

AD-A124 987

FINITE ELEMENT PROGRAM FOR CALCULATING FLOWS IN  
TURBOMACHINES WITH RESULTS FOR NASA TASK-1 COMPRESSOR  
(U) NAVAL POSTGRADUATE SCHOOL MONTEREY CA J A FERGUSON

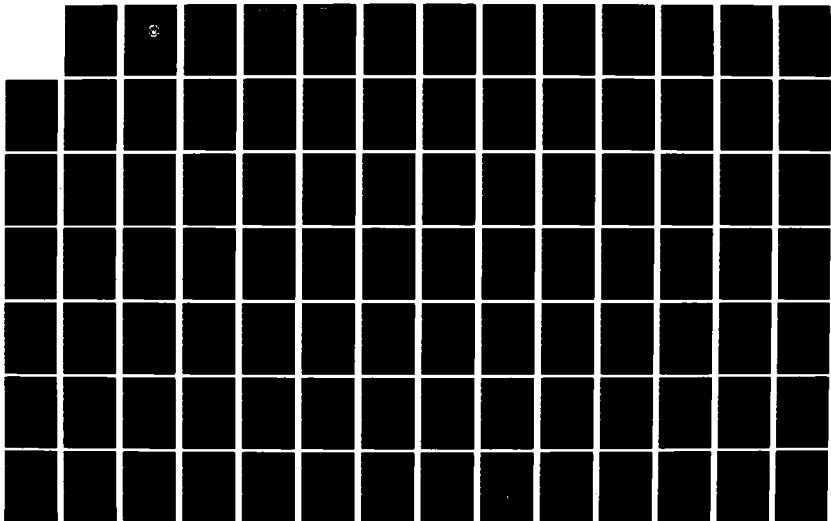
1/3

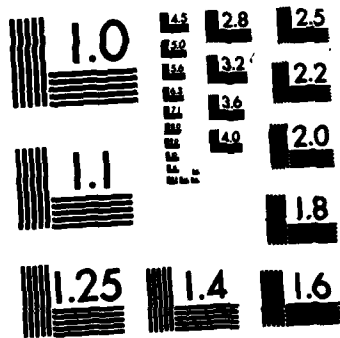
UNCLASSIFIED

OCT 82

F/G 2874

NL





MICROCOPY RESOLUTION TEST CHART  
NATIONAL BUREAU OF STANDARDS-1963-A

2

AD A1 24587

# NAVAL POSTGRADUATE SCHOOL Monterey, California



Copy available to DTIC does not permit fully legible reproduction

## THESIS

FINITE ELEMENT PROGRAM FOR CALCULATING  
FLOWS IN TURBOMACHINES WITH RESULTS  
FOR NASA TASK-1 COMPRESSOR

BY

Julian A. Ferguson III

October 1982

Thesis Advisor:

Raymond P. Shreeve

Approved for public release; distribution unlimited

DTIC FILE COPY

028

092

DTIC  
ELECTED  
1983

E

## **DISCLAIMER NOTICE**

**THIS DOCUMENT IS BEST QUALITY PRACTICABLE. THE COPY FURNISHED TO DTIC CONTAINED A SIGNIFICANT NUMBER OF PAGES WHICH DO NOT REPRODUCE LEGIBLY.**

UNCLASSIFIED

SECURITY CLASSIFICATION OF THIS PAGE (When Data Entered)

REPORT DOCUMENTATION PAGE		READ INSTRUCTIONS BEFORE COMPLETING FORM
1. REPORT NUMBER	2. GOVT ACCESSION NO. AD-A124987	3. RECIPIENT'S CATALOG NUMBER
4. TITLE (and Subtitle) Finite Element Program for Calculating Flows in Turbomachines with Results for NASA Task-1 Compressor		5. TYPE OF REPORT & PERIOD COVERED Engineer's Thesis October 1982
7. AUTHOR(s) Julian A. Ferguson III		6. PERFORMING ORG. REPORT NUMBER
9. PERFORMING ORGANIZATION NAME AND ADDRESS Naval Postgraduate School Monterey, California 93940		8. CONTRACT OR GRANT NUMBER(s)
11. CONTROLLING OFFICE NAME AND ADDRESS Naval Postgraduate School Monterey, California 93940		10. PROGRAM ELEMENT, PROJECT, TASK AREA & WORK UNIT NUMBERS
14. MONITORING AGENCY NAME & ADDRESS (if different from Controlling Office)		12. REPORT DATE October 1982
		13. NUMBER OF PAGES 247
		15. SECURITY CLASS. (of this report) Unclassified
		15a. DECLASSIFICATION/DOWNGRADING SCHEDULE
16. DISTRIBUTION STATEMENT (of this Report)  Approved for public release; distribution unlimited		
17. DISTRIBUTION STATEMENT (of the abstract entered in Block 20, if different from Report)		
18. SUPPLEMENTARY NOTES		
19. KEY WORDS (Continue on reverse side if necessary and identify by block number) Finite Element Method Flow in Turbomachines Compressor Flow Field		
20. ABSTRACT (Continue on reverse side if necessary and identify by block number) A general mesh generation code (MESHGEN) and finite element flow solver (TURBO) for calculating the flow development through axial turbomachines are fully documented. The finite element approach followed Hirsch and Warzee. Excellent results were obtained for the NASA Task-1 compressor operating with subsonic flow conditions. Construction of the code will allow		

UNCLASSIFIED

SECURITY CLASSIFICATION OF THIS PAGE/When Data Entered

straightforward extension to transonic flows, turbine stages and multiple stage machines.

A

Accession For	
NTIS GRA&I	<input checked="" type="checkbox"/>
DTIC TAB	<input type="checkbox"/>
Unannounced	<input type="checkbox"/>
Justification	
By	
Distribution/	
Availability Codes	
Dist	Avail and/or Special
A	23 CP



Approved for public release; distribution unlimited

Finite Element Program for Calculating Flows in  
Turbomachines with Results for NASA Task-1 Compressor

by

Julian A. Ferguson III  
Lieutenant, United States Navy  
B.S., Auburn University, 1975

Submitted in partial fulfillment of the  
requirements for the degree of

MASTER OF SCIENCE IN AERONAUTICAL ENGINEERING

and

AERONAUTICAL ENGINEER

from the

NAVAL POSTGRADUATE SCHOOL  
October 1982

Author:

Julian A. Ferguson III

Approved by:

[Signature]  
Thesis Advisor

Max F. Platzer  
Second Reader

Max F. Platzer  
Chairman, Department of Aeronautics

William M. Tolles  
Dean of Science and Engineering

## ABSTRACT

A general mesh generation code (MESHGEN) and finite element flow solver (TURBO) for calculating the flow development through axial turbomachines are fully documented. The finite element approach followed Hirsch and Warzee. Excellent results were obtained for the NASA Task-1 compressor operating with subsonic flow conditions. Construction of the code will allow straightforward extension to transonic flows, turbine stages and multiple stage machines.



## TABLE OF CONTENTS

I.	INTRODUCTION . . . . .	15
	A. STATEMENT OF TASK . . . . .	15
	B. DESCRIPTION OF THE PROBLEM . . . . .	16
II.	MATHEMATICAL MODEL . . . . .	19
III.	FINITE ELEMENT METHOD . . . . .	24
	A. INTRODUCTION . . . . .	24
	B. APPLICATION OF THE WEIGHTED RESIDUAL PROCESS	25
	C. APPLICATION OF THE FINITE ELEMENT METHOD . .	27
	D. NUMERICAL INTEGRATION TECHNIQUE . . . . .	30
	1. Stiffness Matrix Evaluation . . . . .	31
	2. Right-hand Side Vector Evaluation . . .	35
IV.	DESCRIPTION OF THE PROGRAM MESHGEN . . . . .	36
	A. MAIN PROGRAM DESCRIPTION . . . . .	36
	B. SUBROUTINE DESCRIPTIONS . . . . .	38
	1. Subroutine INIT1 . . . . .	38
	2. Subroutine INPUT . . . . .	39
	3. Subroutine TMESH . . . . .	40
	4. Subroutine CONEC . . . . .	41
	5. Subroutine INIT2 . . . . .	41
	6. Subroutine FLOFCT . . . . .	42
	7. Subroutine TASK1 . . . . .	43
	8. Subroutine FILGEN . . . . .	44
	9. Subroutine MPLOT . . . . .	44

10.	Subroutine ERR1 . . . . .	45
11.	Subroutine ERR2 . . . . .	45
12.	Subroutine ERR3 . . . . .	45
V.	DESCRIPTION OF THE PROGRAM TURBO . . . . .	47
A.	MAIN PROGRAM DESCRIPTION . . . . .	47
B.	SUBROUTINE DESCRIPTIONS . . . . .	49
1.	Subroutine RDATA . . . . .	49
2.	Subroutine INIT1 . . . . .	50
3.	Subroutine ZEROI . . . . .	50
4.	Subroutine INPUT . . . . .	50
5.	Subroutine DIST . . . . .	51
6.	Subroutine SLINE . . . . .	53
7.	Subroutine DUCT . . . . .	57
8.	Subroutine ROTO . . . . .	58
9.	Subroutine STAT . . . . .	60
10.	Subroutine FCAL . . . . .	61
11.	Subroutine STIFF . . . . .	64
12.	Subroutine DSIMQ . . . . .	66
13.	Subroutine REPLA . . . . .	66
14.	Subroutine TEST . . . . .	67
15.	Subroutine RELAX . . . . .	67
16.	Subroutine NOCON . . . . .	67
17.	Subroutine OUTPUT . . . . .	68
18.	Subroutine MPLOT . . . . .	68
19.	Subroutine SHAPE . . . . .	69
20.	Subroutine JACOB . . . . .	69

21.	Subroutine ERR1 . . . . .	70
22.	Subroutine ERR2 . . . . .	70
23.	Subroutine ERR3 . . . . .	71
VI.	RESULTS AND DISCUSSION . . . . .	72
A.	PROGRAM VERIFICATION . . . . .	72
1.	Test Case 1 . . . . .	72
2.	Test Case 2 . . . . .	74
3.	Test Case 3 . . . . .	74
4.	Test Case 4 . . . . .	75
B.	POINTS OF INTEREST . . . . .	76
VII.	CONCLUSIONS AND RECOMMENDATIONS . . . . .	78
A.	PROGRAM MESHGEN . . . . .	78
B.	PROGRAM TURBO . . . . .	78
	LIST OF REFERENCES . . . . .	80
	TABLES . . . . .	83
	FIGURES . . . . .	87
APPENDIX A.	STORAGE ALLOCATION FOR THE PROGRAM MESHGEN . . . . .	163
APPENDIX B.	LISTING OF THE OUTPUT VARIABLES FOR PROGRAM MESHGEN . . . . .	165
APPENDIX C.	STORAGE ALLOCATION FOR THE PROGRAM TURBO	167
APPENDIX D.	LISTING OF THE OUTPUT VARIABLES FOR PROGRAM TURBO . . . . .	170
APPENDIX E.	LISTING OF THE PROGRAM MESHGEN . . . . .	171
APPENDIX F.	LISTING OF THE PROGRAM TURBO . . . . .	183
APPENDIX G.	SAMPLE PROGRAM OUTPUT . . . . .	216
	INITIAL DISTRIBUTION LIST . . . . .	247

**LIST OF TABLES**

1.	Connectivity Relationships for Figure 3 . . . . .	83
2.	Comparison of Program Predictions with NASA Task-1 Compressor Measurements at 50% Design Speed . . .	84
3.	Comparison of Program Predictions with NASA Task-1 Compressor Measurements at 70% Design Speed . . .	85
4.	Comparison of Program Predictions with NASA Task-1 Compressor Measurements at 80% Design Speed . . .	86

## LIST OF FIGURES

1.	S1 and S2 Stream Surfaces . . . . .	87
2.	Nomenclature of an Eight-Node Element . . . . .	88
3.	Example of a Three Element Mesh . . . . .	89
4.	Mapping Relationships from the $\xi, \eta$ to the $z, r$ Plane . . . . .	90
5.	Mesh Generation . . . . .	91
6.	MESHGEN Generated Plot of the 222 Node Mesh Used in the Calculations of the Meridional Through- Flow . . . . .	92
7.	A TURBO Generated Tektonix 618 Plot of the Rotor Inlet Axial Velocity at 50% Design Speed . . . . .	93
8.	A TURBO Generated Tektonix 618 Plot of the Rotor Inlet Relative Flow Angles . . . . .	94
9.	A TURBO Generated Tektonix 618 Plot of the Total Pressure Ratio of the Rotor vs Inlet Radius . . . . .	95
10.	A TURBO Generated Tektonix 618 Plot of the Adiabatic Efficiency of the Rotor vs Inlet Radius . . . . .	96
11.	A TURBO Generated Tektonix 618 Plot of the Rotor Outlet Axial Velocity . . . . .	97
12.	A TURBO Generated Tektonix 618 Plot of the Rotor Outlet Relative Flow Angles . . . . .	98
13.	A TURBO Generated Tektonix 618 Plot of the Rotor Outlet Absolute Flow Angles . . . . .	99
14.	A TURBO Generated Tektonix 618 Plot of the Rotor Outlet Deviation Flow Angles . . . . .	100
15.	A TURBO Generated Tektonix 618 Plot of the Stator Inlet Axial Velocity . . . . .	101
16.	A TURBO Generated Tektonix 618 Plot of the Stator Inlet Absolute Flow Angles . . . . .	102

17.	A TURBO Generated Tektonix 618 Plot of the Stator Total Pressure Ratio vs Inlet Radius . . . . .	103
18.	A TURBO Generated Tektonix 618 Plot of the Stator Outlet Axial Velocity . . . . .	104
19.	A TURBO Generated Tektonix 618 Plot of the Stator Outlet Absolute Flow Angles . . . . .	105
20.	A TURBO Generated Tektonix 618 Plot of the Stator Outlet Deviation Flow Angles . . . . .	106
21.	Comparison of Predictions to Gavito and Observations for Rotor Inlet Axial Velocity, 50% Design	107
22.	Comparison of Predictions to Gavito and Observations for Rotor Outlet Axial Velocity, 50% Design	108
23.	Comparison of Predictions to Gavito and Observations for Stator Inlet Axial Velocity, 50% Design	109
24.	Comparison of Predictions to Gavito and Observations for Stator Outlet Axial Velocity, 50% Design . . . . .	110
25.	Comparison of Predictions to Hirsch and Observations for Rotor Inlet Axial Velocity, 50% Design	111
26.	Comparison of Predictions to Hirsch and Observations for Rotor Outlet Axial Velocity, 50% Design	112
27.	Comparison of Predictions to Hirsch and Observations for Rotor Outlet Relative Flow Angles, 50% Design . . . . .	113
28.	Comparison of Predictions to Hirsch and Observations for Rotor Outlet Absolute Flow Angles, 50% Design . . . . .	114
29.	Comparison of Predictions to Hirsch and Observations for Stator Inlet Axial Velocity, 50% Design	115
30.	Comparison of Predictions to Hirsch and Observations for Stator Outlet Axial Velocity, 50% Design . . . . .	116
31.	Axial Velocity at the Rotor Inlet, 50% Design . .	117
32.	Relative Flow Angles at Rotor Inlet, 50% Design .	118
33.	Total Pressure Ratio of the Rotor, 50% Design . .	119

34.	Adiabatic Efficiency of the Rotor, 50% Design . .	120
35.	Axial Velocity at the Rotor Outlet, 50% Design .	121
36.	Relative Flow Angles at Rotor Outlet, 50% Design	122
37.	Absolute Flow Angles at Rotor Outlet, 50% Design	123
38.	Deviation Flow Angles at Rotor Outlet, 50% Design	124
39.	Axial Velocity at the Stator Inlet, 50% Design .	125
40.	Absolute Flow Angles at Stator Inlet, 50% Design	126
41.	Total Pressure Ratio at Stator Inlet, 50% Design	127
42.	Axial Velocity at the Stator Outlet, 50% Design .	128
43.	Absolute Flow Angles at Stator Outlet, 50% Design	129
44.	Deviation Flow Angles at Stator Outlet, 50% Design . . . . .	130
45.	Axial Velocity at the Rotor Inlet, 70% Design . .	131
46.	Relative Flow Angles at Rotor Inlet, 70% Design .	132
47.	Total Pressure Ratio of the Rotor, 70% Design . .	133
48.	Adiabatic Efficiency of the Rotor, 70% Design . .	134
49.	Axial Velocity at the Rotor Outlet, 70% Design .	135
50.	Relative Flow Angles at Rotor Outlet, 70% Design	136
51.	Absolute Flow Angles at Rotor Outlet, 70% Design	137
52.	Deviation Flow Angles at Rotor Outlet, 70% Design	138
53.	Axial Velocity at the Stator Inlet, 70% Design .	139
54.	Absolute Flow Angles at Stator Inlet, 70% Design	140
55.	Total Pressure Ratio at Stator Inlet, 70% Design	141
56.	Axial Velocity at the Stator Outlet, 70% Design .	142
57.	Absolute Flow Angles at Stator Outlet, 70% Design	143
58.	Deviation Flow Angles at Stator Outlet, 70% Design . . . . .	144

59.	Axial Velocity at the Rotor Inlet, 80% Design . .	145
60.	Relative Flow Angles at Rotor Inlet, 80% Design .	146
61.	Total Pressure Ratio of the Rotor, 80% Design . .	147
62.	Adiabatic Efficiency of the Rotor, 80% Design . .	148
63.	Axial Velocity at the Rotor Outlet, 80% Design .	149
64.	Relative Flow Angles at Rotor Outlet, 80% Design	150
65.	Absolute Flow Angles at Rotor Outlet, 80% Design	151
66.	Deviation Flow Angles at Rotor Outlet, 80% Design	152
67.	Axial Velocity at the Stator Inlet, 80% Design .	153
68.	Absolute Flow Angles at Stator Inlet, 80% Design	154
69.	Total Pressure Ratio at Stator Inlet, 80% Design	155
70.	Axial Velocity at the Stator Outlet, 80% Design .	156
71.	Absolute Flow Angles at Stator Outlet, 80% Design	157
72.	Deviation Flow Angles at Stator Outlet, 80% Design . . . . .	158
73.	Axial Velocity at the Rotor Inlet, 80% Design, 9% Blockage . . . . .	159
74.	Axial Velocity at the Rotor Outlet, 80% Design, 9% Blockage . . . . .	160
75.	Axial Velocity at the Stator Inlet, 80% Design, 9% Blockage . . . . .	161
76.	Axial Velocity at the Stator Outlet, 80% Design, 9% Blockage . . . . .	162



## LIST OF SYMBOLS

<u>Symbol</u>	<u>Description</u>	<u>Units</u>
$\psi$	Stream function	lbm/sec
$\alpha$	Absolute flow angle whose tangent is the ratio of the absolute tangential-to-meridional velocity	degrees
$\beta$	Relative flow angle whose tangent is the ratio of the absolute tangential-to-meridional velocity	degrees
$\delta$	Deviation angle, difference in flow angle and camber-line angle at trailing edge in cascade projection tangential-to-meridional velocity	degrees
$\kappa_1$	Angle between tangent to the blade meanline and the axial direction	degrees
$\phi$	Camber angle, difference between angles in cascade projection of tangents to camber line at extremes of camber-line arc	degrees
$\sigma$	Solidity, ratio of chord to blade spacing	dimensionless
$\tilde{\omega}$	Total-pressure-loss coefficient	dimensionless
T	Temperature	°R
P	Pressure	psia
$\rho$	Density	lbm/ft <sup>3</sup>

### **Subscripts**

t	Total conditions
1	blade leading edge
2	blade trailing edge
E	Over an element

### **Superscripts**

e	For an element
---	----------------

## I. INTRODUCTION

### A. STATEMENT OF TASK

The original task of this research project was to continue the work of Macchi [Ref. 1] and Cirone [Ref. 2] in the development of a turbine prediction computer code for the Turbopropulsion Laboratory at the Naval Postgraduate School. An analysis of the referenced code by Ferguson [Ref. 3] indicated that a significant amount of work remained to be done in order to make the program operational. In the author's opinion the task could be better accomplished through the use of a different solution technique. After additional study and review of similar work [Refs. 4, 5, 6 and 7] it was decided that a finite element approach to the problem would be adopted. A program developed by Gavito [Ref. 8], which followed the work of Hirsch and Warzee [Ref. 4], was selected as the basis for development of the computer code described in the sections that follow. However, Gavito's program was formulated as a compressor performance prediction which, as it was reported, had not given results similar to those obtained by Hirsch and Warzee. Thus the first goal of the project became the development of an axial compressor prediction code that could produce results comparable to those published by Hirsch and Warzee. The second goal was to revise and document the program so that its

application to any compressor and its extension to turbine analysis could be carried out without excessive difficulty.

#### B. DESCRIPTION OF THE PROBLEM

One purpose of conducting a through-flow analysis is to predict the performance of a turbomachine under design and off-design operating conditions. Through the combination of a mathematical model and empirically determined correlations, it is possible to provide the engineer with a tool that will determine the effects of variations in design parameters and analyze the performance of an existing machine.

The first problem addressed in the formulation of a performance prediction code is that of expressing the analysis in a form that can be accurately and efficiently solved by computer methods. Most methods for through-flow calculations are based on the classic work of Wu [Ref. 9] which stated that the equations of fluid flow in turbomachines can be solved on the intersecting sets of stream surfaces known as the S1 family and S2 family of stream surfaces (Fig. 1). In general the intersection of a S1 surface and a S2 surface is a twisting line with three dimensional variations. However, if an axisymmetric assumption is made, the S2 surface will lie on a meridional plane and the directional derivatives on the S2 surface become the  $\partial(\ )/\partial r$  and  $\partial(\ )/\partial z$  in cylindrical coordinates. As shown by Smith [Ref. 10], circumferentially averaged equations with an axisymmetric

flow assumption can be used to a good first approximation for the through-flow analysis.

Three general methods of solving the so-called radial equilibrium equation of flows in turbomachines which results from the axisymmetric assumption can be found in the literature. The first is called the streamline curvature method [Refs. 1, 2 and 11]. The method derived its name from the fact that the radius of curvature of the streamline is an integral part of the formulation. The second, a matrix method, applies a finite differences technique to the radial equilibrium equation, normally after it has been reduced to a Poisson form [Refs. 12 and 13]. The third method is the finite element method which was used in the present work.

In the mid-1970's, Hirsch and Warzee [Ref. 4] first reported the application of the finite element method to solution of the axisymmetric radial equilibrium equation. They applied the finite element technique to solve the equation expressed in quasi-harmonic form in terms of the stress function. They published extensive comparisons of the predictions obtained using their method with measurements obtained on several machines under various operating conditions. In general, the method produced excellent results for compressors and turbines of single and multi-stage configurations. It was this demonstrated ability of the method over

such a wide range of parameters that let to its selection for use in the present project.

In the sections which follow, the development of programs MESHGEN and TURBO, which are based on the work of Hirsch and Warzee [Ref. 4], is documented. Comparisons are given of the results obtained when the program was applied to analyze the NASA Task-1 compressor with results obtained by the referenced authors.

## II. MATHEMATICAL MODEL

The equation of motion for a fluid has the general form (Vavra [Ref. 14])

$$(\partial\vec{V}/\partial t) + (\vec{V}\cdot\nabla)\vec{V} = -\nabla p/\rho + \vec{F}_f - \nabla(gz) \quad (1)$$

Using the vector identity

$$(\vec{V}\cdot\nabla)\vec{V} = \nabla(v^2/2) - (\vec{V} \times \nabla \times \vec{V}) \quad (2)$$

Eq. (1) can be written as

$$\partial\vec{V}/\partial t + \nabla(v^2/2 + gz) = -\nabla p/\rho + \vec{F}_f + (\vec{V} \times \nabla \times \vec{V}) \quad (3)$$

The first law of thermodynamics for a fluid particle can be written as

$$Tds = dh - dp/\rho \quad (4)$$

which, along an elemental path length  $d\vec{r}$  in a fluid field implies that

$$T(d\vec{r}\cdot\nabla s) = (d\vec{r}\cdot\nabla)h - (d\vec{r}\cdot\nabla)p/\rho \quad (4a)$$

or

$$d\vec{r} \cdot (\nabla h - T\nabla s - \nabla p/\rho) = 0 \quad (5)$$

Since  $dr$  is not equal to zero in general, in a homogeneous fluid flow the first law may be expressed as

$$\nabla h - T\nabla s - \nabla p/\rho = 0 \quad (6)$$

Substituting Eq. (6) into Eq. (3) yields

$$\partial \vec{V} / \partial t + \nabla (h + V^2/2 + gz) = T \nabla s + \vec{F}_f + \vec{V} \times \nabla \times \vec{V} \quad (7)$$

For steady, inviscid flow Eq. (7) reduces to

$$\nabla H = T \nabla s + (\vec{V} \times \nabla \times \vec{V}) \quad (8)$$

As shown by Hirsch and Warzee [Ref. 15], Eq. (8) can be revised to describe the flow through blade rows by introducing a circumferential averaging process and assuming that the flow is axisymmetric at the averaged condition. The averaged equation can be expressed as

$$-(\vec{V} \times \nabla \times \vec{V}) = T \nabla s - \nabla H + \vec{F}_b + \vec{F}_d \quad (9)$$

where  $F_b$  is the body force representing the action of the blades on the flow and  $F_d$  represents the dissipative force whose work generates the irreversible entropies. The  $F_d$  forces are considered to be uniformly distributed in the tangential direction and proportional to the loss coefficients. Equation (9) leads to the following three equations in cylindrical coordinates (with  $\partial(\ )/\partial\theta = 0$ )

$$\begin{aligned} (V_u/r) (\partial(rV_u)/\partial r) - V_z ((\partial V_r/\partial z) - (\partial V_z/\partial r)) = \\ \partial H/\partial r - T(\partial s/\partial r) - F_{b,r} - F_{d,r} \end{aligned} \quad (10a)$$

$$(V_z/r) (\partial(rV_u)/\partial z) + (V_r/r) (\partial(rV_u)/\partial r) = F_u \quad (10b)$$

$$\begin{aligned} V_r ((\partial V_r/\partial z) - (\partial V_z/\partial r)) - (V_u/r) (\partial(rV_u)/\partial z) = \\ \partial H/\partial z - T(\partial s/\partial z) - F_z \end{aligned} \quad (10c)$$



Equation (10a) expresses the radial equilibrium of the meridional through-flow and it is the governing equation to be solved for the velocity components. Equations (10b) and (10c) determine the tangential and axial components of the forces once Eq. (10a) has been solved.

For the solution of Eq. (10a) to have physical meaning, care must be taken to ensure that continuity is satisfied throughout the field. In general, the continuity equation can be expressed as

$$\partial \rho / \partial t + \nabla \cdot (\rho \vec{V}) = 0 \quad (11)$$

which for steady, circumferentially averaged flow can be written as

$$(\partial / \partial r) (\rho r b V_r) + (\partial / \partial z) (\rho r b V_z) = 0 \quad (12)$$

where  $b$  is a blockage factor describing the reduction in the flow area in the tangential direction due to the presence of rotor and stator blades. The tangential blockage is approximated by

$$b = 1 - t/s \quad (12a)$$

where  $t$  is the blade thickness and  $s$  is the blade spacing. As will be discussed in the description of subroutine INPUT, this factor will be modified to account for the end-wall boundary layer contractions. A stream function,  $\psi$ , can be introduced and defined so that Eq. (12) is automatically satisfied as follows:

$$\partial\psi/\partial r = \rho r b V_z \quad (13a)$$

$$\partial\psi/\partial z = -\rho r b V_r \quad (13b)$$

After the substitution of Eqs. (13a) and (13b) into Eq. (10a) one is assured of the implicit satisfaction of continuity as the radial equilibrium equation is solved explicitly. Equation (10a) may now be written as

$$\begin{aligned} (\partial/\partial r) \left( (1/\rho r b) (\partial\psi/\partial r) \right) + (\partial/\partial z) \left( (1/\rho r b) (\partial\psi/\partial z) \right) = \\ (1/V_z) \left( (\partial H/\partial r) - T(\partial s/\partial r) + \right. \\ \left. (V_u/r) (\partial(rV_u)/\partial r) \right) - F_{b,r} - F_{d,r} \end{aligned} \quad (14)$$

The equation is written in a slightly different form for solution in rotor regions where rothalpy remains constant along a streamline. The definition of rothalpy,  $H_R$ , given by

$$H_R = H - UV_u \quad (15)$$

is substituted into Eq. (14) and the terms in brackets on the right-hand side become

$$\left[ \partial H_R/\partial r - T(\partial s/\partial r) - (W_u/r) (\partial(rV_u)/\partial r) - F_{b,r} - F_{d,r} \right] \quad (16)$$

The significance of the  $F_{b,r}$  and  $F_{d,r}$  terms can be analyzed in the following manner. The body force  $F_b$  acts in a direction normal to the mean blade surface, which for radial blading is in the circumferential direction. The term  $F_{b,r}$  accounts for the body force component in the radial direction that results when blade lean is present. For most blading this is a small term that may be neglected.

Similarly,  $F_{d,r}$  is the contribution of the dissipative forces in the radial direction for non-cylindrical stream surfaces. This contribution can normally be neglected for axial-flow machines, which is the case treated here. (Note that the two body force terms are included in the analysis for machines in which the magnitudes of these forces are significant.) With these simplifications the radial equilibrium equation may be written in the form

$$\begin{aligned} (\partial/\partial r) \left( (1/\rho r b) (\partial\psi/\partial r) \right) + (\partial/\partial z) \left( (1/\rho r b) (\partial\psi/\partial z) \right) = \\ (1/V_z) \left( (\partial H/\partial r) - T(\partial s/\partial r) \right) + (V_u/r) \left( \partial(rV_u)/\partial r \right) \end{aligned} \quad (17)$$

with the appropriate modifications for solution in a rotor region.

### III. FINITE ELEMENT METHOD

#### A. INTRODUCTION

The finite element method is a numerical procedure that is particularly well suited to solving problems in continuum mechanics, which invariably involve equations expressed in differential form. As stated by Cook [Ref. 16], the essence of the finite element method is the "piecewise approximation of a function  $\phi$ , by means of polynomials, each defined over a small region (element) and expressed in terms of nodal values of the function."

In order to understand the finite element method and the solution techniques employed in the computer program reported herein, one must first have a complete understanding of the basic element, the terminology used to describe the element, and the relationship between the element and the remainder of the solution domain. The complete problem is solved in a piecewise manner, in which the solution of the derived governing relationship over the discrete region of an element is sought to determine the contribution of the element to the overall solution. Figure 2 illustrates the single element as it is used in the present work and the nomenclature for the element on what is referred to as the "local domain". The number scheme to employ is arbitrary, limited only by the requirement that the system remain

consistent from element to element. Figure 3 shows a vertical stack of three elements to show how elements are connected in what is known as a "global domain". Table 1 lists the relationship between the two reference systems, known as the connectivity. The connectivity is important because the solution of a problem over a computational region involves a careful summation of the local contributions of each element to the global equations. The summation process is tracked by the connectivity. Again the global numbering scheme is arbitrary, influenced mainly by considerations of computer storage and computational efficiency.

The key concept to be grasped is that the finite element method is a series of local solutions that are coupled together through the connectivity relationships to form a solution for the entire computational domain. A more detailed description of the finite element method is contained in Refs. 16 through 18.

#### B. APPLICATION OF THE WEIGHTED RESIDUAL PROCESS

A standard weighted residuals process was used to transform Eq. (17) into a form that can be solved by numerical techniques. As a first step, the equation was written in a more compact form as

$$(\partial/\partial r)[k(\partial\psi/\partial r)] + (\partial/\partial z)[k(\partial\psi/\partial z)] + f = 0 \quad (18)$$

where

$$k(r,z) = (1/\rho r b) \quad (19)$$

$$f(r, z) = (1/V_z) [T(\partial s/\partial r) - \partial H/\partial r + (V_u/r)(\partial(rV_u)/\partial r)] \quad (20)$$

with the boundary conditions

$$k(\partial\psi/\partial n) + \alpha_1(\psi - \psi_0) = 0 \quad (21)$$

on the associated exterior surface S. Equations (18) and (21) may be rewritten as

$$(1/r) \{ (\partial/\partial r) [k(\partial\psi/\partial r)] + (\partial/\partial z) [k(\partial\psi/\partial z)] + f \} = 0 \quad (22)$$

in the volume, V, and

$$(1/r) [k(\partial\psi/\partial n) + \alpha_1(\psi - \psi_0)] = 0 \quad (23)$$

on the surface, S. An approximation,  $\tilde{\psi}(r, z)$ , of the unknown solution is searched for such that the corresponding weighted residual,  $\bar{R}$ , is equal to zero. Analytically this is expressed as

$$\bar{R} = \int_V W(r, z) R_V(r, z) dV + \int_S W(r, z) R_S(r, z) dS = 0 \quad (24)$$

where  $W(r, z)$  is the (known) weight function and  $R_V$  and  $R_S$  are the so-called "residuals" in the volume and on the surface, respectively. As the sum of  $R_V$  and  $R_S$  approaches zero, the approximation,  $\tilde{\psi}$ , approaches the exact solution,  $\psi$ , with  $R_V$  and  $R_S$  defined to be identically zero if  $\tilde{\psi} = \psi$ . By defining  $R_V$  to be equal to the left-hand side of Eq. (22) and  $R_S$  to be equal to the left-hand side of Eq. (23), Eq. (24) can be written as

$$\int_{\Omega} -W(r, z) [ (\partial/\partial r) \{ k(\partial\psi/\partial r) \} + (\partial/\partial z) \{ k(\partial\psi/\partial z) \} + f ] 2\pi d\Omega + \int_C Wk(\partial\psi/\partial n) 2\pi dC = 0 \quad (25)$$

Integration of the first term of Eq. (25) by parts yields

$$\int_{\Omega} [k\{(\partial\psi/\partial r)(\partial W/\partial r) + (\partial\psi/\partial z)(\partial W/\partial z)\} - Wf] d\Omega = 0 \quad (26)$$

if  $\psi$  is selected to equal  $\psi_0$  along the corresponding part of the boundary. The second term of Eq. (26) reduces to zero through the proper application of the boundary conditions.

The boundary conditions must be satisfied in different ways for different portions of the boundary. Along the inlet where  $\alpha_1 = 0$  the conditions may be satisfied by specifying  $(\partial\psi/\partial n)$  to be zero or by specifying the nodal values of  $\psi$  if the inlet conditions are conducive to calculating  $\psi$  for each node. Along the shroud and along the hub the value of  $\psi$  must be specified as  $\psi = (m/2\pi)$  at the shroud and  $\psi = 0$  at the hub. For nodes at the exit plane, the condition that  $(\partial\psi/\partial n) = 0$  is required.

### C. APPLICATION OF THE FINITE ELEMENT METHOD

The first step is to discretize the region into subregions or elements. Within each element the unknown stream function,  $\psi$ , and the coordinates  $r$  and  $z$  are assumed to have the following polynomial variations:

$$\psi(r, z) = \sum_i^n \psi_i N_i(\xi, \eta) \quad (27a)$$

$$r = \sum_i^n r_i N_i(\xi, \eta) \quad (27b)$$

$$z = \sum_i^n z_i N_i(\xi, \eta) \quad (27c)$$

where  $n$  = number of nodes in the element

$N_i$  = the shape or (trial) function for node  $i$

$\psi_i$  = value of  $\psi$  at node  $i$

$r_i$  = value of  $r$  at node  $i$

$z_i$  = value of  $z$  at node  $i$

Equations (27b) and (27c) imply a geometrical as well as functional transformation or mapping, as shown for the present case in Fig. 4.

The second step in the process is the selection of the weight and shape functions. The shape functions are defined when the particular type of finite element is selected for the computational grid [Ref. 16]. The eight-noded quadrilateral was used in the present program and its associated shape functions were entered in a subroutine. The weight function is independent of the shape function and may be chosen at the discretion of the individual. In the present case the standard Galerkin technique was employed and therefore, the weight functions were defined as being equal to the shape functions, so that

$$W(r,z) = N(r,z) \quad (28)$$

Equation (26) may now be expressed in the following form:

$$\int_E \left\{ k \left[ (\partial N_j / \partial r) \sum_i^n (\partial N_i / \partial r) + (\partial N_j / \partial z) \sum_i^n (\partial N_j / \partial z) \sum_i^n (\partial N_i / \partial z) \right] - N_j f(r,z) \right\} d\Omega = 0 \quad (29)$$



where  $\int_E$  represents the integral over an element. In matrix notation this becomes

$$[K]^e \{\delta\}^e = \{f\}^e \quad (30)$$

where

$$k_{ij}^e = \int_E k(r,z) [(\partial N_j / \partial r)(\partial N_i / \partial r) + (\partial N_j / \partial z)(\partial N_i / \partial z)] d\Omega \quad (31a)$$

$$f_i^e = \int_E N_i f(r,z) d\Omega \quad (31b)$$

and

$$\delta_i = \psi_i \quad (31c)$$

The summation of the elemental contributions over the entire region yields the global system of equations needed to solve the problem. In matrix notation the global system of equations is expressed as

$$[K]\{\delta\} = \{f\} \quad (32)$$

where

$$[K] = \sum_i^m [K]_i^e \quad (33a)$$

$$\{\delta\} = \sum_i^m \{\delta\}_i^e \quad (33b)$$

$$\{f\} = \sum_i^m \{f\}_i^e \quad (33c)$$

and  $m$  = number of elements in the mesh

$$\delta_i = \psi_i$$

$[K]$  = system's stiffness matrix

$\{f\}$  = system's right-hand side vector

Since  $k_{ij}$  and  $f_i$  depend on the unknown solution  $\psi$ , Eq. (32) is a nonlinear differential equation to be solved by an iterative procedure. The details of the procedure are contained in section V.

#### D. NUMERICAL INTEGRATION TECHNIQUE

In general, problems are analyzed using a coordinate system in which the boundary conditions can be written and satisfied in the simplest possible way. For problems with irregularly shaped boundaries and/or mixed conditions along different portions of the boundary, obtaining numerical solutions in the original coordinate system can be a formidable task. Very often a scheme must be found to transform the derived equations into a new coordinate system that conforms to the requirements of standard numerical techniques. Traditional transformation techniques tend to be complicated exercises in algebra that require extensive reformulation for each geometry or type of boundary condition. The power of the finite element method is the automatic inclusion of a transformation of the geometry and the function to a rectangular domain where a variety of integration techniques may be employed. This can be seen in Fig. 4, which illustrates what is implied by Eqs. (27a), (27b), and (27c). The method can handle extremely complicated boundary conditions

and shapes with ease and is limited only by the type of element selected by the individual.

The quadratic properties of the eight-node element allows curved boundaries in the physical domain so long as the section of the boundary included within a single element does not have a point of inflection. The use of a quadratic element also ensures continuity of the approximated function along the elemental boundaries regardless of the direction of approach from within the mesh. The specific numerical technique used in the program is discussed in the following section.

#### 1. Stiffness Matrix Evaluation

In section C the following relationship was derived for the individual elements of the stiffness matrix, [K]:

$$k_{ij}^e = \int_E k(r,z) [(\partial N_j / \partial r)(\partial N_i / \partial r) + (\partial N_j / \partial z)(\partial N_i / \partial z)] d\Omega \quad (31a)$$

In order to take advantage of well established numerical integration techniques, Eq. (31a) must be transformed from the (z,r) domain and its irregular elemental boundaries to the rectangular ( $\xi, \eta$ ) domain. Equations (27a) through (27c) describe the variation of the function and the (r,z) coordinate values in the ( $\xi, \eta$ ) plane. In order to transform Eq. (31a) it is necessary to determine the relationship of the variations of the derivatives in the two domains. These relationships can be derived in a straightforward manner through the use of the chain rule as follows:

$$(\partial N_i / \partial \xi) = (\partial N_i / \partial z) (\partial z / \partial \xi) + (\partial N_i / \partial r) (\partial r / \partial \xi) \quad (34)$$

and

$$(\partial N_i / \partial \eta) = (\partial N_i / \partial z) (\partial z / \partial \eta) + (\partial N_i / \partial r) (\partial r / \partial \eta) \quad (35)$$

Equations (34) and (35) can be combined in matrix form as

$$\begin{Bmatrix} \frac{\partial N_i}{\partial \xi} \\ \frac{\partial N_i}{\partial \eta} \end{Bmatrix} = \begin{bmatrix} \frac{\partial z}{\partial \xi} & \frac{\partial r}{\partial \xi} \\ \frac{\partial z}{\partial \eta} & \frac{\partial r}{\partial \eta} \end{bmatrix} \begin{Bmatrix} \frac{\partial N_i}{\partial z} \\ \frac{\partial N_i}{\partial r} \end{Bmatrix} \quad (36)$$

Through the selection of the type element to be used in the mesh,  $N_i(\xi, \eta)$  is a known function [Ref. 16], which makes possible the computation of the left-hand side vector for any point within the element boundaries. Similarly, by taking the appropriate derivatives of Eqs. (27b) and (27c) the 2x2 matrix, known as the Jacobian matrix [J], can be determined. It follows that the r and z derivatives of the shape/weight functions can be determined for any point of an element from

$$\begin{Bmatrix} \frac{\partial N_i}{\partial z} \\ \frac{\partial N_i}{\partial r} \end{Bmatrix} = \begin{bmatrix} \frac{\partial z}{\partial \xi} & \frac{\partial r}{\partial \xi} \\ \frac{\partial z}{\partial \eta} & \frac{\partial r}{\partial \eta} \end{bmatrix}^{-1} \begin{Bmatrix} \frac{\partial N_i}{\partial \xi} \\ \frac{\partial N_i}{\partial \eta} \end{Bmatrix} \quad (37)$$

An examination of Eqs. (27a) through (27c) shows that once the derivatives of the shape/weight functions are known for a point then it is a simple procedure to determine the

derivatives of any other elemental property that has a value specified at the nodes.

The final relationship that is needed for the transformation is the relationship between the differential change in the coordinate directions of the  $(r,z)$  plane and the  $(\xi,\eta)$  plane. As shown by Kaplan [Ref. 19], the required relationship is

$$dzdr = |J|d\xi d\eta \quad (38)$$

Equation (31a) can now be transformed for integration in the  $(\xi,\eta)$  plane to the form

$$k_{ij}^e = \int_{-1}^1 \int_{-1}^1 \sum_k^n N_k k_k ([B]^T [B]) |J| d\xi d\eta \quad (39)$$

where

$$[B] = [J]^{-1} \begin{Bmatrix} \frac{\partial N}{\partial \xi} \\ \frac{\partial N}{\partial \eta} \end{Bmatrix} \quad (40)$$

and  $k = (1/\rho r b) \quad (41)$

The Gauss-Legendre method of numerical integration was used to obtain a solution to Eq. (39). It was selected because its determined accuracy was easily determined and the simple summing procedure used in the solution could be efficiently coded. A one dimensional example is used here to illustrate the use of the method.

The definite integral

$$I = \int_{-1}^1 \phi(\xi) d\xi \quad (42)$$

may be written in the form

$$I = W_1\phi_1 + W_2\phi_2 + W_3\phi_3 + \dots + W_n\phi_n \quad (43)$$

where  $\phi_i = \phi(\xi_i)$

$W_i$  = Gaussian weight function for  $\xi_i$

The values of the points, called abscissas, and their corresponding weighting function values are catalogued for use.

The number of points to be used is determined by the order of the function to be approximated. In general, a polynomial of  $(2n - 1)$  is integrated exactly by the use of  $n$  Gauss points. In two dimensions the Gauss method can be written as

$$I = \int_{-1}^1 \int_{-1}^1 \phi(\xi, \eta) d\xi d\eta \quad (44)$$

which can be written as

$$I = \sum_i^n \sum_j^m W_i W_j \phi(\xi_i, \eta_j) \quad (45)$$

Equation (39) can now be written in a form that can be coded for solution by the computer as

$$k_{ij}^e = \sum_k \sum_l W_k W_l \sum_m N_m k_m ([B]^T [B]) |J| \quad (46)$$

The scheme used in the program is a two dimensional, three-point Gauss integration. A detailed description of the evaluation of  $[B]^T[B]$  and the method used to obtain  $k_m$  is contained in the description of subroutine STIFF.

## 2. Right-hand Side Vector Evaluation

In Section C the following relationship for  $f$  was derived:

$$f_i^e = \int_E N_i f(r, z) d\Omega \quad (31b)$$

By using the techniques of Section D1, Eq. (31b) can be replaced by

$$f_i^e = \sum_j \sum_k W_j W_k \sum_i N_i \sum_l N_l F_l |J| \quad (47)$$

A more detailed description of the specific methods used to solve Eq. (47) is contained in the description of subroutine FCAL.

#### IV. DESCRIPTION OF PROGRAM MESHGEN

##### A. MAIN PROGRAM DESCRIPTION

MESHGEN was developed in order that the required inputs for the program TURBO could be generated in a fast, accurate, and conceptually correct manner. The program generates an eight-node isoparametric element mesh, computes the related connectivity matrix, defines the type of region enclosed by each element, computes the tangential blockage factor and an estimate of the stream function for each node in the mesh, and computes the thermodynamic conditions and velocity at the inlet. The inputs required to operate the program are the mass flow rate, total temperature, and total pressure at the inlet, the blading and machine geometries, RPM,  $C_p$ ,  $\gamma$ ,  $R$ , and scaling constants for the plot of the mesh. The blading geometries must be coded in the program as a subroutine that uses approximations or design information to express the blade variables as functions of radius. The user provides the other information in response to interactive prompts. The program has two modes of operation, one which generates a complete mesh and all of the associated information and another which uses a previously generated mesh to compute the changes in specific arrays that result from a change in the inlet conditions.



The program is completely general and may be used for either single-stage axial compressor or turbine, and, with very minor modifications, can be expanded for use with multi-stage machines. The mesh size that can be generated by the program is limited only by computer storage considerations. To use the program for another machine, the user is required to replace subroutine TASK1 with a subroutine that can compute the tangential blockage factor,  $b$ , for the desired blading. The functioning of the program and its subroutines for both modes of operation is described in the section B.

The program's algorithm in outline form is as follows:

Algorithm:

Determine the value of the appropriate operating conditions and whether a new mesh is desired (Subroutine INIT1).

Obtain the coordinates of the super element corners and a description of the division of the super elements into the final mesh. Compute the storage allocation parameters (Subroutine INPUT).

Compute the  $(r,z)$  coordinates for all nodes in the mesh (Subroutine TMESH).

Compute the connectivity relationships for the mesh and determine the beginning and ending node numbers for the rotor and stator (Subroutine CONEC).

Compute the array of node numbers where the value of  $\psi$  is to be specified. Compute an initial estimate of the nodal stream function distribution and call subroutine FLOFCT to determine the inlet conditions (Subroutine INIT2).

Compute the nodal tangential blockage factor,  $b$ , for the rotor and stator nodes (Subroutine TASK1).

Place the computed values in disk storage (Subroutine FILGEN).

Plot the generated mesh on the Tektronix 618 terminal for inspection (Subroutine MPlot).

END

## B. SUBROUTINE DESCRIPTIONS

### 1. Subroutine INIT1

Subroutine INIT1 obtains the value of thermodynamic variables and plotting parameters that are required for the program in either mode of operation. The user is required to provide the values of the mass flow (lbm/sec), total temperature ( $^{\circ}$ R), and total pressure (psia), ratio of specific heats ( $\gamma$ ), gas constant (ft-lbf/lbm- $^{\circ}$ R), and the specific heat at constant pressure (BTU/lbm- $^{\circ}$ R). The scaling constants are convenient values of  $r$  and  $z$  used to frame the plot of the mesh. If a new mesh is not desired, the program exits the subroutine.

Subroutine INIT1 determines if a new mesh is to be generated by the response of the user to an interactive question. If a mesh is to be generated, the subroutine obtains some preliminary information about the flow region. Figure 5 shows how the user must first divide the flow region into a coarse mesh known as super elements, recording the  $(z,r)$  coordinates of the corner points. The minimum number of super elements for a single-stage compressor is five so that the three duct regions, the rotor, and the stator may be represented. The maximum number of super elements and the subsequent division into mesh elements is limited only by the

storage limitations of the machine. In practice, the maximum number of elements is limited by the number of equations that may be solved by the program TURBO. It is also limited by the fact that only one super element may be used to describe a rotor or duct region and that the super elements for these regions may only be further subdivided into a single column of elements. The latter restrictions are for compatibility with the computation procedures used in the program TURBO. A decision must then be reached on what subdivision of the super elements will provide a mesh that is sufficiently fine to yield accurate results efficiently. Once the flow region has been divided into super elements and a determination as to the total number of rows and columns of mesh elements has been made, the user can input the appropriate values in response to the prompts provided by the program.

## 2. Subroutine INPUT

Subroutine INPUT uses interactive prompts to obtain a description of the turbomachine's flow passage geometry and the desired mesh characteristics. The user must provide the program with the coordinate values of the super element nodes as shown in Fig. 5. The values are entered as nodal pairs on a station-by-station basis. The first (z,r) coordinate entered is the node on the shroud and the second lies on the hub. The program then asks the user to identify the type of region enclosed in each super element and into how many columns each super element is to be divided.

Enough information is now available for the program to compute and store the information required for the program TURBO. Subroutine INPUT stores the responses to the interactive prompts, determines the values of the storage location pointers, and determines if any storage limitation has been exceeded. If any storage limitation is exceeded, the subroutine calls the appropriate error subroutine to halt execution. The interactive portion of the subroutine is omitted if a new mesh is not desired. However, the values of the pointers are calculated and storage requirements are evaluated as before. A listing of the pointers and the corresponding variables is given in Appendix A.

### 3. Subroutine TMESH

Subroutine TMESH computes the nodal coordinate values from the information obtained in subroutines INIT1 and INPUT. The subroutine uses linear interpolation in the axial direction and a quadratic scheme in the radial direction. The radial interpolation scheme maintains the difference in the squares of the radius of the nodes as a constant. This allows the assumption of equal mass flow between the nodes for uniform axial velocity which is used to determine the initial estimate of the nodal stream function distribution. The nodes are numbered with the assumption that the fluid flow is from left-to-right in the mesh and that the number of columns of elements is greater than or equal to the number of rows of elements. The node at the inlet shroud is labeled

1 and the node at the outlet hub is labeled n for an n node mesh. The numbering proceeds on a column-by-column basis from top-to-bottom. The total number of rows, columns, and mesh elements is displayed to the user. The mesh computations are omitted if a new mesh is not created and elemental count information is displayed as before.

#### 4. Subroutine CONEC

Subroutine CONEC generates the connectivity matrix for the mesh. The connectivity matrix is used to keep track of which nodes are assigned to which elements and the arrangement of the assigned nodes within the element. The connectivity relationships for a three element stack is shown in Fig. 3. Additionally, the subroutine determines the first and last nodes of the rotor and stator.

#### 5. Subroutine INIT2

Subroutine INIT2 stores the node numbers for nodes where the value of  $\psi$  is specified as a known quantity. The array is used in the program TURBO to apply the boundary conditions. The array is not computed if a new mesh is not desired. For either mode of operation, subroutine INIT2 computes the values of the inlet thermodynamic variables, the inlet axial velocity, and an initial estimate of the nodal stream function distribution. Subroutine FLOFCT is used to calculate the inlet conditions and is described in the next section. The initial stream function is computed from the boundary conditions at the shroud and hub. Along

the shroud,  $\psi$  is specified to be equal to  $(\dot{m}/2\pi)$  and along the hub to be zero. The value of  $\psi$  along the inlet is determined by a linear interpolation because of the quadratic node spacing in the radial direction. The remaining nodal values of  $\psi$  are obtained by an assumption that  $\psi$  is a constant along the streamwise boundaries of the elements. The assumption is obviously in error, but it observes the boundary conditions and provides a reasonable first estimate to begin the iteration scheme used in the program TURBO.

#### 6. Subroutine FLOFCT

Subroutine FLOFCT computes the inlet conditions for a passage with a specified geometry, mass flow rate, total temperature, total pressure, and an assumed uniform inlet velocity. The method followed is the "total flow function" formulation proposed by Shreeve [Ref. 20]. The total flow function is defined as the ratio of the mass flux to the limiting or stagnation mass flux. The following definitions and equations are required for the method:

$$V_t = [2H]^{0.5} \quad (48)$$

$$X = V/V_t \quad (49)$$

$$T/T_t = 1 - X^2 \quad (50)$$

$$p/p_t = (1 - X^2)^{\frac{\gamma}{(\gamma-1)}} \quad (51)$$

$$\rho/\rho_t = (1 - X^2)^{\frac{1}{(\gamma-1)}} \quad (52)$$

From the definition of the total flow function,  $\phi$ , it follows that

$$\phi = \rho V / \rho_t V_t = X(1 - X^2)^{\frac{1}{\gamma-1}} \quad (53)$$

The value of  $\phi$  at the inlet can be calculated at the inlet from the assumed uniform conditions by the expression

$$\phi_1 = \dot{m} / (\rho_t V_t A) \quad (54)$$

The value of  $X$  at the inlet is found through the following Newtonian iteration:

$$\phi_1 = \dot{m} / (\rho_t V_t A) \quad (54)$$

Assume  $X = 0.1$  to assure the selection of the subsonic root.

Calculate:  $\phi = X(1 - X^2)^{\frac{1}{\gamma-1}} \quad (53)$

and  $d\phi/dX = \{1/X - 2X/[(\gamma - 1)(1 - X^2)]\}$

Test  $|\phi_1 - \phi| < \epsilon$

If the test fails then calculate

$$X = X + (\phi_1 - \phi) (d\phi/dX)$$

and recalculate  $\phi$  until convergence is reached. Once convergence is reached the inlet conditions are computed by equations (50) through (52).

#### 7. Subroutine TASK1

Subroutine TASK1 computes the nodal tangential blockage factor for the blading of the NASA TASK1 transonic compressor. The value of the blockage factor is determined by

$$b = 1 - t/s$$

(12a)

The values of  $t$  and  $s$  are obtained by approximations to the known blading geometry that are expressed as functions of radius. The maximum thickness of the blade is artificially defined to be at the mid-point of the chordline to ensure that the factor is accounted for in the calculations in the program TURBO. This artificiality could easily be removed through a modification to the axial interpolation scheme used in rotor and stator super elements. Subroutine TASK1 is the only machine dependent subroutine in use in the program and would need to be replaced with an appropriate substitute in order for the program to be used on another machine. The use of the subroutine is omitted if the user does not desire a new mesh.

#### 8. Subroutine FILGEN

Subroutine FILGEN places the computed mesh parameters on disk storage for use in the program TURBO. If the limited mode of operation was selected by the user, the subroutine only updates the values of the parameters that change for a new inlet condition. A listing of the output parameters and their corresponding storage location is given in Appendix B.

#### 9. Subroutine MPLOT

Subroutine MPLOT provides an on-line plot of the computed mesh on the Tektonix 618 graphics terminal. Figure 6 shows the 63 element, 222 node mesh used in the computations of the test cases. The subroutine displayed the mesh through



direct calls to the subroutines of the library plotting package, GRAFF. The subroutine's algorithm is as follows:

Algorithm:

Form two Real\*4 arrays from the information in the r coordinate and the z coordinate arrays for plotting compatibility.

Sort the arrays and plot the streamwise boundaries of the mesh elements.

Sort the arrays and plot the transverse boundaries of the mesh elements.

END

10. Subroutine ERR1

Subroutine ERR1 is called by subroutine INPUT if the storage limitation for Real\*8 variables has been exceeded. The subroutine displays the amount by which the limitation was exceeded and terminates the program's execution. The user response would be to increase the value of LIMR if possible or reduce the size of the mesh.

11. Subroutine ERR2

Subroutine ERR2 is called by subroutine INPUT if the storage limitation for Real\*4 variables has been exceeded. The subroutine displays the amount by which the limitation was exceeded and terminates the program's execution. The user response would be to increase the value of LIM4 if possible or reduce the size of the mesh.

12. Subroutine ERR3

Subroutine ERR3 is called by subroutine INPUT if the storage limitation for Integer\*4 variables has been exceeded.

The subroutine displays the amount by which the limitation was exceeded and terminates the program's execution. The user response would be to increase the value of LIM1 if possible or reduce the size of the mesh.

## V. DESCRIPTION OF PROGRAM TURBO

Program TURBO solves the quasi-harmonic stream function radial equilibrium equation for flow in an axial compressor. The program uses the information computed by the program MESHGEN to calculate the desired thermodynamic information at all nodal points and displays selected values on a graphics terminal for inspection.

### A. MAIN PROGRAM DESCRIPTION

The program obtains a solution of the equation

$$[K]\{\psi\} = \{f\} \quad (32)$$

An iterative scheme was adopted for this nonlinear problem, whereby an estimate of the stream function distribution is used to calculate values of the velocity components and thermodynamic variables at the nodes of the mesh. These computed values are then substituted into Eq. (32) and a new value of the stream function distribution is calculated. The estimate of the distribution is compared to the calculated value to determine if the solution has reached convergence according to the following criterion:

$$\epsilon > \left| \frac{\psi_i^n - \tilde{\psi}_i^{n+1}}{\tilde{\psi}_i^{n+1}} \right| \quad (47)$$

where  $\psi_i^n$  = estimate of  $\psi$  at node  $i$

$\tilde{\psi}_i^{n+1}$  = solution for  $\psi$  at node  $i$

If the maximum difference for all nodes is less than  $\epsilon$ , the procedure is terminated. If the maximum difference exceeds some specified value of  $\epsilon$ , the new estimate of  $\psi$  to be used for the next iteration is determined using

$$\psi_i^{n+1} = \psi_i^n + \alpha [\tilde{\psi}_i^{n+1} - \psi_i^n] \quad (48)$$

where  $\psi_i^{n+1}$  = new estimate of  $\psi$  for the next iteration

$\alpha$  = under relaxation factor required for convergence because of the strong nonlinear properties of Eq. (32).

The process of constructing the inputs required for Eq. (32) is repeated until convergence is obtained. The details of calculating the inputs and constructing the stiffness matrix and the right-hand side vector are contained in descriptions of the program's subroutines.

The program's algorithm follows in outline form:

Obtain the computational constants (SUBROUTINE RDATA).

Determine the values of the pointers used to partition the storage arrays (SUBROUTINE INIT1).

Set the initial values for all storage locations to 0.0 or 0 as appropriate (SUBROUTINE ZERO1).

Recall from storage the externally computed input values and initialize the inlet conditions (SUBROUTINE INPUT).

Calculate a velocity and thermodynamic variable distribution based on the assumed stream function distribution and the inlet conditions (SUBROUTINE DIST).

From the distributions obtained in DIST, calculate the right-hand side vector {f} (SUBROUTINE FCAL).

Using the density and blockage factor distributions, form the stiffness matrix [K] (SUBROUTINE STIFF).

Solve the system of linear equations to obtain a new stream function distribution (SUBROUTINE DSIMQ).

Place the solution vector in its proper storage location (SUBROUTINE REPLA).

Compare the original stream function distribution to the solution vector to determine the maximum difference in the distributions for all nodes (SUBROUTINE TEST).

Determine if the convergence criterion has been satisfied.

If convergence has not been obtained, perform the relaxation iteration to update the estimate of the stream function distribution (SUBROUTINE RELAX), prepare for another cycle (SUBROUTINE NOCON), and then return to SUBROUTINE DIST for further calculations.

If the convergence criterion has been satisfied, print the results (SUBROUTINE OUTPUT) and display selected information on the graphics terminal (SUBROUTINE MPLOT).

END

## B. SUBROUTINE DESCRIPTIONS

Sections 1 through 23 provide a detailed description of the subroutines of program TURBO.

### 1. Subroutine RDATA

Subroutine RDATA is used to store the following computational constants:

- (a) Logical Input/Output variable NREAD and NWRITE.
- (b) Relaxation factor.
- (c) Limits for the storage arrays.

- (d) Three-point Gaussian abscissas and weighting values.
- (e) Constants used for conversions between different units.

## 2. Subroutine INIT1

Subroutine INIT1 determines the values of the pointers used to partition the Real\*8, Real\*4, and Integer\*4 arrays and determines whether the storage limitations for any of the arrays has been exceeded. If the storage limitations have been exceeded the subroutine will halt execution by calling the appropriate error subroutine. A listing of the pointers and their corresponding array names is contained in Appendix C.

## 3. Subroutine ZEROI

Subroutine ZEROI sets the initial value of all arrays equal to 0.0 or 0 as appropriate.

## 4. Subroutine INPUT

Subroutine INPUT retrieves required input information from its corresponding disk storage location. The information must be placed in storage before running program TURBO. The usual method of generating the information and placing it in storage is through the use of the program MESHGEN.

Subroutine INPUT also initializes the inlet conditions to their proper values, and modifies the nodal blockage factors to account for end-wall boundary layer effects. No attempt was made to include a global method for calculating the blockage factors; rather, a method similar to the one used by Hirsch and Warzee [Ref. 4] was used. The full method

used by Hirsch and Warzee was to artificially reduce the size of the flow passage by reducing the boundaries of the mesh, followed by the application of a general blockage factor to the nodes of the mesh. In the program TURBO, no mesh modifications are made. The procedure followed was to apply a general blockage factor to all nodes, followed by the application of an additional blockage factor to nodes in the outer elements in the rotor, stator, and the passage in between. Though reasonable results were obtained by this method, the handling of the end-wall boundary layers remains the most obvious weakness in the code. This is addressed specifically in section VII.

#### 5. Subroutine DIST

Subroutine *DIST* calculates the distributions of velocity, density, temperature, pressure, fluid flow angles, entropy, and enthalpy using the known blade and machine geometry, inlet conditions, and the assumed distribution of the stream function. Properties of nodes at the mid-line of the rotor or stator blades were assumed to have a value equal to the average of the inlet and exit conditions of the blade. The elemental calculations are accomplished through the control of subroutines *SLINE*, *DUCT*, *ROTO*, and *STAT*.

The following is the subroutine *DIST*'s algorithm in outline form:

For each element in the mesh.

Determine type element for appropriate computations.

### Duct Elements

For each node at stations 2 and 3:

Determine the location of the streamline and thermodynamic conditions at station one (Subroutine SLINE).

(If the element is along the machine exit plane, ensure that  $(\partial\psi/\partial z) = 0$ .)

Compute the thermodynamic conditions (Subroutine DUCT).

Assign the appropriate values to the proper storage location.

### Rotor Elements

For each node at stations 1:

Determine the location of the streamline at station 3 and the  $\partial\psi/\partial z$  and the  $\partial\psi/\partial r$  at stations 1 and 3 (Subroutine SLINE).

Determine the inlet and outlet relative flow angles and the outlet absolute flow angle.

Compute the total-to-total pressure ratio and the adiabatic efficiency for the streamline (Subroutine ROTO).

Assign the appropriate values to the proper storage location.

For each node at stations 2:

Determine the location of the streamline and the thermodynamic conditions and the  $\partial\psi/\partial z$  and the  $\partial\psi/\partial r$  at stations 1 (Subroutine SLINE).

Determine the location of the streamline and the  $\partial\psi/\partial z$  and the  $\partial\psi/\partial r$  at station 3 (Subroutine SLINE).

Determine the inlet and outlet relative flow angles and the outlet absolute flow angle and the relative deviation angle.

Compute the thermodynamic conditions at station 3 (Subroutine ROTO).

Compute the value of all properties for the node as being the average of the values at station 1 and station 3.



Assign the appropriate values to the proper storage location.

For each node at stations 3:

Determine the location of the streamline and thermodynamic conditions at station 1 and the value of  $\partial\psi/\partial z$  and  $\partial\psi/\partial r$  at stations 1 and 3 (Subroutine SLINE).

Determine the inlet and outlet relative flow angles and the outlet absolute flow angle and compute the thermodynamic conditions (Subroutine ROTO).

Assign the appropriate values to the proper storage location.

#### Stator Elements

The stator algorithm is the same as the rotor algorithm except the outlet absolute flow angle is the only angle calculated. The inlet absolute flow angle is determined through interpolation.

#### 6. Subroutine SLINE

In order to understand the functioning of this subroutine and others to follow, one must refer to the nomenclature used to describe the eight-node element. Figures 2 and 3 show the nomenclature clearly and Table 1 demonstrates the connectivity. All of the calculations in the program for the distributions of velocity, flow angles, and thermodynamic properties are founded on the assumption that the points in question lie on the same stream surface. Thus the objective of the subroutine is to obtain the location of a given value of the stream function at a specified station in the flow region. The location of the streamline is required in order to compute the variables used in  $\{K\}$  and  $\{f\}$ .

Through the application of the boundary conditions, the nodes along the shroud are defined to lie on one stream surface and the nodes along the hub are on another. It is possible for all other nodes in the mesh to be on different stream surfaces. For these nodes an interpolation scheme must be followed to find the  $(\xi, \eta)$  coordinates of a specified stream surface at a given station in the mesh.

The solution sequence that the program follows starts at the top element of the first column of elements in the mesh and solves the thermodynamic and velocity conditions for all nodes in the element using the assumed stream function distribution and the specified inlet conditions. When the calculations for the first element are complete, the program continues down the column until the calculations are complete for the element along the hub. The program then sequences to the top element for the next column and continues until the calculations are complete for the last element in the mesh. In this sequence it is always possible to calculate the conditions at station 1 of an element for any interim nodal values of the stream function.

The process will be described by way of an example for one node as shown in Fig. 3.

Example: Find the  $(\xi, \eta)$  coordinates of the streamline that passes through node 7 of element 1, Node (1,7).

From the connectivity relationships it is known that

$$(\text{Node } (1,7)) = (14)$$

The value of (14) is known and the search is begun to find two nodal values of  $\xi$  at station 1 that bracket the desired value, (14). The program first tests to see if (Node (1,7)) is greater than (Node (1,5)). In this case it is not and the program would automatically shift and test to see if (Node (1,7)) is greater than (Node (2,5)). In this example the value is larger and the same test would be applied to (node (2,4)). Again the answer would be true. The program would then test to see if the value of (Node (2,3)) were larger than (Node (1,7)). The answer being true would signal the program that the location of the streamline had been bracketed and a half-interval technique would be applied to find the location. As shown in Fig. 4, the value of  $\xi$  for all locations along station 1 is -1. This fact is important for two reasons. One, with  $\xi$  known the program is only required to iterate on  $\eta$  to obtain convergence. Two, the Kronecker delta property of the shape functions means that only the shape functions at station 1 have nonzero values [Ref. 16]. For the half interval method, the program uses the average  $\eta$  of the most recent bracketing as its estimate for  $\eta$ . In this example the first estimate of  $\eta$  is equal to 0.5 and the solution for  $\psi$  at (-1., 0.5) can be written as

$$\psi(-1., 0.5) = N_3(-1., 0.5)\psi_3 + N_4(-1., 0.5)\psi_4 + N_5(-1., 0.5)\psi_5$$

The solution is then compared to  $\psi(\text{Node } (1,7))$  to determine if the difference is less than some  $\epsilon$ . If the difference exceeds  $\epsilon$ , the new estimate for  $\eta$  becomes 0.25 or 0.75 depending on whether the solution is larger than or less than the value of  $\psi(\text{Node } (1,7))$ . The process is continued until convergence is reached. Once  $\xi$  and  $\eta$  for the streamline location at station 1 are known, all of the properties for station 1 can be determined. (The same method is used to find the location of the streamline at station 3 for rotor and stator elements.) Having determined the coordinates of streamlines at all desired locations it is possible to calculate the required  $(\partial N_i / \partial r)$  and  $(\partial N_i / \partial z)$ . The computed inlet and exit coordinates and conditions are then passed to subroutine DIST for use in subroutines DUCT, ROTO, and STAT as appropriate for the calculation of the conditions at Node (1,7).

The following is the subroutine's algorithm in outline form:

#### Duct Element

If the node being investigated is on station one, exit the subroutine.

For stations two and three, determine the streamline coordinates and the thermodynamic conditions at station one and compute the  $\partial\psi/\partial z$  and  $\partial\psi/\partial r$  at the node. Exit the subroutine.

#### Rotor/Stator Element

If the node being investigated is on station one, set all inlet thermodynamic variables equal to the corresponding

nodal value and compute the  $\partial\psi/\partial z$  and the  $\partial\psi/\partial r$  at station three. Exit the subroutine.

For station two, determine the streamline coordinates and the thermodynamic conditions at station one and compute the streamline location and the  $\partial\psi/\partial z$  and the  $\partial\psi/\partial r$  at station three. Exit the subroutine.

For station three, determine the streamline coordinates and the thermodynamic conditions at station one and compute the  $\partial\psi/\partial z$  and the  $\partial\psi/\partial r$  at station three. Exit the subroutine.

#### 7. Subroutine DUCT

Subroutine DUCT determines the values of temperature, pressure, and density for the elemental nodes at stations two and three. An iterative procedure is used with the knowledge that angular momentum is a constant in a duct. The initial estimate of the velocity at station 1 is made using the computed values of  $\partial\psi/\partial z$ ,  $\partial\psi/\partial r$ ,  $r$ , and  $b$  at the node (Subroutine SLINE) and by choosing the estimate of the density at the node to be equal to the density at station 1. The following sequence of calculations is repeated until convergence on a value of the exit velocity:

$$V_{m2} = (1/(\rho_2 r_2 b_2)) * [(\partial\psi/\partial z_2)^2 + (\partial\psi/\partial r_2)^2]^{0.5}$$

$$\alpha_2 = \tan^{-1} [(r_1 V_{m1} \tan \alpha_1) / (r_2 V_{m2})]$$

$$T_2 = T_{T1} - (\gamma - 1) / 2 * (V_{m2}^2 (1 + \tan^2 \alpha_2)) / (\gamma R G_c)$$

$$P_2 = P_{T1} (T_2 / T_{T1})^{**} (\gamma / (\gamma - 1))$$

$$\rho_2 = P_2 / (RT_2)$$

$$V_{m2n} = (1/(\rho_2 r_2 b_2)) * [(\partial\psi/\partial z)_2^2 + (\partial\psi/\partial r)_2^2]^{0.5}$$

$$\text{Test if } |V_{m2n} - V_{m2}| < \epsilon$$

The total conditions are then calculated from the static conditions and the computed velocity.

#### 8. Subroutine ROTO

Subroutine ROTO calculates the change in the relative flow angles, the velocity, and the thermodynamic properties along a streamline across a (compressor) rotor element. The program uses the conditions at station one and the location of the streamline and the partial derivatives of the stream function at station 3, all of which were calculated in subroutine SLINE. The relationships in subroutine ROTO are derived from cascade correlations and known property relationships for a streamline in a rotor.

The first step is the calculation of the inlet and exit relative flow angles. For inlet flow without swirl, the relative inlet flow angle can be calculated using

$$\beta_1 = \tan^{-1}(U_1/V_{m1})$$

The incidence angle is calculated using the known blade geometry and inlet angle, since

$$i = \beta_1 - \kappa_1$$

where  $\kappa_1$  is the angle formed between the tangent to the blade chordline and the axial direction. In order to calculate the exit relative flow angle one must determine the deviation angle,  $\delta$ . The program uses the correlations and equations

derived by NASA [Ref. 21]. The specific sequence of equations, using the notation of Ref. 21, is as follows:

$$i_C - i_{2D} = f(M, r)$$

$$i_{2D} = (K_i)_t (K_i)_{SH} (i_0)_{10} + n\phi$$

$$i_{ref} = i_{2D} + (i_C - i_{2D})$$

$$\delta_{2D} = (K_\delta)_t (K_\delta)_{SH} (\delta_0)_{10} + (m/\sigma^b) + (i_C - i_{2D}) (d\delta/di)_{2D}$$

$$\delta_C - \delta_{2D} = f(M_R, r)$$

$$\delta_{ref} = \delta_{2D} + (\delta_C - \delta_{2D})$$

$$\delta = \delta_{ref} + (i - i_{ref}) (d\delta/di)_{2D}$$

$$\beta_2 = \beta_1 - \phi - i + \delta$$

The expressions used to approximate the NASA correlation curves were those obtained by Crouse of NASA Lewis and were provided to the author by Okiishi [Ref. 22].

When the inlet conditions and relative flow angles are known it is possible to determine the conditions at the rotor element exit. The initial exit velocity is obtained in the same way as in subroutine DUCT. The following sequence of equations is solved iteratively until convergence for the exit velocity is reached:

$$\alpha_2 = \tan^{-1} [(\omega r_2 - v_{m2} \tan \beta_2) / v_{m2}]$$

$$D = 1 - (W_2/W_1) + (r_1 W_{u1} - r_2 W_{u2}) / (2 W_1 \bar{r})$$

$$\tilde{\omega} = \text{curve fit to } \tilde{\omega}(D, \cos \beta, \sigma)$$

$$T_{E1} = T_{R1} + \omega^2 (r_2^2 - r_1^2) / \text{constant}$$

$$P_{E1} = P_{T1} (T_{E1} / T_{T1})^{(\gamma/\gamma-1)}$$

$$P_{R1} = P_{T1} (T_{R1} / T_{T1})^{(\gamma/\gamma-1)}$$

$$P_{E2} = P_{E1} - \tilde{\omega} (P_{R1} - P_1)$$

$$W_2 = V_{m2} / \cos \beta_2$$

$$T_2 = T_{E1} - W_2^2 / \text{constant}$$

$$P_2 = P_{E2} (T_2 / T_{E1})^{(\gamma/\gamma-1)}$$

$$\rho_2 = P_2 / (RT_2)$$

$$V_{\min} = (1 / (\rho_2 r_2 b_2)) * [(\partial\psi/\partial z)_2^2 + (\partial\psi/\partial r)_2^2]^{0.5}$$

$$\text{Test if } |V_{\min} - V_{m2}| < \epsilon$$

When convergence is reached the total conditions are calculated from the static conditions and the computed velocity. The value of the entropy change is calculated by:

$$S = R \ln(P_{T2} / P_{T1}) * \text{constant}$$

#### 9. Subroutine STAT

Subroutine STAT calculates the stator element exit absolute flow angle and thermodynamic conditions using the knowledge that the total enthalpy is a constant across the stator. The initial estimate of the exit velocity is obtained in the same way as in subroutine DUCT. The following sequence of equations is used until convergence for the exit velocity is reached:



$$V_1 = [V_{m1}^2 (1 + \tan^2 \alpha_1)]^{0.5}$$

$$D = 1 - (V_2/V_1) + (r_1 V_{u1} - r_2 V_{u2}) / (2 \sigma V \bar{r})$$

$$\tilde{\omega} = \text{curve fit to } \omega(D, \cos \beta, \sigma)$$

$$P_{T2} = P_{T1} - \tilde{\omega}(P_{T1} - P_1)$$

$$T_2 = T_{T1} - (\gamma - 1) / 2 * (V_{m2}^2 (1 + \tan^2 \alpha_2)) / (\gamma R G)$$

$$P_2 = P_{T2} (T_2 / T_{T2})^{**} (\gamma / \gamma - 1)$$

$$\rho_2 = P_2 / (R T_2)$$

$$V_{\min} = (1 / (\rho_2 r_2 b_2)) * [(\partial \psi / \partial z)_2^2 + (\partial \psi / \partial r)_2^2]^{0.5}$$

$$\text{Test if } |V_{\min} - V_{m2}| < \epsilon$$

When convergence is reached the total conditions are calculated from the static conditions and the computed velocity. The value of the entropy change is calculated by the same method used by subroutine ROTO.

#### 10. Subroutine FCAL

Subroutine FCAL uses the previously computed distributions of total temperature, entropy, enthalpy, axial velocity, and tangential velocity to compute the right-hand side vector for the global system of equations. In the absolute frame of reference,  $f(r, z)$  can be expressed in the form

$$f(r, z) = (1/V_z) T(\partial s / \partial r) - \partial H / \partial r + (V_u / r) (\partial (r V_u) / \partial r) \quad (20)$$

The value of  $f(r, z)$  within an element is determined using the following relationships:

$$T(z,r) = \sum_i^n N_i(\xi,\eta) T_i$$

$$H(z,r) = \sum_i^n N_i(\xi,\eta) H_i$$

$$s(z,r) = \sum_i^n N_i(\xi,\eta) s_i$$

$$V(z,r) = \sum_i^n N_i(\xi,\eta) V_i$$

$$V(z,r) = \sum_i^n N_i(\xi,\eta) V_i$$

$$r = \sum_i^n N_i(\xi,\eta) r_i$$

where the value of  $N_i(\xi,\eta)$  is determined by the value of  $\xi$  and  $\eta$  for a specified Gaussian integration point within the element. The required partial derivatives are found in a simple and direct way. To illustrate, the  $(\partial H/\partial r)$  is derived as follows:

$$H(z,r) = \sum_i^n N_i H_i$$

$$(\partial H/\partial r) = \sum_i^n (\partial N_i/\partial r) H_i + \sum_i^n N_i (\partial H_i/\partial r)$$

and since  $H_i$  is a constant then

$$\partial H/\partial r = \sum_i^n (\partial N_i/\partial r) H_i$$

where  $(\partial N_i/\partial r)$  is found by Eq. (37), and  $H_i$  is the appropriate nodal value of  $H$ . The radial variations in entropy and angular momentum are found in the same manner. The same procedure is followed for the values of rothalpy and relative tangential velocity for rotor elements.

It is now possible to calculate the quantities in the expression for the right-hand side vector at a point. All that remains is to apply an integration technique to

obtain the value over an element and to assemble the resulting local contributions into the global equations. As shown in section III.D.2, the local contribution for node  $i$  in an element can be expressed as:

$$f_i^e = \sum_j \sum_k W_j W_k \sum_i N_i \sum_\ell N_\ell f_\ell |J| \quad (47)$$

In the program Eq. (47) is modified to

$$f_i^e = \sum_m^9 W_m \sum_i^n N_i \sum_k^n N_k f_k |J|$$

where the Gaussian abscissas and the corresponding product of the weight functions are grouped into three one-dimensional arrays. At the completion of the summing process, the local contribution for  $f$  has been calculated for each node in the element. The global system is then updated by adding the local contributions to the global values through the use of the connectivity relationships.

The following is the subroutine's algorithm in outline form:

**Algorithm:**

Iterate for each element in the mesh.

Iterate for each Gaussian point.

Find shape functions,  $|J|$ , and  $[J]^{-1}$ .

Find  $V_z$ ,  $T_T$ ,  $V_u$ ,  $r$ ,  $rV_u$ ,  $(\partial s/\partial r)$ , and  $(\partial H/\partial r)$ .

Compute the contributions of the value  $f$  at the Gauss point to the value of  $f$  at each node of the element.

Upon completion of the Gaussian integration, add the local contribution to the global system.

END

The same algorithm is followed for rotor elements with the appropriate substitutions of  $H_R$  and  $W_u$ .

#### 11. Subroutine STIFF

Subroutine STIFF uses the computed distributions of density and blockage factors to form the stiffness matrix for the global system of equations. It was shown earlier that the contribution to the elemental stiffness is expressed as

$$k_{ij}^e = \int_E k(r,z) [(\partial N_j / \partial r)(\partial N_i / \partial r) + (\partial N_j / \partial z)(\partial N_i / \partial z)] d\Omega \quad (31a)$$

$$\text{where} \quad k(r,z) = (1/\rho r b) \quad (19)$$

Again, the elemental properties are considered to have a polynomial variation of the form

$$\rho(z,r) = \sum_i^n N_i \rho_i, \quad r_i = \sum_i^n N_i r_i, \quad \text{and} \quad b(z,r) = \sum_i^n N_i b_i$$

As shown earlier, Eq. (31a) can be converted by the Gauss-Legendre method to

$$k_{ij}^e = \sum_{k\lambda} W_k W_\lambda \sum_m^n N_m k_m ([B]^T [B]) |J| \quad (46)$$

The value of  $k_m$  is determined from the definitions of  $\rho$ ,  $b$ , and  $r$  by the same methods used in subroutine FCAL. The evaluation of  $[B]^T [B]$  is a simple matter to perform. The

matrix [B] is simply the column vector  $\{(\partial N_i/\partial z), (\partial N_i/\partial r)\}$ . Therefore,  $[B]^T[B]$  can be written  $\{(\partial N_i/\partial r)(\partial N_j/\partial r) + (\partial N_i/\partial z)(\partial N_j/\partial z)\}$ . The value of  $(\partial N_i/\partial z)$  and  $(\partial N_i/\partial r)$  is found for all nodes in the element in one step through the use of subroutine JACOB. The matrix product can be evaluated at a point (z,r) as

$$\sum_i^n \sum_j^n [(\partial N_i/\partial r)(\partial N_j/\partial r) + (\partial N_i/\partial z)(\partial N_j/\partial z)]$$

By using the same Gaussian weighting scheme used in subroutine FCAL, Eq. (46) may be written in the form

$$k_{ij}^e = \sum_k^9 W_k \sum_\ell^n N_\ell k_\ell \sum_{ij}^{nn} [(\partial N_i/\partial r)(\partial N_j/\partial r) + (\partial N_i/\partial z)(\partial N_j/\partial z)] |J|$$

The resulting 8x8 elemental matrix is then added to the global stiffness matrix through the connectivity relationships.

Up to this point [K] and {f} have been assembled without regard to the boundary conditions except at the exit plane where the  $(\partial\psi/\partial n) = 0$  was enforced explicitly during the procedures used by Subroutine DIST. Care must be taken to ensure that the boundary conditions for the other three segments of the boundary are not violated. As shown in section III.B, the boundary condition for the nodes along the shroud, along the hub and at the inlet plane of the machine is that the value of  $\psi$  is specified. If the value of  $\psi$  is specified at these locations the Eq. (32) must be modified so that  $\psi$  is no longer free at these nodes. A standard technique is

employed to remove individual equations from a system of equations when the degree of freedom represented by the individual equations has been removed.

The following is the subroutine's algorithm in outline form:

Algorithm:

Iterate for each element in the mesh.

Iterate for each Gaussian point.

Find shape functions,  $|J|$ , and  $[J]^{-1}$ .

Find the value of  $k$  at the Gauss point.

Compute the elemental stiffness matrix.

Upon completion of the Gaussian integration, add the local contribution to the global system.

Upon completion of the addition of the last element's contribution, modify the system of equations to include the boundary conditions.

END

12. Subroutine DSIMQ

Subroutine DSIMQ is a non-IMSL library, double precision subroutine that solves a set of  $n$  simultaneous equations of the form

$$[A]\{X\} = \{B\}$$

where  $[A]$  is an  $n \times n$  matrix

$\{X\}$  and  $\{B\}$  are  $n \times 1$  vectors.

13. Subroutine REPLA

Subroutine REPLA places the solution vector obtained from subroutine DSIMQ into its proper storage location.

#### 14. Subroutine TEST

Subroutine TEST determines the maximum difference in the assumed nodal distribution of the stream function at the beginning of an iteration to the solution of the radial equilibrium equation calculated using the assumed distribution. The difference in the distributions at a node is defined as

$$\text{Diff} = \left| \left[ \frac{\psi_i^n - \tilde{\psi}_i^{n+1}}{\tilde{\psi}_i^{n+1}} \right] \right|$$

where  $\psi_i^n$  is the assumed value at node  $i$  and  $\tilde{\psi}^{n+1}$  is the calculated value for node  $i$ . Convergence is considered to be reached when the maximum difference for any node is less than a selected reference value,  $\epsilon$ .

#### 15. Subroutine RELAX

Subroutine RELAX performs the relaxation scheme to obtain an updated estimate of the stream function distribution for the next program iteration. The new estimate for stream function distribution is calculated as follows:

$$\psi_i^{n+1} = \psi_i^n + \alpha \left[ \tilde{\psi}_i^{n+1} - \psi_i^n \right] \quad (48)$$

#### 16. Subroutine NOCON

Subroutine NOCON prepares the program for the next iteration by setting the elements of the right-hand side vector,  $\{f\}$ , and the stiffness matrix,  $[K]$ , equal to zero.

## 17. Subroutine OUTPUT

Subroutine OUTPUT prints the computed nodal values of a majority of the velocities and thermodynamic properties. A listing of the values that are printed and the corresponding units is contained in Appendix D. A sample output listing is contained in Appendix G.

## 18. Subroutine MPLOT

Subroutine MPLOT uses the Tektronix 618 terminal to make an online graphical presentation of selected variables at the rotor inlet, rotor outlet, stator inlet and the stator outlet. Figures 7 through 20 provide examples of the plots available for display to the individual on request. The user is given the option of terminating the plotting sequence at any stage of the presentation through the use of interactive prompts.

The following is the subroutine's algorithm in outline form:

### Algorithm:

Convert the appropriate variables to Real 4 for compatibility with the library plotting package GRAFF.

Determine the values of axial velocity, relative flow angles, total-to-total pressure ratio, and the adiabatic efficiency for the rotor inlet, display if requested.

Determine the values of axial velocity, and relative, absolute, and deviation angles for the rotor exit, display if requested.

Determine the values of axial velocity, absolute flow angles, and total-to-total pressure ratio for the stator inlet, display if requested.



Determine the values of axial velocity, and absolute and deviation angles for the stator exit, display if requested.

END

19. Subroutine SHAPE

Subroutine SHAPE calculates the eight nodal shape functions for a given point  $(\xi, \eta)$ . The equations for the nodal shape functions are:

$$N(1) = (\xi\eta + \xi^2 + \eta^2 + \xi^2\eta + \xi\eta^2 - 1)/4$$

$$N(2) = (1 + \eta - \xi^2 - \xi^2\eta)/2$$

$$N(3) = (-\xi\eta + \xi^2 + \eta^2 + \xi^2\eta - \xi\eta^2 - 1)/4$$

$$N(4) = (1 - \eta^2 - \xi + \xi\eta^2)/2$$

$$N(5) = (\xi\eta + \xi^2 + \eta^2 - \xi^2\eta - \xi\eta^2 - 1)/4$$

$$N(6) = (1 - \eta - \xi^2 + \xi\eta^2)/2$$

$$N(7) = (-\xi\eta + \xi^2 + \eta^2 - \xi^2\eta + \xi\eta^2 - 1)/4$$

$$N(8) = (1 - \eta^2 + \xi - \xi\eta^2 - 1)/2$$

The values of the shape functions are stored in the array SF, and are returned to the calling portion of the program.

20. Subroutine JACOB

Subroutine JACOB computes the partial derivatives of the shape functions with respect to  $\xi$  and  $\eta$  and computes the elements of the Jacobian matrix, [J], for a specific point  $(\xi, \eta)$ . The equations for the partial derivatives were obtained directly from the differentiation of the functions shown in the description of subroutine SHAPE. The arrays D

and E store the values of the  $(\partial N/\partial \xi)$  and  $(\partial N/\partial \eta)$  respectively. The Jacobian matrix is calculated by the following sequence of equations:

$$J(1,1) = (\partial z/\partial \xi) = \sum_i^n (\partial N_i/\partial \xi) z_i$$

$$J(1,2) = (\partial r/\partial \xi) = \sum_i^n (\partial N_i/\partial \xi) r_i$$

$$J(2,1) = (\partial z/\partial \eta) = \sum_i^n (\partial N_i/\partial \eta) z_i$$

$$J(2,2) = (\partial r/\partial \eta) = \sum_i^n (\partial N_i/\partial \eta) r_i$$

Arrays D and E and the Jacobian matrix are returned to the calling location in the program.

#### 21. Subroutine ERR1

Subroutine ERR1 is called by subroutine INPUT if the storage limitation for Real 8 variables has been exceeded. The subroutine displays the amount by which the limitation was exceeded and terminates the program's execution. The user response would be to increase the value of LIMR if possible or reduce the size of the mesh.

#### 22. Subroutine ERR2

Subroutine ERR2 is called by subroutine INPUT if the storage limitation for Real 4 variables has been exceeded. The subroutine displays the amount by which the limitation was exceeded and terminates the program's execution. The

user response would be to increase the value of LIM4 if possible or reduce the size of the mesh.

23. Subroutine ERR3

Subroutine ERR3 is called by subroutine INPUT if the storage limitation for Integer 4 variables has been exceeded. The subroutine displays the amount by which the limitation was exceeded and terminates the program's execution. The user response would be to increase the value of LIM1 if possible or reduce the size of the mesh.

## VI. RESULTS AND DISCUSSION

### A. PROGRAM VERIFICATION

Four operating conditions of the NASA TASK-1 compressor were used to test the capabilities of the programs MESHGEN and TURBO. In all cases the 63 element, 222 node mesh with an under-relaxation factor of 0.24 as recommended by Hirsch and Warzee [Ref. 4] were used. Selected portions of the results obtained are presented in Figs. 7 through 76. The points annotated as "observed values" were obtained from the material published in Refs. 23 and 24. The values attributed to Gavito were obtained from Ref. 8 and those attributed to Hirsch from Ref. 4. A discussion of the predictions for the various conditions are presented in the sections that follow.

#### 1. Test Case 1

For test case 1 the operating point was defined as a rotor speed of 50% design speed and an inlet mass flow rate of 107.6 lbm/sec. The author was unable to locate this specific operating point in Ref. 23 or 24 and must assume that in Ref. 4 the mass flow rate was modified to conform to the end-wall boundary layer scheme described in that reference. Therefore, it was necessary to use the observed values published by Hirsch and Warzee in Figs. 21 through 30. The relative differences found between the present predictions and the reported observations are given in Table 1.

a. Comparison to the Work of Gavito

Figures 21, 22, 23 and 24 compare the results obtained by Gavito with the predictions of the present program. A significant improvement has been obtained at all locations. That this was possible was due in large measure to the solid foundation to the present work provided by Gavito's program and to the excellent documentation given in Ref. 8.

b. Comparison to the Work of Hirsch and Warzee

The predictions of the program TURBO compare quite favorably with those of Hirsch and Warzee. As shown in Figs. 25, 26, 29 and 30 the predictions of the two programs have almost identical average relative errors for the velocity profiles. The predictions of Hirsch and Warzee tend to have better agreement in the rotor and stator tip regions, while the program TURBO has slightly better agreement near the hub. The program TURBO's predictions had a 3.7% and 2.5% average error at the rotor inlet and exit respectively with a maximum error of 4.6% at the inlet and 7.0% at the outlet. The stator inlet velocity predictions had an average relative error of 2.6% and maximum error of 5.8% and the outlet predictions had a 2.0% average error with a maximum error of 6.0%. The prediction of both programs for the velocity profiles show excellent agreement with the observed values.

Hirsch and Warzee's program consistently produced flow angle predictions with closer agreement to the observed

values for the published rotor outlet angles. Though the two programs had the same average errors of  $3.3^\circ$  for the relative flow angles and  $4.8^\circ$  for the absolute flow angles, Hirsch and Warzee's program provided better qualitative distributions. The difference is clearly shown in Figs. 27 and 28.

Hirsch and Warzee did not publish predictions of total pressure ratios or adiabatic efficiencies, so the predictions made by TURBO for these parameters were not presented. It is assumed that no significant differences could have occurred because of the similarity of the results for the velocity profile and flow angles discussed earlier.

## 2. Test Case 2

Because of the apparent modification in the mass flow rate which was assumed in test case 1 and the lack of comparative data for all quantities predicted by the program TURBO, another operating point at 50% design speed was compared. The operating condition for case 2 was defined as a mass flow rate of 114.7 lbm/sec at a speed equal to 50% of design, which corresponded to reading 38 of Ref. 24. The results for case 2 are presented in Figs. 31 through 44, and a summary of the relative differences between the predictions and observations is contained in Table 2.

## 3. Test Case 3

Test case 3 corresponded to reading 45 of Ref. 24, which was defined as a speed equal to 70% design and a mass flow rate of 151.55 lbm/sec. When reviewing the results

presented for this case, one should note the decline in the agreement between the program's predictions and the observed values. It is the author's opinion that the degradation is primarily caused by two factors. The first is the formulation used to compute the meridional velocity change across the rotor and the other is the application of a single blockage factor to all nodes to account for the end-wall boundary layers. Both factors are much more significant at 70% design speed than they were at 50%. At 70% design speed the rotor tip relative Mach number is about 0.94. This would require the program to account for transonic effects at the tip. Second, the mass flow and absolute Mach number of the flow in all regions is significantly higher at 70% design speed. Therefore, it is unlikely that a single blockage factor will work satisfactorily in all regions of the machine. It is hoped that both areas will be addressed in any future work on the program.

The results for test case 3 are presented in Figs. 45 through 58 with the corresponding differences between the predictions and observations summarized in Table 3.

#### 4. Test Case 4

The operating condition of test case 4 was at 80% design speed point with a mass flow rate of 174.54 lbm/sec, corresponding to reading 50 of Ref. 24. Figures 59 through 72 and Table 4 present the results of the program's predictions and comparisons to the observed values. As expected,

and for similar reasons to those cited in test case 3, the agreement between the program's predictions and observed values is significantly poorer than any of the three previous cases.

#### B. POINTS OF INTEREST

The results produced by the program are highly dependent on the value of the general blockage factor used to account for the end-wall boundary layers. This factor influences both the quality, in terms of agreement with observations, and the stability of the solution. Figures 73 through 76 show the axial velocity distributions for the rotor and stator for test case 4 with a blockage factor of 9% instead of the 6% factor used to obtain the results shown in Figs. 59 through 72. A comparison of corresponding velocity profiles clearly demonstrates the factor's pronounced influence on the program's solution. The general blockage factor also has a strong influence on the program's convergence rate. In some cases the factor can cause the program to become oscillatory or even divergent.

For the low speed cases of 50% and 70% design, additional blockage factors had to be applied to the duct element between the rotor and stator tips to obtain accurate results. As shown in the program listing for subroutine INPUT of program TURBO, the factors used for 50% design speed were much higher than the factors used for 70% design speed and that



no additional factors were used for 80% design speed. A global method of calculating the end-wall blockage factor must be incorporated if the program is to become independent of inputs other than physical constants.

The deterioration of the program's predictions with increasing Mach number and its failure to run for test cases with strong supersonic relative velocities at the tip demonstrate the need to provide the program with a method of handling supersonic relative velocities. Hirsch and Warzee [Ref. 15] showed a method of extending the radial equilibrium formulation used in the present code to supersonic flow. They presented comparisons of predictions obtained by this method to observations of the NASA TASK-1 transonic compressor at 100% design speed. The results were impressive and clearly showed that the method is valid for relative velocities in excess of Mach 1.4. It is strongly recommended that the first effort at improving the code be an effort to modify TURBO to include the method shown in Ref. 15.

## VII. CONCLUSIONS AND RECOMMENDATIONS

A computer program based on the finite element technique has been developed and has been verified satisfactorily for computing flows through subsonic axial flow compressor stages. Minor modifications have been suggested to allow transonic stages to be calculated.

The code was written in such a way that it could be readily adapted to compute either turbines or compressors with multiple stages. Before such extensions are attempted however, the following specific recommendations are made to improve the present compressor code.

### A. PROGRAM MESHGEN

1. Incorporate some of the two-dimensional techniques of Adamek [Ref. 25] to improve the efficiency of the code.
2. Review the code to find improvements in storage allocations and computational efficiencies.
3. Modify the program to track the first and last nodes of the rotor and stator as subscripted variables so that the program can be used to generate the appropriate mesh parameters for a multi-stage machine.
4. Convert subroutine MPLOT to the DISPLA system.

### B. PROGRAM TURBO

1. Incorporate a method for the global calculation of the blockage and losses created by the end-wall boundary layers.

2. Convert the storage of [K] and the solution technique for the program to at least a symmetric banded scheme or if possible to a skyline equivalent scheme.
3. Test the program on a variety of machines and operating conditions.
4. Obtain expressions that approximate the NASA correlation curves for 65-series blading.
5. Incorporate methods for the prediction of stall/surge.
6. Take advantage of the modular form of the program and include a variety of correlation techniques as a user selected option.
7. Review the program for improved storage and computational techniques. Specifically, determine ways to take fuller advantage of the dynamic dimensioning scheme [Ref. 16] used by the program.
8. Convert the rotor inlet calculations to allow the value of  $\beta_1$  to have nonzero values so that the program can be extended to multi-stage analysis.
9. Modify the use of the values of the beginning nodes of the rotor and stator to subscripted variables so that the analysis can be extended to multi-stage machines.
10. Convert subroutine MPLOT to the DISPLA system.
11. Develop iterative schemes for calculating the flow angle, the velocity distribution changes and the thermodynamic property changes across a turbine rotor and stator for inclusion in subroutines ROTO and STAT.

## LIST OF REFERENCES

1. Naval Postgraduate School Technical Report NPS-57MA70081A, Computer Program for Prediction of Axial Flow Turbine Performance, by E. Macchi, August 1970.
2. Cirone, R., Computer Evaluation of the On- and Off-Design Performance of an Axial Air Turbine, M.S. Thesis, Naval Postgraduate School, Monterey, California, March 1981.
3. Naval Postgraduate School TPL Technical Note 82-02, Verification of a Single Stage Axial Turbine Performance Prediction Program for the HP 21-MX Computer System, by J. A. Ferguson, May 1982.
4. Hirsch, C., and Warzee, G., "A Finite Element Method for the Axisymmetric Flow Computation in a Turbomachine," International Journal for Numerical Methods in Engineering, v. 10, pp. 93-113, 1976.
5. Adler, D., and Krimerman, Y., "The Numerical Calculation of the Meridional Flow Field in Turbomachines Using the Finite Element Method," Israel Journal of Technology, v. 12, pp. 268-274, 1974.
6. Hirsch, C., and Deconinck, H., Finite Element Methods for Transonic Blade-to-Blade Calculation in Turbomachines, ASME Paper 81-GT-5.
7. Bettencourt, J., Finite Element Analysis Program (FEAP) for Conduction Heat Transfer, Engineer's Thesis, Naval Postgraduate School, Monterey, California, December 1979.
8. Gavito, F. V., The Finite Element Method Applied to Flows in Turbomachines, M.S. Thesis, Naval Postgraduate School, Monterey, California, December 1976.
9. NACA TN2604, A General Theory of Three-dimensional Flow in Subsonic and Supersonic Turbomachines of Axial, Radial, and Mixed Flow Types, by C. H. Wu, 1952.
10. Smith, H. L., "The Radial Equilibrium Equation of Turbomachinery," Transactions of the ASME, Journal of Engineering for Power, v. 88A, pp. 1-12, 1966.

11. Novak, R. A., "Streamline Curvature Computing Procedures for Fluid Flow Problems," Transactions of the ASME, Journal of Engineering for Power, v. 89A, p. 478, 1967.
12. Aeronautical Research Council R&M 3509, A Digital Computer Program for the Through-flow Fluid Mechanics in an Arbitrary Turbomachine Using a Matrix Method, by H. Marsh, 1966.
13. Carleton University, Division of Aerothermodynamics, ME/A 73-1, Axial Flow Compressor Analysis Using a Matrix Method, by W. R. Davis and D. A. J. Miller, 1973.
14. Vavra, M. H., Aero-Thermodynamics and Flow in Turbo-machines, Kriger, 1981.
15. Hirsch, C., and Warzee, G., "A Finite Element Method for Through-flow Calculations in Turbomachines," Transactions of the ASME, Journal of Fluids Engineering, v. 98, pp. 403-422, 1976.
16. Cook, R. D., Concepts and Applications of Finite Element Analysis, pp. 2, 399-401, Wiley, 1981.
17. Huebner, K. H., The Finite Element Method for Engineers, Wiley, 1975.
18. Zienkiewicz, O. C., The Finite Element Method, 3rd Ed., McGraw-Hill, 1977.
19. Kaplan, W., Advanced Calculus, p. 93, Addison-Wesley, 1952.
20. Naval Postgraduate School Technical Report NPS-57Sf74081, Flow Into a Transonic Compressor Rotor, Part 1, Analysis, by R. P. Shreeve, August 1974.
21. NASA SP-36, Aerodynamic Design of Axial Flow Compressors, by NASA Staff, 1965.
22. Okiishi, T. H., private communication, June 1982.
23. NASA CR-72806, Evaluation of Range and Distortion Tolerance for High Mach Number Transonic Fan Stages, Volume 1, by C. C. Koch, K. R. Bilwakesh, and V. L. Doyle, August 1971.
24. NASA CR-72964, Evaluation of Range and Distortion Tolerance for High Mach Number Transonic Fan Stages, Volume 2, by C. C. Koch, K. R. Bilwakesh, and V. L. Doyle, August 1971.

25. Adamek, J. M. An Automatic Mesh Generator Using Two- and Three-dimensional Isoparametric Finite Elements, M.S. Thesis, Naval Postgraduate School, Monterey, California, 1973.

TABLE 1

Connectivity Relationships for Figure Three

<u>Element Number</u>	<u>Local Node Number</u>	<u>Global Number</u>
1	1	12
1	2	8
1	3	1
1	4	2
1	5	3
1	6	9
1	7	14
1	8	13
2	1	14
2	2	9
2	3	3
2	4	4
2	5	5
2	6	10
2	7	16
2	8	15
3	1	16
3	2	10
3	3	5
3	4	6
3	5	7
3	6	11
3	7	18
3	8	17

TABLE 2

Comparison of Program Predictions with NASA Task-1  
Compressor Measurements at 50% Design Speed

	<u>Average Difference</u>	<u>Maximum Difference</u>
Rotor Inlet		
Axial Velocity	4.6%	7.2%
Relative Angles	1.5°	3.1°
Total Pressure Ratio	0.7%	1.4%
Efficiencies	4.3%	11.4%
Rotor Outlet		
Axial Velocity	3.2%	6.7%
Relative Angles	1.6°	2.8°
Absolute Angles	1.5°	4.2°
Deviation Angles	2.2°	3.0°
Stator Inlet		
Axial Velocity	3.4%	6.8%
Absolute Angles	2.5°	4.2°
Total Pressure Ratio	0.3%	1.2%
Stator Outlet		
Axial Velocity	1.7%	5.7%
Absolute Angles	0.6°	1.5°
Deviation Angles	1.4°	2.6°



TABLE 3

Comparison of Program Predictions with NASA Task-1  
Compressor Measurements at 70% Design Speed

	<u>Average Difference</u>	<u>Maximum Difference</u>
Rotor Inlet		
Axial Velocity	4.8%	7.4%
Relative Angles	1.14°	1.8°
Total Pressure Ratio	1.1%	2.0%
Efficiencies	3.2%	4.8%
Rotor Outlet		
Axial Velocity	4.1%	7.4%
Relative Angles	2.0°	3.2°
Absolute Angles	3.6°	5.5°
Deviation Angles	1.6°	3.5°
Stator Inlet		
Axial Velocity	4.0%	8.8%
Absolute Angles	3.9°	5.5°
Total Pressure Ratio	0.5%	2.1%
Stator Outlet		
Axial Velocity	3.6%	7.4%
Absolute Angles	0.6°	1.1°
Deviation Angles	1.5°	2.4°

TABLE 4

Comparison of Program Predictions with NASA Task-1  
Compressor Measurements at 80% Design Speed

	<u>Average Difference</u>	<u>Maximum Difference</u>
Rotor Inlet		
Axial Velocity	7.9%	11.4%
Relative Angles	1.3°	1.5°
Total Pressure Ratio	1.5%	2.5%
Efficiencies	3.1%	7.9%
Rotor Outlet		
Axial Velocity	6.6%	8.9%
Relative Angles	2.9°	5.5°
Absolute Angles	6.8°	8.5°
Deviation Angles	2.4°	4.7°
Stator Inlet		
Axial Velocity	6.9%	13.9%
Absolute Angles	5.6°	7.0°
Total Pressure Ratio	0.9%	3.1%
Stator Outlet		
Axial Velocity	8.0%	20.0%
Absolute Angles	0.8°	1.4°
Deviation Angles	1.5°	2.3°

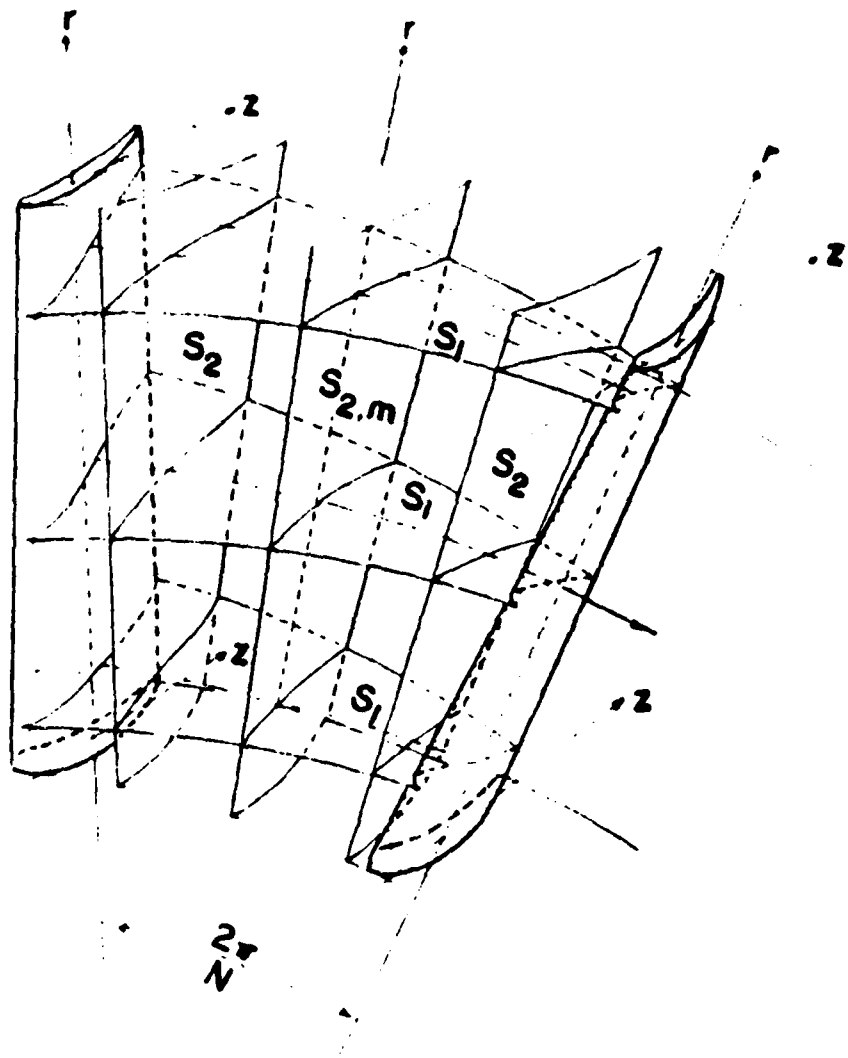


Figure 1. S1 and S2 Stream Surfaces

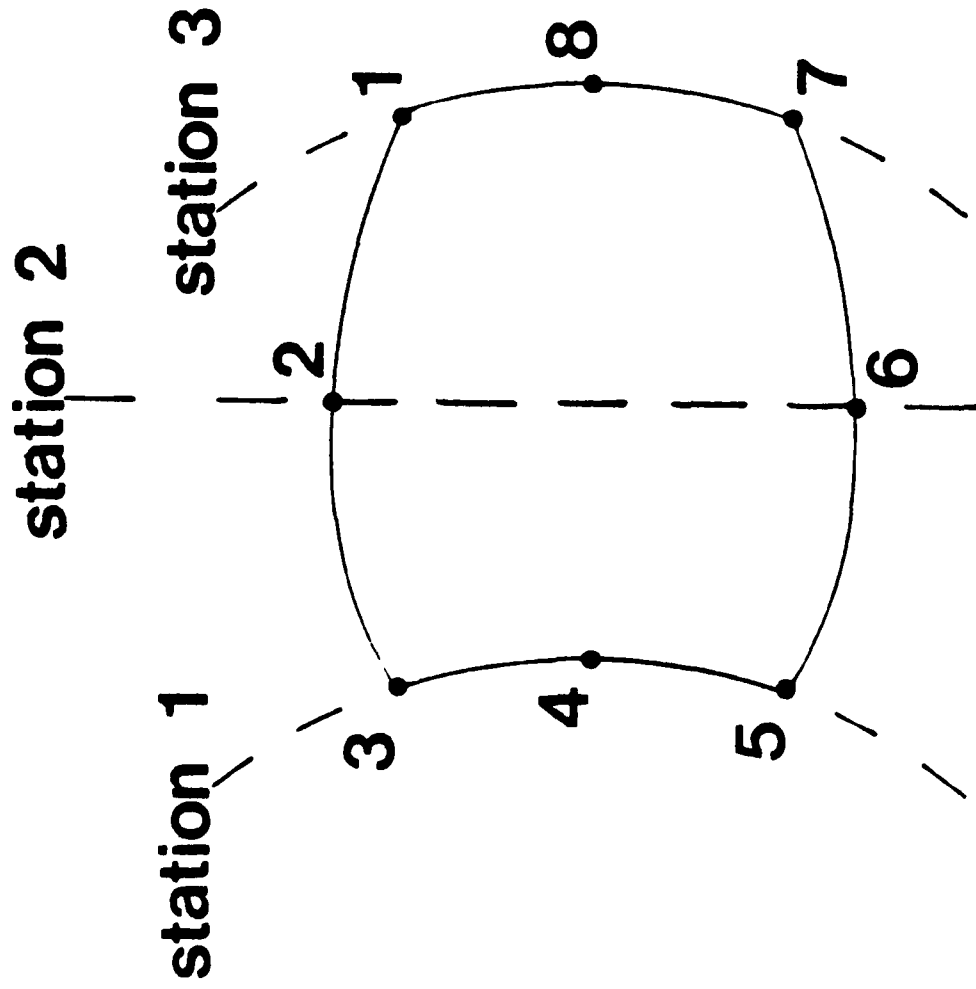


Figure 2. Nomenclature of an Eight-Node Element

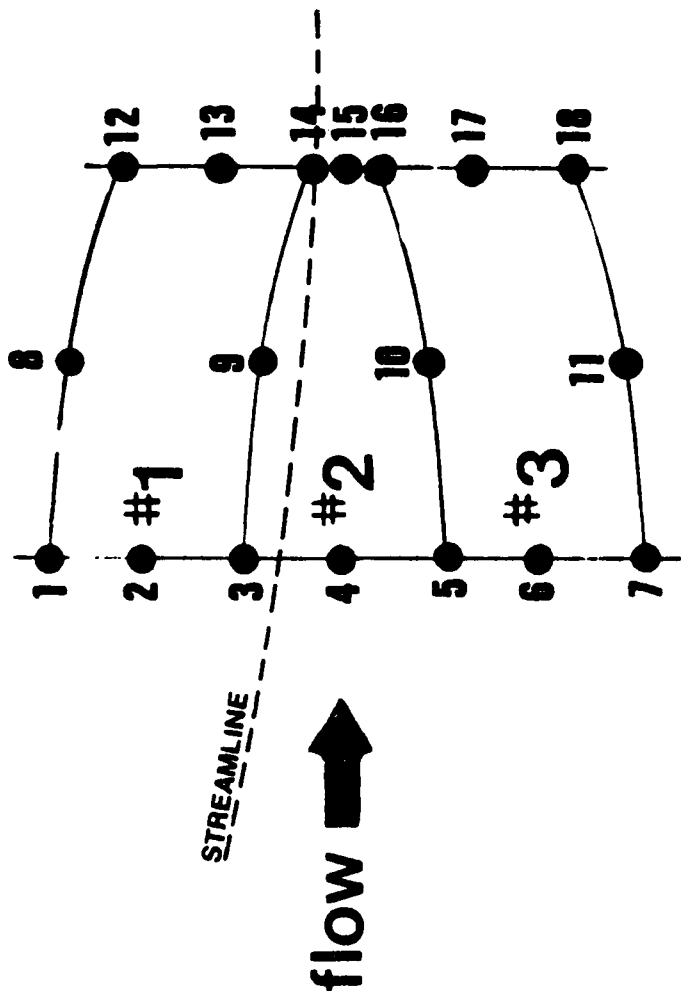


Figure 3. Example of a Three Element Mesh

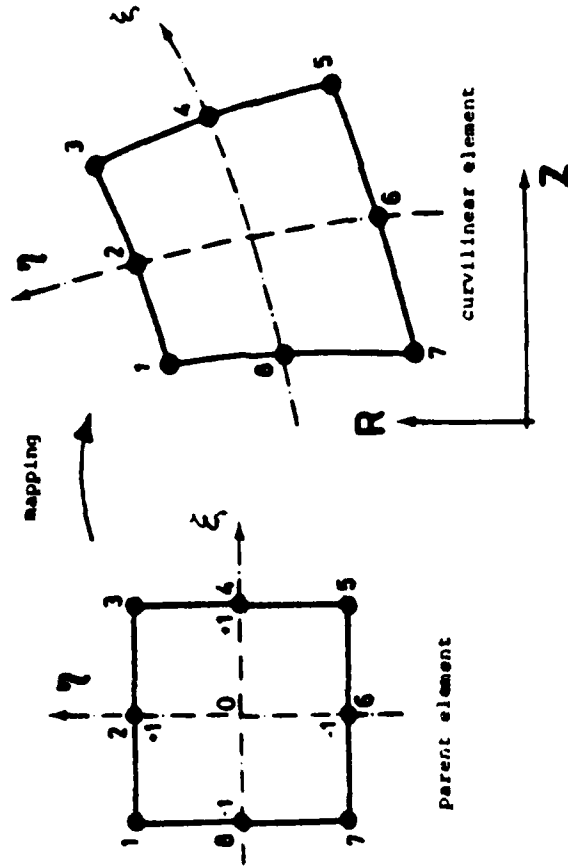


Figure 4. Mapping Relationships from the  $\xi, \eta$  to the  $z, r$  Plane

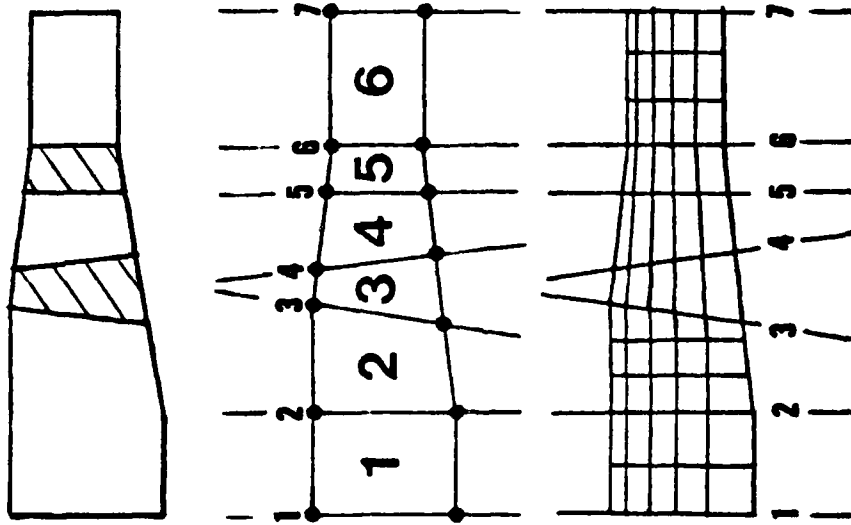


Figure 5. Mesh Generation

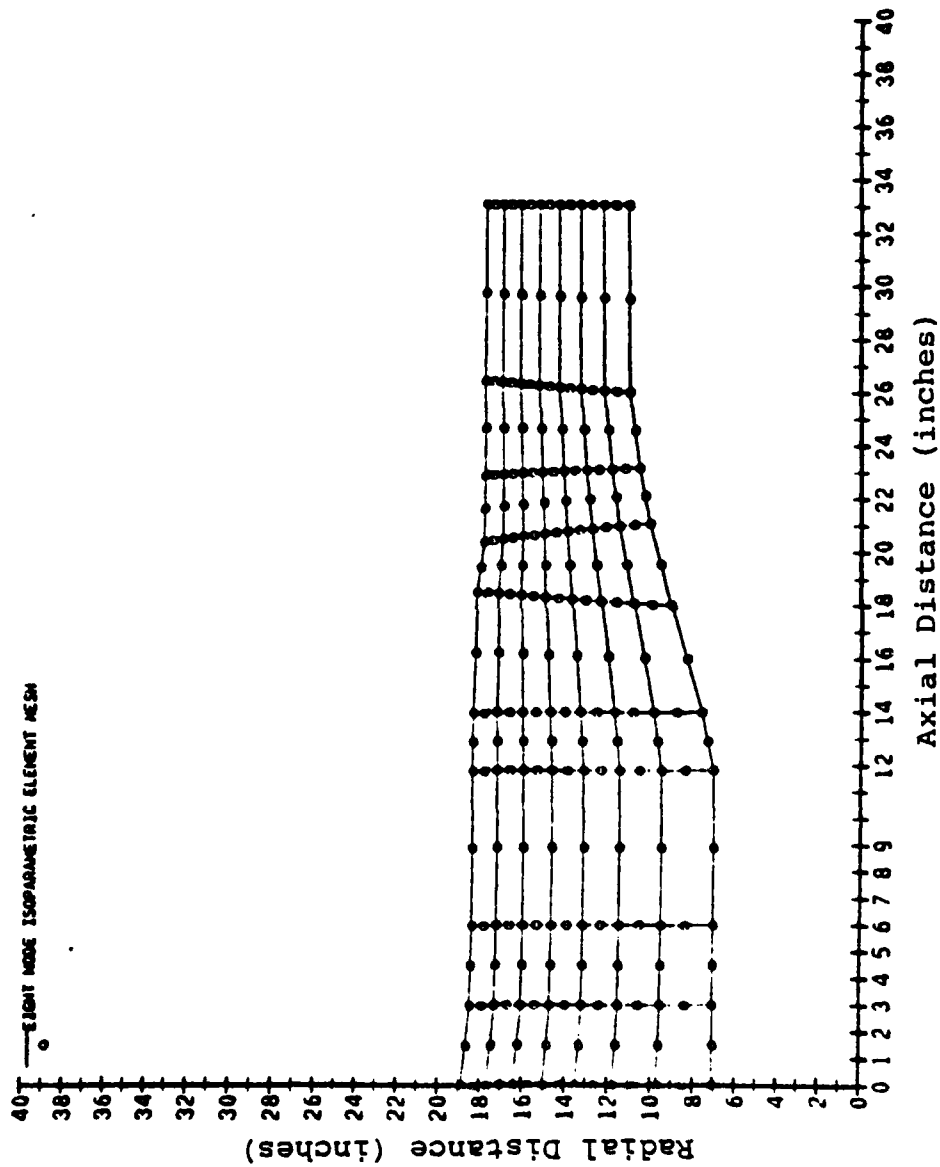


Figure 6. MESHGEN Generated Plot of the 222 Node Mesh Used in the Calculations of the Meridional Through-Flow



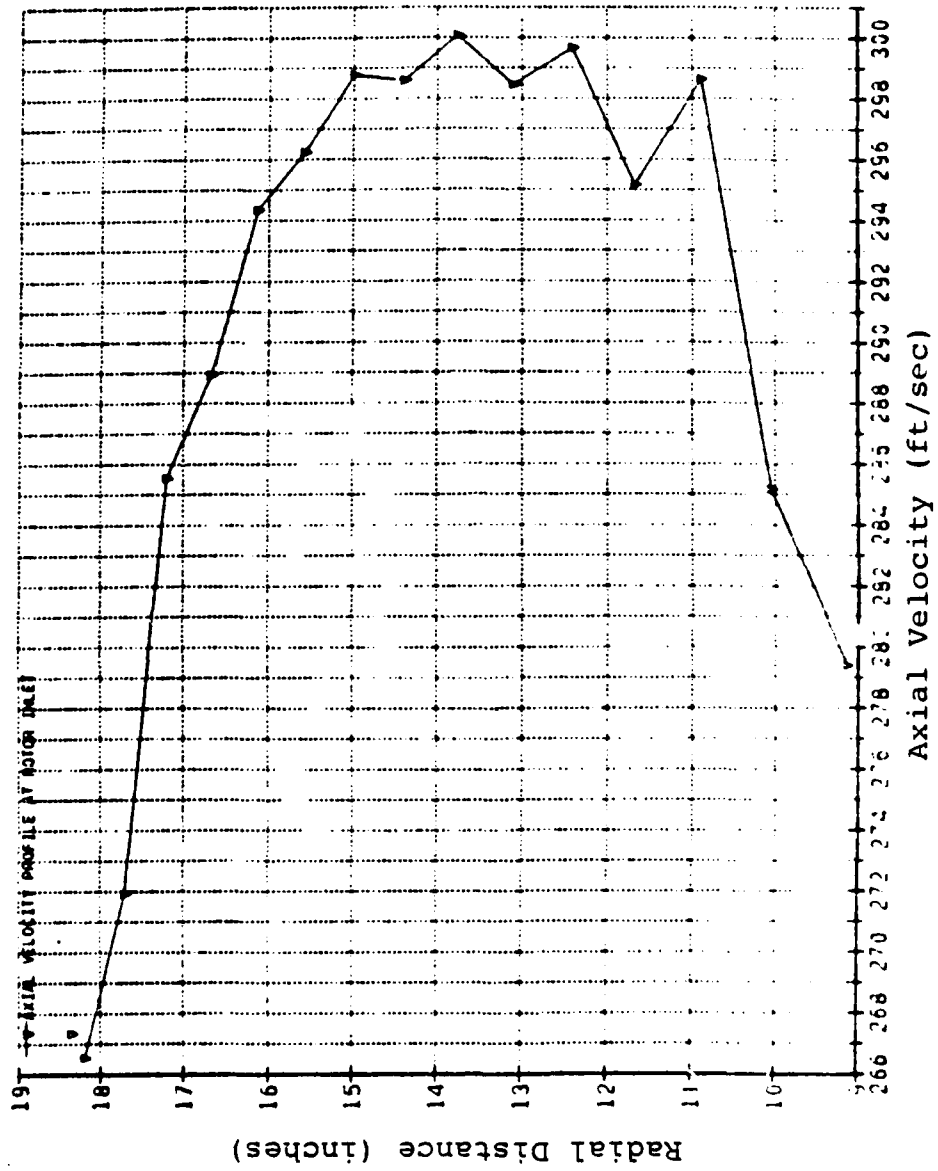


Figure 7. A TURBO Generated Tektonix 618 Plot of the Rotor inlet Axial Velocity at 50% Design Speed

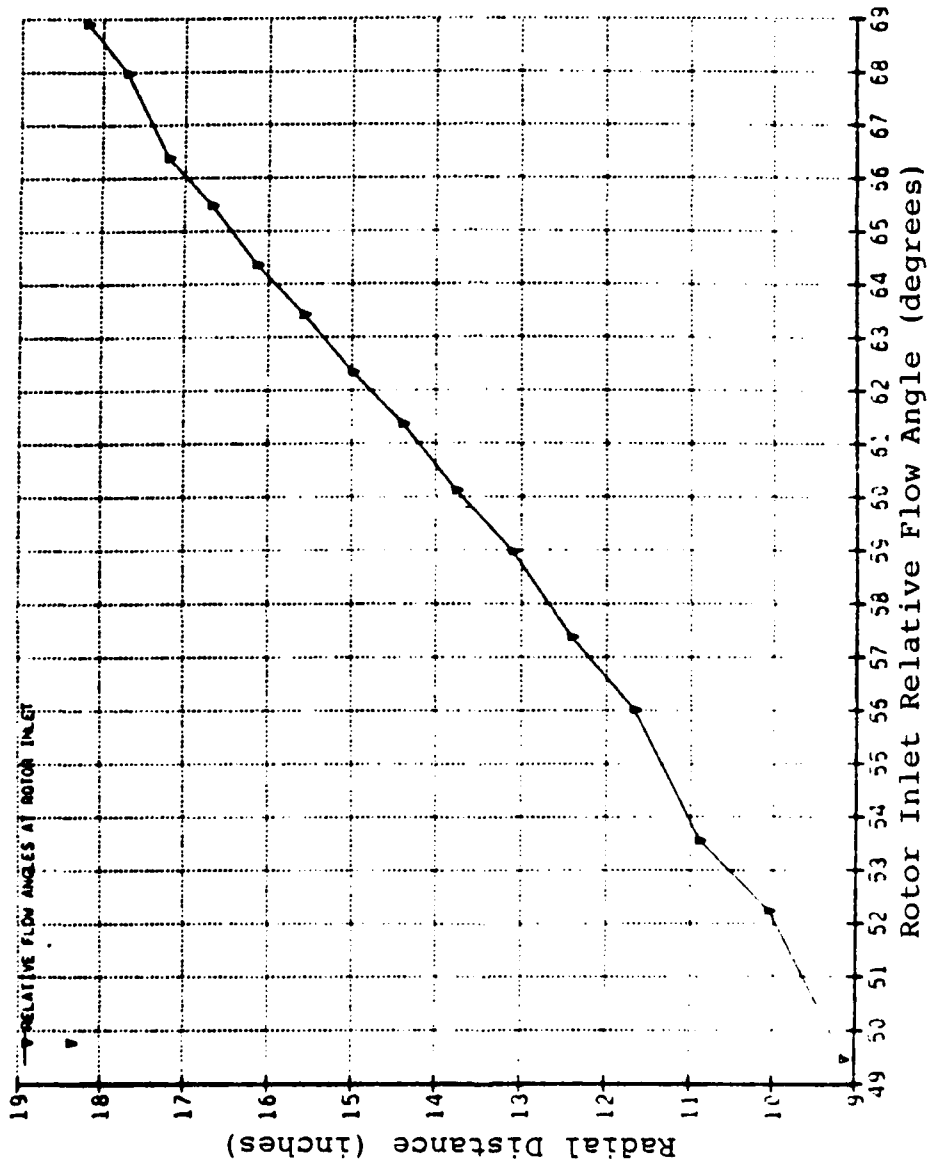


Figure 8. A TURBO Generated Tektonix 618 Plot of the Rotor Inlet Relative Flow Angles

AD-A124 987

FINITE ELEMENT PROGRAM FOR CALCULATING FLOWS IN  
TURBOMACHINES WITH RESULTS FOR NASA TASK-1 COMPRESSOR  
(U) NAVAL POSTGRADUATE SCHOOL MONTEREY CA J A FERGUSON

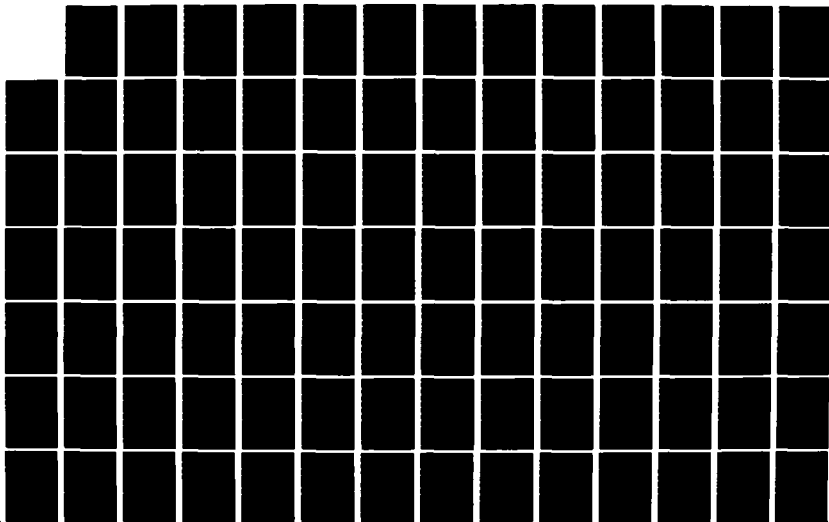
2/3

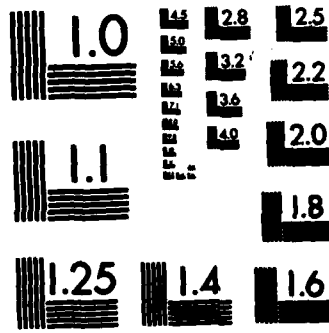
UNCLASSIFIED

OCT 82

F/G 20/4

NL





MICROCOPY RESOLUTION TEST CHART  
NATIONAL BUREAU OF STANDARDS-1963-A

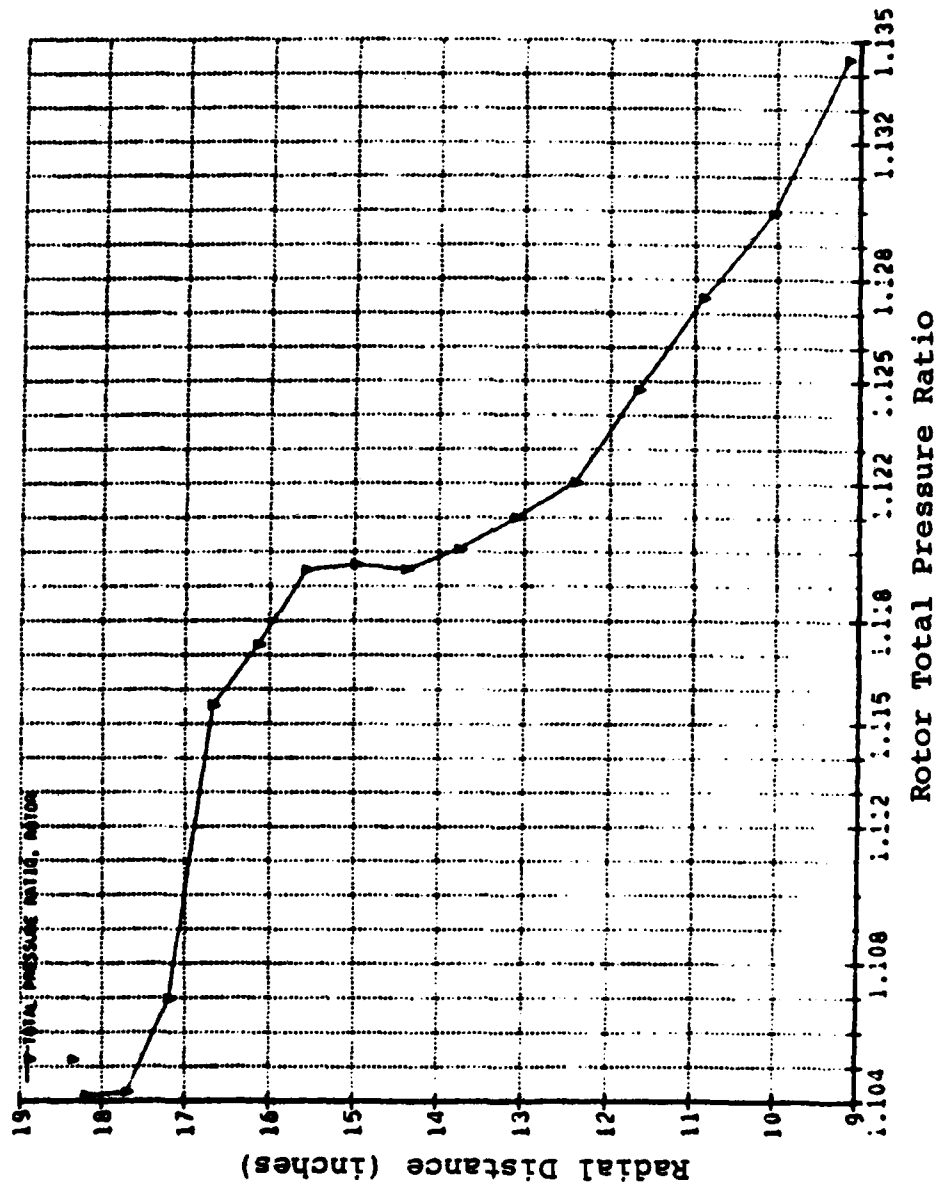


Figure 9. A TURBO Generated Tektonix 618 Plot of the Total Pressure Ratio of the Rotor vs Inlet Radius

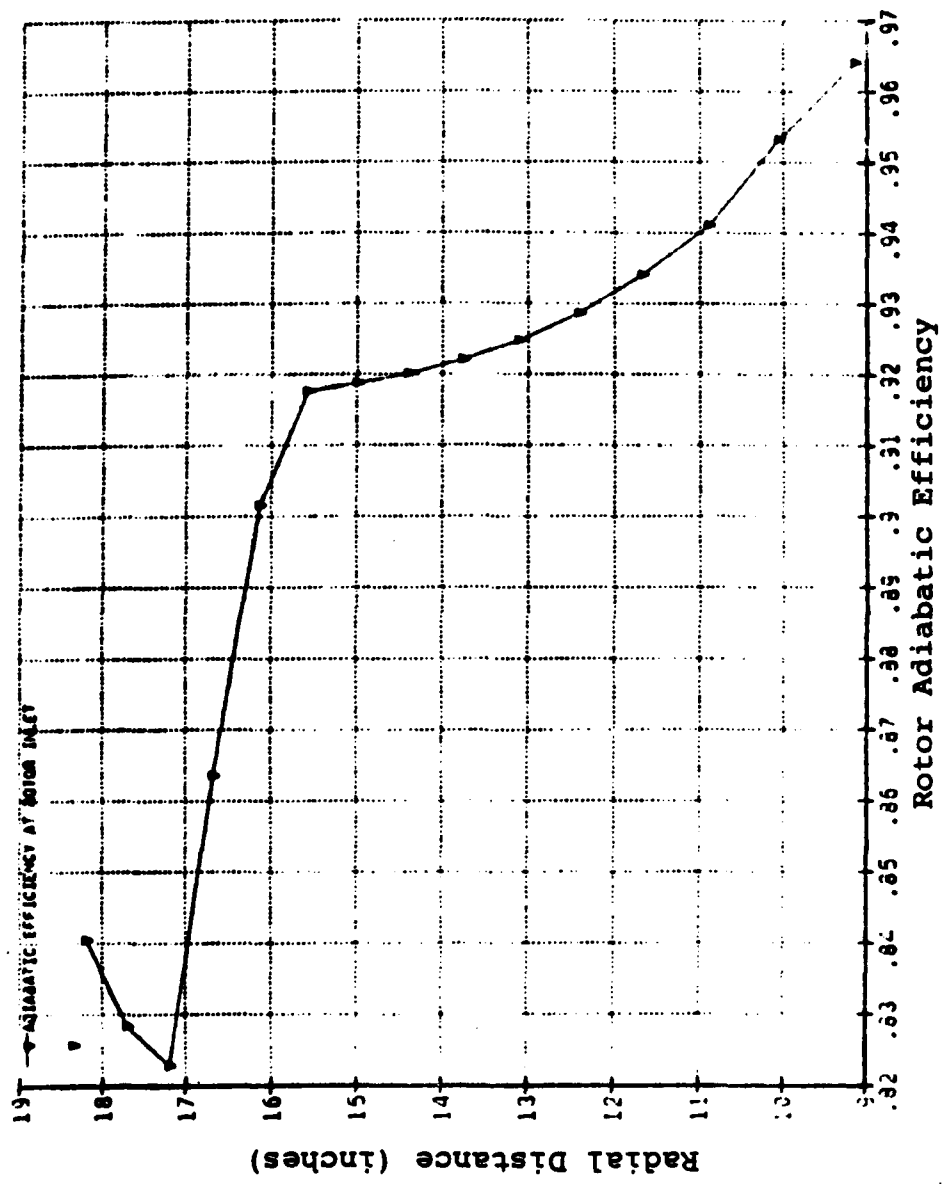


Figure 10. A TURBO Generated Tektonix 618 Plot of the Adiabatic Efficiency of the Rotor vs Inlet Radius

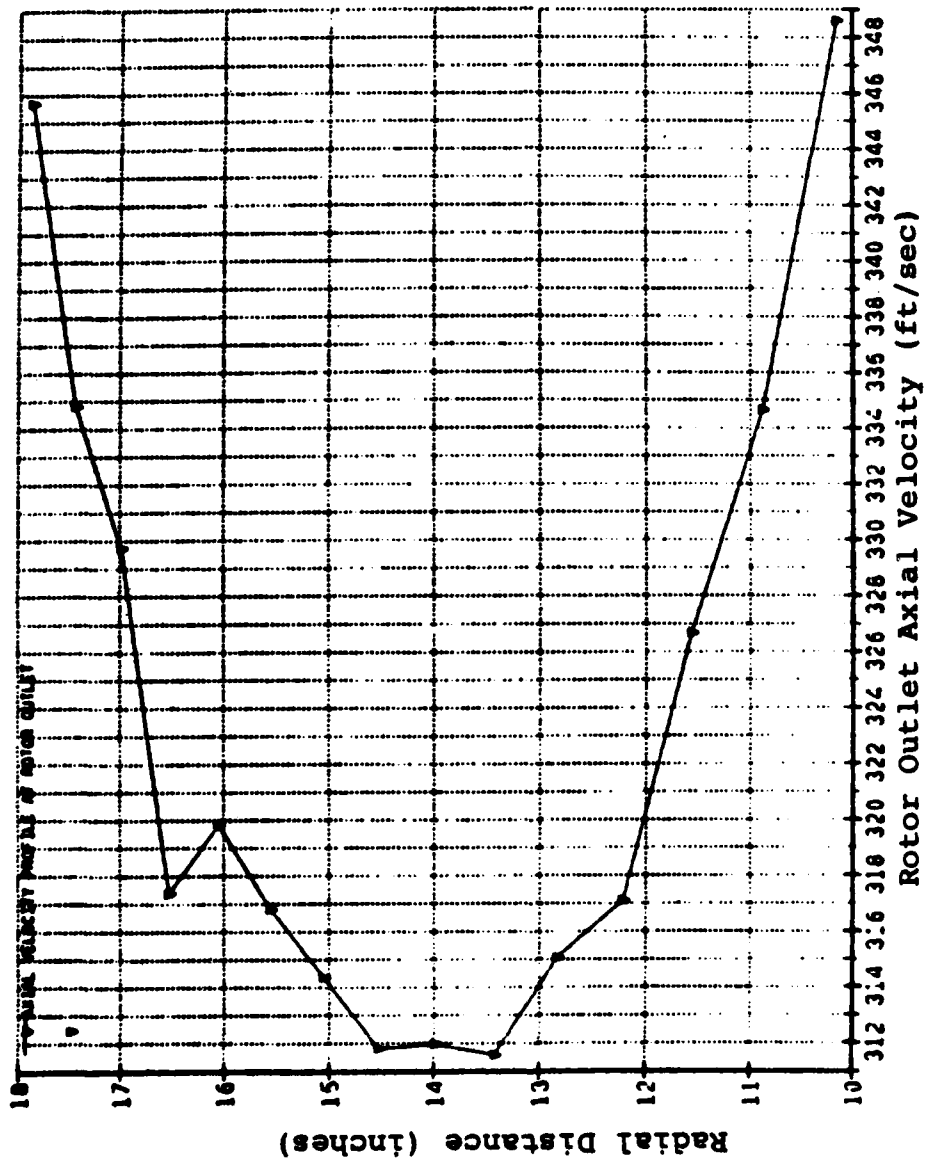


Figure 11. A TURBO Generated Tektonix 618 Plot of the Rotor Outlet Axial Velocity

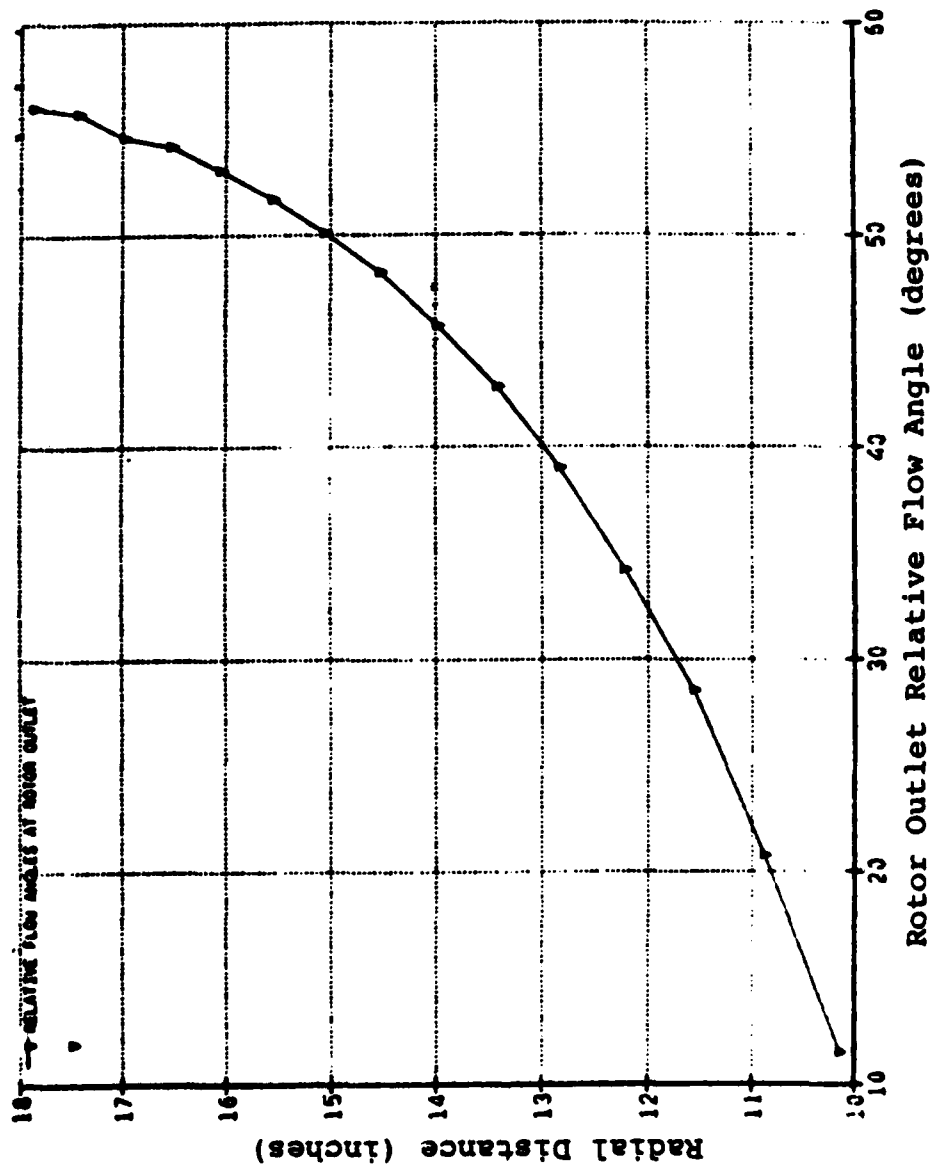


Figure 12. A TURBO Generated Tektonix 618 Plot of the Rotor Outlet Relative Flow Angles



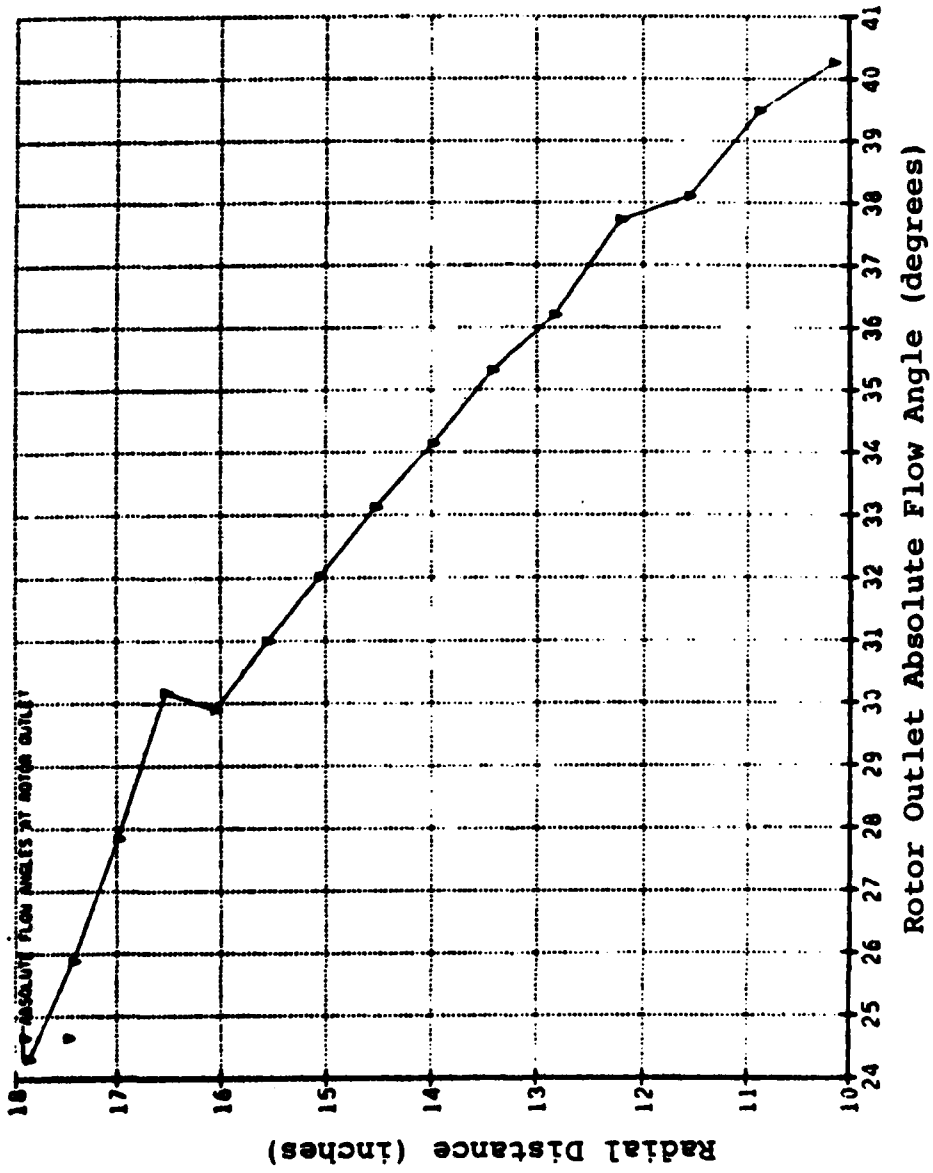


Figure 13. A TURBO Generated Tektonix 618 Plot of the Rotor Outlet Absolute Flow Angles

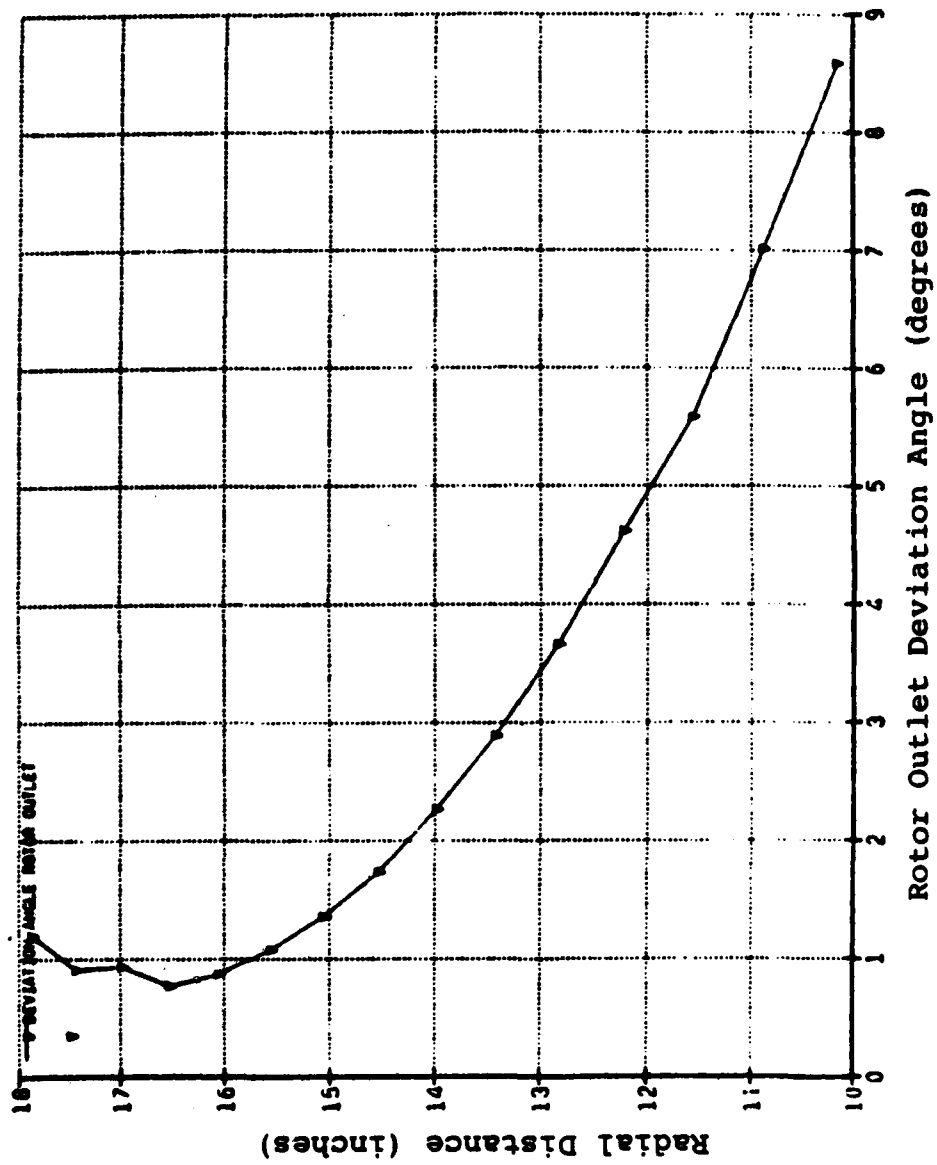


Figure 14. A TURBO Generated Tektonix 618 Plot of the Rotor Outlet Deviation Flow Angles

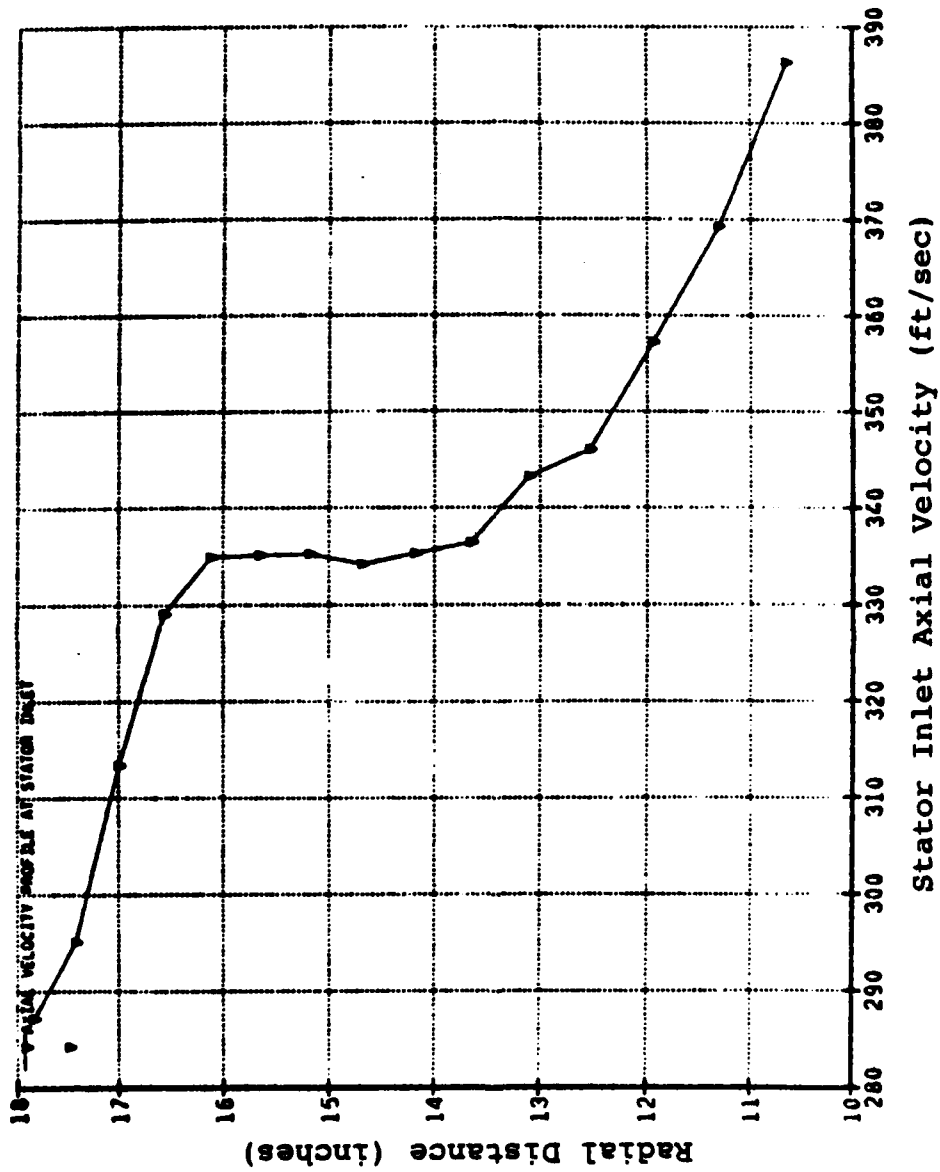


Figure 15. A TURBO Generated Tektonix 618 Plot of the Stator Inlet Axial Velocity

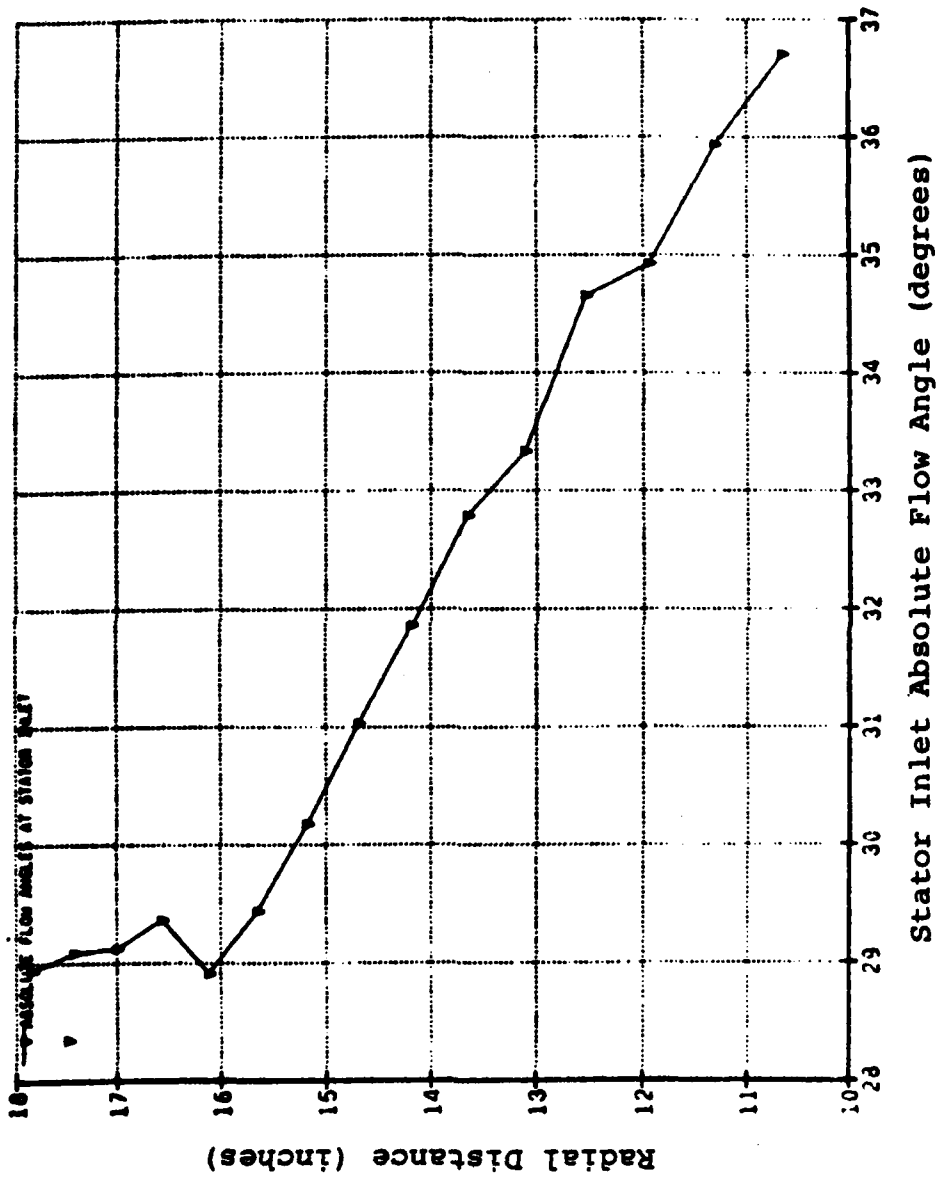


Figure 16. A TURBO Generated Tektonix 618 Plot of the Stator Inlet Absolute Flow Angles

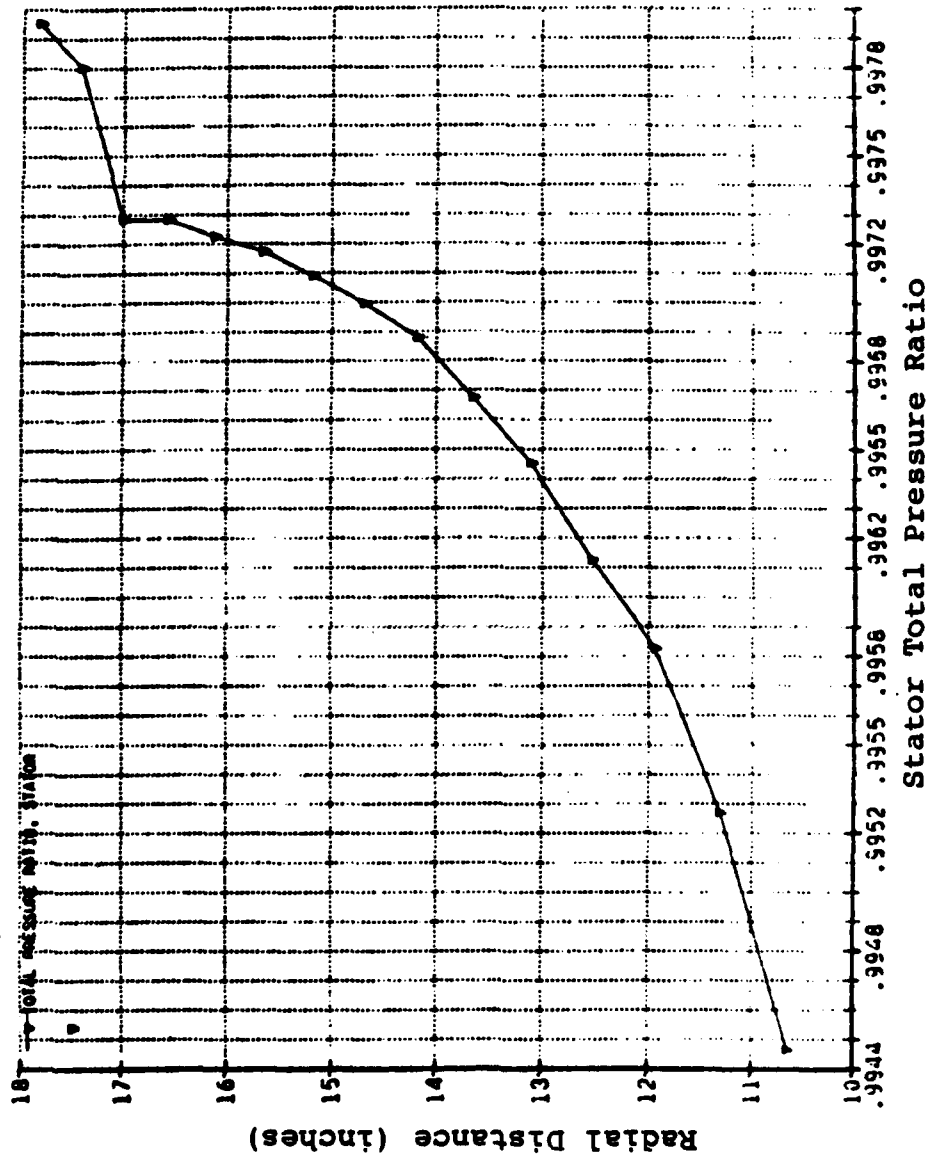


Figure 17. A TURBO Generated Tektonix 618 Plot of the Stator Total Pressure Ratio vs Inlet Radius

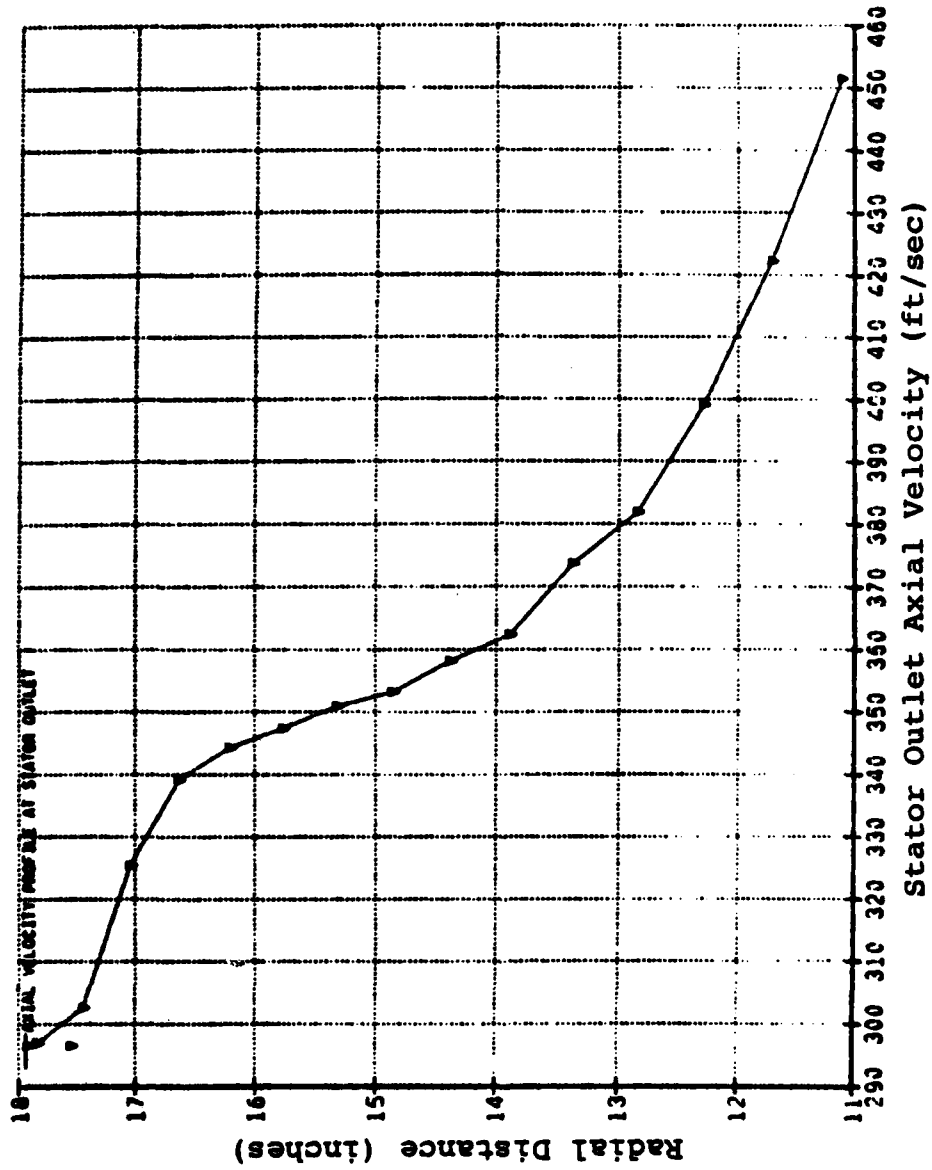


Figure 18. A TURBO Generated Tektonix 618 Plot of the Stator Outlet Axial Velocity

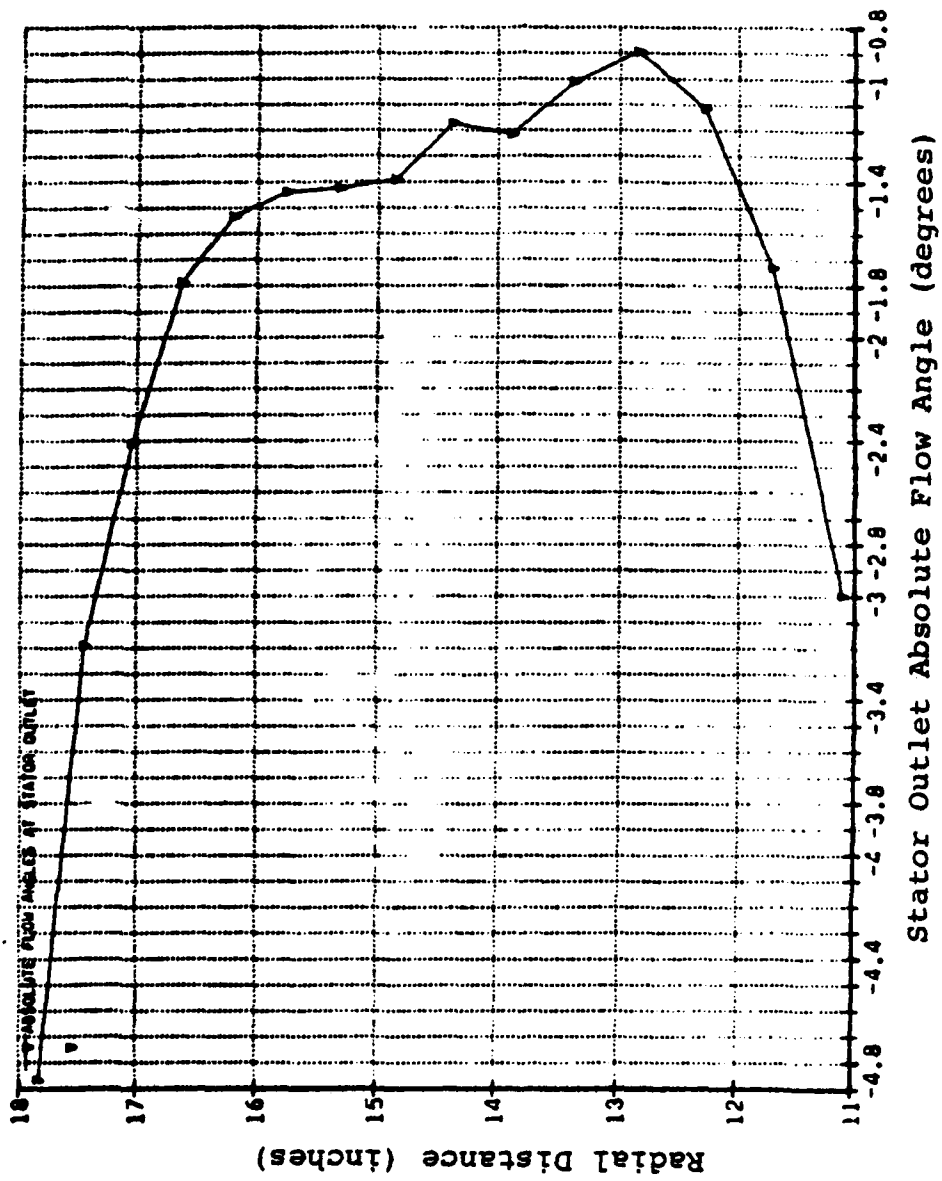


Figure 19. A TURBO Generated Tektonix 618 Plot of the Stator Outlet Absolute Flow Angles

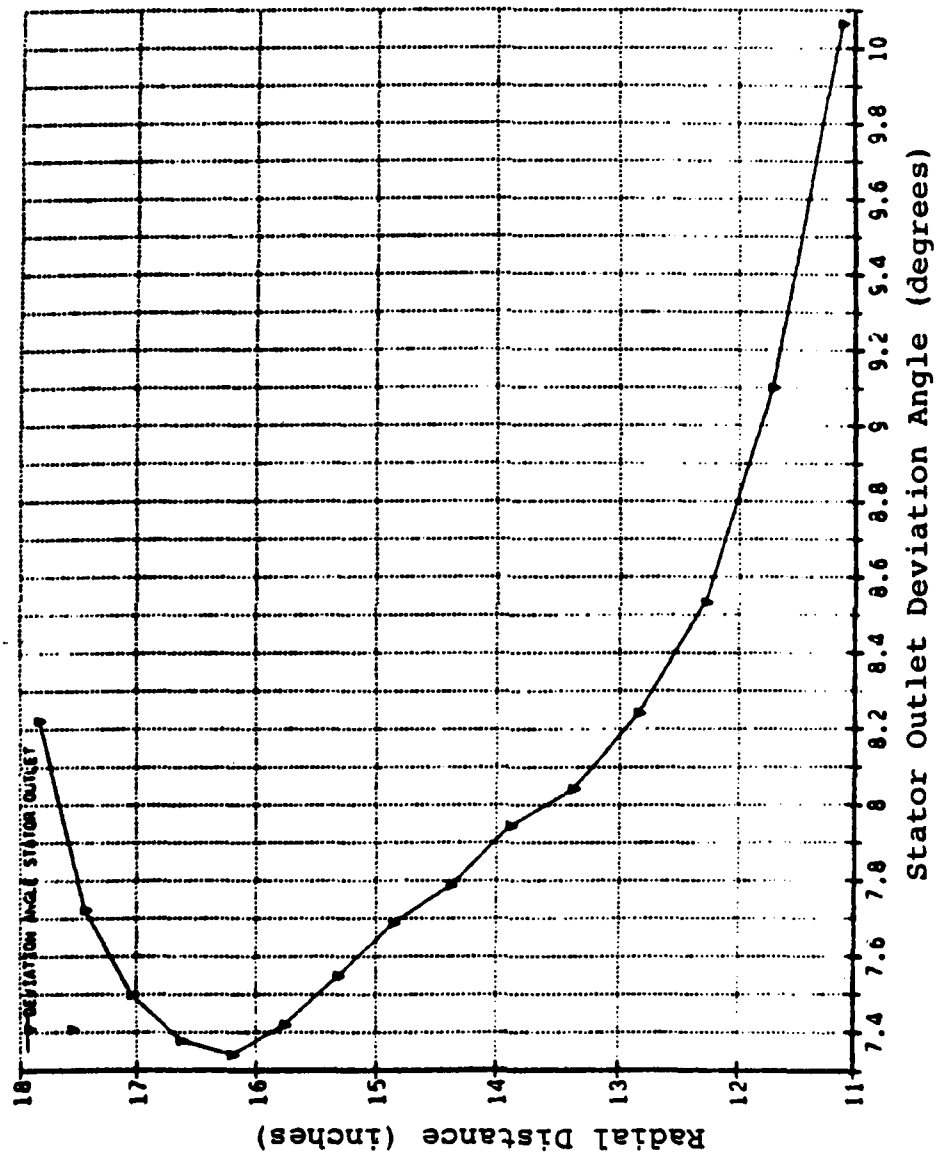


Figure 20. A TURBO Generated Tektonix 618 Plot of the Stator Outlet Deviation Flow Angles



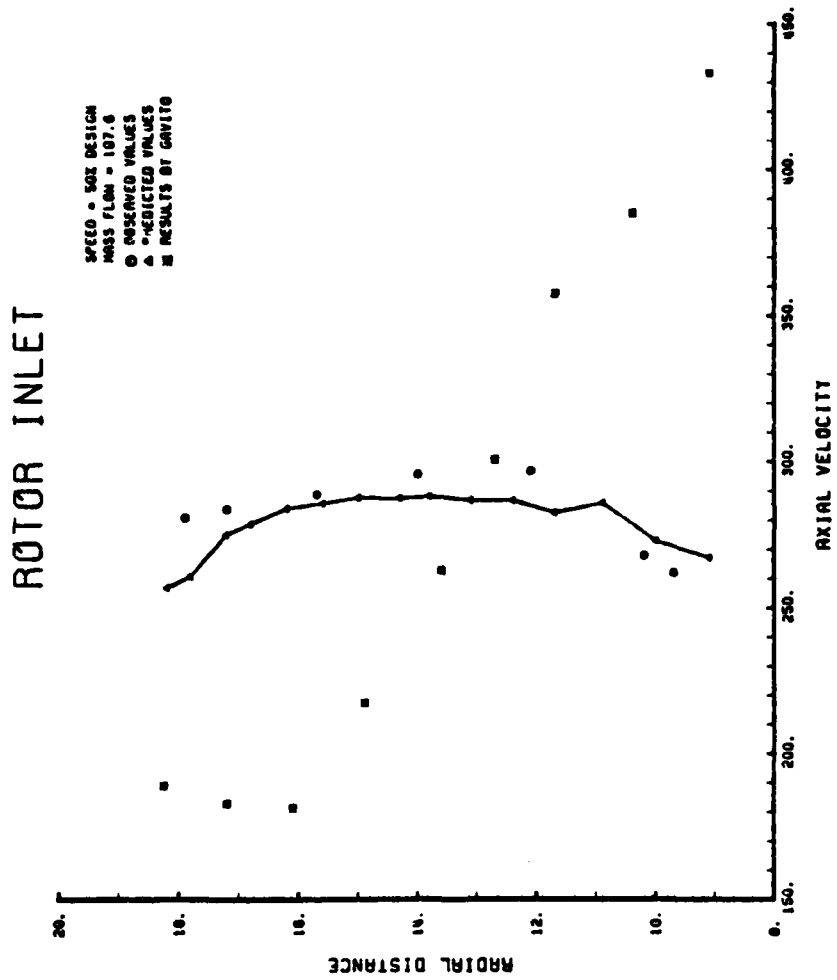


Figure 21. Comparison of Predictions to Gavito and Observations for Rotor Inlet Axial Velocity, 50% Design

# ROTOR OUTLET

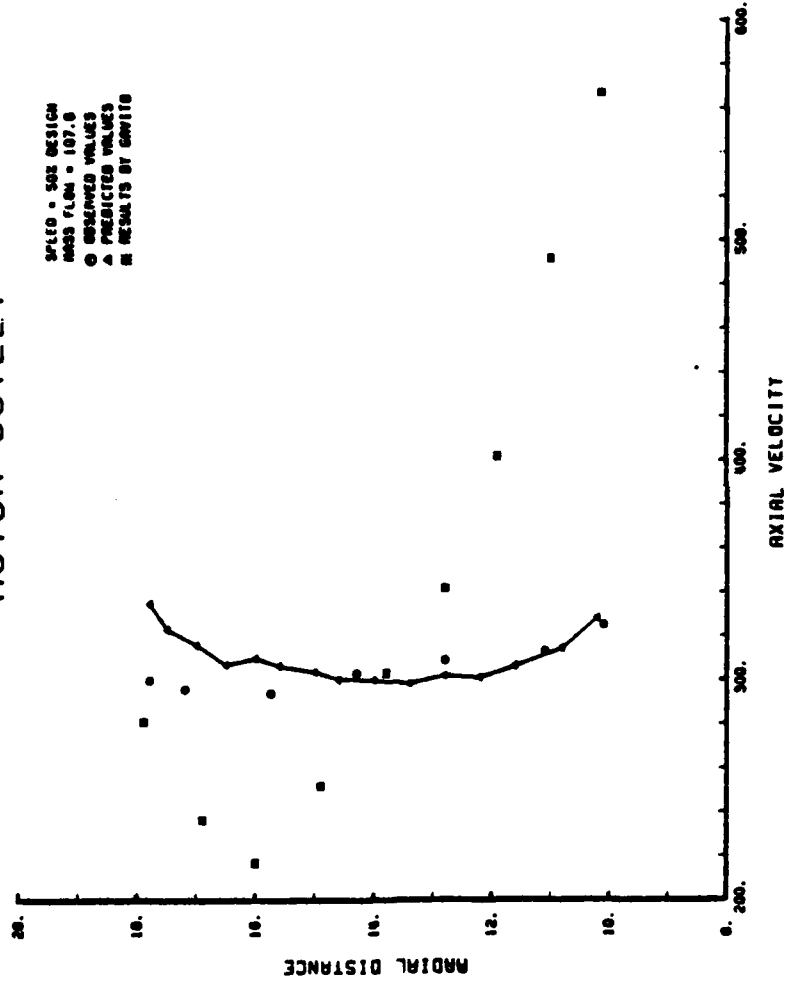


Figure 22. Comparison of Predictions to Gavito and Observations for Rotor Outlet Axial Velocity, 50% Design

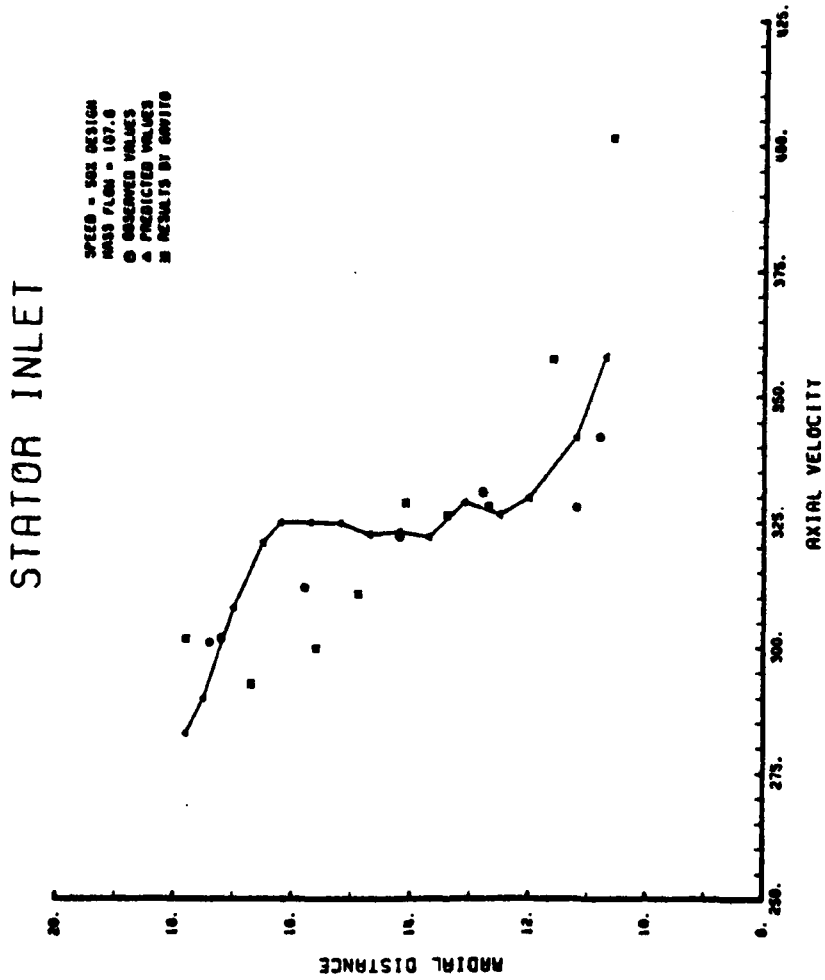


Figure 23. Comparison of Predictions to Gavito and Observations for Stator Inlet Axial Velocity, 50% Design

# STATOR OUTLET

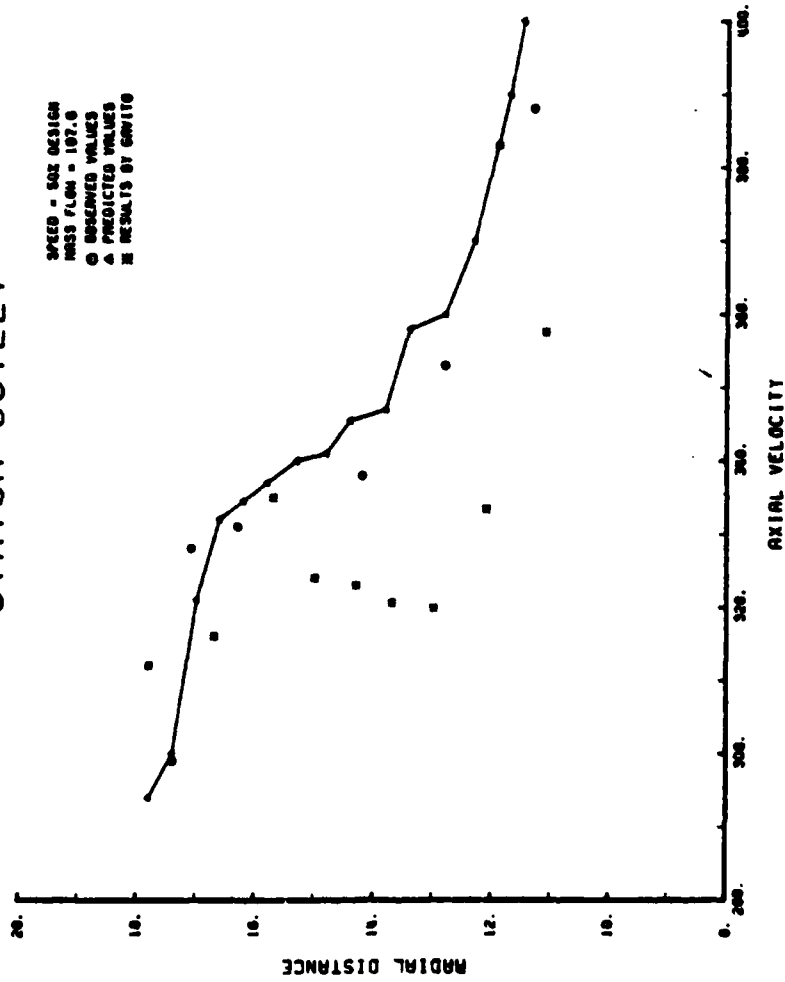


Figure 24. Comparison of Predictions to Gavito and Observations for Stator Outlet Axial Velocity, 50% Design

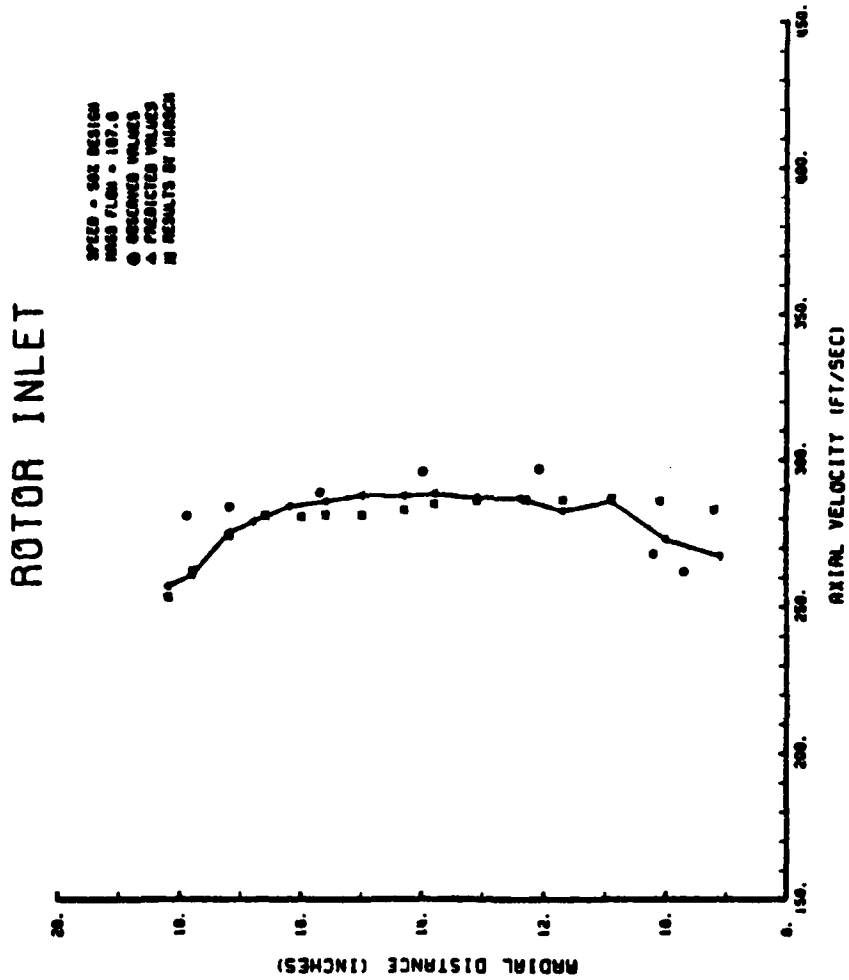


Figure 25. Comparison of Predictions to Hirsch and Observations for Rotor Inlet Axial Velocity, 50% Design

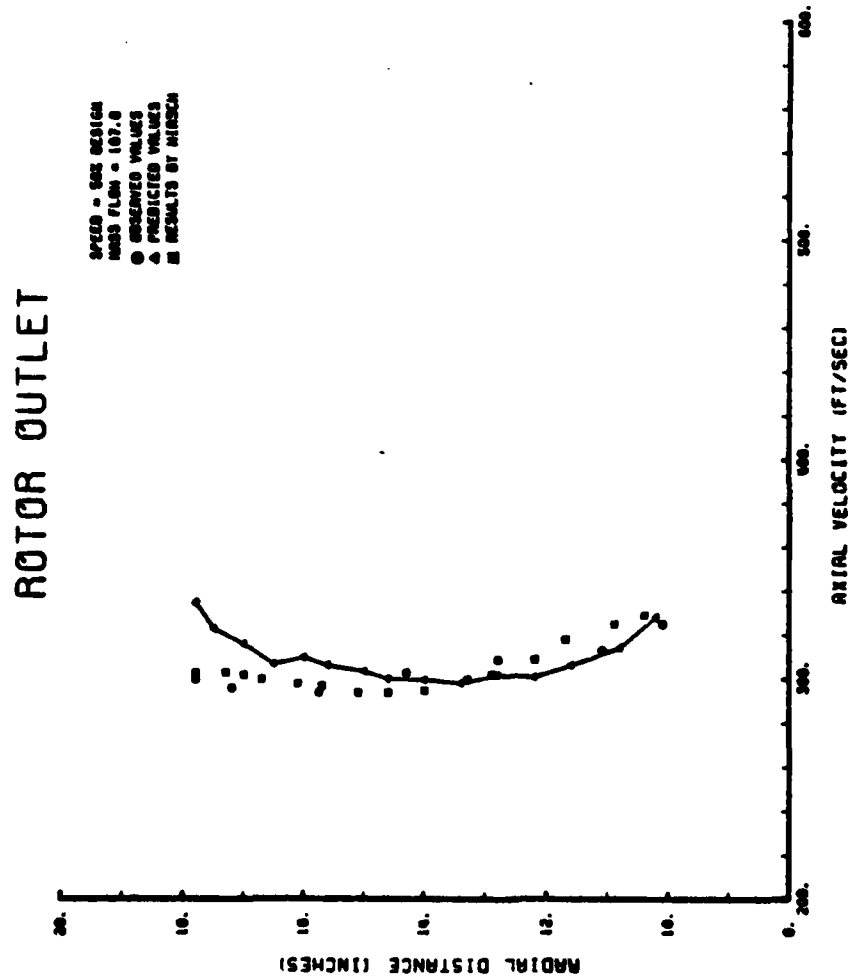


Figure 26. Comparison of Predictions to Hirsch and Observations for Rotor Outlet Axial Velocity, 50% Design

# ROTOR OUTLET

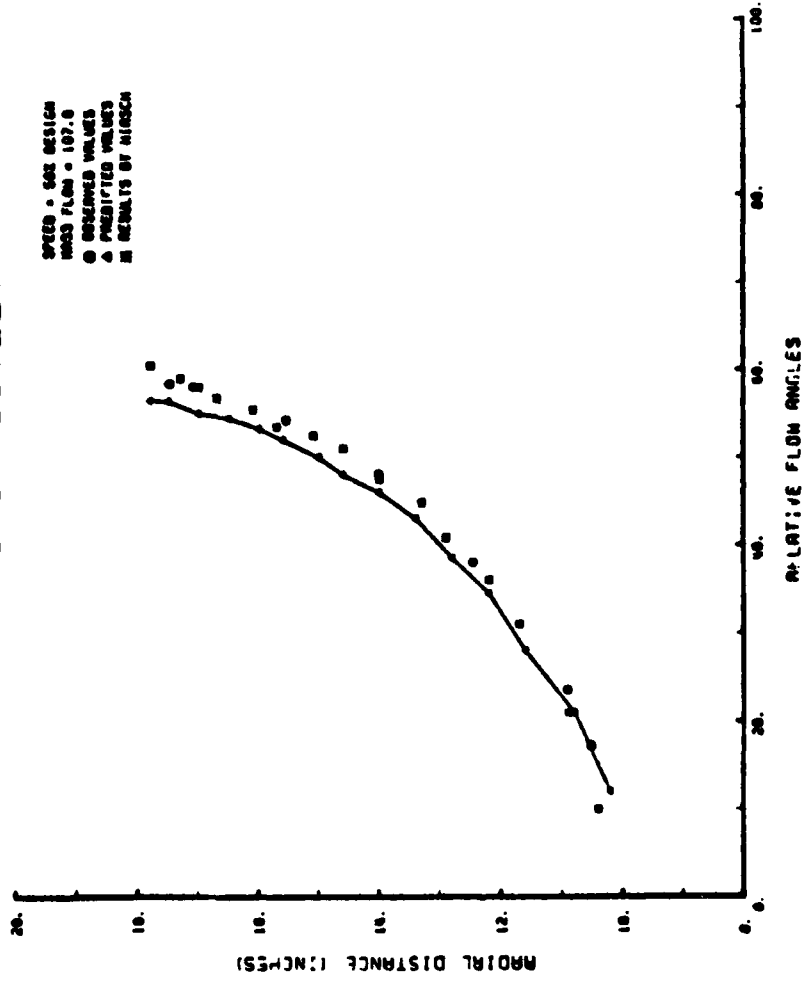


Figure 27. Comparison of Predictions to Hirsch and Observations for Rotor Outlet Relative Flow Angles, 50% Design

# ROTOR OUTLET

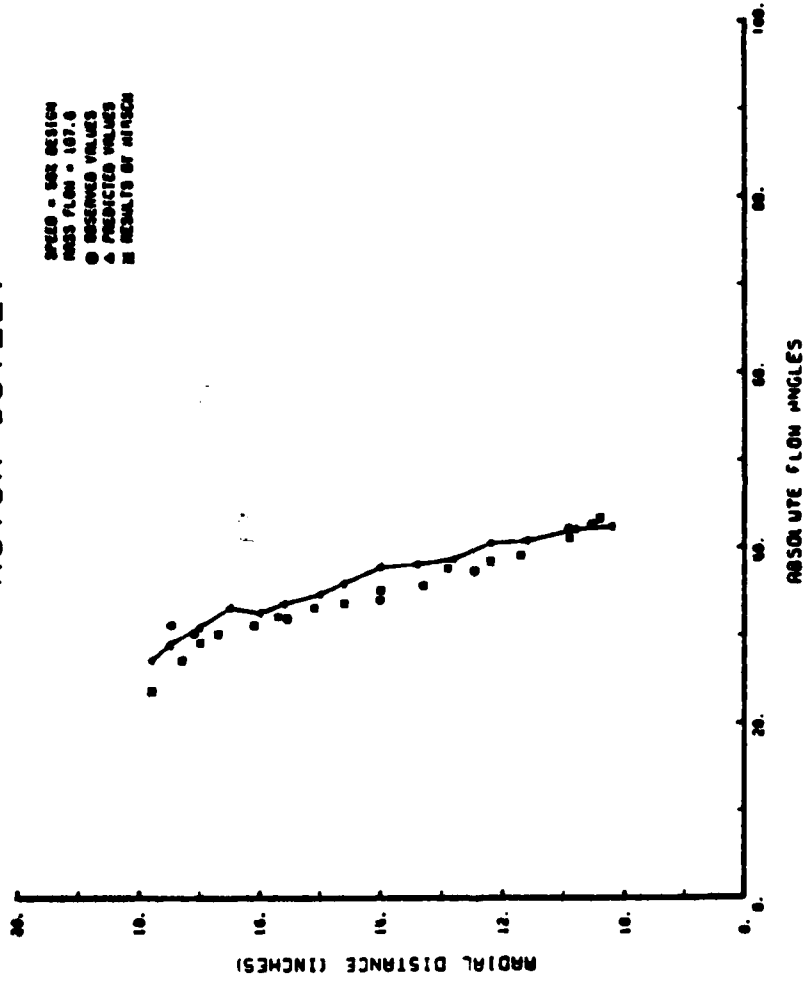


Figure 28. Comparison of Predictions to Hirsch and Observations for Rotor Outlet Absolute Flow Angles, 50% Design



# STATOR INLET

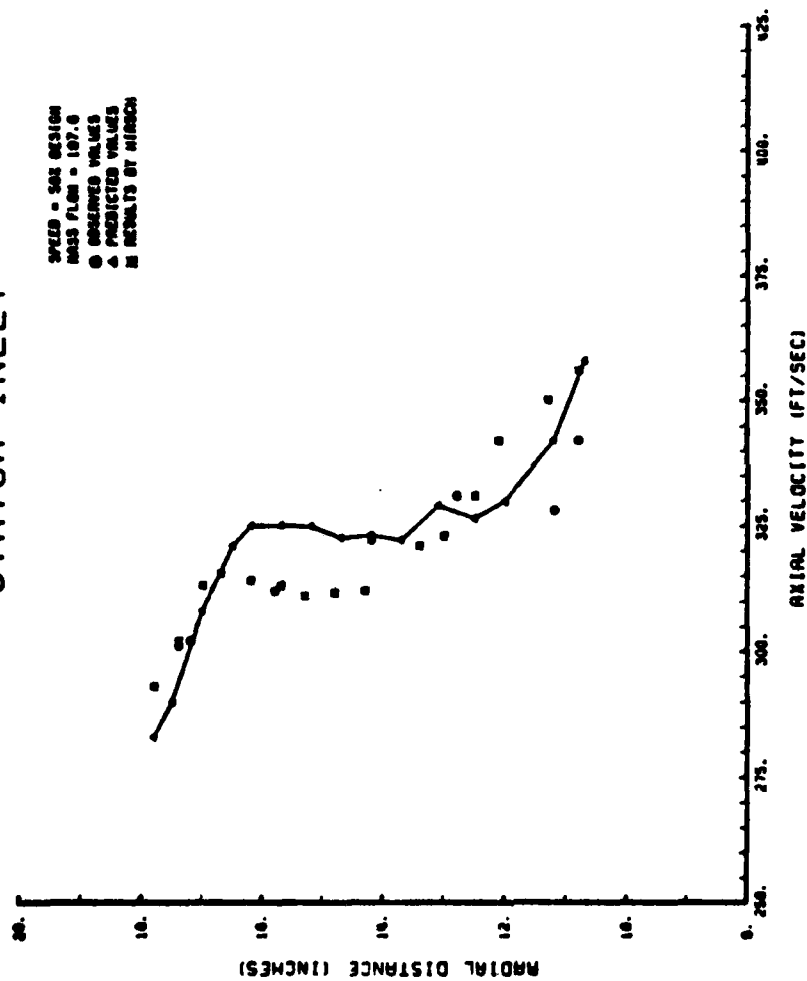


Figure 29. Comparison of Predictions to Hirsch and Observations for Stator Inlet Axial Velocity, 50% Design

# STATOR OUTLET

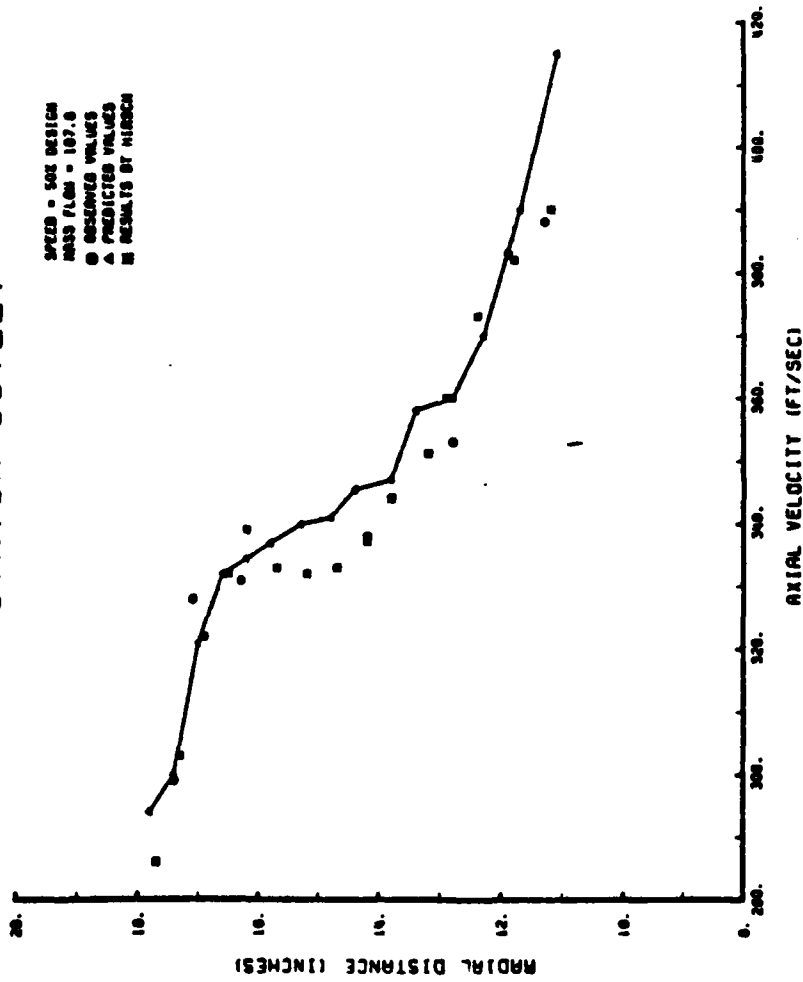


Figure 30. Comparison of Predictions to Hirsch and Observations for Stator Outlet Axial Velocity, 50% Design

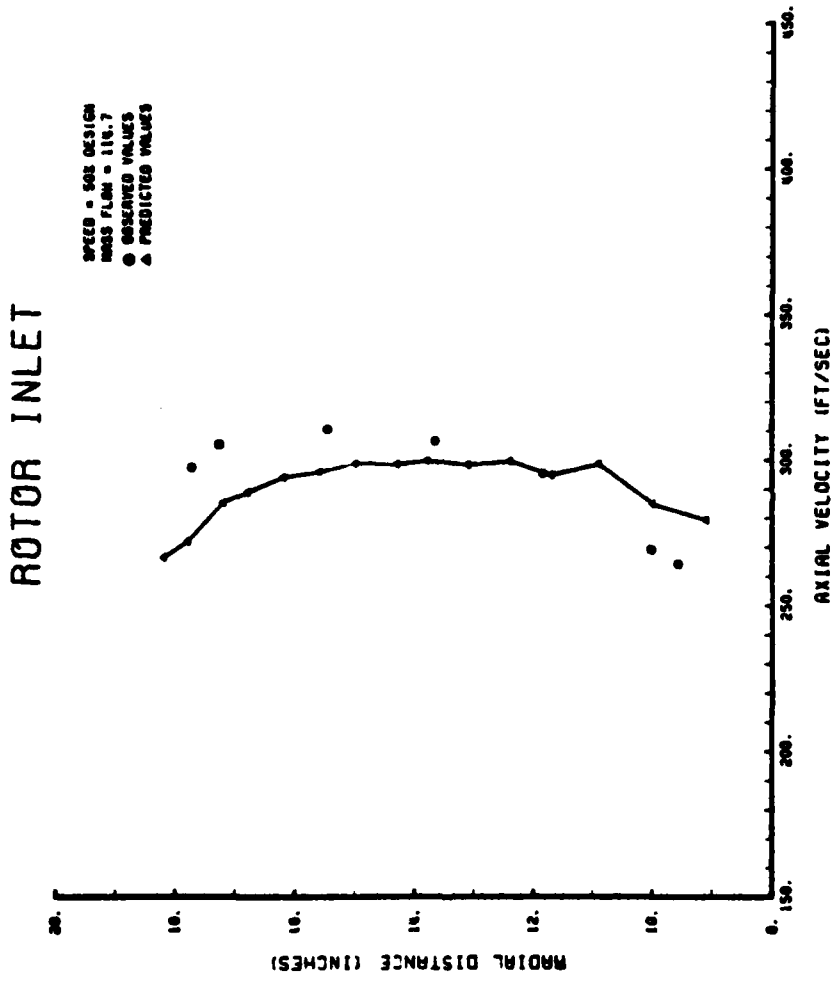


Figure 31. Axial Velocity at the Rotor Inlet, 50% Design

# ROTOR INLET

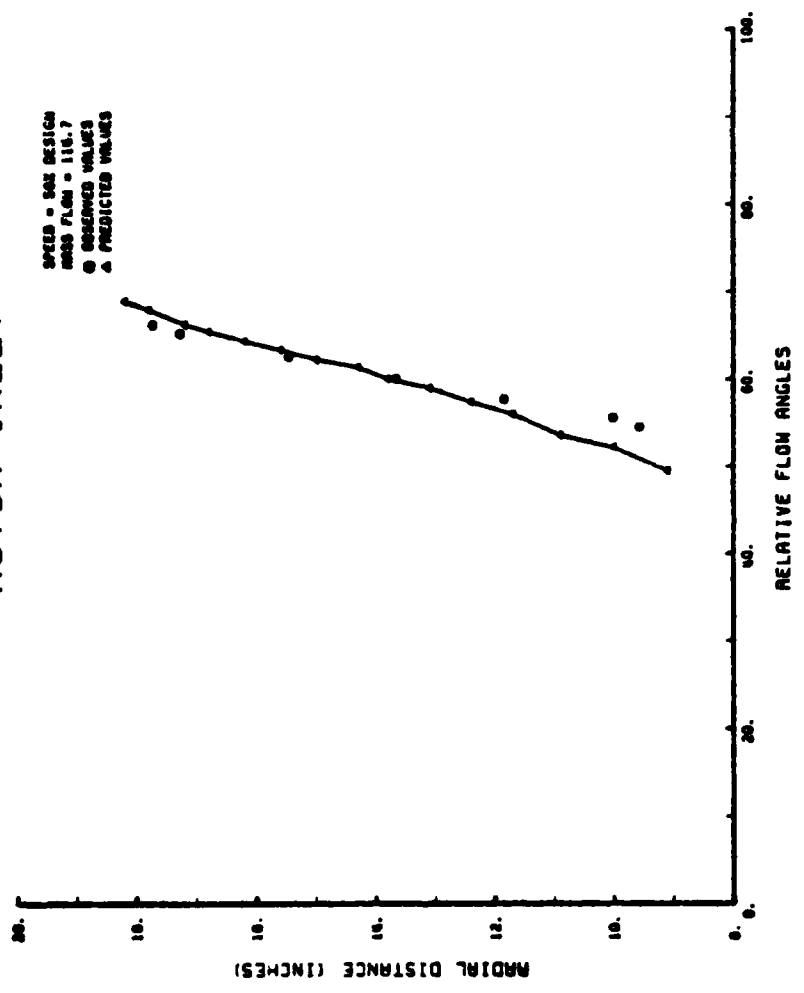


Figure 32. Relative Flow Angles at Rotor Inlet, 50% Design

# ROTOR INLET

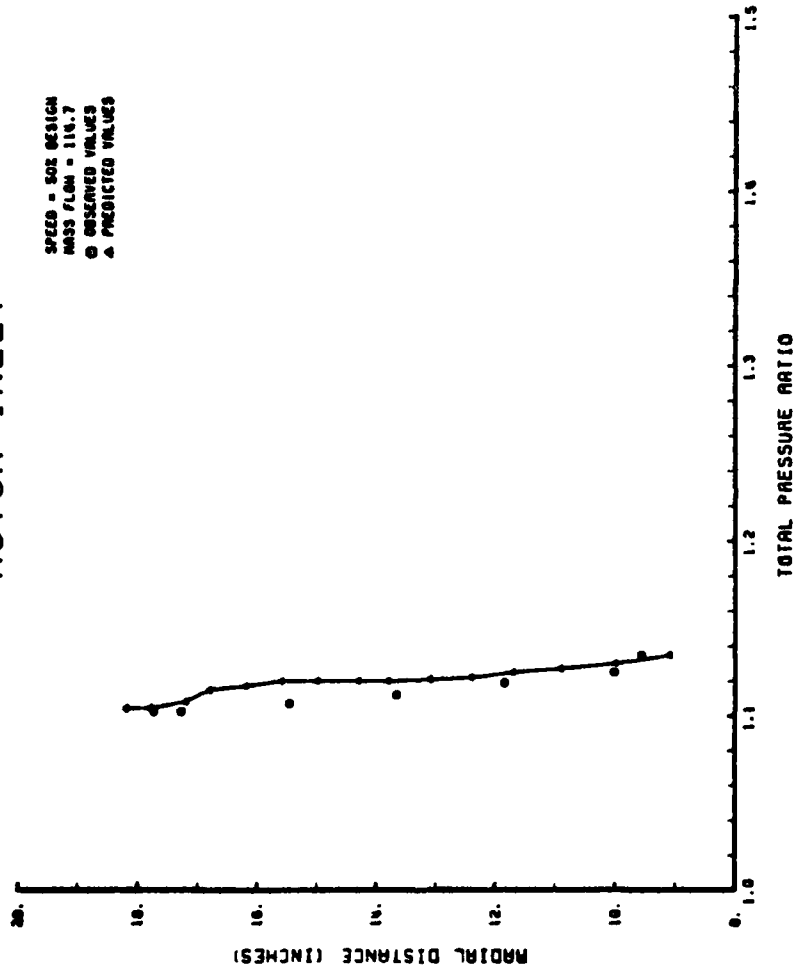


Figure 33. Total Pressure Ratio of the Rotor, 50% Design

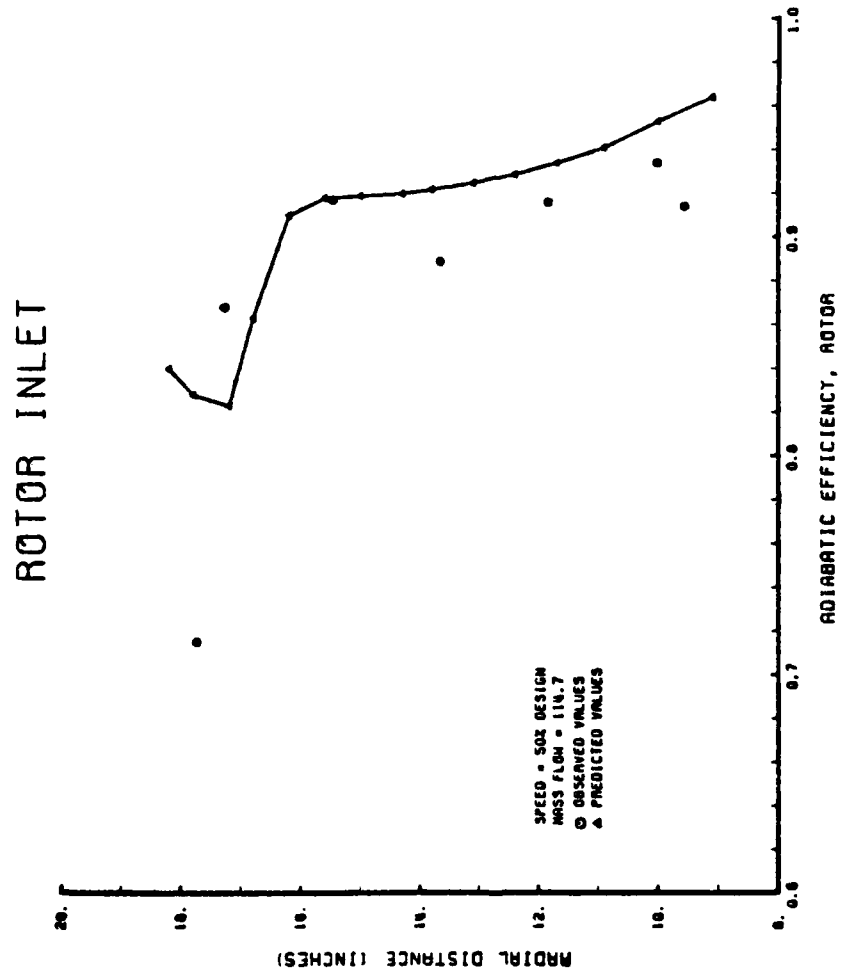


Figure 34. Adiabatic Efficiency of the Rotor, 50% Design

# ROTOR OUTLET

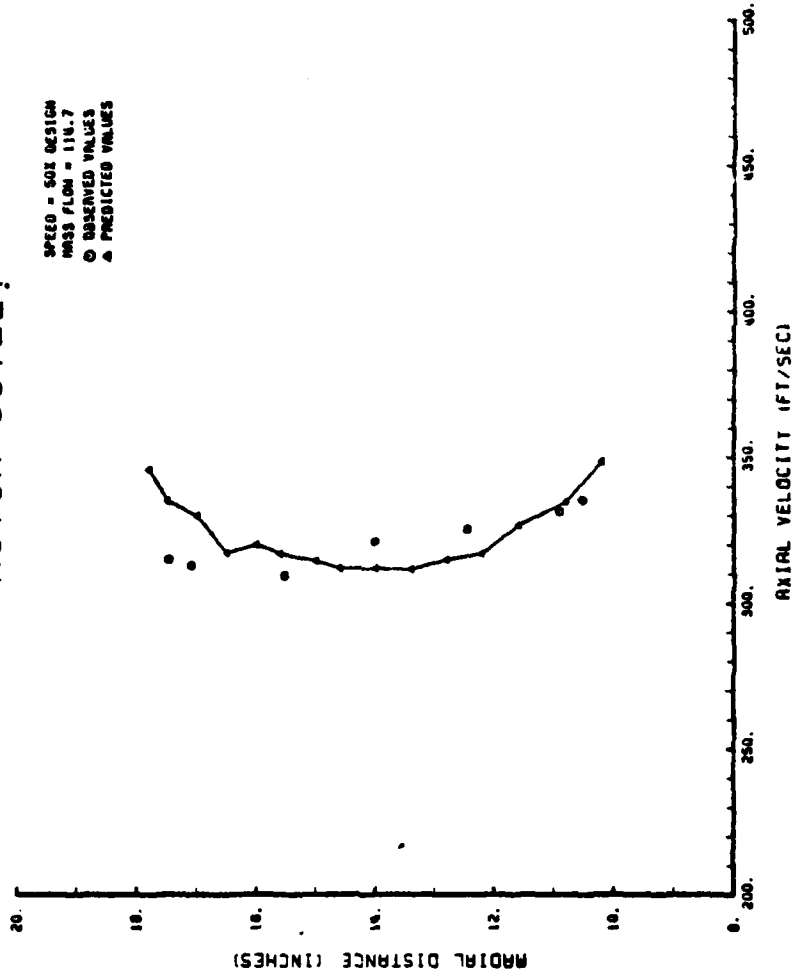


Figure 35. Axial Velocity at the Rotor Outlet, 50% Design

# ROTOR OUTLET

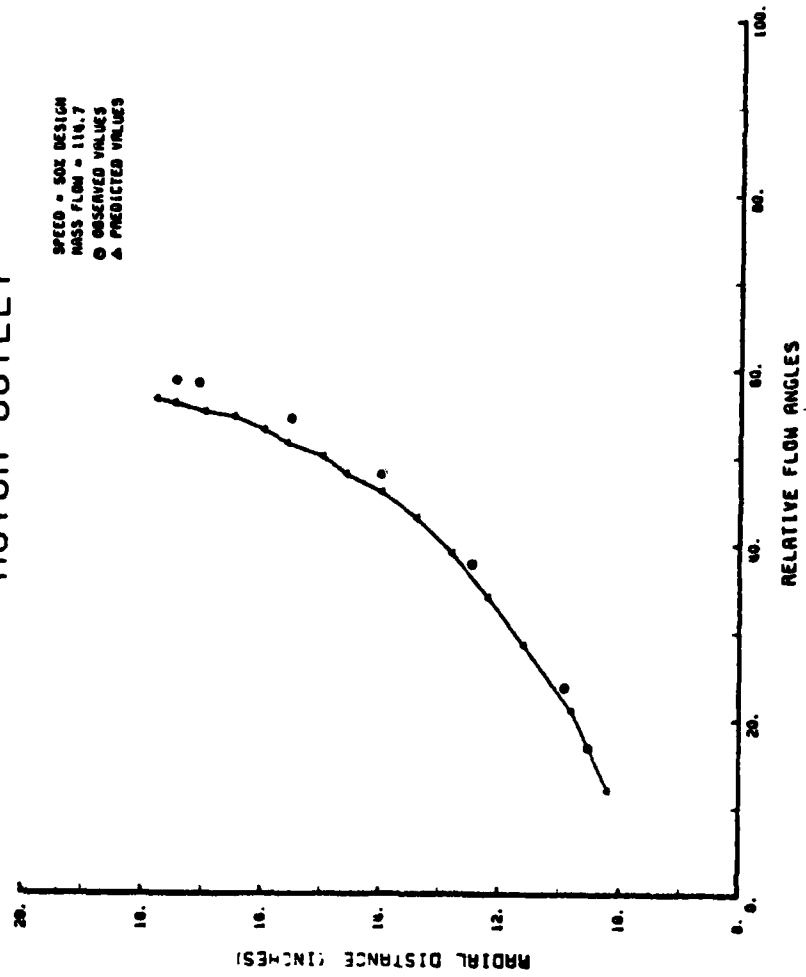


Figure 36. Relative Flow Angles at Rotor Outlet, 50% Design



# ROTOR OUTLET

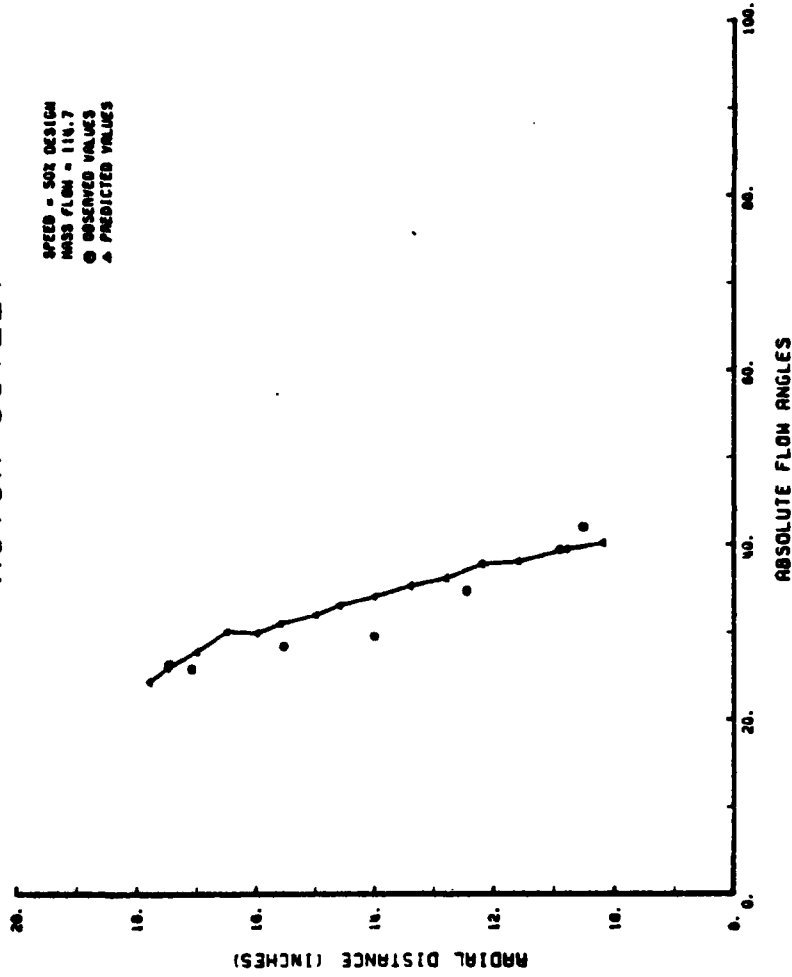


Figure 37. Absolute Flow Angles at Rotor Outlet, 50% Design

# ROTOR OUTLET

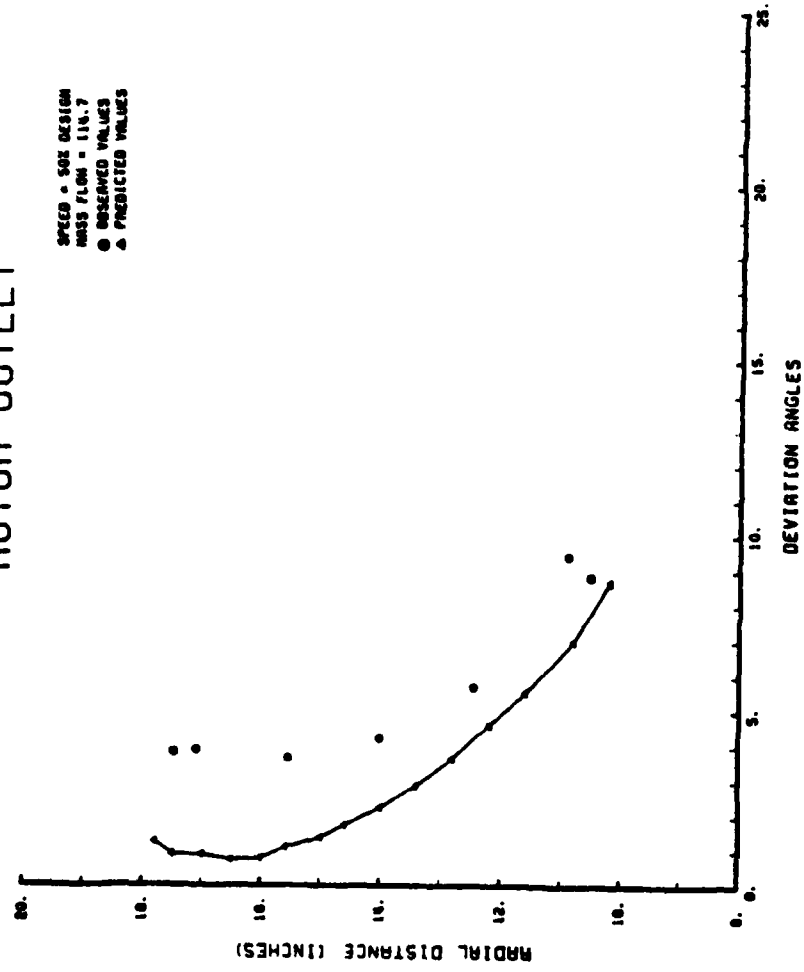


Figure 38. Deviation Flow Angles at Rotor Outlet, 50% Design

# STATOR INLET

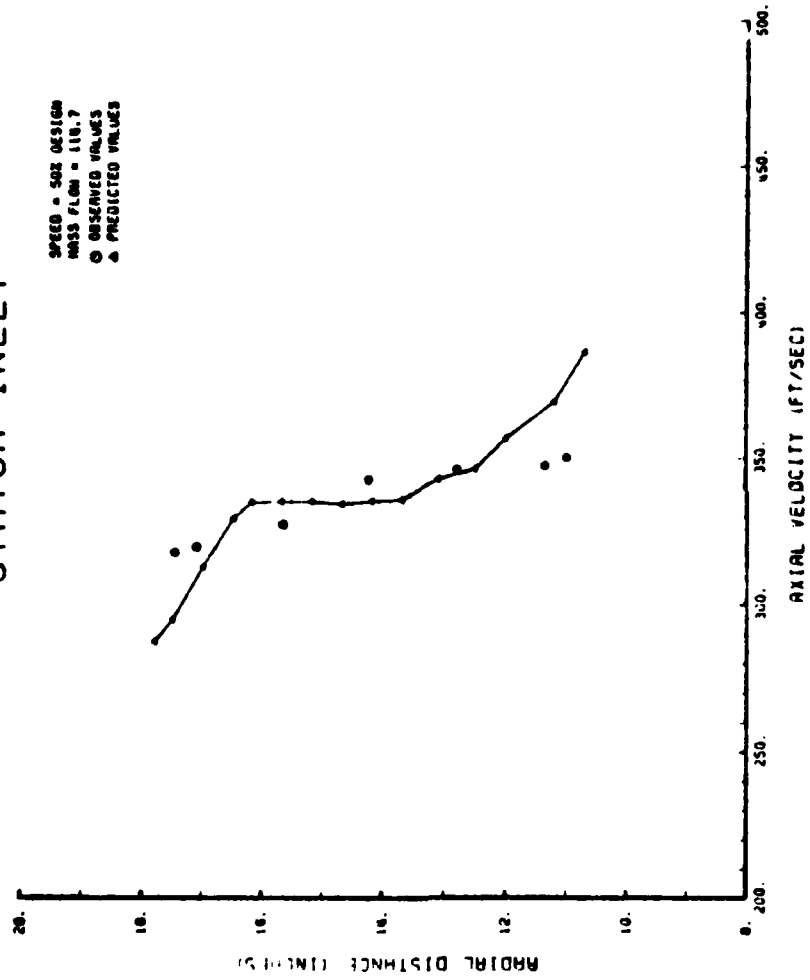


Figure 39. Axial Velocity at the Stator Inlet, 50% Design

# STATOR INLET

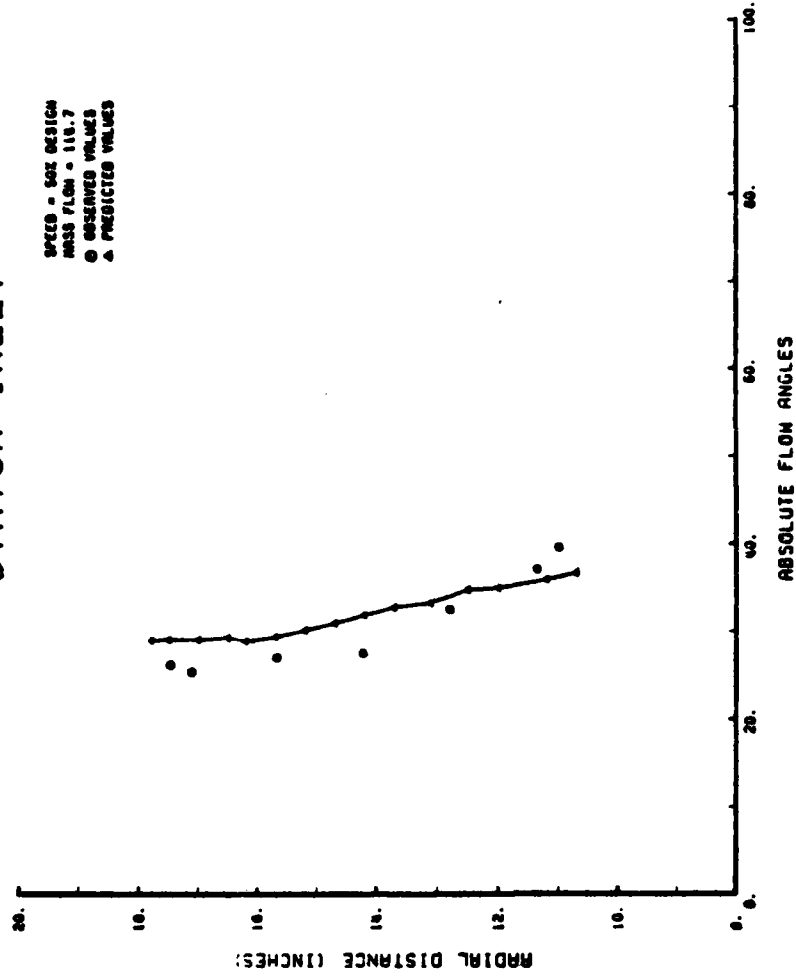


Figure 40. Absolute Flow Angles at Stator Inlet, 50% Design

# STATOR INLET

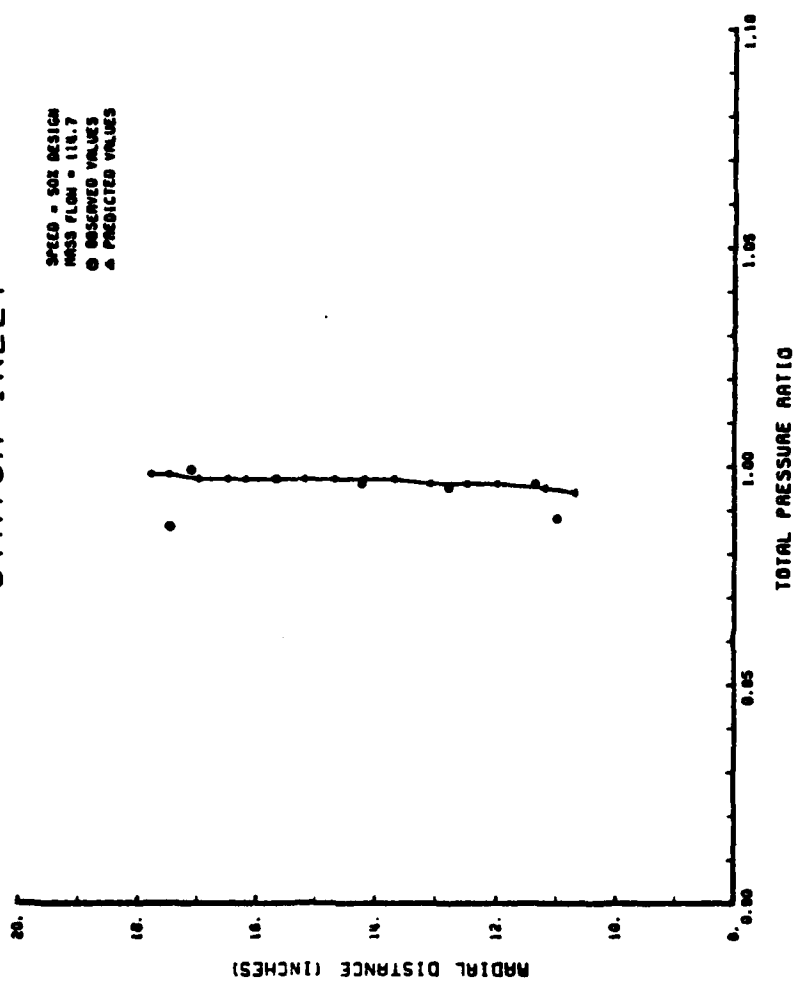


Figure 41. Total Pressure Ratio at Stator Inlet, 50% Design

# STATOR OUTLET

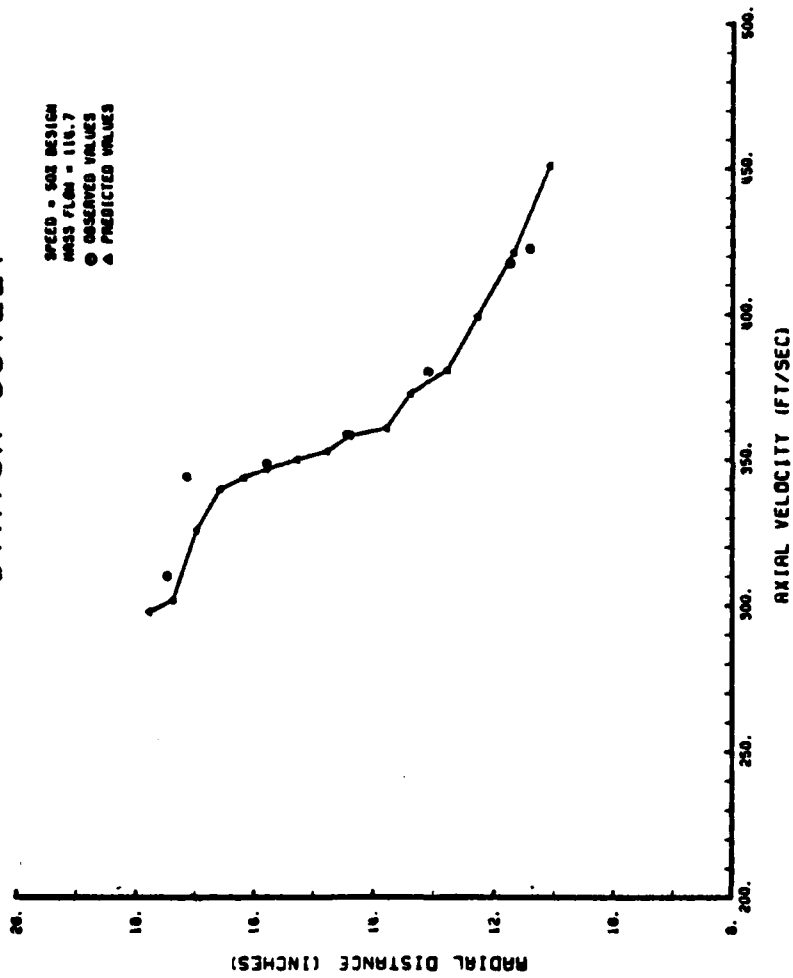


Figure 42. Axial Velocity at the Stator Outlet, 50% Design

# STATOR OUTLET

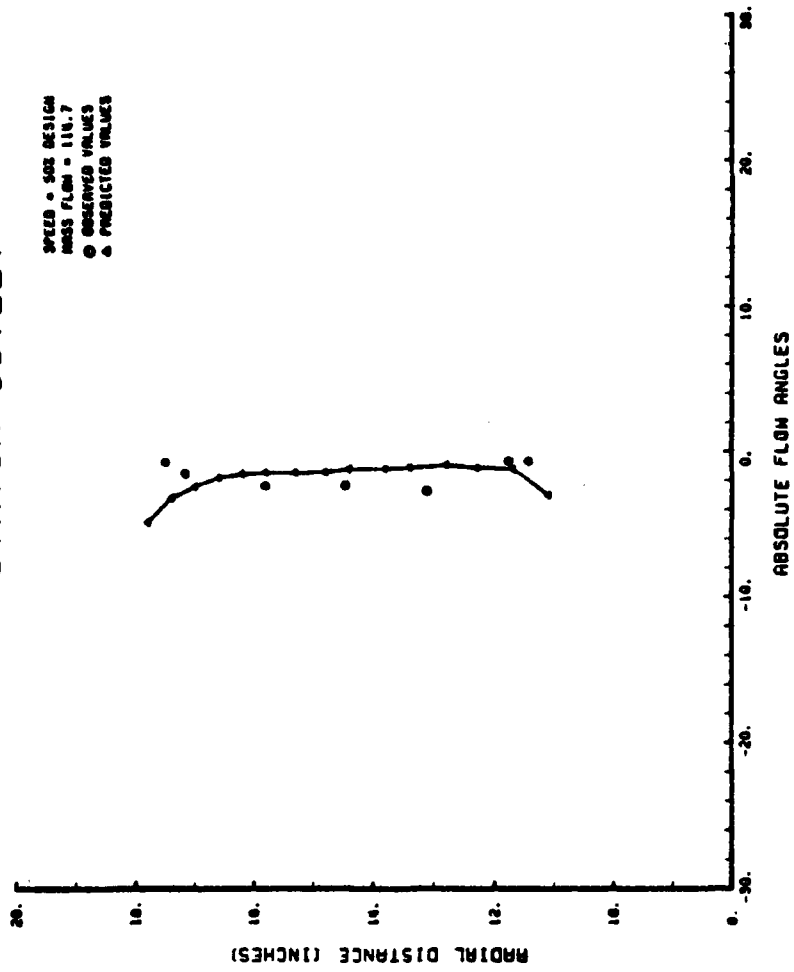


Figure 43. Absolute Flow Angles at Stator Outlet, 50% Design

STATOR OUTLET

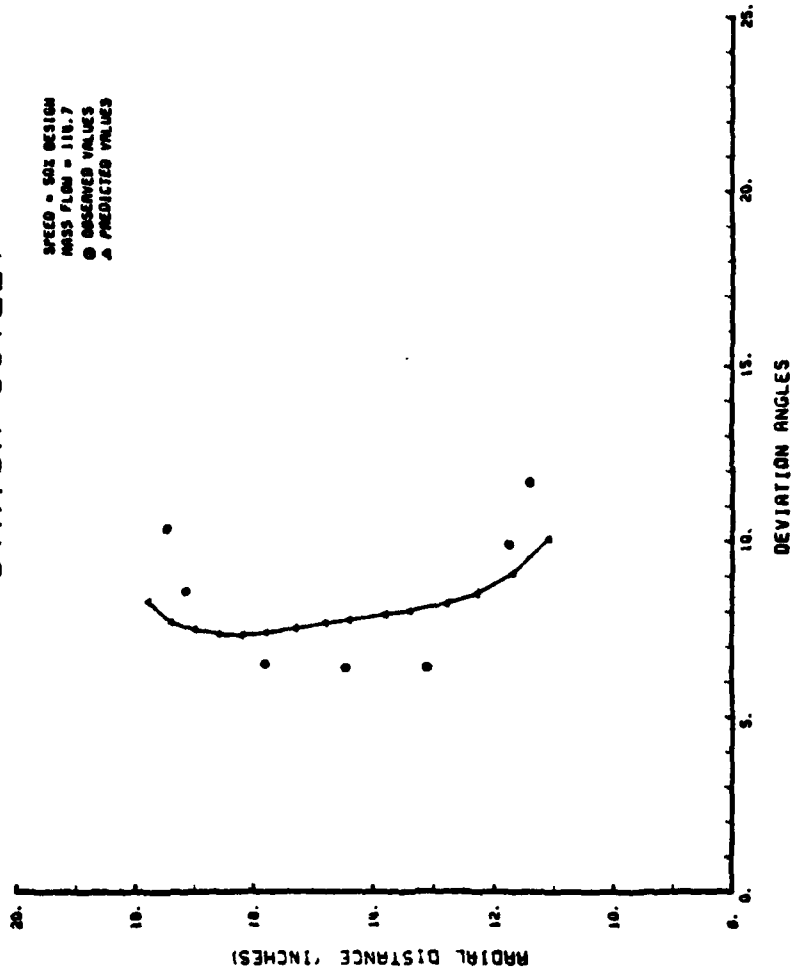


Figure 44. Deviation Flow Angles at Stator Outlet, 50% Design



# ROTOR INLET

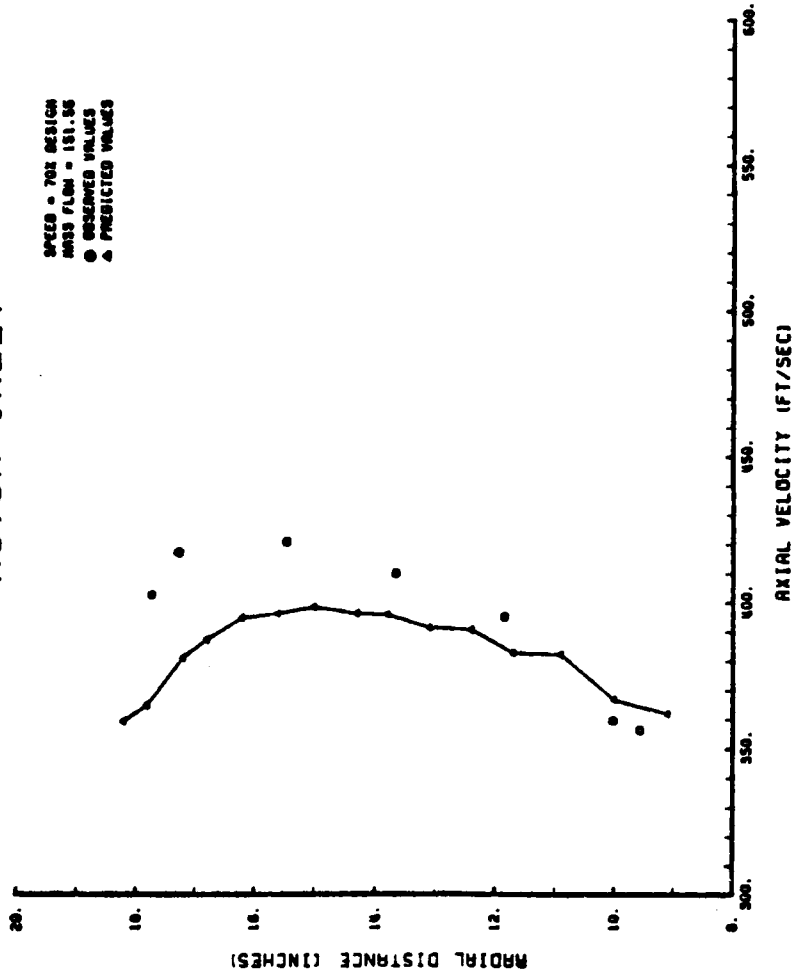


Figure 45. Axial Velocity at the Rotor Inlet, 70% Design

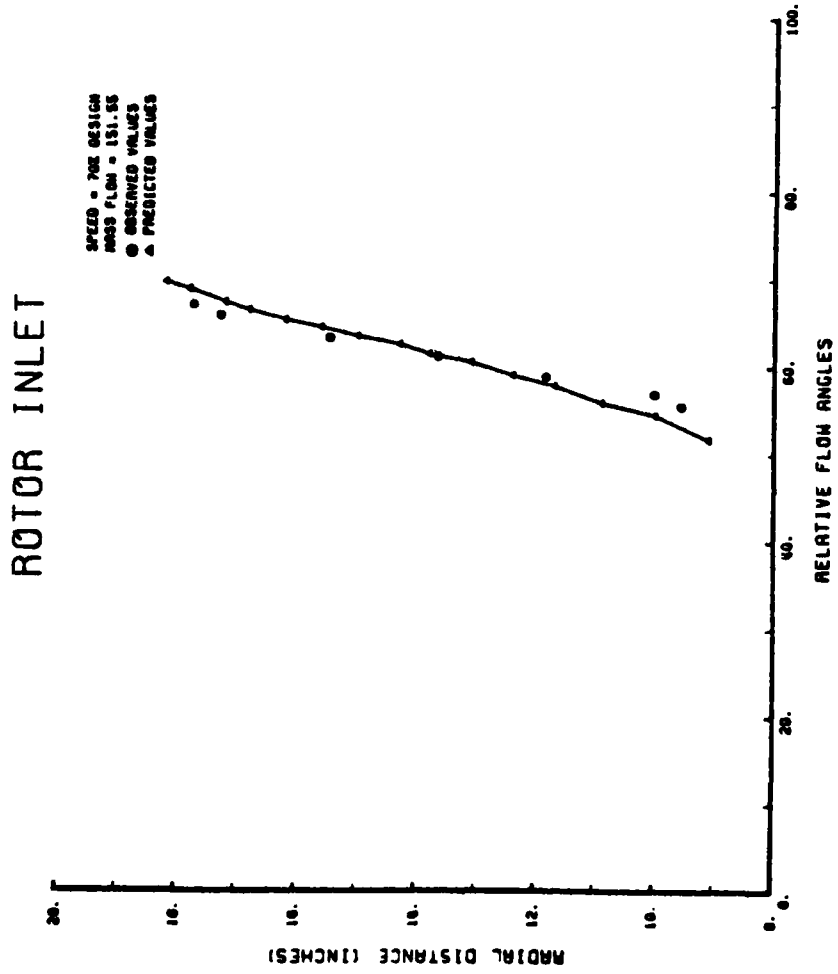


Figure 46. Relative Flow Angles at Rotor Inlet, 70% Design

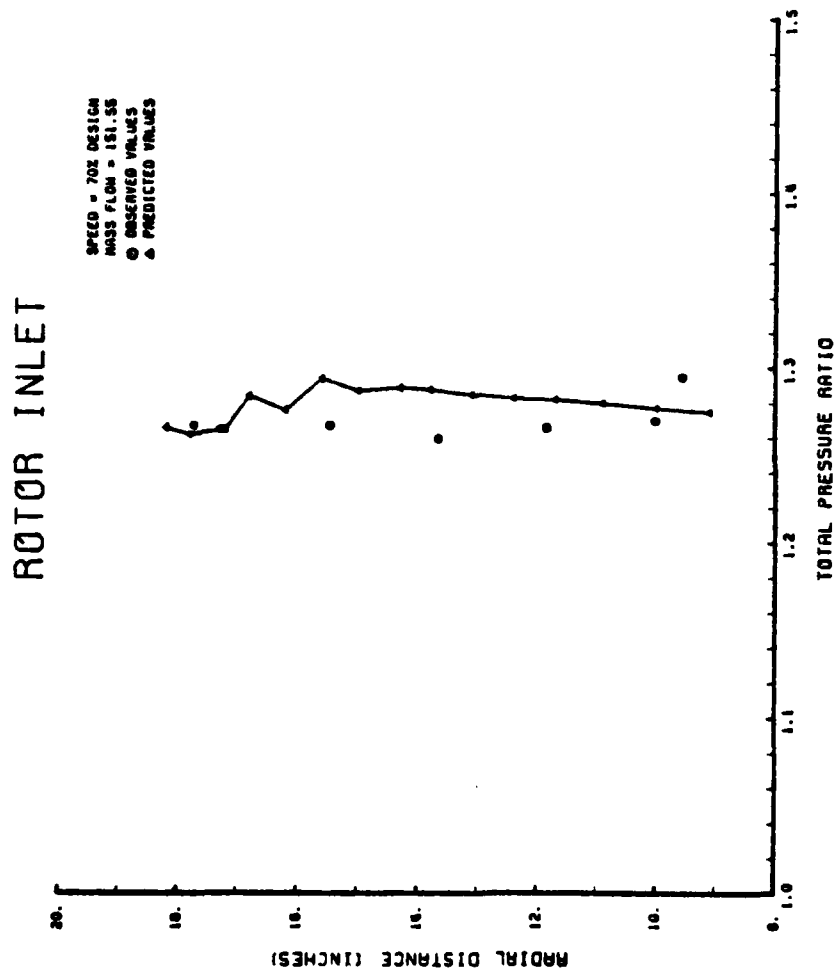


Figure 47. Total Pressure Ratio of the Rotor, 70% Design

# ROTOR INLET

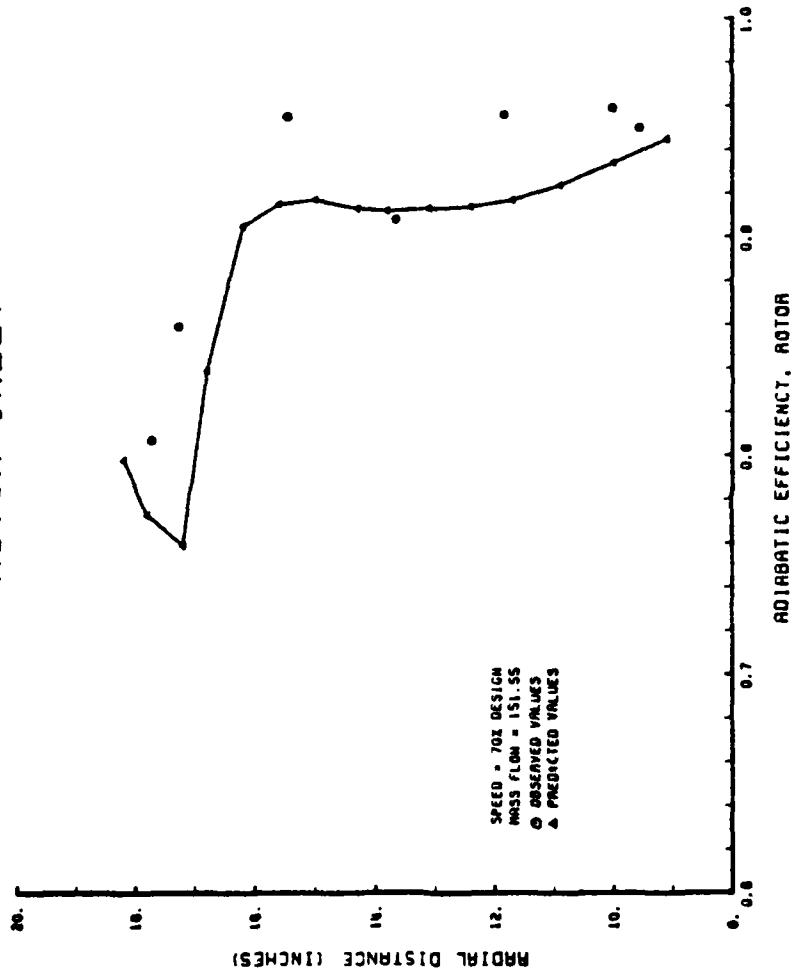


Figure 48. Adiabatic Efficiency of the Rotor, 70% Design

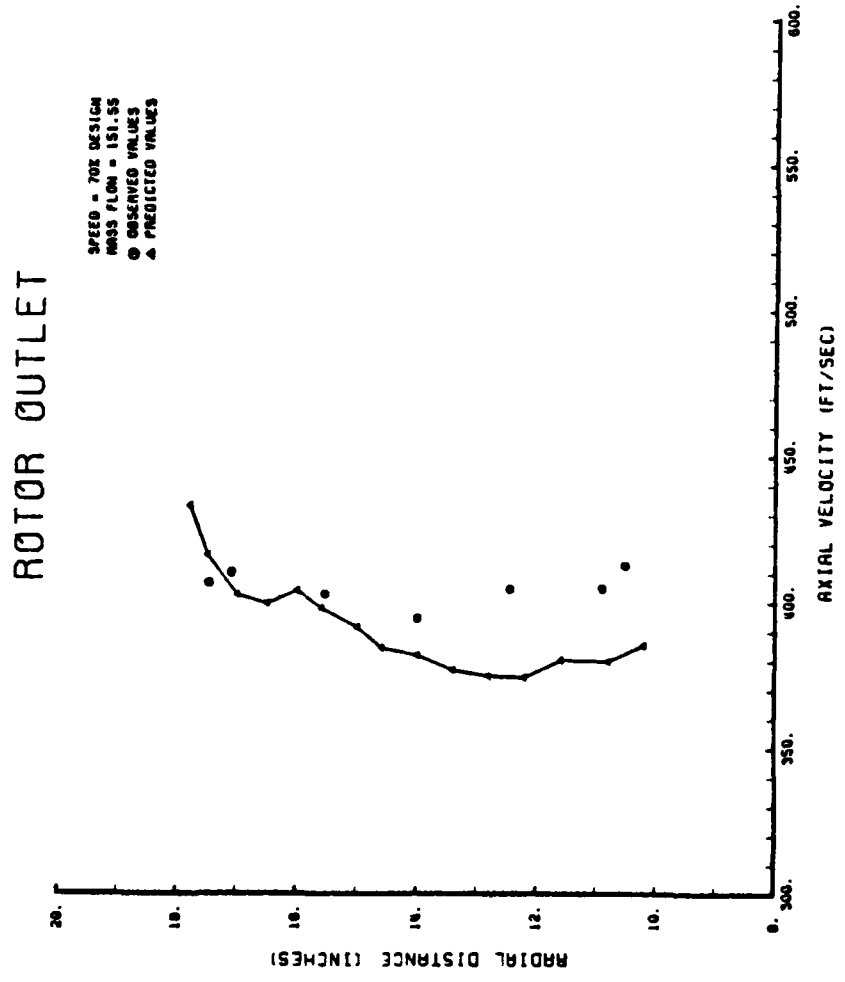


Figure 49. Axial Velocity at the Rotor Outlet, 70% Design

# ROTOR OUTLET

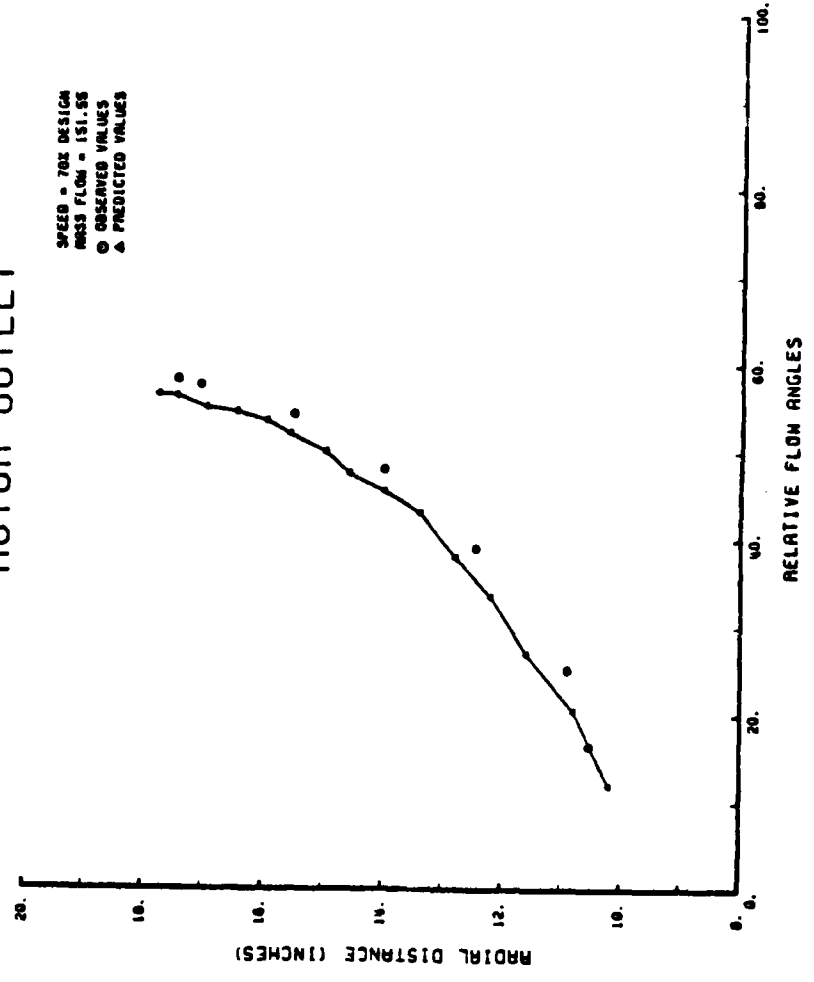


Figure 50. Relative Flow Angles at Rotor Outlet, 70% Design

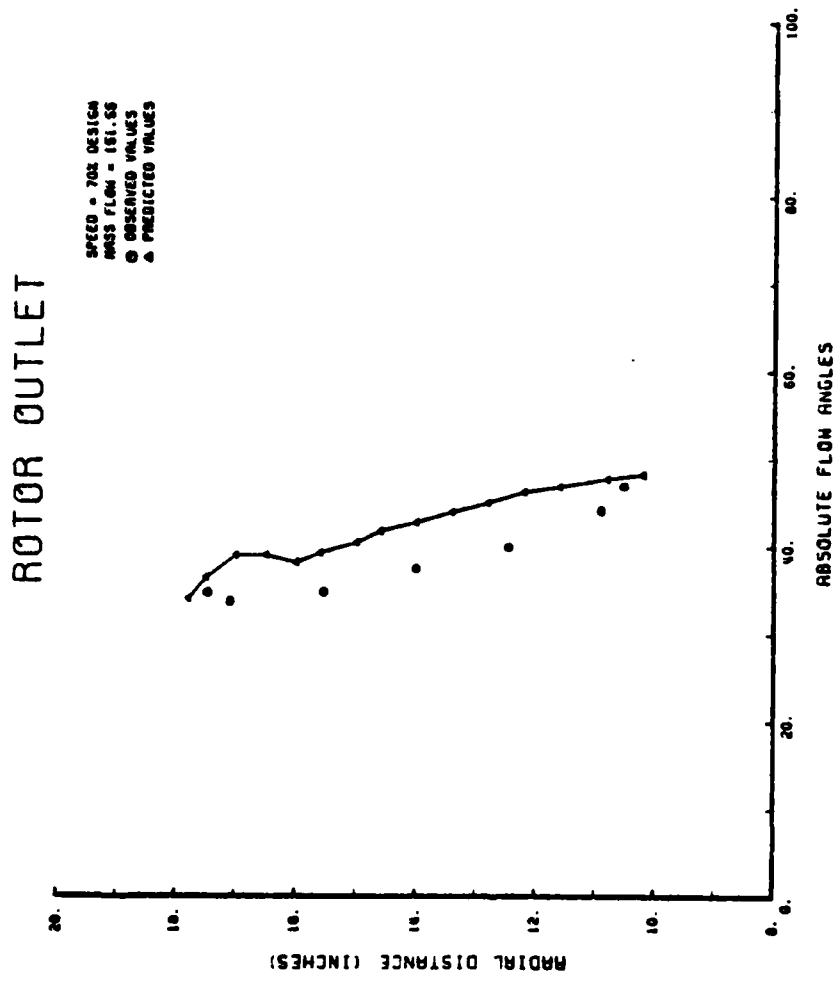


Figure 51. Absolute Flow Angles at Rotor Outlet, 70% Design

# ROTOR OUTLET

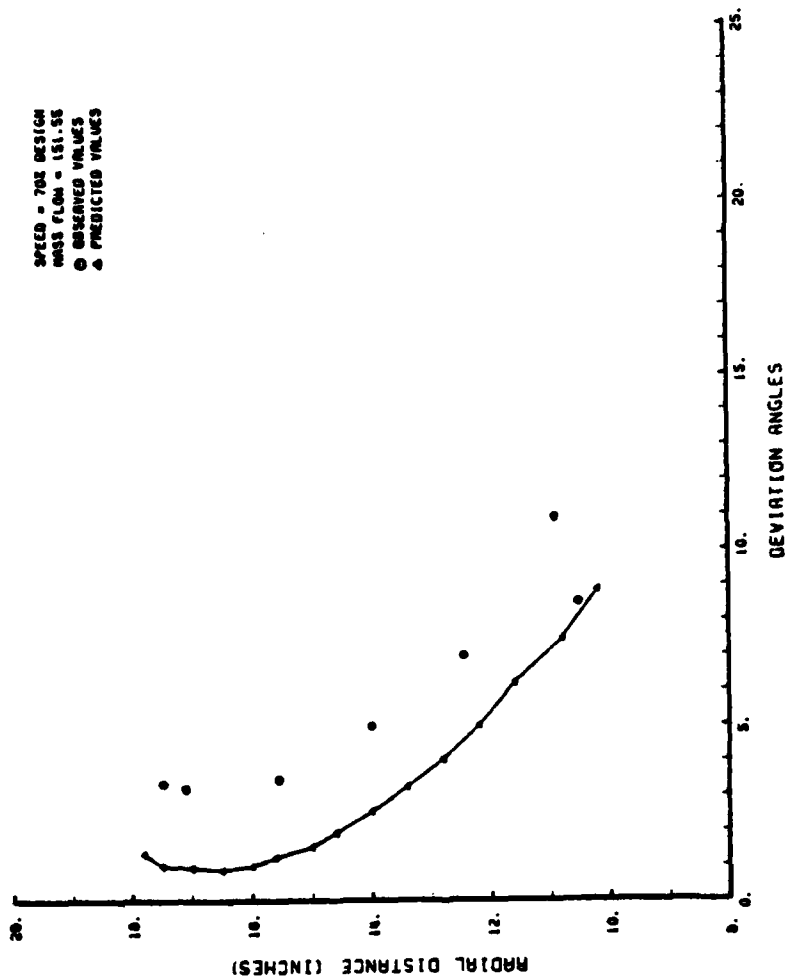


Figure 52. Deviation Flow Angles at Rotor Outlet, 70% Design



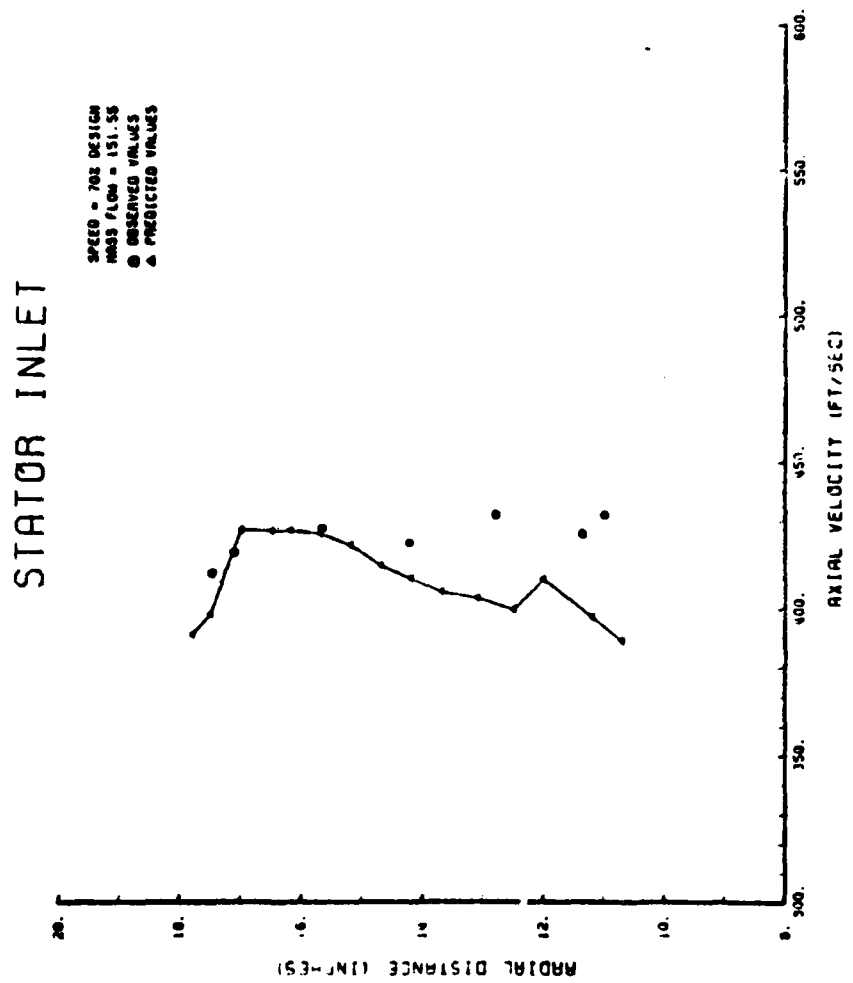


Figure 53. Axial Velocity at the Stator Inlet, 70% Design

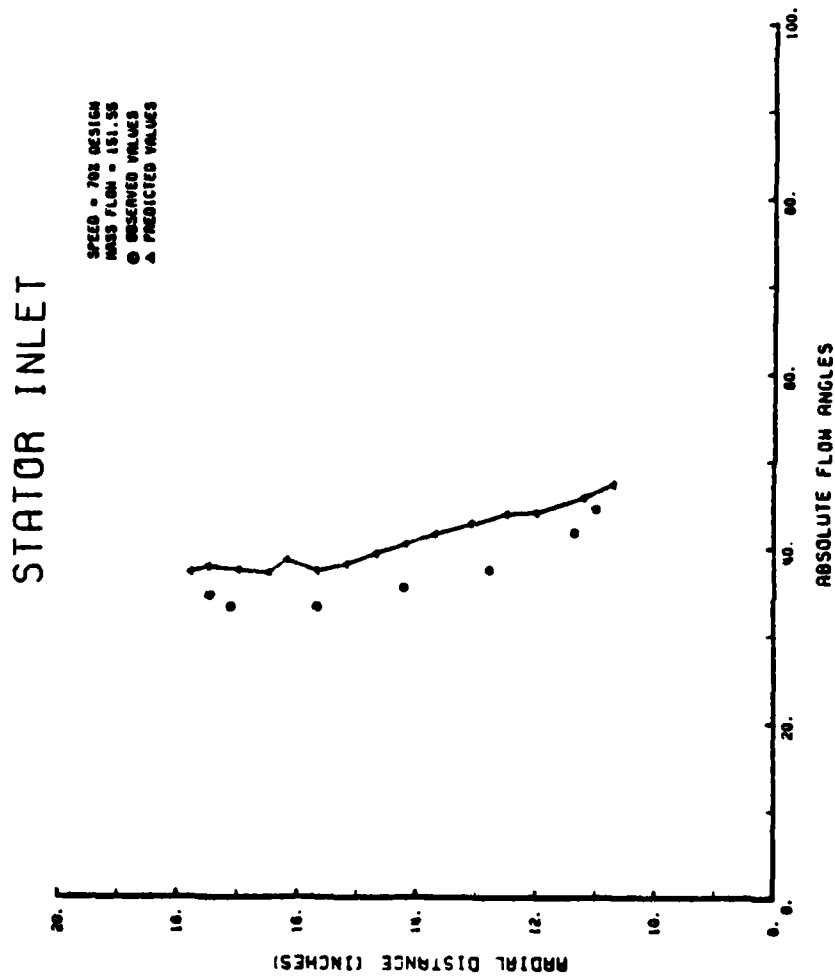


Figure 54. Absolute Flow Angles at Stator Inlet, 70% Design

# STATOR INLET

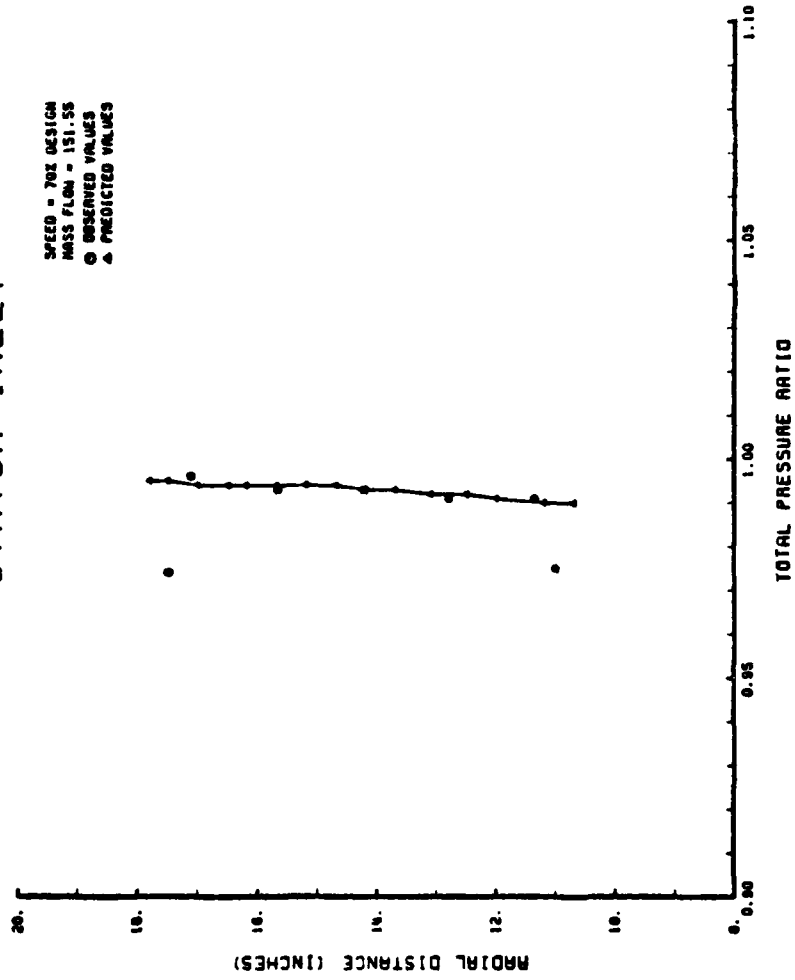


Figure 55. Total Pressure Ratio at Stator Inlet, 70% Design

# STATOR OUTLET

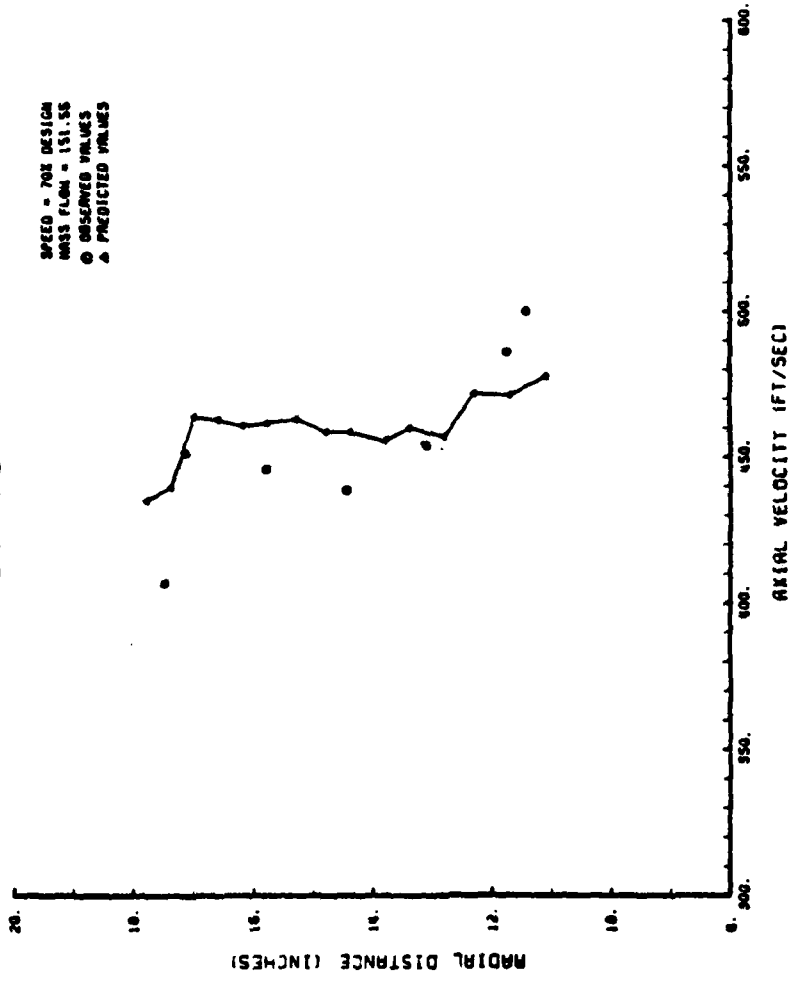


Figure 56. Axial Velocity at the Stator Outlet, 70% Design

# STATOR OUTLET

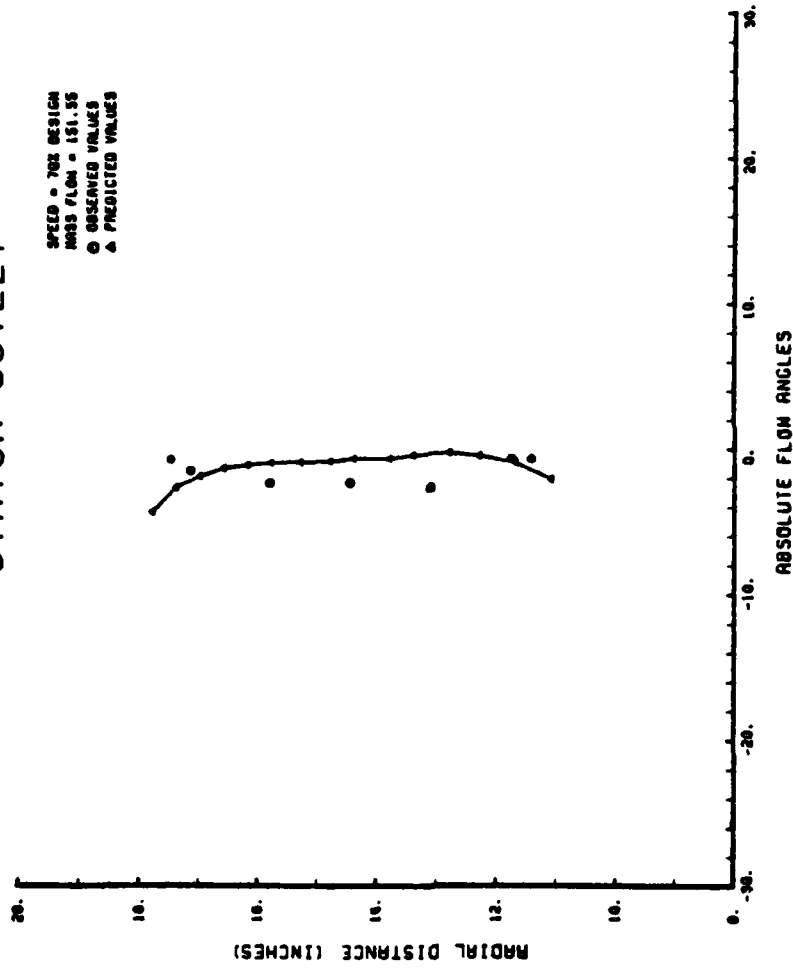


Figure 57. Absolute Flow Angles at Stator Outlet, 70% Design

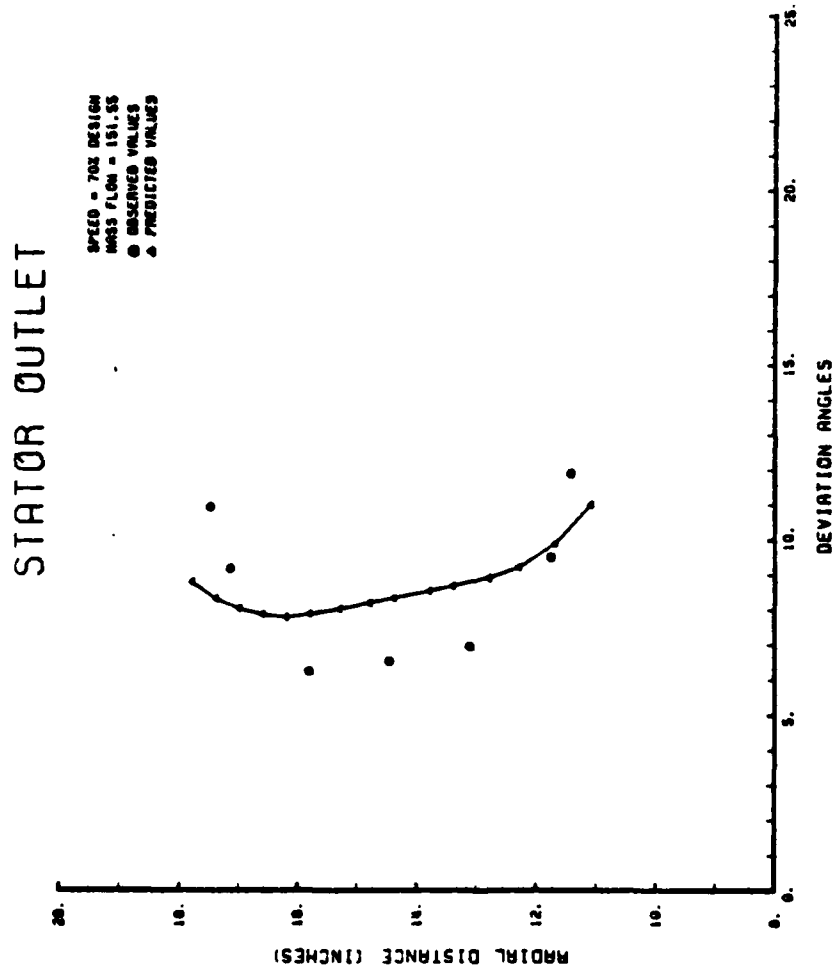


Figure 58. Deviation Flow Angles at Stator Outlet, 70% Design

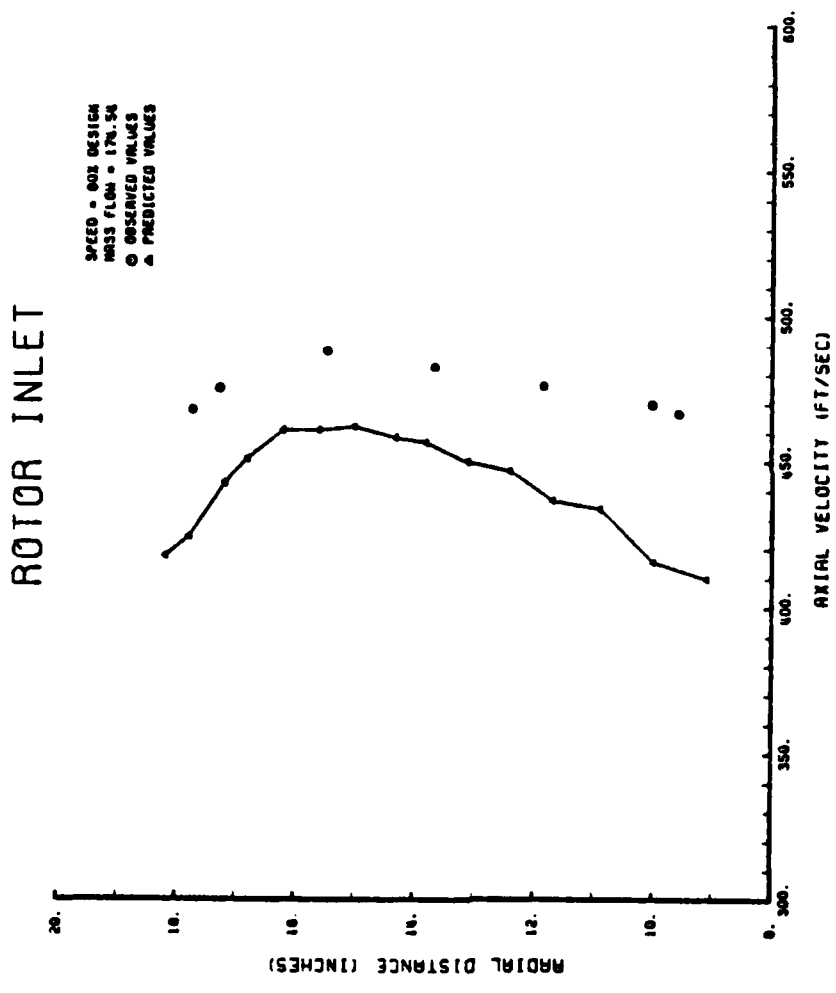


Figure 59. Axial Velocity at the Rotor Inlet, 80% Design

# ROTOR INLET

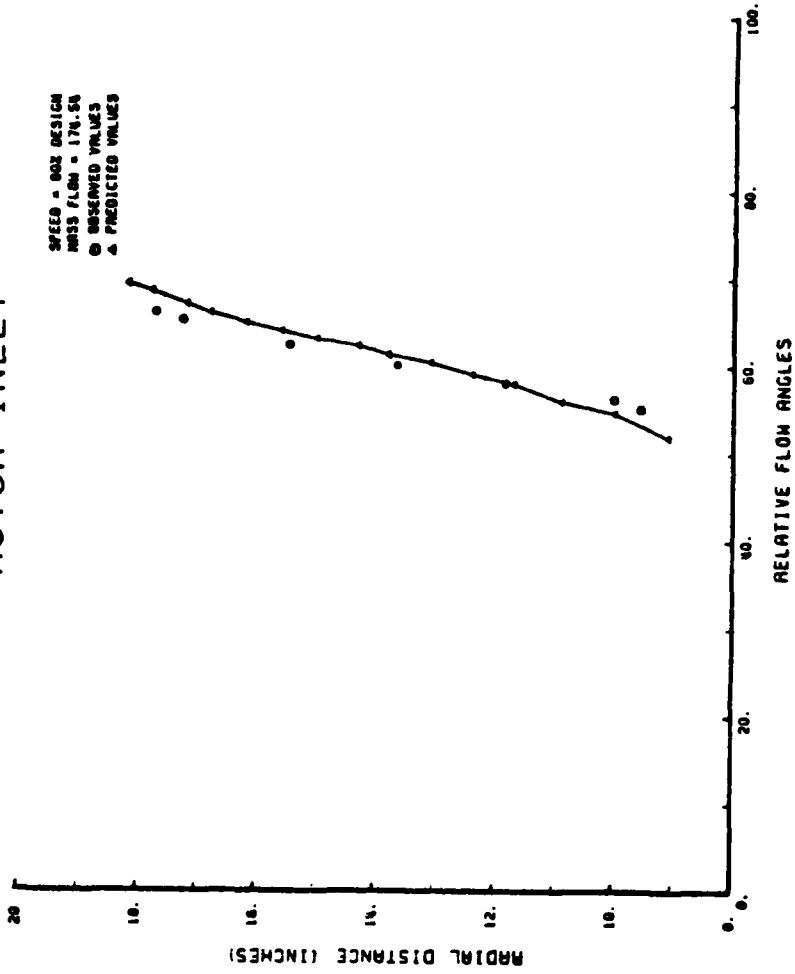


Figure 60. Relative Flow Angles at Rotor Inlet, 80% Design



# ROTOR INLET

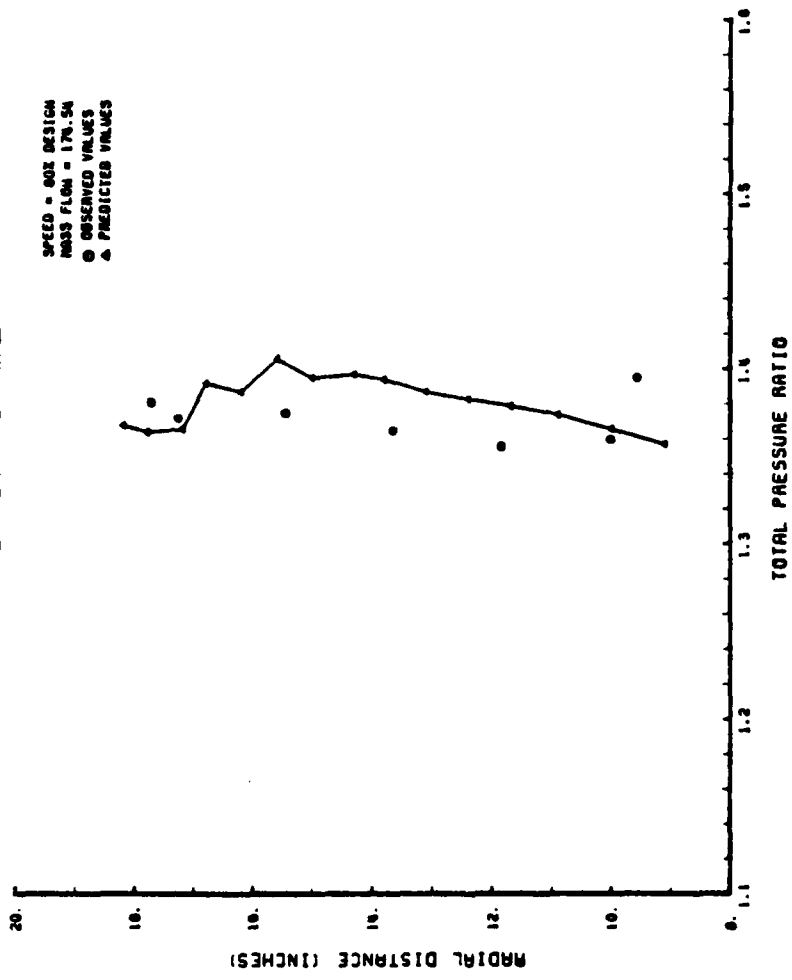


Figure 61. Total Pressure Ratio of the Rotor, 80% Design

# ROTOR INLET

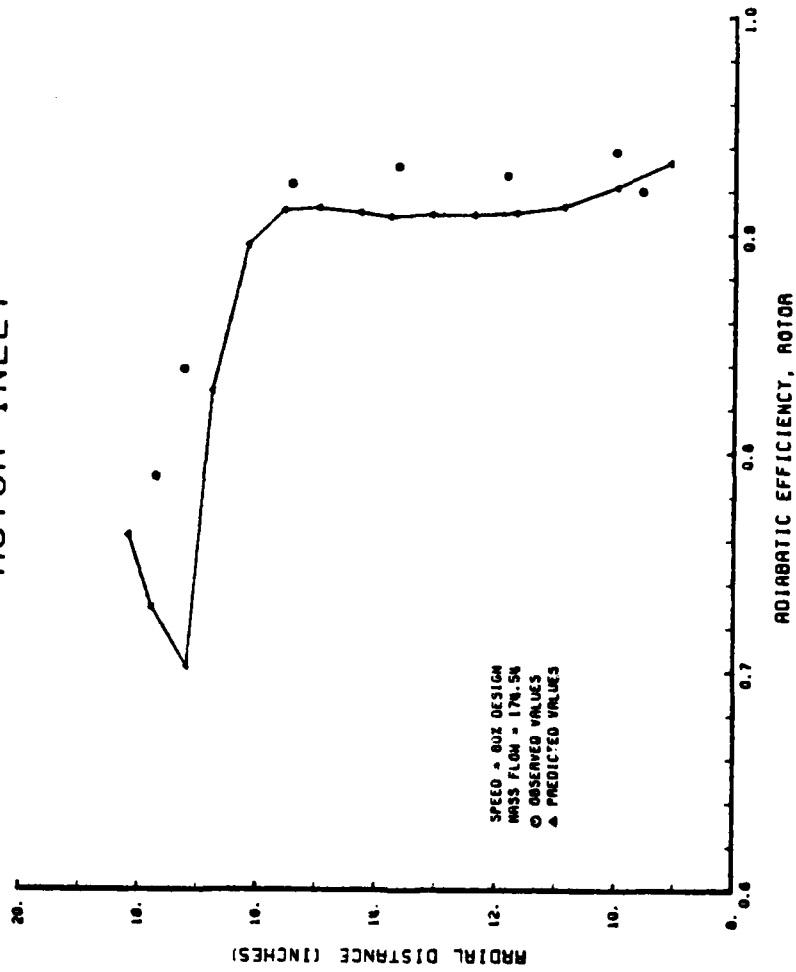


Figure 62. Adiabatic Efficiency of the Rotor, 80% Design

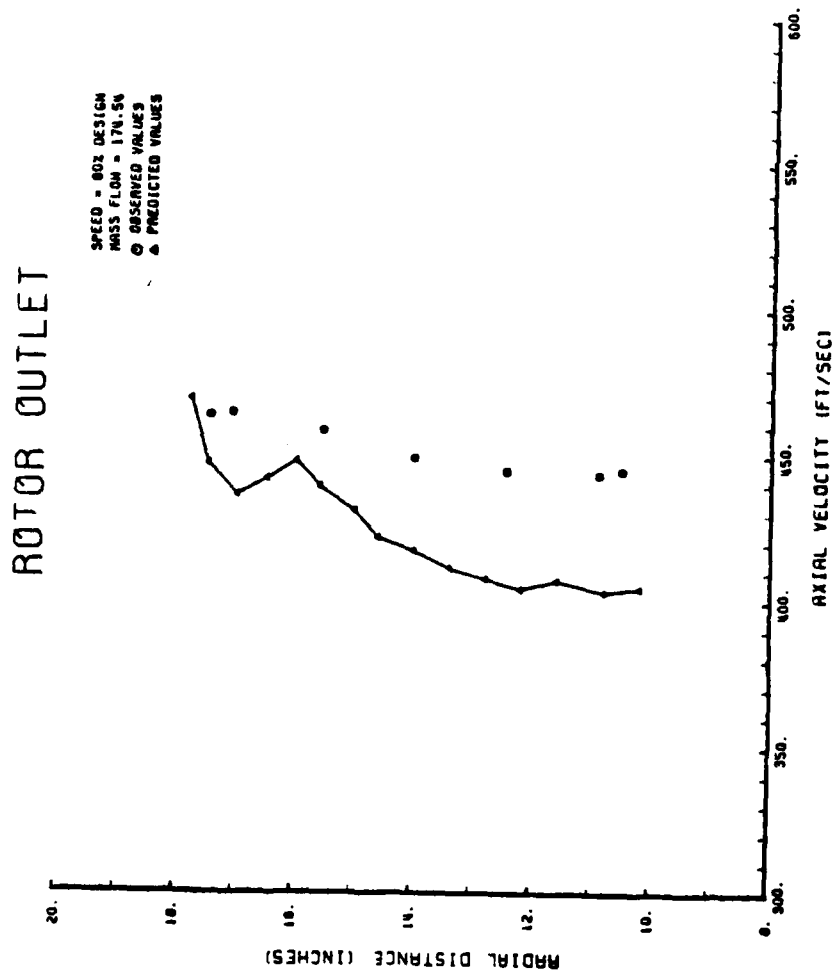


Figure 63. Axial Velocity at the Rotor Outlet, 80% Design

# ROTOR OUTLET

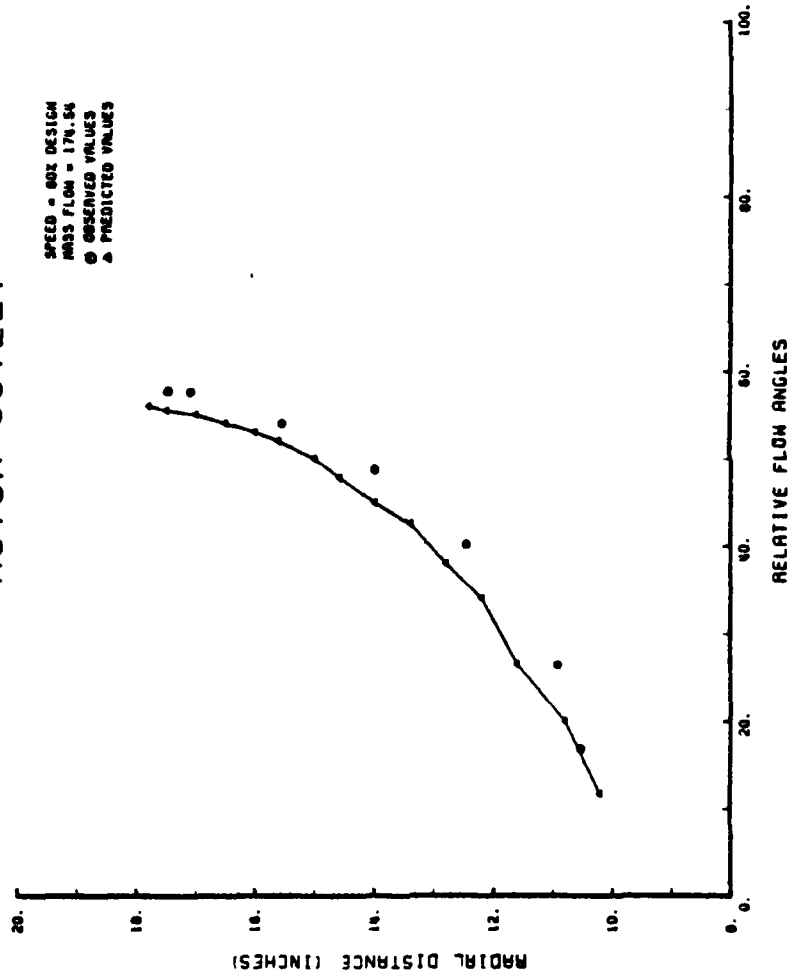


Figure 64. Relative Flow Angles at Rotor Outlet, 80% Design

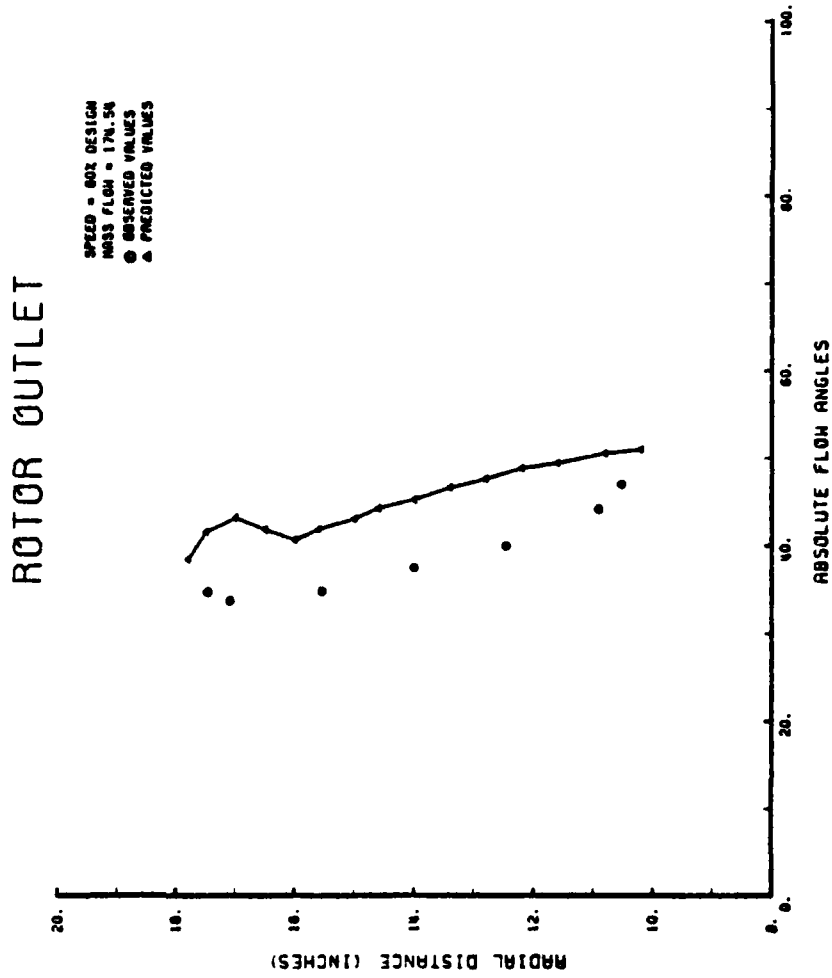


Figure 65. Absolute Flow Angles at Rotor Outlet, 80% Design

# ROTOR OUTLET

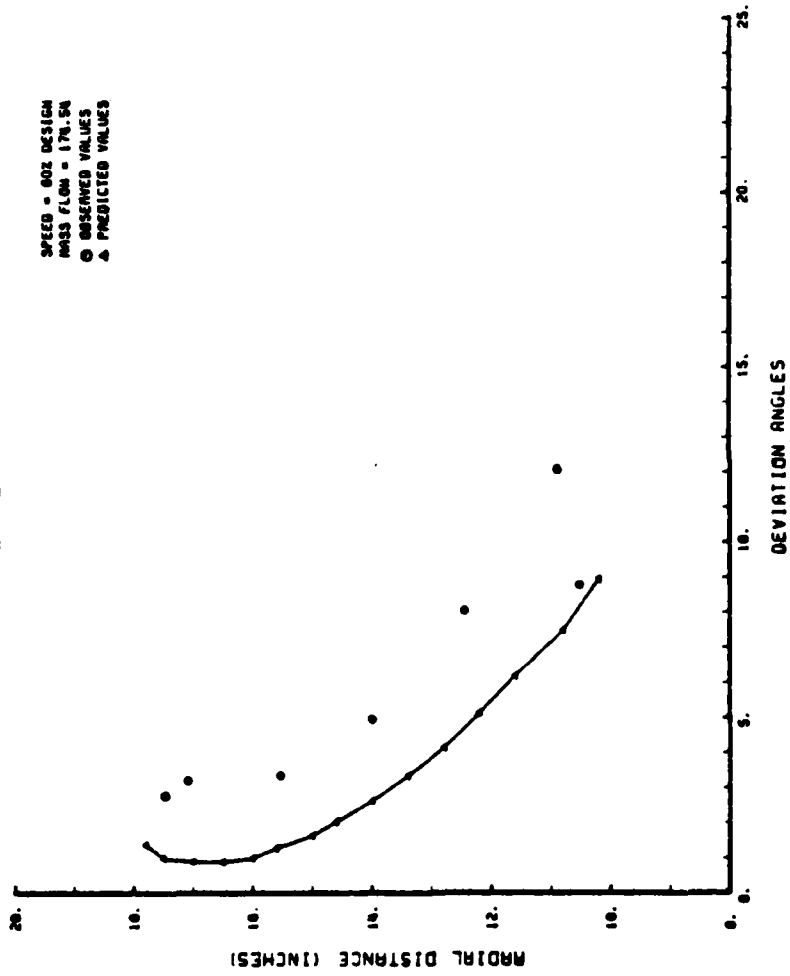


Figure 66. Deviation Flow Angles at Rotor Outlet, 80% Design

# STATOR INLET

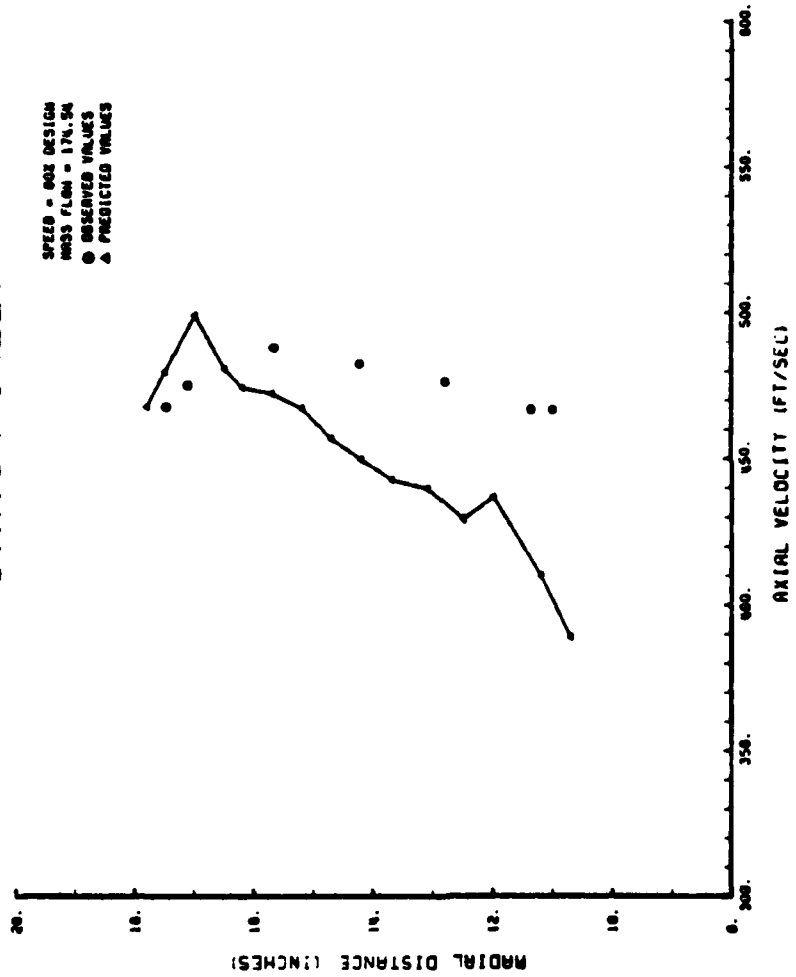


Figure 67. Axial Velocity at the Stator Inlet, 80% Design

# STATOR INLET

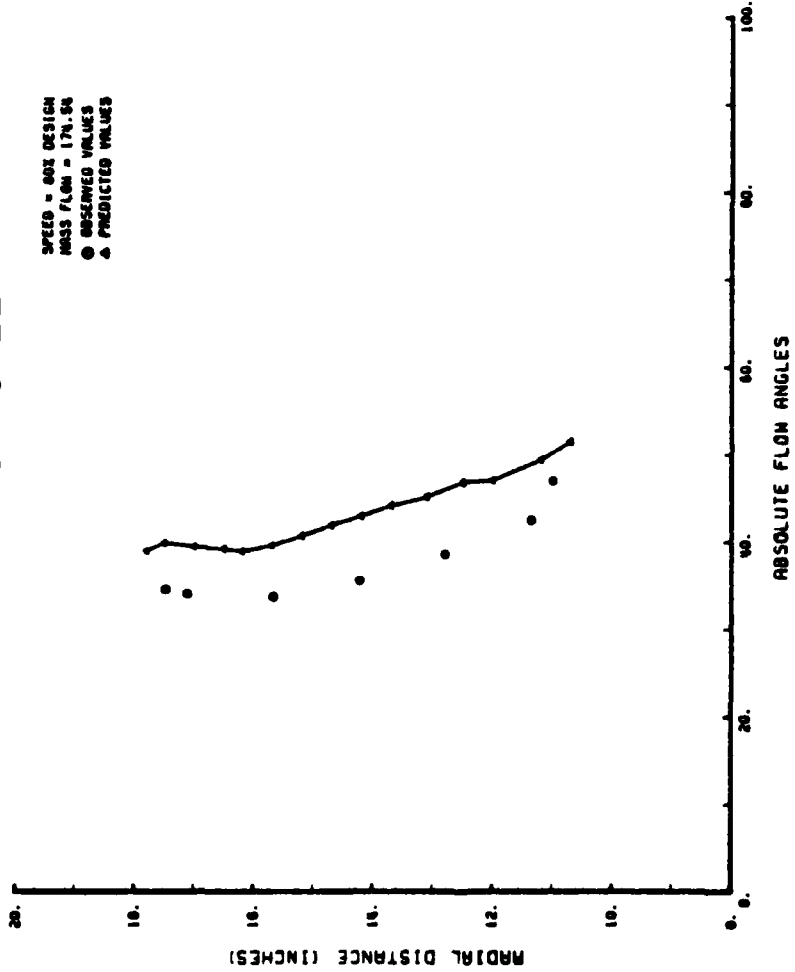


Figure 68. Absolute Flow Angles at Stator Inlet, 80% Design



# STATOR INLET

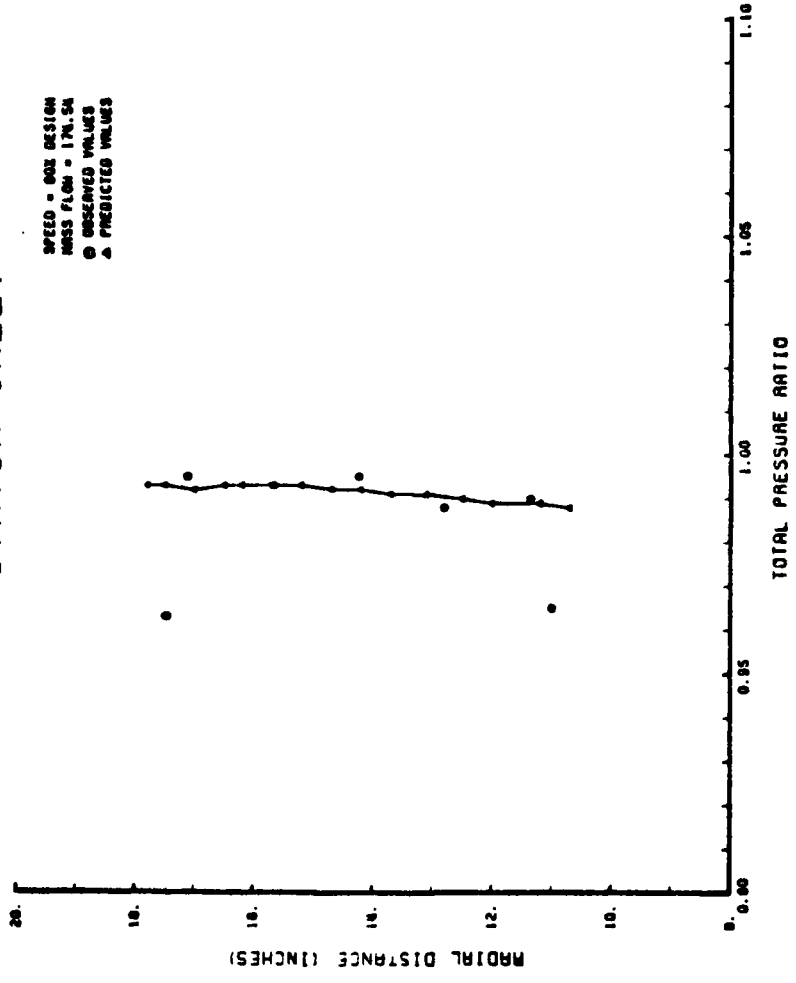


Figure 69. Total Pressure Ratio at Stator Inlet, 80% Design

# STATOR OUTLET

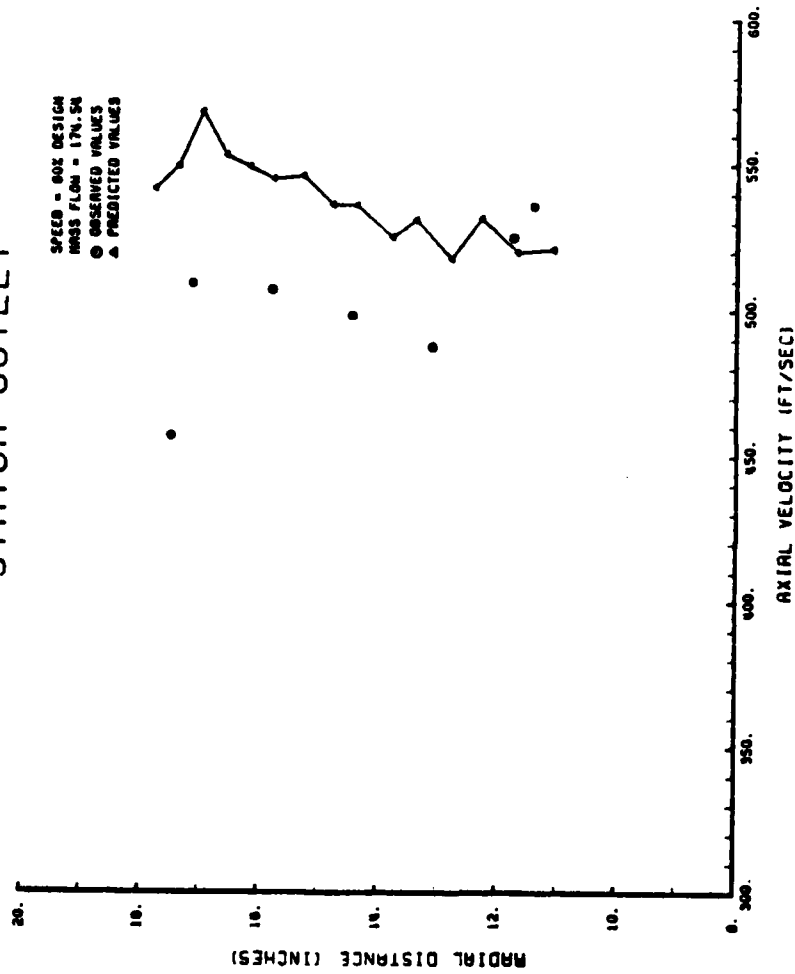


Figure 70. Axial Velocity at the Stator Outlet, 80% Design

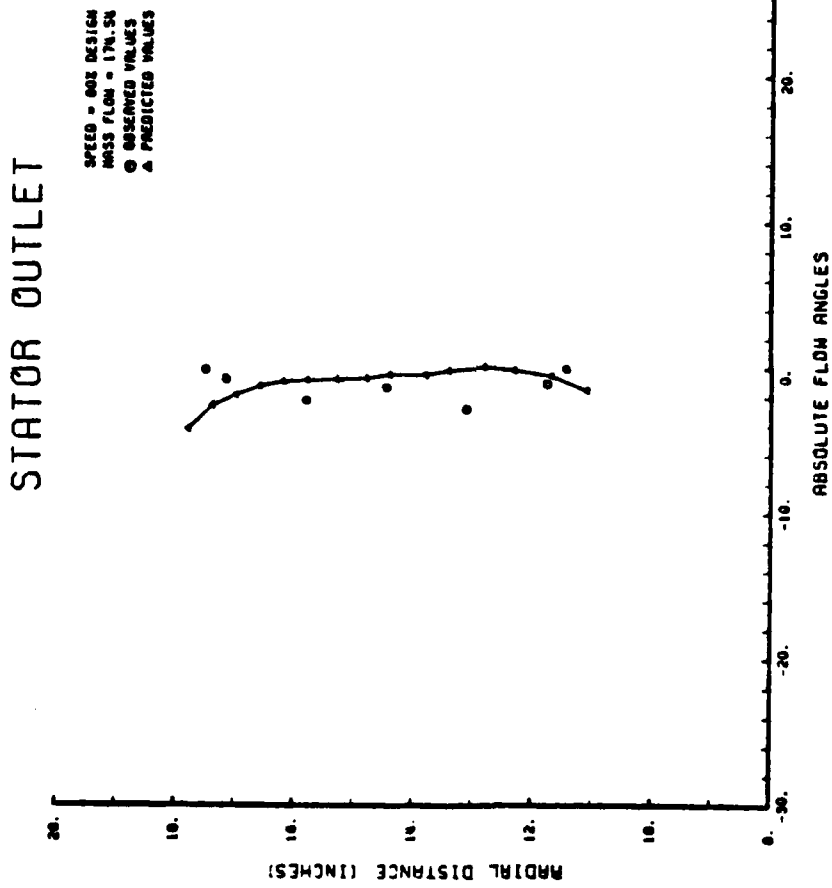


Figure 71. Absolute Flow Angles at Stator Outlet, 80% Design

# STATOR OUTLET

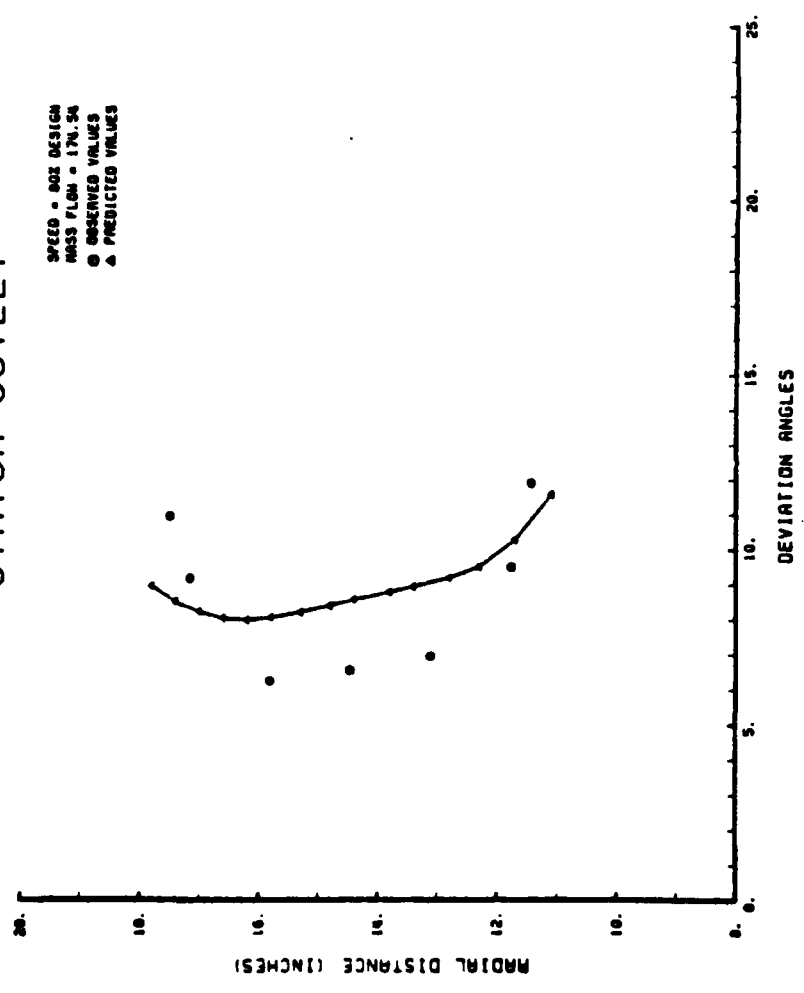


Figure 72. Deviation Flow Angles at Stator Outlet, 80% Design

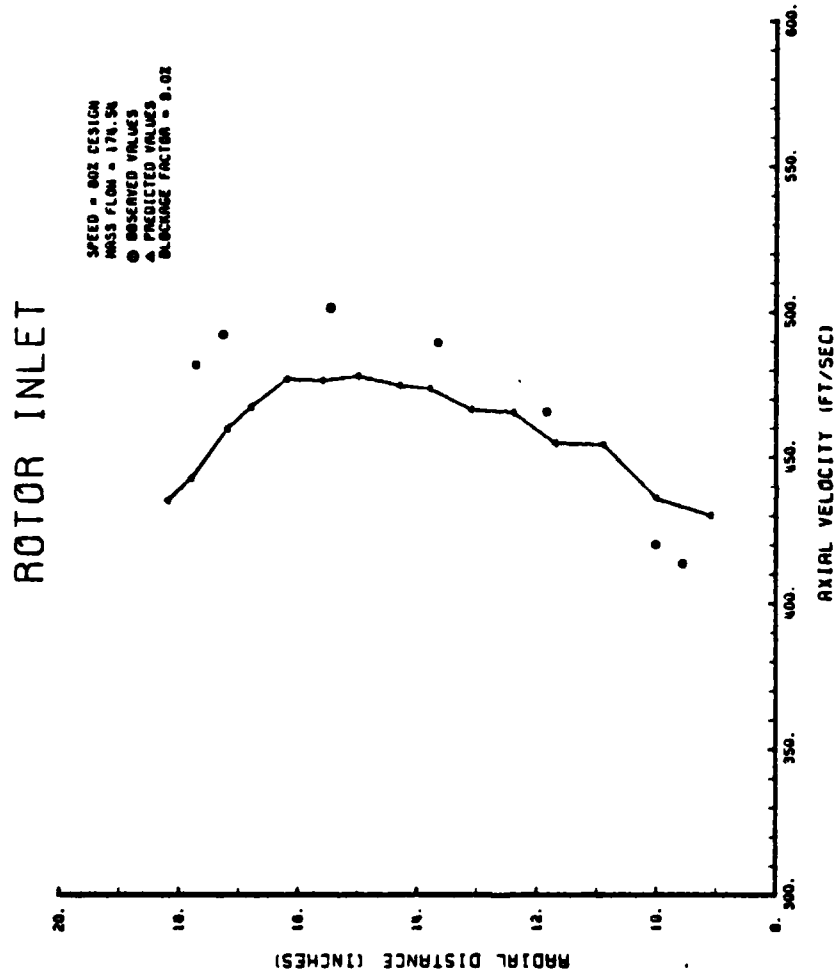


Figure 73. Axial Velocity at the Rotor Inlet, 80% Design, 9% Blockage

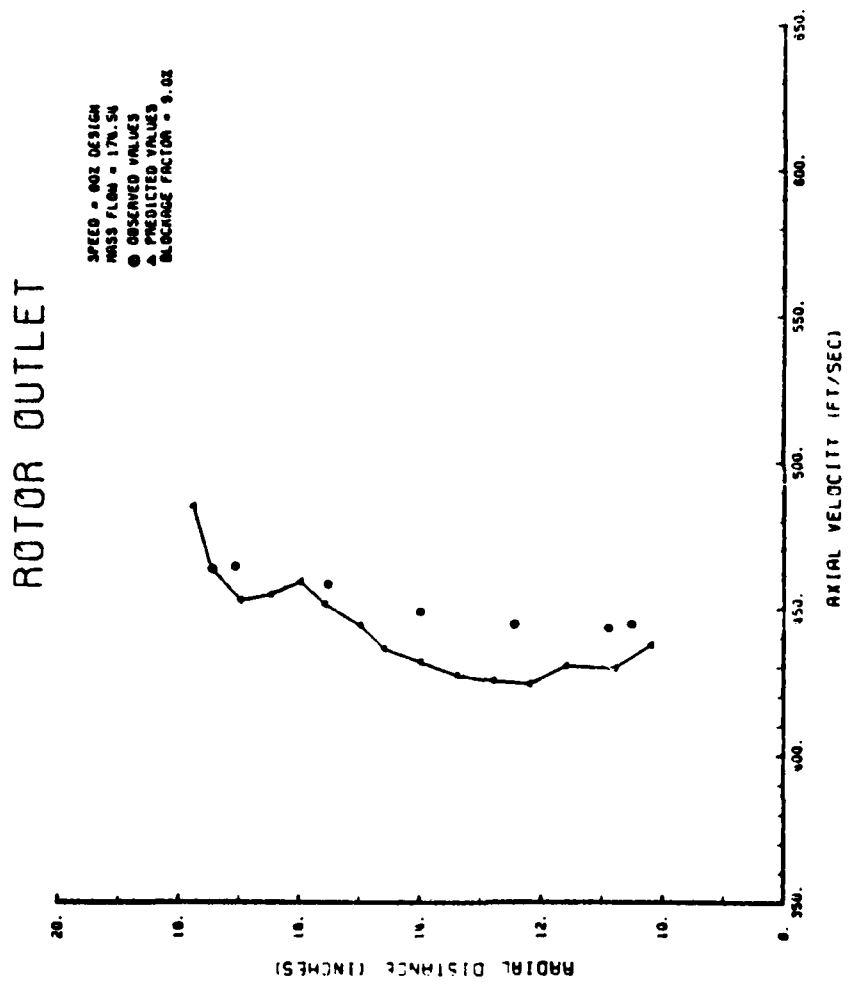


Figure 74. Axial Velocity at the Rotor Outlet, 80% Design, 9% Blockage

# STATOR INLET

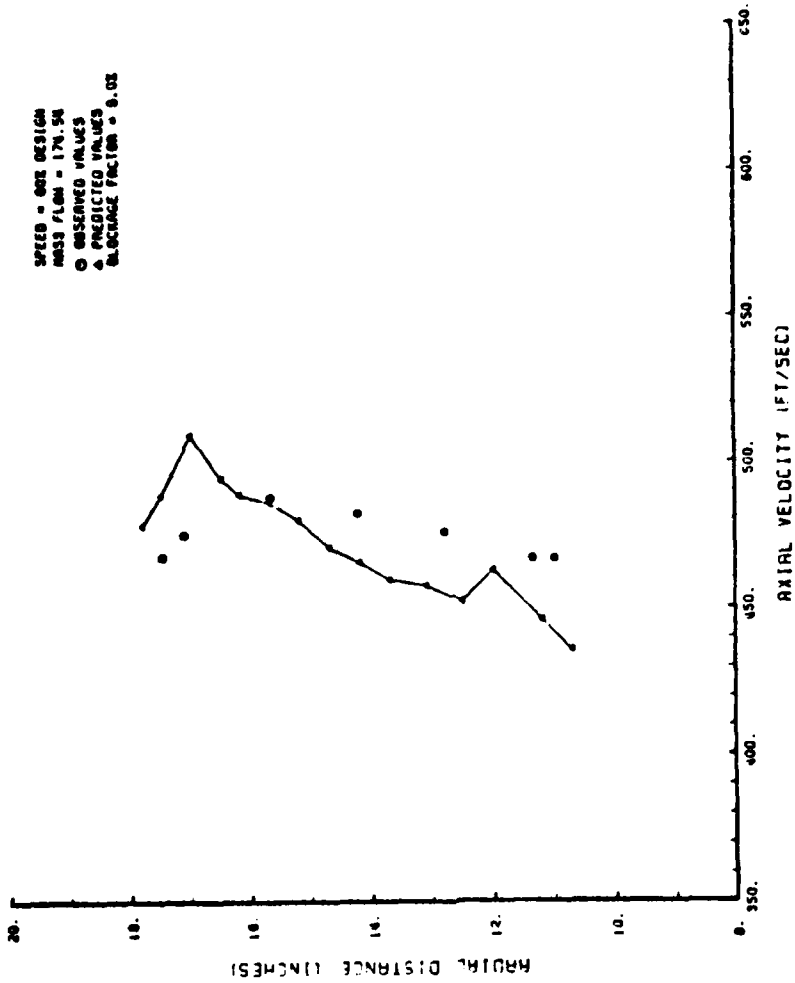


Figure 75. Axial Velocity at the Stator Inlet, 80% Design, 9% Blockage

# STATOR OUTLET

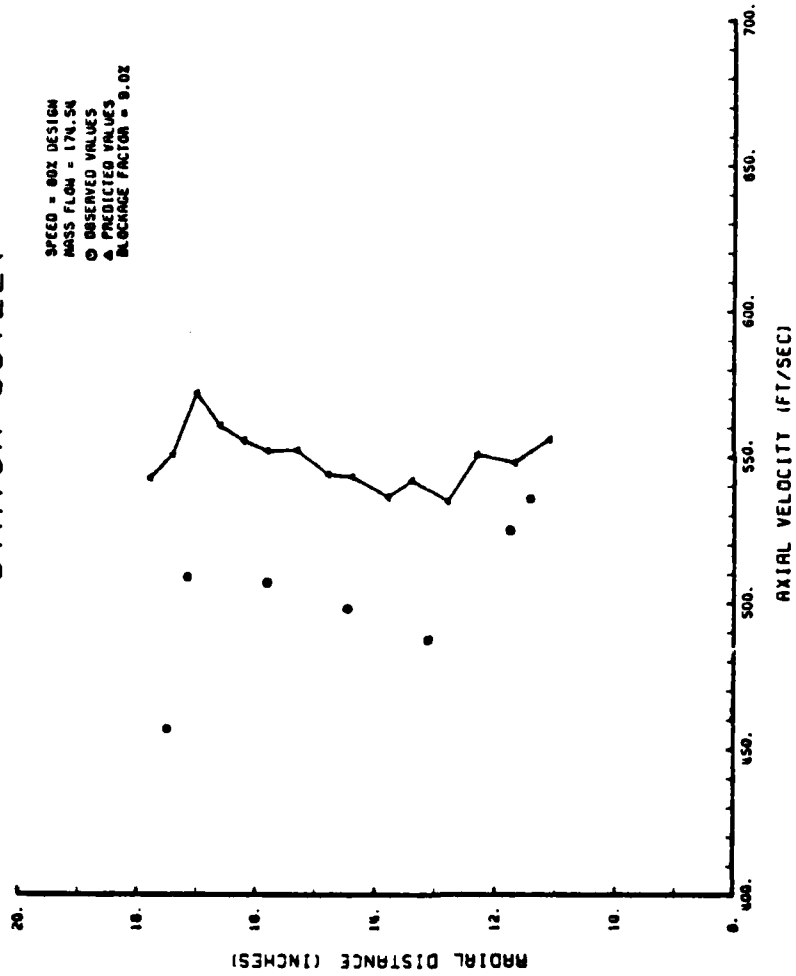


Figure 76. Axial Velocity at the Stator Outlet, 80% Design, 9% Blockage



APPENDIX A

STORAGE ALLOCATION FOR THE PROGRAM MESHGEN

The following list of pointers and variable names indicates the storage location of the first value of the corresponding array:

REAL 8 Variables (Array R8)

<u>Pointer Name</u>	<u>Array Name</u>	<u>Array Contents</u>
J1	XSE	Z Coordinates of the Super Elements
J2	YSE	R Coordinates of the Super Elements
J3	XXSE	Temporary Storage of the Z Coordinates of the Super Element Subdivision
J4	YYSE	Temporary Storage of the R Coordinates of the Super Element Subdivision
J5	ZC	Z Coordinates
J6	RC	R Coordinates
J7	PSI	Stream Function
J8	B	Blockage Factor
J9		End of Stored Values

REAL 4 Variables (Array 04)

<u>Pointer Name</u>	<u>Array Name</u>	<u>Array Contents</u>
M1	OHZC	Z Coordinates of Streamwise Element Boundaries
M2	OHRC	R Coordinates of Streamwise Element Boundaries
M3	OVZC	Z Coordinates of Transverse Element Boundaries
M4	OVRC	R Coordinates of Transverse Element Boundaries
M5	OHZC1	Z Coordinates of Streamwise Element Boundaries
M6	OHRC1	R Coordinates of Streamwise Element Boundaries
M7	OZC	Real 4 Z Coordinates of Mesh
M8	ORC	Real 4 R Coordinates of Mesh
M9		End of Stored Values

INTEGER 4 Variables (Array I2)

<u>Pointer Name</u>	<u>Array Name</u>	<u>Array Contents</u>
L1	NSEC	Number of Columns per Super Element
L2	NTSE	Super Element Type
L3	NTE	Element Type Identifier
L4	NODE	Connectivity Matrix
L5	NBC	Boundary Condition Nodes
L6		End of Stored Values

APPENDIX B

LISTING OF THE OUTPUT VARIABLES FOR THE PROGRAM MESHGEN

<u>FORTRAN Name</u>	<u>Variable</u>	<u>File</u>
ZC	Z Coordinate	TMESH DATA
RC	R Coordinate	TMESH DATA
B	Blockage Factor	TMESH DATA
PRESS	Inlet Static Pressure	FLUID DATA
PTOT	Inlet Total Pressure	FLUID DATA
TEMP	Inlet Static Temperature	FLUID DATA
TTOT	Inlet Total Temperature	FLUID DATA
RHOSTA	Inlet Static Density	FLUID DATA
RHOTT	Inlet Total Density	FLUID DATA
WDOT	Inlet Mass Flow	FLUID DATA
CP	Specific Heat	FLUID DATA
R	Gas Constant	FLUID DATA
G		FLUID DATA
RPM	RPM	FLUID DATA
VZI	Inlet Axial Velocity	FLUID DATA
NODE	Connectivity Matrix	NODE DATA
NTE	Element Type ID	NODE DATA

NBC

Boundary Nodes  
Where  $\psi$  Specified

BC DATA

PSI

Stream Function

STREAM DATA

## APPENDIX C

### STORAGE ALLOCATION FOR THE PROGRAM TURBO

The following list of pointers and variable names indicates the storage location of the first value of the corresponding array:

#### REAL 8 Variables (Array R8)

<u>Pointer Name</u>	<u>Array Name</u>	<u>Array Contents</u>
NP1	ZC	Z Coordinates
NP2	RC	R Coordinates
NP3	B	Blockage Factors
NP4	ALP	Absolute Flow Angles
NP5	BE	Relative Flow Angles
NP6	H	Total Enthalpy
NP7	HS	Static Enthalpy
NP8	VZ	Axial Velocity
NP9	VR	Radial Velocity
NP10	VU	Absolute Tangential Velocity
NP11	WU	Relative Tangential Velocity
NP12	PSI	Current Streamfunction Values
NP13	PSIO	Previous Streamfunction Value
NP14	F	Right-hand Side Vector
NP15	RHS	Temporary Storage for F
NP16	RHO	Static Density

NP17	RHON	Not Used
NP18	WRL	Angular Momentum Vector
NP19	ETA	Adiabatic Efficiencies
NP20	EM	Stiffness Matrix Elements
NP21	DEV1	Rotor/Stator Deviation Angles
NP22	PRAT	Total-to-Total Pressure Ratio
NP23	TEMP	Static Temperature
NP24	TTOT	Total Temperature
NP25	PRESS	Static Pressure
NP26	PTOT	Total Pressure
NP27	RHOTT	Total Density
NP28	HR	Rhothalpy
NP29	ENTROP	Entropy
NP30		End of Stored Values

REAL 4 Variables (Array 04)

<u>Pointer Name</u>	<u>Array Name</u>	<u>Array Contents</u>
NPO1	OVEL	Velocity at a Given Station
NPO2	ORC	R Coordinates
NPO3	OBE	Relative Flow Angles
NPO4	OALP	Absolute Flow Angles
NPO5		End of Stored Values

INTEGER 4 Variables (Array I2)

<u>Pointer Name</u>	<u>Array Name</u>	<u>Array Contents</u>
NPI1	NFS	Nodes for F Calculation
NPI2	NBC	Boundary Nodes
NPI3	NTE	Element Type Identifier
NPI4	NODE	Connectivity Matrix
NPI5		End of Stored Values

APPENDIX D

LISTING OF THE OUTPUT VARIABLES FOR THE PROGRAM TURBO

<u>Listing Name</u>	<u>Variable</u>	<u>Units</u>
PSI	Stream Function	lbm/sec
VZ	Axial Velocity	ft/sec
VR	Radial Velocity	ft/sec
R	Radius	inches
DENSITY	Static Density	lbm/ft <sup>3</sup>
WRL	Angular Momentum	ft <sup>2</sup> /sec
HT	Total Enthalpy	BTU/lbm
VT	Absolute Tangential Velocity	ft/sec
WT	Relative Tangential Velocity	ft/sec
HS	Static Enthalpy	BTU/lbm
TEMP	Static Temperature	°R
TTOT	Total Temperature	°R
PRESS	Static Pressure	psia
PTOT	Total Pressure	psia
RHOT	Total Density	lbm/ft <sup>3</sup>
ALPHA	Absolute Flow Angle	Degrees
BETA	Relative Flow Angle	Degrees



## APPENDIX E

## LISTING OF THE PROGRAM MESHGEN

FILE: MESHGEN FORTRAN AT NAVAL POSTGRADUATE SCHOOL

```
C *****
C *****
C                PROGRAM MESHGEN
C *****
C *****
C    THIS PROGRAM PRODUCES A RECTANGULAR EIGHT-NODED
C    ISOPARAMETRIC GRID OF ARBITRARY DIMENSION M X N GIVEN
C    THE CORNER COORDS OF THE MESH'S "SUPER ELEMENTS".
C    THE PROGRAM ALSO COMPUTES AN INITIAL STREAM FUNCTION
C    DISTRIBUTION, TANGENTIAL BLOCKAGE FACTORS AND THE
C    APPROPRIATE INLET CONDITIONS NEED FOR THE PROGRAM TURBO.
C    THE PROGRAM IS ONLY LIMITED BY THE SPACE ALLOCATED IN
C    THE ARRAYS R4, C4. 12 OR MACHINE LIMITATIONS.
C *****
C *****
C    IMPLICIT REAL*8(A-G,P-Z), REAL*4(H)
C    INTEGER*4 NR,MR,NC,NC1,IC,VRP 1,NE1, *M1, *M2, *M3, *M4, *NSF2, *N2
C    INTEGER*4 IANS
C    COMMON /INT4/  NR,MR,NC,NC1,IC
C    COMMON /ACCNT/  *M1,*M2,*M3,*M4,*NSF2,*N2
C    COMMON /NODES/  NR,NB,NC1,NC2,NE,NR1,NR2,NR3,NR4,NS1,NS2
C    COMMON /APRT/  J1,J2,J3,J4,J5,J6,J7,J8,J9,J10,J11,J12,J13,J14,
C    I1,I2,I3,I4,I5,I6,I7,I8,I9,I10,I11,I12,I13,I14,
C    I15,I16,I17,I18,I19,I20,I21,I22,I23,I24,I25,I26,I27,I28,I29,I30,
C    I31,I32,I33,I34,I35,I36,I37,I38,I39,I40,I41,I42,I43,I44,I45,I46,I47,
C    I48,I49,I50,I51,I52,I53,I54,I55,I56,I57,I58,I59,I60,I61,I62,
C    I63,I64,I65,I66,I67,I68,I69,I70,I71,I72,I73,I74,I75,I76,I77,I78,
C    I79,I80,I81,I82,I83,I84,I85,I86,I87,I88,I89,I90,I91,I92,I93,I94,I95,
C    I96,I97,I98,I99,I100
C    LIMIT = 3000
C    LIMIT = 3000
C    LIMIT = 3000
C
C    CALL INIT1(MR,NC,ACCL2,NSF,NSE2,WDDT,PTCT,TTCT,FRM,G,R,CP,ZMAX,
C    IZMIN,RMAX,PMIN,IANS)
C
C    CALL INPLT(RR(J1),RR(J2),I2(L1),I2(L2),NE1,NSE2,NSE,MR1,N2,I1V,
C    LIMT,LIM4,IANS)
C
C    CALL TMSH(RR(J1),RR(J2),RR(J3),RR(J4),RR(J5),RR(J6),I2(L1),
C    I2(L2),I2(L3),RR(J13),NSE2,NSE,N2,MR1,IANS)
C
C    CALL CONEC(I2(L2),I2(L3),I2(L4),NSF,N2,NE1,NR1O3,NR2O6,
C    INSTATB,NSTATE,IANS)
C
C    CALL INIT2(RR(6),I2(L4),I2(L5),RR(J7),PHOSTA,PHOTT,TTCT,WDDT,
C    IPTCT,PRSS,TEMP,VZ1,R,CP,G,NSF2,MR1,N2,NSE,RR1,IANS)
C
C    IF (IANS.EQ.2) GOTO 100
C
C    CALL TASK1(RR(J6),RR(J13),NSE2,MR1,N2,NR1O3,NR2O6,NSTATE,
C    INSTATE)
C
C 100 CALL FILENV(RR(J5),RR(J6),RR(J13),RR(J7),I2(L4),I2(L3),I2(L5),
C    IPRESS,PTCT,TEMP,TTCT,PHOSTA,PHOTT,VZ1,WDDT,RPM,CP,P,G,NR1O6,
C    INSTATB,NSE2,NSE,N2,MR1,NE1,IANS)
C
C 200 WRITE (15,200)
C     FORMAT(6X,' DO YOU WANT A PLOT OF THE MESH?',/, ' 1 = YES
C     ' 2 = NO.')
C *****
```

FILE: MESHGEN FORTRAN A1 NAVAL POSTGRADUATE SCHOOL

```
      READ(15,*) IANS
      IF(IANS.EQ.2) GOTO 300
C
      CALL MFLCT(2*(J5),F8(J6),ZMAX,ZMIN,RMAX,RMIN,C4(M1),C4(M2),
1    IC4(M3),C4(M4),C4(M5),C4(M6),C4(M7),C4(M8),I2(L5),NSE2,MRF1,
2    ZA2,ASE,NE1,NC2,M42)
C
C
300   STOP
     FAC
C
C
      SUBROUTINE INIT1(MROW2,NCCL2,NSE,NSE2,WOOT,PTOT,TTCT,RPM,G,R,CP,
1    ZMAX,ZMIN,FMAX,RMIN,IANS)
      IMPLICIT REAL*(A-G,P-Z), REAL*4(H)
      INTEGER*4 MR,MRI,NC,NC1,IC,MRF1,NE1,MN1,MN2,MN3,MN4,NSE2,N2
      INTEGER*4 IANS
      COMMON /INT4/ MR,MRI,NC,NC1,IC
      COMMON /MROW/ MROW,MROW1,MNSEC
      COMMON /MROW2/ MR,MRF1,NC,NCL1,NE,PTOT,NSTAT
      COMMON /MPOINT/ J1,J2,J3,J4,J5,J6,J7,J8,J9,J10,J11,J12,J13,J14,
1    L1,L2,L3,L4,L5,L6,M1,M2,M3,M4,M5,M6,M7,M8,M9
      WRITE(15,100)
      FCMMAT(5X,1) >ENTER INLET CONDITIONS: '/,.' MASS FLOW(LBM PER SEC)
1    1 TOTAL TEMP(DLG R) AND TOTAL PRESS(PSIA)'/)
      READ(15,*) WOOT,TTCT,PTOT
      WRITE(15,110)
      FCMMAT(5X,1) >ENTER OPERATING CONSTANTS: '/,.' RPM'/,.' RATIO OF
1    SPECIFIC HEATS (GAMMA)'/,.' GAS CONSTANT (FT-LBF/LBM-DEG R)'/,.'
2    SPECIFIC HEAT CONSTANT PRESSURE CP(BTU/LBM-DEG R)'/,.'
      READ(15,*) RPM,G,R,CP
      WRITE(15,120)
      FCMMAT(5X,1) >ENTER GRAPH SCALING CONSTANTS: '/,.' Z MAX'/,.' Z
1    MIN'/,.' Z MAX'/,.' R MIN'/,.'
      READ(15,*) ZMAX,ZMIN,RMAX,RMIN
      WRITE(15,50)
      FCMMAT(5X,1) >DO YOU WANT TO CREATE A NEW MESH ?'/,.' 1 = YES
1    2 = NO'/)
      READ(15,*) IANS
      IF(IANS.EQ.1) GOTO 140
130   READ(15,130) MR,MROW,NCCL,MROW1,NCCL1,MROW2,NSTATS
      FCMMAT(7I5)
      GOTO 201
145   WRITE(15,200)
200   FCMMAT(5X,1) >ENTER NO OF SUPER ELEMENTS AND NO ELEMENT ROWS',/ )
201   READ(15,*) ISEC,MROW
      MROW1 = 2 * MROW + 1
      MRI = MROW1 - 1
      MR = MROW
      MROW2 = MROW1
      NCCL2 = NCCL1
      NSE2 = 2*NSE + 2
      J1 = 1
      J2 = J1 + NSE2
      J3 = J2 + NSE2
      L1 = 1
      L2 = L1 + NSE
      L3 = L2 + NSE
      RETURN
     END
C
C
      SUBROUTINE INPUT(XSE,YSE,NSEC,ATSE,NE1,NSE2,NSE,MRR1,N2,LIMP,
1    LIMP1,LIMP4,IANS)
      *****
      *****
      *****
      *****
      THIS SUBROUTINE CONTAINS THE DESCRIPTION OF THE SUPER ELEMENTS
      *****
      *****
      *****
      *****
C
```

FILE: MESHGEN FORTRAN A1 NAVAL POSTGRADUATE SCHOOL

```
C
  IMPLICIT REAL*8(A-H,P-Z)
  INTEGER*4 NR,MF1,NC,NC1,IC,MRR1,NE1,MN1,MN2,MN3,MN4,NSE2,N2
  INTEGER*4 IANS
  COMMON /INT4/ NR,MF1,NC,NC1,IC
  COMMON /NCCOUNT/ MR0W,MROW1,MNSEC
  COMMON /ACOUNT/ AN,ACCL,ACCL1,AE,NPOTC,NSTAT
  COMMON /MPINT/ J1,J2,J3,J4,J5,J6,J7,J8,J9,J10,J11,J12,J13,J14,
  I1,I2,I3,I4,I5,I6,I7,I8,I9,I10,I11,I12,I13,I14,
  I1,I2,I3,I4,I5,I6,I7,I8,I9,I10,I11,I12,I13,I14,
  DIMENSION XSE(1),YSE(1)
  DIMENSION NSEC(1),NTSE(1)
```

```
C
  IF(IANS.EQ.2) GOTO 202
  NCCL = 0
  J = 1
  NSE22 = NSE2/2
  DO 100 I = 1,NSE22
    WRITE(15,101) I
    FOR MAT(5X,' ENTER 2, R COORDINATE PAIRS FOR STATION ',I2/)
    READ(15,*) XSE(J),YSE(J),XSE(J+1),YSE(J+1)
    J = J + 2
  100 CONTINUE
  DO 200 I = 1,NSE
    WRITE(15,201) I
    FOR MAT(5X,' ENTER TYPE OF SUPER ELEMENT AND THE NO OF COLUMNS F
  201 OR SUPER ELEMENT ',I2/)
    READ(15,*) NTSE(I),NSEC(I)
    NCCL = NCCL + NSEC(I)
  200 CONTINUE
  402
  NE1 = MR0W + NCCL
  NE1 = NE
  NCCL1 = 2 * NCCL + 1
  MN = NCCL1 * MROW1 - MROW * NCCL
  MN2 = MN
  MRR1 = MROW1
  J1 = 1
  J2 = J1 + NSE2
  J3 = J2 + NSEC22
  J4 = J3 + NSEC22
  J5 = J4 + MRR1
  J6 = J5 + N2
  J7 = J6 + N2
  J8 = J7 + N2
  J9 = J8 + N2
  J10 = J9 + N2
  J11 = J10 + N2
  J12 = J11 + N2
  J13 = J12 + N2
  J14 = J13 + N2
  I1 = 1
  I2 = I1 + NSE
  I3 = I2 + NSEC1
  I4 = I3 + NSEC1
  I5 = I4 + 3*NSE1
  I6 = I5 + NSE1
  N1 = 1
  N2 = N1 + NCCL1
  N3 = N2 + NCCL1
  N4 = N3 + MRR1
  N5 = N4 + MRR1
  N6 = N5 + NCCL1
  N7 = N6 + NCCL1
  N8 = N7 + N2
  N9 = N8 + N2
  NEXCR = LIVR - J14
  NEXCI = LIVR - I6
  NEXC4 = LIVR - MRR1
  IF(NEXCR.LT.0) CALL SUBR1(NEXCR)
  IF(NEXCI.LT.0) CALL SUBR2(NEXCI)
  IF(NEXC4.LT.0) CALL SUBR3(NEXC4)
  WRITE(6,200) NEXC4,NEXCI
```

FILE: MESHGEN FCRTFRAN A1 NAVAL POSTGRADUATE SCHOOL

```
300  FORMAT(1CX,' MEMCFY SPACE AVAILABLE : REAL =',I5,2X,' INTEGER = '  
1, I5//')  
RETURN  
END
```

C  
C

```
      SUBROUTINE TRESH(XSE,YSE,XXSE,YYSE,ZC,RC,NSEC,NTSE,NTE,  
1B,NSEC2,NSE,N2,MFC1,IANS)
```

```
C *****  
C *****  
C *****  
C *****  
C *****  
C *****  
C *****  
C *****  
C *****  
C *****  
C *****
```

```
      ** THIS SUBROUTINE PRODUCES A RECTANGULAR EIGHT-NODED  
      ** ISOPARAMETRIC GRID OF ARBITRARY DIMENSION M X N GIVEN  
      ** THE CORNER NODES OF THE MESH'S "SUPER ELEMENTS"  
      **
```

C

```
      IMPLICIT REAL*8(A-H,F-Z)  
      INTEGER*4 NR,MRI,NC,NC1,IC,MRR1,NE1,MN1,MN2,MN3,MN4,NSEC2,N2  
      INTEGER*4 IANS  
      COMMON /INT4/ NR,MRI,NC,NC1,IC  
      COMMON /NCCOUNT/ MRCW,MRCW1  
      COMMON /NCCOAT/ MN,NCOL,NCOL1,NE,IPJTC,NSTAT  
      DIMENSION XSE(1),YSE(1),XXSE(1),YYSE(1),ZC(1),RC(1),B(1)  
      DIMENSION NSEC(1),NTSE(1),NTE(1)
```

12

```
      IF(IANS.EC.1) GOTO 20  
      DO 11 I=1,MN  
        READ(2C,12) ZC(I),RC(I),B(I)  
        FORMAT(2F15.11)
```

11

```
      CONTINUE  
      GOTO 100  
      YDIV1 = FLCAT(MR1)  
      YDIV2 = FLCAT(M2)
```

20

```
      I = 1  
      J = 1  
      IL = 1  
      IM = 1  
      NSTAT = C  
      MFC1 = C  
      DO 10 N = 1, MN  
        ZC(N) = J.DC  
        RC(N) = O.DC
```

10

```
      CONTINUE  
      DO 140 J = 1, NSEC  
        IF(J.EC.1) GOTO 120  
        IF(NTSE(J)-NTSE(J-1)) 120,120,140  
        IF(IM.LT.3) GOTO 150  
        AROT = IL  
        IM = C - IM
```

140

```
        GOTO 120  
        NSTAT = IL  
        IM = C - IM  
        IT = NSEC(J) + MRCW  
        DO 110 L = 1, IT  
          NTE(IL) = NTSE(J)  
          IL = IL + 1
```

150

120

110

```
      CONTINUE  
      NNCOL1 = 2 + NSEC(J) + 1  
      NC1 = NCOL1  
      NC = NC1 - 1  
      XDIV1 = FLCAT(NC1)  
      XDIV2 = FLCAT(NC)  
      X1 = XSE(I)  
      X2 = XSE(I + 1)  
      X3 = XSE(I + 2)  
      X4 = XSE(I + 3)  
      Y1 = YSE(I)  
      Y2 = YSE(I + 1)  
      Y3 = YSE(I + 2)
```

```

Y4 = YSE(I + 3)
XDIF2 = X3 - X1
XDIF3 = X4 - X2
YDIF2 = Y1 - Y3
YDIF3 = Y2 - Y4
XINT2 = XDIF2 / XDIV2
XINT3 = XDIF3 / XDIV3
YINT2 = YDIF2 / YDIV2
YINT3 = YDIF3 / YDIV3
ISEL = -1
DO 200 K = 1, NCL
  XCIF1 = X1 - X2
  YCIF1 = Y1 - Y2
  IF (ISEL) 210, 210, 220
  XINT1 = XCIF1 / YDIV1
  YINT1 = YCIF1 / YDIV1
  MRR = MRCW1
  GOTO 230
210 XINT1 = XCIF1 / YDIV2
  YINT1 = YCIF1 / YDIV2
  MRR = MRCW + 1
220 DC 230 IC = 1, MPR
  ICI = IC - 1
  XXSE(ICI) = X1 - FLOAT(IC - 1)*XINT1
  IF (IC.NE.1) GOTO 231
  YYSE(IC) = Y1
  GOTO 232
231 YYSE(IC) = CSOPT(YYSE(ICI)*YYSE(ICI) - YINT1)
232 ZC(IJ) = XXSE(IC)
  RC(IJ) = YYSE(IC)
  IJ = IJ + 1
200 CONTINUE
  X1 = X1 + XINT2
  X2 = X2 + XINT3
  Y1 = Y1 - YINT2
  Y2 = Y2 - YINT3
  ISEL = -ISEL
200 CONTINUE
  ISEL = -ISEL
  IJ = IJ - MRCW1
  I = 2*IJ + 1
100 CONTINUE
WRITE(6,400) MRCW, NCOL
400 FORMAT(1CX, ' NUMBER OF ROWS = ', I3, '1EX, ' NUMBER OF COLUMNS = ',
1, I3)
WRITE(6,410) NE, AN
410 FORMAT(5X, ' TOTAL NUMBER OF ELEMENTS = ', I4, '10X,
1, ' TOTAL NUMBER OF NODES = ', I4//)
RETURN
END

C
C
SUBROUTINE CONEC (NTSE, NTE, NODE, NSE, N2, NE1, MPROT09, NROTC, NSTAT8,
INSTATE, IANS)
C
C *****
C
C THIS SUBROUTINE PRODUCES THE CONNECTIVITY MATRIX
C
C *****
C
IMPLICIT REAL*8 (A-H, I-Z)
INTEGER*4 M, M1, NC, NCL, IC, MRR1, NE1, MA1, MN2, MN3, MN4, NSEC, N2
INTEGER*4 IANS
COMMON /ACCOUNT/ M, MRCW, MRCW1, MNSC
COMMON /ACOUNT/ M, NCOL, NCL1, NE, NROTC, NSTAT
COMMON /INTS/ M, M1, NC, NCL, IC
DIMENSION NODE (M, 1, 1), NTSE(1), NTE(1)
IF (IANS.EC.2) GO TO 601
K = 1
MK = 1

```

```

NRCTOR = C
NRCTCR = C
NSTATR = C
NSTATE = C
C = 1.00
40 IC = 1, NE1
K1 = K + MRCW1 + MRCW + 1
K2 = K1 - MRCW - MK
K3 = K
K4 = K + 1
K5 = K2 + 2
K6 = K2 + 2
K7 = K1 + 2
K8 = K1 + 1
NODER(IC,1) = K1
NODER(IC,2) = K2
NODER(IC,3) = K3
NODER(IC,4) = K4
NODER(IC,5) = K5
NODER(IC,6) = K6
NODER(IC,7) = K7
NODER(IC,8) = K8
K = K + 2
MK = MK + 1
CO = FLCAT(IC)/FLCAT(MR)
IF(CO.NE.0) GOTO 40
K = 2 + 4R + 2
MK = 1
C = C + 1.00
40 CONTINUE
64 WRITE(6,64)
FORMAT(10)
WRITE(6,64)
IF(INOTE.EQ.0.AND.NSTAT.EQ.0) GOTO 600
IJK1 = NRCTCR
IJK2 = NRCTCR + MRCW - 1
IJK3 = NSTATR
IJK4 = NSTATR + MRCW - 1
NRCTCR = NODER(IJK1,3)
NRCTCR = NODER(IJK2,7)
NSTATR = NODER(IJK3,3)
NSTATR = NODER(IJK4,7)
CONTINUE
GOTO 600
601 CC 700 I = 1, NE1
      REAC(1,IC) = NODER(I,1),NODER(I,2),NODER(I,3),NODER(I,4),
1      NODER(I,5),NODER(I,6),NODER(I,7),NODER(I,8),ITE(I)
710   FOR MAT(1,1)
700   CONTINUE
600   RETURN
      END
C
C
SUBROUTINE INIT2(IC,NODE,NBC,PSI,XHO,STA,SHOTT,TTCT,WDCY,PTCT,
1 PRESS,TEMP,VZ1,C,CP,B,NSF2,MRP1,MR2,NSF,NE1,INS)
C
C *****
C
C THIS SUBROUTINE COMPUTES THE INLET CONDITIONS
C THROUGH THE USE OF SUBROUTINE FLOCT.
C SUBROUTINE ALSO DETERMINES THE NODER NUMBERS
C WHERE THE VALUES OF PSI ARE TO BE SPECIFIED.
C THE SUBROUTINE COMPUTES THE INITIAL DISTRIBUTION
C OF THE STREAM FUNCTION FROM THE INLET CONDITIONS
C AND THE BOUNDARY CONDITIONS OF THE PROGRAM TUBC.
C *****
C
IMPLICIT REAL*8(A-H,P-Z)
INTEGER*4 MR, MRP1,NC,NC1,IC,MRP1,NE1,MN1,MN2,MN3,MN4,NSF2,N2

```

FILE: MESHGEN FORTRAN A1 NAVAL POSTGRADUATE SCHOOL

```
INTEGER*4 IANS
COMMON /ACCOUNT/ MRCH, MROW1, MNSFC
COMMON /ACCOUNT/ MR, MCOL, NCOL1, NE, NROTC, NSTAT
COMMON /INT4/ MR, MRP1, NC, NCI, IC
DIMENSION FC(1), PSI(1)
DIMENSION NODE(NEL,1), NBC(1)
G = 1.4CC
R = 53.2CC
CC = 32.17400
IF(IANS.EQ.1) GOTO 10
NMC = 2 * NCOL1 + MROW1 - 2
CC 700 I = 1, NMC
    READ(25,710) NEC(I)
    FORMAT(15)
71C
70C CCNTINUE
    GOTO 300
10 CC 100 I = 1, MRR1
    NBC(I) = I
10C CCNTINUE
    MN = I
    MK = I
    K = MRR1 + 1
    JK = K
    L = MRP1 + 1
    M = 2 * (NCOL1 - 1) + K
    CC 200 J = K, M
        IF(MN.GT.0) GOTO 210
        NBC(K) = L
        K = K + 1
        L = L + 1
        MM = C - MM
21C GOTO 200
        IF(MK.GT.0) GOTO 220
        NRC(K) = L
        L = L + MRCH1 - 1
        MK = C - MK
        K = K + 1
        MM = C - MM
22C GOTO 200
        NBC(K) = L
        L = L + 4RCH
        MK = C - MK
        K = K + 1
        MM = C - MM
20C CCNTINUE
    K = MRR1 + 2 * (NCOL1 - 2) + 1
    JK = N2 - MRR1 + 1
    NBC(K) = J
    NBC(K+1) = N2
300 CCNTINUE
    GM1 = G - 1.00
    GM2 = 1.00 / GM1
    RFLC2 = FC(MRCH1) * FC(MROW1)
    ARF1 = 3.141592654 * (RC(1) * RC(1) - RHUR2) / 144.000
    CALL FLCFCT(WOCT, PTCT, TTCT, RHCTT, VTDJ, XVEL, CP, R, GM1, GM2,
1 AFEA)
    CLANT = 1.000 - XVEL * XVEL
    TEMP = TTCT * CLANT
    PRESS = FTCT * CLANT** (G*GM1)
    RFLCSTA = *HOTT * CLANT**GM1
    VZ1 = VICT * XVEL
    NC = MRCH1 - 1
    PS11 = WOCT / (2.000 * 3.141592654)
    PS10 = PS11 / FLCAT(NC)
    J = 0
    CC 500 I = 1, NC
        PSI(I) = PS11 - FLCAT(J) * PS10
        J = J + 1
500 CCNTINUE
    PSI(MRCH1) = 0.0000000000000000
    CC 600 I = 1, NEL
        N11 = NODE(I,1)
```

FILE: MESHGEN FORTRAN A1 NAVAL POSTGRADUATE SCHOOL

```
N12 = NCDEF(1,2)
N13 = NCDEF(1,3)
N14 = NCDEF(1,4)
N15 = NCDEF(1,5)
N16 = NCDEF(1,6)
N17 = NCDEF(1,7)
N18 = NCDEF(1,8)
PSI(N11) = PSI(N13)
PSI(N12) = PSI(N13)
PSI(N18) = PSI(N12)
PSI(N16) = PSI(N15)
PSI(N17) = PSI(N15)
```

```
600 CONTINUE
RETURN
END
```

```
C
C
C
```

```
100 SUBROUTINE ERR1(NEXCR)
NEXCR = -NEXCR
WRITE(6,100) NEXCR
FORMAT(' EXCEEDED MAXIMUM ALLOWABLE SPACE FOR REAL*8 VARIABLES BY
1,15//')
STOP
END
```

```
C
C
C
```

```
100 SUBROUTINE ERR2(NEXCI)
NEXCI = -NEXCI
WRITE(6,100) NEXCI
FORMAT(' EXCEEDED MAXIMUM ALLOWABLE SPACE FOR INT*2 VARIABLES BY
1,15//')
STOP
END
```

```
C
C
C
```

```
100 SUBROUTINE ERR3(NEXC4)
NEXC4 = -NEXC4
WRITE(6,100) NEXC4
FORMAT(' EXCEEDED MAXIMUM ALLOWABLE SPACE FOR INT*4 VARIABLES BY
1,15//')
STOP
END
```

```
C
C
C
```

```
100 SUBROUTINE TASK1(RC,R,NSE2,NR4,N2,NROTOR,NPROTGE,NSTATB,NSTATE)
+++++
+++++
+++++
THIS SUBROUTINE COMPUTES THE TANGENTIAL BLOCKAGE
FACTOR S FOR THE ROTOR AND STATOR OF THE NASA TASK1
CONFRESSCP.
+++++
+++++
+++++
```

```
C
C
C
```

```
IMPLICIT REAL*8(A-H,P-Z)
INTEGER*4 NR,MF1,AC,NC1,IC,MR41,NE1,MN1,MN2,MN3,MN4,NSP2,N2
COMMON /ACCOUNT/ MR4,MR41,MR4W,MR4W1,MASEC
COMMON /ACCOUNT/ AN,ACPL,ACPL1,NE,NROTC,NSTAT
COMMON /INT2/ NR,MN1,NC,NC1,IC
DIMENSION FC(1),P(1)
IF(IANS.EC.2) GO TO 700
MN1 = NC1*3 + MR4W1 - 1
MN2 = MN1 + 1
MN3 = MN2 + MR4W
MN4 = MN3 + 1
MN5 = MN4 + 1
MN6 = MN5 + MR4W1 - 1
```



```

MM7 = MM6 + MRCW
MME = MM1 + 1
CC 100 I = 1.0AN
E(I) = 1.0DO
100 CC CONTINUE
CC 200 I = NFACTC,MM1
RCI = RC(I)
RTCL = C.0131143 - 2.49672D-4 * RCI - 1.03091D-5 * RCI * RCI +
14.24339D-10 * RCI * RCI * RCI * RCI * RCI * RCI
RSIGL = 1.04973 + 1.22251D-3 * RCI * RCI + 1.46066D-8 * RCI * RCI *
1 RCI * RCI * RCI - 1.33865D-3 * DCOS(RCI) - 7.42494D-4 * DSIN(RCI)
2 + 2.395621D-5 * DTAN(RCI) - 2.12971 * DLOG(RCI)
B(I) = 1.00 - RTCL * RSIGL
200 CC CONTINUE
CC 300 I = MM2,MM3
RCI = RC(I)
FTCM = C.140493 - 5.89061D-3 * RCI - 3.28044D-11 * RCI * RCI * RCI
1 * RCI * RCI * RCI + 2.15909D-15 * RCI * RCI * RCI * RCI * RCI *
2 RCI * RCI * RCI * RCI * RCI + 4.55276D-4 * DCOS(RCI) - 1.2162D-4 *
3 DSIN(RCI) - 3.87042D-6 * DTAN(RCI)
RCI = RC(I)
RSIGM = 10.9594 + .255785 * RCI - 2.6207D-6 * RCI * RCI * RCI *
1 RCI + 4.45133D-3 * DSIN(RCI) - 1.04378D-4 * DTAN(RCI)
2 - 4.83569 * DLOG(RCI)
E(I) = 1.00 - FTCM * RSIGM
300 CC CONTINUE
CC 400 I = MM4,NFACTC
RCI = RC(I)
RTCI = C.0199726 - 1.11132D-3 * RCI + 1.3479D-6 * RCI * RCI * RCI -
1 1.06835E-14 * RCI * RCI * RCI * RCI * RCI * RCI * RCI * RCI * RCI
2 + 8.41726D-5 * DCOS(RCI) + 2.68422D-5 * DSIN(RCI) - 5.72139D-7 *
3 DTAN(RCI)
RSIGT = 17.9259 + .656044 * RCI - 3.56691D-6 * RCI * RCI * RCI *
1 RCI + 1.65520D-2 * DSIN(RCI) - 1.35477D-4 * DTAN(RCI)
2 - 9.50883 * DLOG(RCI)
E(I) = 1.00 - RTCI * RSIGT
400 CC CONTINUE
CC 500 I = NSTATE,MM5
RCI = RC(I)
STMCI = C.013089 + 2.31157D-3 * RCI + 1.60096D-5 * RCI * RCI -
1 7.69643D-5 * DCOS(RCI) + 4.83218D-5 * DSIN(RCI) + 3.84003D-7 *
2 DTAN(RCI)
SSIGL = 4.77577 - C.350357 * RCI + 9.45492D-3 * RCI * RCI -
1 5.52663E-13 * RCI * RCI * RCI * RCI * RCI * RCI * RCI * RCI * RCI
2 - 1.31164E-3 * DSIN(RCI) - 1.72748D-5 * DTAN(RCI)
STEML = C.272807 - 5.02565D-3 * RCI + 1.9943D-11 *
1 RCI * RCI * RCI * RCI * RCI * RCI + 3.0662D-4 * DCOS(RCI)
2 + 2.25631D-4 * DSIN(RCI) - 0.87345D-5 * DTAN(RCI)
B(I) = 1.000 - STEML * STMCI * SSIGL
500 CC CONTINUE
CC 600 I = MM6,MM7
RCI = RC(I)
SINCM = C.0158763 + 2.58621D-3 * RCI + 9.85191D-6 * RCI * RCI -
1 7.56625E-5 * DCOS(RCI) + 6.89499D-5 * DSIN(RCI) - 4.16541E-6 *
2 DTAN(RCI)
SSIGM = 5.17732 - .401549 * RCI + 1.12424D-2 * RCI * RCI -
1 6.59085E-13 * RCI * RCI * RCI * RCI * RCI * RCI * RCI * RCI * RCI
2 2.01135E-4 * DTAN(RCI)
B(I) = 1.000 - SINCM * SSIGM
600 CC CONTINUE
CC 700 I = MM8, NSTATE
RCI = RC(I)
SINCT = C.03994821 + 3.14858D-3 * RCI - 3.60047D-11 * RCI * RCI * RCI
1 * RCI * RCI * RCI + 1.80029D-5 * DCOS(RCI) - 3.03125D-5 * DSIN(RCI) -
2 1.39128E-5 * DTAN(RCI)
SSIGT = 1.50125 - .505055 * RCI + 1.52234D-2 * RCI * RCI -
1 2.16170E-11 * RCI * RCI * RCI * RCI * RCI * RCI * RCI * RCI * RCI
2 + 1.07797D-4 * DTAN(RCI)
STETMT = C.515185 + 3.5254D-4 * RCI * RCI - 6.34D-14 * RCI *
1 RCI * RCI * RCI * RCI * RCI * RCI * RCI * RCI + 1.64098D-3 * DCOS(RCI)
2 - C.194717 * DLOG(RCI)
E(I) = 1.000 - STETMT * SINCT * SSIGT

```

FILE: MESH-GEN FORTRAN A1 NAVAL POSTGRADUATE SCHOOL

700 CONTINUE  
RETURN  
END

C  
C  
C

SUBROUTINE FILGEN(ZC,RC,R,PSI,NODE,NTE,NBC,PRESS,PTOT,TEMP,TTOT,  
1 RHCSTA,RHCTT,VZI,WDCR,RDV,CP,R,G,NROTCB,NSTATB,  
2 NSE2,NSE,NZ,MNR1,MN1,IAN5)

C  
C  
C  
C  
C  
C  
C  
C  
C  
C  
C

\*\*\*\*\*  
\*\* THIS SUBROUTINE WRITES THE OUTPUT OF THE PROGRAM \*\*  
\*\* ONTO DISK STORAGE. THE FILE DEFINITIONS ARE LISTED \*\*  
\*\* IN THE EXEC FILES TURBO1 AND TURBO1A. \*\*  
\*\*\*\*\*

IMPLICIT REAL\*8(A-H,P-Z)  
INTEGER\*4 NR,MNR1,NC,NC1,IC,MNR1,MN1,MN2,MN3,MN4,NSE2,NZ  
INTEGER\*4 IAN5  
COMMON /INT4/ NR,MNR1,NC,NC1,IC  
COMMON /ACCOUNT/ MROW,MROW1,MSACC  
COMMON /ACCOUNT/ MN,NCCL,NCCL1,NE,NPOTC,NSTAT  
DIMENSION ZC(1),RC(1),R(1),PSI(1)  
DIMENSION NODE(MN1,1),NTE(1),NEC(1)

C

IF (IAN5.EC.2) GOTO 101  
CC 100 I=1,MN  
WRITE(20,110) ZC(I),RC(I),R(I)  
FORMAT(3F15.11)

11C  
10C

CONTINUE  
WRITE(25,120) MN,NPOTC,NCCL,MROW1,NCCL1,NROTCB,NSTATB  
WRITE(25,121) PRESS,PTOT,TEMP,TTOT,RHCSTA,RHCTT,WDCR,CP,R,G,RPM,VZI  
FORMAT(7F15)

101  
12C  
121

IF (IAN5.EC.2) GOTO 301  
CC 200 I=1, MN  
WRITE(30,210) NODE(I,1),NODE(I,2),NODE(I,3),NODE(I,4),  
1 NODE(I,5),NODE(I,6),NODE(I,7),NODE(I,8),NTE(I)

21C  
20C

FORMAT(9F5)  
CONTINUE  
L=2\*NCCL1+2\*MROW1-4  
CC 300 I=1,L

31C  
30C

WRITE(35,310) NBC(I)  
FORMAT(F5)

301

CONTINUE  
CC 400 I=1,MN  
WRITE(40,410) PSI(I)  
FORMAT(F15.11)

41C  
40C

CONTINUE  
RETURN  
END

C  
C  
C

SUBROUTINE FLFCCT(WDCT,PTOT,TTOT,RHOTT,VTOT,XVEL,CP,R,GML,GYII,  
1 AFEA)

C  
C  
C  
C  
C  
C  
C  
C

\*\*\*\*\*  
\*\* THIS COMPUTES THE NONDIMENSIONAL VELOCITY X \*\*  
\*\*\*\*\*

IMPLICIT REAL\*8(A-G,P-Z), REAL\*4(H)  
INTEGER\*4 NR,MNR1,NC,NC1,IC,MNR1,MN1,MN2,MN3,MN4,NSE2,NZ  
COMMON /INT4/ NR,MNR1,NC,NC1,IC  
COMMON /ACCOUNT/ MROW,MROW1,MSACC  
COMMON /ACCOUNT/ MN,NCCL,NCCL1,NE,NPOTC,NSTAT

FILE: MESHGEN FORTRAN AI NAVAL POSTGRADUATE SCHOOL

```

IT = 0
XVEL = C,100
EPS = 1.E-06
RJ = 778.2 * 32.174
RHCTT = (FIJT * 14.000)/(R * TTOT)
VTCT = CSCAT(2.0CC * CP * RJ * TTCT)
PHI1 = WCT / (RFET * VTCT * APEA)
100 PHI = XVEL * (1.000 - XVEL * XVEL)**GM1
    CIFF = CABS(PHI1 - PHI)
    IF(CIFF.LT.EPS) GOTO 200
    DPHIDX = PHI*(1.00/XVEL - (2.00*XVEL)/(GM1*(1.000 - XVEL*XVEL)))
    XVEL = XVEL + (PHI1 - PHI) / DPHIDX
    IT = IT + 1
    IF(IT.LT.21) GOTO 100
    WRITE(5,110)
110  FORMAT(' CONVERGENCE NOT REACHED',/)
200  CONTINUE
    VZI = XVEL * VTGT
    RETURN
    END

```

```

C
C
C
C      SUBROUTINE MPLOT(ZC,PC,ZMAX,ZMIN,RMAX,RMIN,DHZC,DHRC,
C      1CVZC,OVFC,CHZC1,CHRC1,CZC,ORC,CLK,NS E2,ARR1,N2,NS E,
C      2NE1,NCZ,MM2)
C
C *****
C
C      THIS SUBROUTINE CREATES A TEKTRONIX 418 PLOT OF
C      EIGHT-NODE ISOPARAMETRIC ELEMENT MESH.
C *****
C
C *****

```

MPLOO01

```

C
C
C
C      IMPLICIT REAL*8(A-H,P-Z), REAL*4(C)
C      INTEGER*4 NP, NR1,NC,NC1,IC,NE1,N14,MR14,NC14,NC01
C      LOGICAL*4 TITL1
C      COMMON /FPAR/ FB(5000)
C      COMMON /APAR/ I2(2000)
C      COMMON /CPAR/ O4(3000)
C      COMMON /INT4/ NR1,NE1,NC,IC
C      COMMON /ACOUNT/ YCOW,AROW1,MNSEC,LIMI,LIMR,LIM4
C      COMMON /ACCOUNT/ NA,NCL1,NCCL1,NE,NPDTG,NSTAT
C      DIMENSION CHZC(1),CHRC(1),OVZC(1),OVRC(1),CXYL(4)
C      DIMENSION CHZC1(1),CHRC1(1),CZC(1),ORC(1),OPS(10)
C      DIMENSION ZC(1),PC(1)
C      DIMENSION CLK(1)
C      DIMENSION TITL1(7)
C      DATA TITL1/' EIGHT NODE ISOPARAMETRIC ELEMENT MESH'/
C *****
C
C      CONVERT THE NODAL COORDINATES TO REAL*4
C      TO MAKE THEM COMPATIBLE WITH PLOTG CALLS
C *****
C
C      CC 30 I = 1,MN
C      OZC(I) = ZC(I)
C      OFC(I) = PC(I)
30  CONTINUE
    CXYL(1) = ZMIN
    CXYL(2) = RMIN
    CXYL(3) = ZMAX
    CXYL(4) = RMAX
    CALL D5INIT
    CALL D5PSE
C *****
C
C      PLCT NODAL POINTS
C *****
C
C      CC 5 I = 1,NCCL1
C      CHZC(I) = C.C

```

FILE: MESHGEN FORTRAN A1 NAVAL POSTGRADUATE SCHOOL

```

      CHRC(I) = C.C
5    CCNTINUE
      DC 6 I = 1, MFCW1
      CVZC(I) = C.C
      CVRC(I) = C.C
6    CCNTINUE
      MM1 = MFCW1 + 1
      ACC1 = ACCL1 + 1
      NI4 = NN
      MF14 = MFCW1
      NC14 = ACCL1
      NI1 = NN + 1
      MP1 = MFCW + 1
      CALL PLCT('MMMMNNNNL', NI4, CZC, CPC, OXYL, 37, TITL1)
C ****
C **          PLCT HORIZONTAL ELEMENT BOUNDARIES          **
C ****
      MM = 1
      KKK = 1
      DO 100 J = 1, NCCL1
        CHZC(J) = CZC(MM)
        CHFC(J) = CFC(MM)
        KKH(J) = MM
        IF(KKK.LT.C) GOTC 90
        MM = MM + MFCW1
        KKH = 0 - KKH
90     GOTC 100
        MM = MM + MP1
        KKH = 0 - KKH
100    CCNTINUE
      CALL PLCT('MMMMNNNNL', NC14, CHZC, CHRC, OXYL, 37, TITL1)
      DO 200 I = 1, MFCW
        MLK = 2 * I
        KKK = 1
        DC 800 II = 1, ACCL1
          IF(KKK.LT.C) GOTC 850
          III = KKH(II) + MLK
          GHZC1(III) = CZC(III)
          CHRC1(III) = CFC(III)
          KKK = 0 - KKK
800     GOTC 800
          III = KKH(II) + 1
          CHZC1(III) = CZC(III)
          CHRC1(III) = CFC(III)
          KKK = C - KKH
800    CCNTINUE
      MM = (2 * I) + 1
      MLK = MLK + 1
      CALL PLCT('MMMMNNNNL', NC14, CHZC1, CHRC1, OXYL, 37, TITL1)
200    CCNTINUE
C ****
C **          PLCT VERTICAL BOUNDARIES          **
C ****
      MM = 1
      AC11 = ACCL + 1
      DC 400 I = 1, AC11
        DO 300 J = 1, MFCW1
          OVZC(J) = ZC(MM)
          OVFC(J) = FC(MM)
          MM = MM + 1
300    CCNTINUE
      CALL PLCT('MMMMNNNNL', NI14, CVZC, CVFC, OXYL, 37, TITL1)
400    CCNTINUE
      CALL OSTERN
      RETURN
      END
```

## APPENDIX F

LISTING OF THE PROGRAM TURBO

FILE: TURBO FORTRAN A1 NAVAL POSTGRADUATE SCHOOL

## PROGRAM TURBO

THIS MERIDIONAL THROUGH-FLOW ANALYSIS PROGRAM APPLIES A GALERKIN FINITE ELEMENT METHOD TO A STREAM FUNCTION FORMULATION. THE PROGRAM USES EIGHT NODE, ISOPARAMETRIC ELEMENTS AND THREE-POINT GAUSS-LEGENDRE QUADRATURE NUMERICAL INTEGRATION. SELECTED RESULTS ARE DISPLAYED ON THE TEKTRONIX 619 GRAPHICS TERMINAL.

```
IMPLICIT REAL*(A-H,O-Z), REAL*4(C)
INTEGER*4 NREAD,NWRITE,IC,NNOD,NE4,NNE4,NROWS,LIMR,LIM4
      DIMENSION ALL ARRAY VARIABLES
```

```
COMMON /REAL2/ B2(56000)
COMMON /REAL4/ C4(500)
COMMON /INT2/ I2(2000)
COMMON /ACCUNT/ NCOL,NCOL1,NN,NE
1,NNE,NNFC,NNASC
COMMON /ECON/ RC,GC,CY,PT,TT,AG,WOOD,RHCT,RHSTA,
LUINLET,UCULET,PS,TI,RTU,E212,FIL1,SC
COMMON /ACCUNT/ NCO,NFE,NKI,KN
COMMON /LTC/ NRETC,NEXIT
COMMON /NPOINT/ NP1,NP2,NP3,NP4,NP5,NP6,NP7,NP8,NP9,NP10,NP11,
NP12,NP13,NP14,NP15,NP16,NP17,NP18,NP19,NP20,NP21,NP22,NP23,
NP24,NP25,NP26,NP27,NP28,NP29,NP30,NP31,NP32,NP33,NP34,NP35,
NP36,NP37,NP38,NP39,NP40,NP41,NP42,NP43,NP44,NP45
DIMENSION CA(3),EB(3),J(3),E(3),SF(3)
DIMENSION FOS(3),ZC(1),BH(3,3),BB(3)
DIMENSION N(3),L1(2),L11(2)
DIMENSION TITL(10),RJAC(2,2),RIJAC(2,2)
DATA STOP/'STOP'/
```

```
CALL RDATA(ZA,EA,w,RELX,KK,LIM1,LIMR,LIM4)
```

```
CALL INIT1(LIM1,LIMR,TITL,I,PTOB,NSTATS,LIM4,NNOD,NE4,NNE4,
1,NROWS)
```

```
CALL ZEROI(RP(NP14),R2(NP12),R6(NP15),R8(NP8),R9(NP9)
2,R(NP10),R(NP25),R2(NP2),R(NP11),R8(NP3),
3I2(NP11),I2(NP12),R4(NP13),R(NP14),R(NP17),R(NP5),R(NP7)
4,R(NP4),R(NP11),R(NP5),R2(NP21),R(NP22),R(NP23),
5EM8,I2(NP13),I2(NP14),R3(NP18),R4(NP23),R3(NP19),NNOD,NE4,
6NNE4,NPC4S)
```

```
CALL INFL(R4(NP1),R(NP2),R3(NP3),R6(NP4),R3(NP5),I2(NP13),
1I2(NP14),R2(NP22),R(NP21),R(NP15),R(NP8),R(NP12),R(NP13),
2R(NP23),R(NP24),R(NP25),R(NP26),R(NP27),
3I2(NP11),I2(NP12),TITL,I,PTOB,NNOD,NE4,NNE4,NROWS)
```











```

GM1 = G - 1. CDC
IESTA(1) = 3
IESTA(2) = 2
IESTA(3) = 1
IESTA(4) = 1
IESTA(5) = 1
IESTA(6) = 2
IESTA(7) = 3
IESTA(8) = 3
CC 100 I = 1, MPOW1
H(I) = CP * (TCT(I) * BTU * GC * 144.000
HS(I) = CP * TEMP(I) * BTU * GC * 144.000
100 CC CONTINUE
CC 200 II = 1, NE
NTE1 = NTE(II)
IF(NTE1 - 2) 210, 220, 230

C
C
C 210
CC 240 M = 1, AAE
IESTA1 = IESTA(M)
CALL SLIN(FC, PSI, VZ, VE, NCDF, VM1, RC11, RC12, ALP1, NTE1, RHC1,
2PHCT1, H1, FS1, B2, OPSIR2, OPSIZ2, F, HS, Z1, VZ1, VR1, ZC, ENTROP, ENT1,
3NACD, NE4, NNE4, NNE5)
IJK = AAE - 1
IF(II, LE, IJK) GOTO 211
IF(IESTA1, EQ, 3) GOTO 211
DPSIZ2 = 0.000
211 CALL ELOC(FC, RC11, RC12, T1, P1, TT1, FT1, RHCT1, H1, FS1,
2RHC1, ALP1, ALP2, OPSIZ2, OPSIZ2, IESTA1, T2, TT2, P2, FT2, RHC2, RHCT2,
3VW1, VM2, NACD, NNE4, NNE5, NACWS1)
IF(IESTA1, EQ, 1) GOTO 240
NIM = AAE(II, M)
PRESS(NIM) = P2
PTOT(NIM) = PT1
TTOT(NIM) = TT2
TEMP(NIM) = T2
F(NIM) = F1
FS(NIM) = FS1
RHC(NIM) = RHC2
RHOT(NIM) = RHCT2
ALP(NIM) = ALP2
VZ(NIM) = 144.000 * OPSIR2 / (AHC2 * B2 * RC12 / 12.00)
VR(NIM) = -144.000 * OPSIZ2 / (AHC2 * B2 * RC12 / 12.00)
VU(NIM) = VM2 * DTAN(ALP2)
WFL(NIM) = RC12 * VL(NIM)
ENTROCF(NIM) = ENT1
240 CC CONTINUE
GOTO 200

C
C
C 220
CC 250 M = 1, AAE
IESTA1 = IESTA(M)
RMAX1 = RC12(INPCTOB)
RMIN1 = RC12(INPCTOB + MPOW1 - 1)
CALL SLIN(FC, PSI, VZ, VE, NCDF, VM1, RC11, RC12, ALP1, NTE1, RHC1,
1RHC, ALP, EL, I, IESTA1, K, RHCT1, TEMP, TT21, PRESS, PTOT, R, F1, T1, TT1, PT1,
2PHCT1, H1, FS1, B2, OPSIR2, OPSIZ2, F, HS, Z1, VZ1, VR1, ZC, ENTROP, ENT1,
3NACD, NE4, NNE4, NNE5)
CALL ELOC(FC, RC11, VM1, BET11, BET12, AMACH1, RMAX1, RMIN1,
1CFV, RC12, RHC1, RC12, T1, TT1, P1, FT1, ALP1, RHCT1, RHCT2, AC, ENT, OPSIR2,
2OPSIZ2, OFAC, ALP2, P2, PT2, T2, TT2, TOMC3, VM2, RPASS, NACD, NE4, NNE4,
3NACWS1)
NIM = AAE(II, M)
RFACT = (1.00 - OPASS) * (1.00 - RPASS)
IF(IESTA1 - 2) 251, 251, 252
PRESS(NIM) = (P2 + P1) / 2.000
PTOT(NIM) = (PT2 + PT1) / 2.000
TTOT(NIM) = (TT2 + TT1) / 2.000
TEMP(NIM) = (T2 + T1) / 2.000
251

```

```

H(NIM) = CP * TTCT(NIM) * BTU * GC * 144.000
HS(NIM) = CP * TEMP(NIM) * BTU * GC * 144.000
RHO(NIM) = (RHC2 + RHC1) / 2.000
RHOTT(NIM) = (RHCT2 + RHCT1) / 2.000
ALP(NIM) = (ALP2 + ALP1) / 2.000
BE(NIM) = (BETA2 + BETA1) / 2.000
VZ2 = 144.000 * OPSIZ2 / (RHC2 * H2 * RC12 / 12.00)
VP2 = -1.000 * OPSIZ2 / (RHC2 * H2 * RC12 / 12.00)
VZ(NIM) = (VZ1 + VZ2) / 2.000
VR(NIM) = (VR1 + VR2) / 2.000
VU(NIM) = (VM2 + VM1) * DTAN(ALP(NIM)) / 2.000
WU(NIM) = (VM2 + VM1) * DTAN(BETA2) / 2.000
WPL(NIM) = (RC11 + RC12) * VU(NIM) / 2.000
FR(NIM) = H(NIM) - WG * (RC11 + RC12) * VU(NIM) / 2.000
ENTRCF(NIM) = C.5000 * ENT
GOTO 250
252
PRESS(NIM) = P2
PTCT(NIM) = PT2
TTCT(NIM) = TT2
TEMP(NIM) = T2
DEV1(NIM) = DEV
H(NIM) = CP * TT2 * BTU * GC * 144.000
HS(NIM) = CP * T2 * BTU * GC * 144.000
RHO(NIM) = RHC2
RHOTT(NIM) = RHCT2
ALP(NIM) = ALP2
BE(NIM) = BETA2
VZ(NIM) = 144.000 * OPSIZ2 / (RHC2 * H2 * RC12 / 12.00)
VP(NIM) = -144.000 * OPSIZ2 / (RHC2 * H2 * RC12 / 12.00)
VU(NIM) = VM2 * DTAN(ALP2)
WU(NIM) = VM2 * DTAN(BETA2)
WPL(NIM) = RC12 * VU(NIM)
FR(NIM) = H(NIM) - WG * RC12 * VU(NIM)
ENTRCF(NIM) = ENT
GOTO 250
253
BE(NIM) = BETA1
WU(NIM) = VM1 * DTAN(BETA1)
FR(NIM) = H(NIM) - WG * RC11 * VU(NIM)
ETA(NIM) = (TT1/TT2 - TT1) * ((PT2/PT1)**(GM/G)) - 1.000
PRAT(NIM) = PT2/PT1
CONTINUE
GOTO 200
C
C
C
230
DO 260 M = 1, N
  ISTAT1 = ISTAT(M)
  RMAX1 = RC(ISTATB)
  RMINI = RC(ISTATB + NRCM1 - 1)
  NIM = NCOE(I1, M)
  CALL SLIME(FC, FSI, VZ, VE, NCOE, VM1, RC11, RC12, ALP1, BETA1, RHO1,
    1RHC, ALP, EI, I1, ISTAT1, N, RHOTT, TEMP, TTCT, PRESS, PTCT, P, P1, T1, TT1, PT1,
    2RHC1, ALP1, FSI, B2, OPSIZ2, OPSIZ2, F, HS, Z1, VZ1, VR1, ZC, ENTRCF, ENT1,
    3NRC, NRC4, NRC4, NRC4)
  IF (ISTAT1.EQ.1) GOTO 264
  BETA1 = ALP1
  GOTO 265
264
  BETA1 = ALP(NIM)
265
  CALL STAT(RC11, VM1, BETA1, BETA2, R1, R2, R3, R4, R5, R6, R7, R8, R9, R10, R11, R12, R13, R14, R15, R16, R17, R18, R19, R20, R21, R22, R23, R24, R25, R26, R27, R28, R29, R30, R31, R32, R33, R34, R35, R36, R37, R38, R39, R40, R41, R42, R43, R44, R45, R46, R47, R48, R49, R50, R51, R52, R53, R54, R55, R56, R57, R58, R59, R60, R61, R62, R63, R64, R65, R66, R67, R68, R69, R70, R71, R72, R73, R74, R75, R76, R77, R78, R79, R80, R81, R82, R83, R84, R85, R86, R87, R88, R89, R90, R91, R92, R93, R94, R95, R96, R97, R98, R99, R100)
  1CEV, RC12, RHO1, RHO2, T1, TT1, P1, PT1, ALP1, RHCT1, RHCT2, RC, ENT, OPSIZ2,
  2OPSIZ2, CFAC, ALP2, P2, PT2, T2, TT2, TC, FC, VP2, RPASS, NCOE, NRC4, NRC4,
  3NRC4)
  REACT = (1.00 - RPASS) * (1.00 - RPASS)
  IF (ISTAT1.EQ.2) GOTO 263, 261, 262
  PRESS(NIM) = (P2 + P1) / 2.000
  PTCT(NIM) = (PT2 + PT1) / 2.000
  TTCT(NIM) = (TT2 + TT1) / 2.000
  TEMP(NIM) = (T2 + T1) / 2.000
  H(NIM) = F1
  FS(NIM) = FSI
  RHO(NIM) = (RHC2 + RHC1) / 2.000
  RHOTT(NIM) = (RHCT2 + RHCT1) / 2.000
261

```

```

ALP(NIM) = (BETA2 + BETA1) / 2.000
VZ2 = 144.000 * DPSIZ2 / (RHO2 * B2 * RCI2 / 12.00)
VP2 = -144.000 * DPSIZ2 / (RHO2 * B2 * RCI2 / 12.00)
VZ(NIM) = (VZ1 + VZ2) / 2.000
VR(NIM) = (VR1 + VR2) / 2.000
VU(NIM) = (VM2 + VM1) * CTAN(ALP(NIM)) / 2.000
ENTRCF(NIM) = 0.5000 * ENT + ENT1
WRL(NIM) = RCI2 * VU(NIM)
GOTO 260
262 PRESS(NIM) = P2
TTOT(NIM) = PT2
TTOT(NIM) = T12
TEMP(NIM) = T2
CFV1(NIM) = C2V
H(NIM) = T1
FS(NIM) = FS1
RHC(NIM) = RHC2
RHOT1(NIM) = RHOT2
ALP(NIM) = BETA2
VZ(NIM) = 144.000 * DPSIZ2 / (RHO2 * B2 * RCI2 / 12.00)
VR(NIM) = -144.000 * DPSIZ2 / (RHO2 * B2 * RCI2 / 12.00)
VU(NIM) = VM2 * CTAN(ALP2)
WRL(NIM) = RCI2 * VU(NIM)
ENTRCF(NIM) = ENT + ENT1
GOTO 260
263 ETA(NIM) = PT2/PT1
264 PRAT(NIM) = PT2/PT1
265 CONTINUE
266 CONTINUE
267 RETURN
268 END

```

```

SUBROUTINE SHAPE(E,Z,SF)
+++++
++
++ THIS SUBROUTINE CALCULATES THE SHAPE FUNCTIONS FOR
++ LOCAL NODES FROM LEFT TO RIGHT, BOTTOM TO TOP
++ IN THE Z-E PLANE
++ CALL STATEMENT DEFINITIONS:
++ Z = VALUE OF THE EXCISE INPUT
++ E = VALUE OF THE ETA INPUT
++ SF = SHAPE FUNCTION VECTOR
+++++

```

```

IMPLICIT REAL*8(A-H,P-Z)
DIMENSION SF(8)
SF(1) = (Z*E + Z*Z + E*E + Z*Z*E + Z*E*E - 1.00)/4.00
SF(2) = (1.00 + Z*Z - Z*Z*E - Z*Z*E*E)/2.00
SF(3) = (-Z*E + Z*Z + E*E + Z*Z*E - Z*E*E - 1.00)/4.00
SF(4) = (1.00 - Z*Z - Z*Z*E + Z*E*E)/2.00
SF(5) = (Z*E + Z*Z + E*E - Z*Z*E - Z*E*E - 1.00)/4.00
SF(6) = (1.00 - Z*Z + Z*Z*E + E*Z*Z)/2.00
SF(7) = (-Z*E + Z*Z + E*E - E*Z*Z + Z*E*E - 1.00)/4.00
SF(8) = (1.00 - E*E + Z*Z - Z*E*E)/2.00
RETURN
END

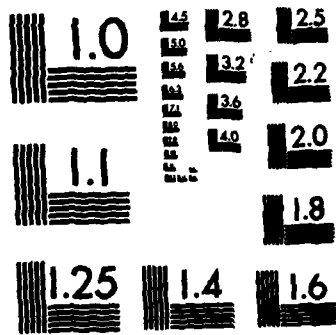
```

```

SUBROUTINE INPUT(ZC,HC,B,ALP,RE,NTS,NODE,PRAT,DEVI,RHC,
1 UVEL,PSI,PSIC,TEN,TTOT,PRESS,PTOT,RHOT,RFSS,ABC,TITLE,
2 NARCTOP,NACC,NB4,NB34,NFCWC)

```





MICROCOPY RESOLUTION TEST CHART  
NATIONAL BUREAU OF STANDARDS-1963-A











FILE: TLRB0 FORTRAN A1 NAVAL POSTGRADUATE SCHOOL

```
C      GCTC1104
45C    WRITE(NWRITE,12CC)KK,X
1200   FORMAT(' ***** FINITE ELEMENT CONVERGENCE CRITERION SATISFIED ON ITE
IRATION NUMBER ',I3,'//', ' RESULTS ARE AS FOLLOWS FOR CONVEGENCE
2EPSILON = ',D15,12)
C      WRITE(CUT RESULTS
C      GCTC 131C
C      CHANGE UNITS OF VELOCITY TO FT/SEC
1104   CC 600 I = 1,NN
      UVEL(I) = UVEL(I)/12.00
      VVEL(I) = VVEL(I)/12.00
      TVEL(I) = TVEL(I)/12.00
      TWEL(I) = TWEL(I)/12.00
      ALP(I) = ALP(I) * 57.25578
      WRL(I) = WRL(I) / 144.000
      BE(I) = BE(I) * 57.25578
      H(I) = H(I) / (GC*144.000*BTU)
      HS(I) = HS(I) / (GC*144.000*BTU)
600    CONTINUE
      WRITE(NWRITE,1109)
1109   FORMAT(' ')
      WRITE(NWRITE,1110)
1110   FORMAT(' //////////////// 27X, 'FINITE ELEMENT RESULTS',///,
1 ' ACCE',5X,' PSI(I)',10X,' VZ',13X,' VR',12X,' R(I)',10X,' DENSITY'//)
C      I122 I = 1,NN
      WRITE(NWRITE,1120)(I,PSI(I),UVEL(I),VVEL(I),AC(I),R+C(I))
      IF(I.EQ.NN) GOTO 1124
      IC = I
      CC = FLCAT(IC)/40.
      IF(C.NE.CC) GCTC 1123
      C = C + 1
      WRITE(NWRITE,1053)
      WRITE(NWRITE,1110)
      GCTC 1122
1124   WRITE(NWRITE,1053)
1123   CONTINUE
1122   CONTINUE
1120   FORMAT(' // 13,2X,D13.6,2X,D13.6,2X,D13.6,2X,D13.6,2X,D13.6,2X,D13.6)
1111   WRITE(NWRITE,1121)
1121   FORMAT(' // ACCE',5X,' WRL(I)',10X,' HT',13X,' VT',12X,' WT',14X,' HS' )
C      I1322 I = 1,NN
      WRITE(NWRITE,1300)(I,WRL(I),H(I),TVEL(I),TWEL(I),HS(I))
1300   FORMAT(' // 13,2X,D13.5,2X,D13.6,2X,D13.6,2X,D13.5,2X,D13.6)
      IF(I.EQ.NN) GCTC 1324
      IC = I
      CC = FLCAT(IC)/40.
      IF(C.NE.CC) GCTC 1323
      C = C + 1
      WRITE(NWRITE,1053)
      WRITE(NWRITE,1121)
      GCTC 1322
1324   WRITE(NWRITE,1053)
1053   FORMAT(' ')
1323   CONTINUE
1322   CONTINUE
1421   WRITE(NWRITE,1421)
1421   FORMAT(' // ACCE',5X,' TEMP',11X,' TTOT',11X,' PRESS',11X,
1 ' FTOT',11X,' RHOT')
C      I1422 I = 1,NN
      WRITE(NWRITE,1400)(I,TEMP(I),TTOT(I),PRESS(I),PTOT(I),RHOT(I))
1400   FORMAT(' // 13,2X,D13.6,2X,D13.6,2X,D13.6,2X,D13.6,2X,D13.6)
      IF(I.EQ.NN) GCTC 1424
      IC = I
      CC = FLCAT(IC)/40.
      IF(C.NE.CC) GCTC 1423
      C = C + 1
      WRITE(NWRITE,1053)
```





FILE: TURBO FORTRAN A1 NAVAL POSTGRADUATE SCHOOL

```
EXPC2 = ((1.0828 - C.344*RPASS + 1.563*RPASS2)/R*MACHR)**EXPC1
RICIFF = -2.5 * 2.55*RPASS + (5.275 + 7.5*RPASS - 2.5 * RPASS2)
1 * RMACHR**XPC2
RIRREF = R120 + RICIFF
RKCELS = C.7JEC
RKCELT = 4.667*TVVC + 24.45*TCVC2
DELTE1 = (-0.0C123 + 0.0257*SIG + 0.000144*SIG2)*BETA1 +
1 (1.510E-4 - 2.55E-4 * SIG - 3.102E-4 * SIG2)*BETA12 +
2 (-2.507E-4 + 7.343 * SIG + 3.621 * SIG2)*1.0D-6*BETA13
SLCPM = 0.25 + 7.06E-4 * BETA1 - 1.2E-5 * BETA12 + 3.10E-7 *
1 BETA13
ACCN = 3.35 - C.0124 * BETA1 - C.000094 * BETA12
BCCN = C.0070 - C.00070 * BETA1 + 1.3E-5 * BETA12
CCELDI = CEXP(-ACCN*SIG) + (BCCN/SIG2)*(CSIN(3.141593*SIG /
2 (1.2*57.29578)))**2
B = 0.566 - 0.00305 * BETA1 + 6.195D-5 * BETA12 - 1.4789D-6 *
1 BETA13
DEL20 = FKCELS * RKCELT * DELTEN + (SLCPM/(SIG**3)) * PHI +
1 RIDIFF + CDELDI
ACCN2 = -1.7E-5 + 2.5*RPASS + RPASS**6.59
BCCN2 = C.29 - 5.5**RPASS + 31.84 * RPASS2 - 57.2*RPASS*RPASS2
1 + 35.15 * RPASS2 * RPASS2
CCCN2 = 1.43 + 5.6 * (RPASS - C.535)**2
CCELDI2 = ACCN2 + BCCN2 * RMACHR**CCCN
CDEL20 = DEL20 + CDELDI
RIRREF = DELREF + (RINCC - RIRREF)*CDELDI
RIRREF = BETA1 - PHI - RINCC + DEV
RIRREF = 1.0D-6
IT = 1
BETA1 = BETA1 / 57.29578
BETA2 = BETA2 / 57.29578
RIRREF = (RCI1 + RC12)/2.0D0
GM1 = G - 1.00
RIRREF = RIRREF / GM1
VM2 = (CSQRT(CPSIR2*DCPSIR2+DPSI22*DCPSI22)) * 144.000 /
1 (RIRREF**2*RC12/12.00)
60C ALF2 = CATAN((W2*RC12 - VM2*CATAN(BETA2))/VM2)
DFAC = 1 - (VM2*DCOS(BETA1))/(VM1*DCOS(BETA2)) + ((VM1*CATAN(BETA1))
1 RC11 - VM2*CATAN(BETA2)*RC12)*DCOS(BETA1)/(2.0D0*SIG*VM1*RIRREF)
DFAC2 = DFAC*DFAC
DFAC3 = DFAC2 * DFAC
DFAC4 = DFAC3 * DFAC3
TCMEG1 = (0.00219558 + 0.0304237*DFAC - 0.338447*DFAC2 +
1 C.55549C*DFAC3 - 0.60274C*DFAC4) * (2.0D0*SIG/DCOS(BETA2))
TCMEG2 = (0.00012009 + 0.0319210*DFAC - C.10647*DFAC2 +
1 C.000000000*DFAC3 - 0.0433925*DFAC4) * (2.0D0*SIG/DCOS(BETA2))
TCIFF = (TCMEG1 - TCMEG2)
IF(RPASS.GE.0.30) GOTO 100
IF(OPASS.LE.0.10) GOTO 110
TCMEG = TCMEG1 + (TCMEG1 - TCMEG2) * ((0.3-RPASS)/0.20)**2
GOTO 120
11C TCMEG = TCMEG1
GOTO 120
1CC TCMEG = TCMEG2
12C TE1 = T2 + W2*WG * (RC12*RC12 - RC11*RC11) / (BCCN3 * 144.000)
PRI = PT1 * (TE1/TE1)**(G*GM1)
PE1 = PE1 * (TE1/TE1)**(G*GM1)
PE2 = PE1 - TCMEG*(PE1 - PE1)
W2 = VM2 / DCOS(BETA2)
TE1 = TE1 - W2*V2 / (BCCN3 * 144.000)
PE2 = PE2 * (TE2 / TE1)**(G*GM1)
RHC2 = (F2*144.00) / (RG * T2)
VM2N = (CSQRT(CPSIR2*DCPSIR2+DPSI22*DCPSI22)) * 144.000 /
1 (RIRREF**2*RC12/12.00)
CTEST = CAPS(VM2 - VM2N)
IT = IT + 1
IF(CTEST.LT.EPS) GOTO 700
VM2 = VM2N
IF(IT.LT.10) GOTO 60C
WRITE(6,65C)
65C PCFMT(' CONVERGENCE NOT REACHED IN 20 ITERATIONS')

```



FILE: TLF80 FORTRAN AI NAVAL POSTGRADUATE SCHOOL

```

1-SIG1)*BETA1-2.145D-8*(26.43-1.0/(SIG*SIG))*BETA13
RI2D = RMISH * RKIT + RITEN + SLOPEN * PHI
EXPC1 = 2.7094 - 1.1375*RPASS + 0.4375*RPASS2
EXPC2 = ((1.0828 - 0.344*RPASS + 1.563*RPASS2)/RMACHR)**EXP01
RICIFF = -2.28 + 2.55*RPASS + (5.275 + 7.5*RPASS - 2.5 * RPASS2)
1 * RMACHF**XPC2
PIREF = FI2D + PICIFF
RKCELS = C.700C
RKCEL = 4.667*TCVC + 24.45*TCVC2
DELTFN = (-0.00143 + 0.0257*SIG + 0.000144*SIG2)*METAL1 +
1 (1.51D-4 - 3.53D-4 * SIG - 3.102D-4 * SIG2)*BETA12 +
2 (-2.07C + 7.043 * SIG + 3.621 * SIG2)*1.0D-4*BETA13
SLOPEM = 0.25 + 7.06D-4 * BETA1 - 1.286D-5 * BETA12 + 3.109D-7 *
1 BETA13
ACCN = 3.35 - C.0124 * BETA1 - 0.000964 * BETA12
BCCN = C.007D - C.000708 * BETA1 + 1.36D-5 * BETA12
CCELD1 = CCXPC(-ACCN/SIG) + (BCCN/SIG2)*(DSIN(3.141593*SIG /
2 (1.2*57.29579)**2
H = C.566 - C.003C5 * BETA1 + 6.195D-5 * BETA12 - 1.4788D-6 *
1 BETA13
CFL2D = FKCELS * FKDEL + DELTEN + (SLOPEM/(SIG*B)) * PHI +
1 RIDIFF + DDEL1
ACCN2 = -1.75 + 2.5*PPASS + RPASS**6.58
BCCN2 = C.29 - 5.55*PPASS + 31.84 * PPASS2 - 57.2*RPASS*PPASS2
1 + 35.15 * PPASS2 * PPASS2
CCCN = .43 + 5.6 * (PPASS - 0.535)**2
CCELDIF = CCXPC2 + BCCN2 * RMACHF**CCCN
CFL2D = CCEL2D + CCEL2DIF
CEV = DELTFN + (FINCD - RIREF)*CDEL1
REAR = (FC11 + RC12)/2.000
FFS = 1.0C-6
IT = 1
BETA1 = BETA1 / 57.29578
BETA2 = BETA2 / 57.29578
GM1 = G - 1.0C
GM11 = 1.0C / GM1
RFC2 = RFC1
TT2 = TT1
VM2 = DSCFT(VM1*VM1*(1.000 + CTAN(BETA1)*DTAN(BETA1)))
VM2 = (DSCFT(DPSIR2*OP SIR2+DPS IZ2*OPS IZ2)) * 144.000 /
1 (RFC2*B2*RC12/12.00)
60C VM2 = DSCFT(VM2*VM2*(1.000 + DTAN(BETA2)*DTAN(BETA2)))
DFAC = 1 - VM2/VM1 + (VM1*CTAN(BETA1)*FC11
1 - VM2*CTAN(BETA2)*FC12)/(2.00*SIG*V1*RBAR)
TCMFG = 10.00312094 + 0.0319210*DFAC - 0.109476*DFAC2 +
1 C.22337E*DFAC3 - 0.0438925*DFAC51 * (2.000*SIG/CCCS(BETA2))
PT2 = PT1 - TCMFG*(PT1 - PT1)
T2 = TT1 - GM1 * (VM2*VM2*(1.00 + (DTAN(ALP2))**2)) / (2.00 *
1 G * RG * GC = 144.000)
F2 = PT2 * (T2 / TT1)**(G*GM11)
FMC2 = (F2*144.00) / (RG * T2)
VM2N = (DSCFT(DPSIR2*OP SIR2+DPS IZ2*OPS IZ2)) * 144.000 /
1 (RFC2*B2*RC12/12.00)
CTEST = CABS(VM2 - VM2N)
IT = IT + 1
IF(DTEST.LT.FFS) GOTO 700
VM2 = VM2N
IF(IT.LT.100) GOTO 600
WRITE(6,ERR)
65C FORNAT(1) CONVERGENCE NOT REACHED IN 20 ITERATIONS!/
70C RMACH2 = VM2N*VM2N*(1.000+(CTAN(BETA2))**2)/(G*RG*GC*T2*144.000)
CL/NT = 1.000 + (GM1/2.00)*RMACH2
RFACT2 = (PT2 * 144.00) / (G * TT2)
FA1 = -RC*CLCC(PT2/PT1) * GC * 144.000
RETURN
ENC

```

```

C
C
C ***** SUBROUTINE RCAT5 (ZA, EA, W, FELX, KK, LIMI, LIMR, LIM4) *****

```



FILE: TURBO FCRTRM A1 NAVAL POSTGRADUATE SCHOOL

```
C *****
C **
C **
C *****
C
```

```
IMPLICIT REAL*8(A-H,P-Z)
INTEGER*4 NR,FAC,NWRITE,IC,NMCD,NF4,NNE4,NROWS,LINR,LIMI
COMMON /FCCM/ PG,G,C3,PT,TT,LG,WDOCT,RHCT,RHCTA,
IUINLET,UCLLET,PSI1,RTU,F2I2,F1I1,GC
COMMON /LIC/ NFEED,NWRITE
DIMENSION ZA(9),EA(9),W(9)
```

C

```
NREAD = 5
NWRITE = 6
RELX = C.24C0C0
```

C

```
INITIALIZE STREAM FUNCTION ITERATION COUNTER ,KK. SET SIZE
FOR REAL*8 AND INTEGER*2 STORAGE
```

C

```
KK = 0
LINR = 56C0C
LIMI = 21C0C
LIM4 = 5C0C
```

C

```
THREE-POINT GAUSSIAN ABSCISSAS
```

```
ZZ1 = C.774596669241483
ZZ2 = C.CC0CCCCC0C0C0
ZA(1) = ZZ1
ZA(2) = ZZ1
ZA(3) = ZZ1
ZA(4) = ZZ2
ZA(5) = ZZ2
ZA(6) = ZZ2
ZA(7) = -ZZ1
ZA(8) = -ZZ1
ZA(9) = -ZZ1
EA(1) = ZZ1
EA(2) = ZZ2
EA(3) = -ZZ1
EA(4) = ZZ1
EA(5) = ZZ2
EA(6) = -ZZ1
EA(7) = ZZ1
EA(8) = ZZ2
EA(9) = -ZZ1
```

C

```
WEIGHTING VALUES FOR 3 PT. GAUSSIAN QUADRATURE
```

```
WH1 = 0.5555555555555556
WH2 = 0.8888888888888889
W(1) = WH1*WH1
W(2) = WH2*WH1
W(3) = WH1*WH1
W(4) = WH2*WH1
W(5) = WH2*WH2
W(6) = WH2*WH1
W(7) = WH1*WH1
W(8) = WH2*WH1
W(9) = WH1*WH1
```

C

```
CONSTANTS USEC FOR UNITS CONVERSIONS
```

```
RTL = 77E.20C
F1I1 = 12.00C0
F2I2 = 144.00C
F3I3 = F1I1 * F2I2
GC = 32.1740C
RETURN
ENC
```



```

C *****
C **
C **          PLOT THE ROTOR INLET VELOCITY DISTRIBUTION
C **
C *****
DATA TITL1/' AXIAL VELOCITY PROFILE AT ROTOR INLET'/
DATA TITL2/' AXIAL VELOCITY PROFILE AT ROTOR OUTLET'/
DATA TITL3/' AXIAL VELOCITY PROFILE AT STATOR INLET'/
DATA TITL4/' AXIAL VELOCITY PROFILE AT STATOR OUTLET'/
DATA TITL5/' RELATIVE FLOW ANGLES AT ROTOR INLET'/
DATA TITL6/' RELATIVE FLOW ANGLES AT ROTOR OUTLET'/
DATA TITL7/' ABSOLUTE FLOW ANGLES AT ROTOR OUTLET'/
DATA TITL8/' ABSOLUTE FLOW ANGLES AT STATOR INLET'/
DATA TITL9/' ABSOLUTE FLOW ANGLES AT STATOR OUTLET'/
DATA TITL10/' ADIABATIC EFFICIENCY AT ROTOR INLET'/
DATA TITL11/' DEVIATION ANGLE ROTOR OUTLET'/
DATA TITL12/' DEVIATION ANGLE STATOR OUTLET'/
DATA TITL13/' TOTAL PRESSURE RATIO, ROTOR'/
DATA TITL14/' TOTAL PRESSURE RATIO, STATOR'/
WRITE(6,100)
100  FORMAT(S,' >DO YOU WISH TO ENTER THE PLOT SEQUENCE? ',/,)
      1 1 = YES; 2 = NO. ',/)
      READ(15,4) NANS
      IF(NANS.EC.2) GOTO 500
      J = NROTC2
      DO 30 I = 1, MRCW1
        ORC(I) = RC(J)
        OVVEL(I) = VZ(J)
        CBEL(I) = BE(J)
        CALP(I) = ET1(J)
        CRAT(I) = PRAT(J)
        J = J + 1
30    CONTINUE
      NR14 = MRCW1
      CXYL(1) = -50.000
      CXYL(2) = RMIN
      CXYL(3) = 700.000
      CXYL(4) = RMAX
      CALL DSINIT
      CALL GSEFSE
      CALL PLOT('MGNM3NWL',NR14,CVEL,ORC,CXYL,37,TITL1)
      CALL PLOT('MGNM3OWL',NR14,CVEL,ORC,CXYL,37,TITL1)
      CALL DSTERM
      WRITE(6,110)
110  FORMAT(S,' >DO YOU WISH TO CONTINUE PLOT SEQUENCE? ',/,)
      1 1 = YES; 2 = NO. ',/)
      READ(15,4) NANS
      IF(NANS.EC.2) GOTO 500
      CALL DSINIT
      CALL GSEFSE
      CALL PLOT('MGNM3NWL',NR14,CBE,ORC,CXYL,35,TITL5)
      CALL PLOT('MGNM3OWL',NR14,CBE,ORC,CXYL,35,TITL5)
      CALL DSTERM
      WRITE(6,110)
      READ(15,4) NANS
      IF(NANS.EC.2) GOTO 500
      CALL DSINIT
      CALL GSEFSE
      CALL PLOT('MGNM3NWL',NR14,CRAT,ORC,CXYL,27,TITL13)
      CALL PLOT('MGNM3OWL',NR14,CRAT,ORC,CXYL,27,TITL13)
      CALL DSTERM
      WRITE(6,110)
      READ(15,4) NANS
      IF(NANS.EC.2) GOTO 500
      CALL DSINIT
      CALL GSEFSE
      CALL PLOT('MGNM3NWL',NR14,CALP,ORC,CXYL,35,TITL10)
      CALL PLOT('MGNM3OWL',NR14,CALP,ORC,CXYL,35,TITL10)
      CALL DSTERM
      WRITE(6,110)
      READ(15,4) NANS
      IF(NANS.EC.2) GOTO 500

```

FILE: TLRBO FCRTRAN A1 NAVAL POSTGRADUATE SCHOOL

```
J = J + MRCW + 1
DC 40 I = 1, MRCW1
   OPC(I) = RC(J)
   OVEL(I) = VZ(J)
   CBE(I) = BE(J)
   CALP(I) = CEV1(J)
   J = J + 1
40 CONTINUE
   CALL DSINIT
   CALL GSEFSE
   CALL PLOT('MMGNNA3NWL', NR14, CVEL, ORC, CXYL, 38, TITL2)
   CALL PLOT('MMGNNA3OWL', NR14, CVEL, ORC, CXYL, 39, TITL2)
   CALL DSTERM
   WRITE(6, IIC)
   READ(15, *) NANS
   IF(NANS.EC.2) GOTC 500
   CALL DSINIT
   CALL GSEFSE
   CALL PLOT('MMGNNA3NWL', NR14, CBE, ORC, CXYL, 36, TITL5)
   CALL PLOT('MMGNNA3OWL', NR14, CBE, ORC, CXYL, 36, TITL5)
   CALL DSTERM
   WRITE(6, IIC)
   READ(15, *) NANS
   IF(NANS.EC.2) GOTC 500
   CALL DSINIT
   CALL GSEFSE
   CALL PLOT('MMGNNA3NWL', NR14, CALP, ORC, CXYL, 28, TITL11)
   CALL PLOT('MMGNNA3OWL', NR14, CALP, ORC, CXYL, 28, TITL11)
   CALL DSTERM
   WRITE(6, IIC)
   READ(15, *) NANS
   IF(NANS.EC.2) GOTC 500
   J = J - MRCW1
   DC 41 I = 1, MRCW1
   OPC(I) = OC(J)
   CBE(I) = ALP(J)
   J = J + 1
41 CONTINUE
   CALL DSINIT
   CALL GSEFSE
   CALL PLOT('MMGNNA3NWL', NR14, CBE, ORC, CXYL, 36, TITL7)
   CALL PLOT('MMGNNA3OWL', NR14, CBE, ORC, CXYL, 36, TITL7)
   CALL DSTERM
   WRITE(6, IIC)
   READ(15, *) NANS
   IF(NANS.EC.2) GOTC 500
   J = J + MRCW + 1
   DC 50 I = 1, MRCW1
   OPC(I) = OC(J)
   CVEL(I) = VZ(J)
   CPAT(I) = PRAT(J)
   CBE(I) = ALP(J)
   J = J + 1
50 CONTINUE
   CALL DSINIT
   CALL GSEFSE
   CALL PLOT('MMGNNA3NWL', NR14, CVEL, ORC, CXYL, 39, TITL3)
   CALL PLOT('MMGNNA3OWL', NR14, CVEL, ORC, CXYL, 38, TITL3)
   CALL DSTERM
   WRITE(6, IIC)
   READ(15, *) NANS
   IF(NANS.EC.2) GOTC 500
   CALL DSINIT
   CALL GSEFSE
   CALL PLOT('MMGNNA3NWL', NR14, CBE, ORC, CXYL, 36, TITL8)
   CALL PLOT('MMGNNA3OWL', NR14, CBE, ORC, CXYL, 36, TITL8)
   CALL DSTERM
   WRITE(6, IIC)
   READ(15, *) NANS
   IF(NANS.EC.2) GOTC 500
   CALL DSINIT
   CALL GSEFSE
```

```

CALL PLCT('MMGNAN3NWL', NR14, CRAT, CRC, CXYL, 29, TITL14)
CALL PLCT('MMGNAN3OWL', NR14, CRAT, CRC, CXYL, 28, TITL14)
CALL DSTERM
WRITE(6, IIC)
READ(15, 4) NANS
IF(NANS.EC.2) GCTC 500
J = J + MRCW + 1
CC 60 I = I, MRCW1
   ORC(I) = PC(J)
   QVEL(I) = VZ(J)
   OBE(I) = ALP(J)
   CALP(I) = CEVI(J)
J = J + 1

```

60

```

CONTINUE
CALL DSINIT
CALL GSEFSE
CALL PLCT('MMGNAN3NWL', NR14, CVEL, CRC, CXYL, 39, TITL4)
CALL PLCT('MMGNAN3OWL', NR14, CVEL, CRC, CXYL, 39, TITL4)
CALL DSTERM
WRITE(6, IIC)
READ(15, 4) NANS
IF(NANS.EC.2) GCTC 500
CALL DSINIT
CALL GSEFSE
CALL PLCT('MMGNAN3NWL', NR14, CBE, OPC, CXYL, 37, TITL9)
CALL PLCT('MMGNAN3OWL', NR14, CBE, OPC, CXYL, 37, TITL9)
CALL DSTERM
WRITE(6, IIC)
READ(15, 4) NANS
IF(NANS.EC.2) GCTC 500
CALL DSINIT
CALL GSEFSE
CALL PLCT('MMGNAN3NWL', NR14, CALP, CRC, CXYL, 29, TITL12)
CALL PLCT('MMGNAN3OWL', NR14, CALP, CRC, CXYL, 29, TITL12)

```

50C

```

CONTINUE
RETURN
END

```

CCCCCCCC

```

SUBROUTINE SLINE(FC, PSI, VZ, VR, ACDE, VM1, RC11, RC12, ALP1, NTE1, PHC1,
1IFC, ALP, E1, I1, I2, AI, M, PHCT, TCM, TTOT, PRESS, PTOT, B, PL, T1, TT1, PT1,
2RFCT1, H1, PSI, Z1, OPSIZ, F, HS, Z1, VZ1, VR1, IC, ENTROP, ENTI,
3NACC, NE4, NNE4, NROWS)

```

CCCCCCCC

```

IMPLICIT REAL*8 (A-H, P-Z)
INTEGER*4 NREAD, NWRITE, IC, NACC, NE4, NNE4, NROWS, LIMR, LIMI
COMMON /ACCOUNT/ NCUL, NCOL1, NR, NE
1, ANE, NNPC, NNAC
COMMON /FCC4/ FC, G, CP, FT, TT, WG, WDTT, FHCT, RHOSTA,
1UINLET, UCULET, PSI, HTU, FZ12, F111, GC
COMMON /ACCOUNT/ VM1, MRCW1, KK
DIMENSION FC(1), VR(1), E1(3), SE(3), PHC(1), PHCT(1), TEMP(1), TTOT(1)
DIMENSION VZ(1), VC(1), POL(1), TWEL(1), PRESS(1), PTOT(1), R(1)
DIMENSION PSI(1), ALP(1), GF(1), F(1), HS(1), Z1(3), D(3), S(3), ZC(1)
DIMENSION RC1(1), ZC(3), RJAC(2,2), Z2(3), OR(3), OPSIZ(3)
DIMENSION ENTROP(1)
DIMENSION INLET(1), NTE(1), NCCF(NR4,1)

```

CCCCCCCC

BEGIN WITH MID NODE OF FIRST ELEMENT AND THEN CYCLE THROUGH EACH ELEMENT.

```

N11 = NODE(11,M)
P = PSI(N11)
IT = 1
K = 1
IF(ISTAT.EQ.1.AND.NTE1.EQ.1) GOTO 700
IF(ISTAT.EQ.1) GOTO 200
RC12 = RC(N11)
BZ = E(N11)
C
13C    CHECK TO SEE IF P IS WITHIN THE PRESENT ELEMENT
C    IF(P.GE.PSI(NCCE(K,5)))GOTO14)
C    CHECK NEXT ELEMENT BELOW THE PRESENT ELEMENT.
K = K + 1
GOTO13C
14C    IF(P.GT.PSI(NODE(K,4))GOTC170
C    IF(ISTAT.EQ.1)GOTO13C
C    IF(ISTAT.EQ.1)GOTO13C
15C    IF(ISTAT.EQ.1)GOTO13C
C    CALL    (EP)/2.00
C          (EP-1.0D0)*SF
C          (3)+PSI(NODE(K,3)) + SF(4)+PSI(NODE(K,4))
C          (5)+PSI(NODE(K,5))
C          CHECK FOR STRAHLIN CONVERGENCE
C          EPS = DABS(FA - P)
C          IF(EPS.LT.1.0-C6)GOTO190
C          IT = IT + 1
C          IF(IT.GT.15)GOTO150
C          IF(PA.LT.P)GOTC1AC
C          GOTO13C
16C    IF(ISTAT.EQ.1)GOTO13C
C          IF(P.GT.PSI(NCCE(K,3)))GOTC135
C          ER = ER + 1
C          IF(ER.GT.10)GOTO13C
C          GOTO13C
C          CHECK NEXT ELEMENT ABOVE PRESENT ELEMENT
C          K = K - 1
C          GOTO14C
C
C          IF CONVERGENCE CRITERIA SATISFIED.
C          CALCULATE WHIRL AND STATIC ENTHALPY
C
C          NK3 = NODE(K,3)
C          NK4 = NODE(K,4)
C          NK5 = NODE(K,5)
C          RCT1 = SF(3)*RC(NK3) + SF(4)*RC(NK4) +
C                SF(5)*RC(NK5)
C          VZ1 = SF(3)*VZ(NK3) + SF(4)*VZ(NK4) +
C                SF(5)*VZ(NK5)
C          VP1 = SF(3)*VP(NK3) + SF(4)*VP(NK4) +
C                SF(5)*VP(NK5)
C          VM1 = DSQRT(VZ1*VZ1 + VP1*VP1)
C          ALP1 = SF(3)*ALP(NK3) + SF(4)*ALP(NK4) +
C                SF(5)*ALP(NK5)
C          RH01 = SF(3)*RHCT(NK3) + SF(4)*RHCT(NK4) +
C                SF(5)*RHCT(NK5)
C          RHOT1 = SF(3)*RHCTT(NK3) + SF(4)*RHCTT(NK4) +
C                SF(5)*RHCTT(NK5)
C          T1 = SF(3)*TEMP(NK3) + SF(4)*TEMP(NK4) +
C                SF(5)*TEMP(NK5)
C          TT1 = SF(3)*TTOT(NK3) + SF(4)*TTOT(NK4) +
C                SF(5)*TTOT(NK5)
C          PT1 = SF(3)*PTOT(NK3) + SF(4)*PTOT(NK4) +
C                SF(5)*PTOT(NK5)
C          P1 = SF(3)*PRESS(NK3) + SF(4)*PRESS(NK4) +
C                SF(5)*PRESS(NK5)
C          ENT1 = SF(3)*ENTROP(NK3) + SF(4)*ENTROP(NK4) +
C                SF(5)*ENTROP(NK5)
C          H1 = SF(3)*H(NK3) + SF(4)*H(NK4) +
C                SF(5)*H(NK5)
C          HS1 = SF(3)*HS(NK3) + SF(4)*HS(NK4) +
C                SF(5)*HS(NK5)

```

```

1      SF(5) * PS(NK5)
20C   K = I
      RC11 = FC(NI1)
      VZ1 = VZ(NI1)
      VRI = VRI(NI1)
      VM1 = CSOFT(VZ1 * VZ1 + VRI * VRI)
      ALP1 = ALP(NI1)
      RHO1 = RHO(NI1)
      RHO11 = RHO11(NI1)
      P1 = PRESS(NI1)
      PT1 = PTOT(NI1)
      TT1 = TTOT(NI1)
      T1 = TEMP(NI1)
      H1 = F(NI1)
      HS1 = FTS(NI1)
      GOTO 215
21C   IF (VT1 .EQ. 1. OR .ISTAL.EQ.3) GOTO 300
215   K = I
      C
      C CHECK TO SEE IF P IS WITHIN THE PRESENT ELEMENT
230   IF (P .GE. PSI(NCDE(K,7))) GOTO 243
      C CHECK NEXT ELEMENT BELOW THE PRESENT ELEMENT.
      K = K + 1
      GOTO 230
24C   IF (P .GT. PSI(NCDE(K,8))) GOTO 270
      REL = F1(S)
      ERR = F1(7)
      CALL ABSE(F1(7) + SF) / 2.0
      PA = (F1(1) * PSI(NCDE(K,1)) + SF(7) * PSI(NCDE(K,7))
      + SF(8) * PSI(NCDE(K,3)))
      C CHECK FOR STREAMLINE CONVERGENCE
      EPS = ABS(PA - P)
      IF (EPS .LT. 1.0E-6) GOTO 29C
      IT = IT + 1
      IF (IT .GT. 15) GOTO 250
      IF (PA .LT. P) GOTO 26C
      GOTO 270
26C   GOTO 270
27C   IF (P .GT. PSI(NCDE(K,1))) GOTO 285
285   REL = F1(1)
      ERR = F1(8)
      GOTO 285
      C CHECK NEXT ELEMENT ABOVE PRESENT ELEMENT
      K = K - 1
      GOTO 24C
      C
      C IF CONVERGENCE CRITERIA SATISFIED.
      C CALCULATE WHIPL AND STATIC ENTHALPY
29C   RC12 = SF(1) * FC(NCDE(K,1)) + SF(7) * FC(NCDE(K,7))
      + SF(8) * FC(NCDE(K,3))
      B2 = SF(1) * F(NCDE(K,1)) + SF(7) * F(NCDE(K,7))
      + SF(8) * F(NCDE(K,3))
      C
      C GOTO NEXT ELEMENT.
30C   N1 = NCDE(K,1)
      N2 = NCDE(K,2)
      N3 = NCDE(K,3)
      N4 = NCDE(K,4)
      N5 = NCDE(K,5)
      N6 = NCDE(K,6)
      N7 = NCDE(K,7)
      N8 = NCDE(K,8)
      RC$(1) = FC(N1)
      RC$(2) = FC(N2)
      RC$(3) = FC(N3)
      RC$(4) = FC(N4)
      RC$(5) = FC(N5)
      RC$(6) = FC(N6)

```

FILE: TLF8G FORTRAN A1 NAVAL POSTGRADUATE SCHOOL

RCS(7) = RC(N7)  
RCS(8) = RC(N8)  
ZCS(1) = ZC(N1)  
ZCS(2) = ZC(N2)  
ZCS(3) = ZC(N3)  
ZCS(4) = ZC(N4)  
ZCS(5) = ZC(N5)  
ZCS(6) = ZC(N6)  
ZCS(7) = ZC(N7)  
ZCS(8) = ZC(N8)  
DO 500 I = 1, N8

C FIND THE JACOBIAN.  
CALL JACCB(F1(1), Z1(1), O, E, PCS, ZCS, RJAC)  
DETJ = RJAC(1,1)\*RJAC(2,2) - RJAC(1,2)\*RJAC(2,1)  
C FIND INVERSE OF JACOBIAN.  
DUM1 = RJAC(1,1) / DETJ  
RJAC(1,1) = RJAC(2,2) / DETJ  
RJAC(1,2) = -RJAC(1,2) / DETJ  
RJAC(2,1) = -RJAC(2,1) / DETJ  
RJAC(2,2) = DUM1

C FIND CNI/OR AND CNI/OZ  
DC 400 L = 1, N8  
CZ(L) = RJAC(1,1)\*D(L) + RJAC(1,2)\*E(L)  
CR(L) = RJAC(2,1)\*D(L) + RJAC(2,2)\*E(L)  
400 CONTINUE

C CHECK TO SEE IF SOLUTION IS AT INLET  
C FIND C(PST)/OR AND C(PST)/OZ  
DPSIR(1) = CR(1)\*PSI(N1) + CR(2)\*PSI(N2) +  
CR(3)\*PSI(N3) + CR(4)\*PSI(N4) +  
CR(5)\*PSI(N5) + CR(6)\*PSI(N6) +  
CR(7)\*PSI(N7) + CR(8)\*PSI(N8)  
DPSIZ(1) = CZ(1)\*PSI(N1) + CZ(2)\*PSI(N2) +  
CZ(3)\*PSI(N3) + CZ(4)\*PSI(N4) +  
CZ(5)\*PSI(N5) + CZ(6)\*PSI(N6) +  
CZ(7)\*PSI(N7) + CZ(8)\*PSI(N8)

500 CONTINUE  
IF(NTEL.EQ.1) GOTO 500  
IF(ISTAL.EQ.3) GOTO 600  
1 DPSIR2 = SF(1) \* DPSIR(1) + SF(7) \* DPSIR(7) +  
SF(8) \* DPSIR(8)  
1 DPSIZ2 = SF(1) \* DPSIZ(1) + SF(7) \* DPSIZ(7) +  
SF(8) \* DPSIZ(8)  
GOTO 700  
600 DPSIR2 = DPSIR(M)  
DPSIZ2 = DPSIZ(M)  
700 CONTINUE

C RETURN  
ENC

SLROUTINE FCALIF, W, H, ZA, EA, VZ, PC, ZC, WRL, VU, NRC, NDCS, WU,  
INTE, HP, ENTA, DP, TTCT, NDCD, NE4, NEE4, NROWS)

\*\*\*\*\*  
\*\* THIS SUBROUTINE CALCULATES THE RIGHT-HAND SIDE VECTOR \*\*  
\*\* F(R, Z) FROM KNOWN RADIAL DISTRIBUTIONS OF WHIRL, \*\*  
\*\* ENTHALPY, RCTHALPY, AND ENTECPY. \*\*  
\*\* CALL STATEMENT DEFINITIONS: \*\*  
\*\* F = RIGHT HAND SIDE VECTOR \*\*  
\*\* H = GAUSSIAN HEIGHT FUNCTION ARRAY \*\*  
\*\* P = NOCAL TOTAL ENTHALPY VECTOR \*\*  
\*\* ZA = ARRAY OF EXCISE GAUSSIAN VALUES \*\*  
\*\* EA = ARRAY OF ETA GAUSSIAN VALUES \*\*  
\*\*



```

**          VZ = NODAL AXIAL VELOCITY
**          VC = ARRAY OF NODAL X COORDINATES
**          ZC = ARRAY OF NODAL Z COORDINATES
**          WVL = NODAL ANGULAR MOMENTUM VECTOR
**          VU = NODAL ABSOLUTE TANGENTIAL VELOCITY VECTOR
**          NDC = NODES WHERE BOUNDARY CONDITIONS APPLY
**          NDC2 = ARRAY OF ELEMENTAL NODE ASSIGNMENTS
**          NN = NUMBER OF NODES IN THE MESH
**          NE = NUMBER OF ELEMENTS IN THE MESH
**          VU = NODAL RELATIVE TANGENTIAL VELOCITY VECTOR
**          NTE = TYPE OF ELEMENT ARRAY
**
**
**

```

```

IMPLICIT REAL*(A-H,O-Z)
INTEGER*4 NR,FAC,NA,ITE,IC,NNO,NE4,NEE4,NROWS,LIMR,LIMI
COMMON /ACOUNT/ NCOL,NCOL1,NA,NE
1,ANE,NNBC,ANNBC
COMMON /ACOUNT/ NROW,MROW,KK
COMMON /PCO/ PG,GP,PT,TT,WG,WGT,FACT,RHOSTA,
LCLLET,LCLLET,PCIT,PTJ,F212,F111,PC
DIMENSION VC(1),WC(1),FC(1),F(1),TTOT(1)
DIMENSION VZ(1),VL(1),WVL(1),VU(1),SF(8)
DIMENSION NDC(1),NTE(1),NDC2(NE4,1)
DIMENSION N(4),ZA(4),SA(4),FS(8),F(1),ENTROP(1)
DIMENSION D(3),E(6),SF(3),RC3(2),ZCS(3),RJAC(2,2)

```

ZERLIZE OUT FS( ) .

```

DO 50 I = 1,NE
  FS(I) = 0.00
CONTINUE

```

CYCLE FOR EACH ELEMENT.

```

DO 100 II = 1,NE
  N1 = NDC2(II,1)
  N2 = NDC2(II,2)
  N3 = NDC2(II,3)
  N4 = NDC2(II,4)
  N5 = NDC2(II,5)
  N6 = NDC2(II,6)
  N7 = NDC2(II,7)
  N8 = NDC2(II,8)
  RC3(1) = VC(N1)
  RC3(2) = VC(N2)
  RC3(3) = VC(N3)
  RC3(4) = VC(N4)
  RC3(5) = VC(N5)
  RC3(6) = VC(N6)
  RC3(7) = VC(N7)
  RC3(8) = VC(N8)
  ZCS(1) = ZC(N1)
  ZCS(2) = ZC(N2)
  ZCS(3) = ZC(N3)
  ZCS(4) = ZC(N4)
  ZCS(5) = ZC(N5)
  ZCS(6) = ZC(N6)
  ZCS(7) = ZC(N7)
  ZCS(8) = ZC(N8)

```

CYCLE FOR EACH LOCAL NODE.

```

DO 300 J = 1,8
  CALL SHAPR(SA(J),ZA(J),SF)
  CALL JACOB(SA(J),ZA(J),D,RC3,ZCS,RJAC)
  DETJ = RJAC(1,1)*RJAC(2,2) - RJAC(1,2)*RJAC(2,1)
  FJAC = INVERSE OF THE JACOBIAN.
  DUM1 = RJAC(1,1) / DETJ
  RJAC(1,1) = RJAC(2,2) / DETJ

```



```

C  **      USAGE
C  **      CALL DSIMG(A,B,N,KS)
C  **
C  **      DESCRIPTION OF PARAMETERS
C  **      A AND B MUST BE REAL*8
C  **      A - MATRIX OF COEFFICIENTS STORED COLUMNWISE.
C  **      THESE ARE DESTROYED IN THE COMPUTATION. THE
C  **      SIZE OF MATRIX A IS N BY N.
C  **      B - VECTOR OF ORIGINAL CONSTANTS (LENGTH N). THESE
C  **      ARE REPLACED BY FINAL SOLUTION VALUES, VECTOR X.
C  **      N - NUMBER OF EQUATIONS AND VARIABLES
C  **      KS - OUTPUT DIGIT
C  **      0 FOR A NORMAL SOLUTION
C  **      1 FOR A SINGULAR SET OF EQUATIONS
C  **
C  **      REMARKS
C  **      MATRIX A MUST BE GENERAL.
C  **      IF MATRIX IS SINGULAR, SOLUTION VALUES ARE MEANING-
C  **      LESS. AN ALTERNATIVE SOLUTION MAY BE OBTAINED BY USING
C  **      MATRIX INVERSION (MINV) AND MATRIX PRODUCT (GMPD).
C  **
C  **      SUBROUTINES AND FUNCTION SUBPROGRAMS REQUIRED
C  **      NONE

```

SLEROUTINE DSIMG(A,B,N,KS)

SLEROUTINE DSIMG NOT INCLUDED NON-IMSL LIBRARY SUBROUTINE

```

SUBROUTINE STIFF(RC,ZC,R,EMS,ZA,EA,W,NODE,RHO,
1 PSI,F,PMS,EM,NPC,NACD,NE4,NNE4,NROWS)

```

```

IMPLICIT REAL*8(A-H,P-Z)
INTEGER*4 NREAC,NWRITE,IC,NMCD,NE4,NNE4,NROWS,LIMR,LIMI
COMMON /ACOUNT/ NCOL,NCOL1,NN,NE
1,NNE,NMPC,MMNEC
COMMON /FCO/ FC,GC,CC,PT,TT,GG,DDT,PHCT,PHCSTA,
1LIMLET,LCOLET,PSI1,STU,F212,F111,CC
COMMON /LIT/ NREAC,NWRITE
DIMENSION ZC(1),PC(1),SC(1),RPF(9),RPF(1)
DIMENSION MFC(1),MFC(MN4,1),L(6)
DIMENSION EM(NMCD,1),RJJAC(2,2),PSI(1),F(1),PMS(1)
DIMENSION O(3),L(6),SF(3),ZA(9),EA(9),S(9),ONDZ(9)
DIMENSION RC(1),ZC(3),EM(8,9),RJJAC(2,2),ONDZ(9)

```

```

CC 400 II = 1,AE
N1 = NREAC (11,1)
N2 = NMCD (11,2)
N3 = NMPC (11,3)
N4 = NNE (11,4)
N5 = MMNEC (11,5)
N6 = MFC (11,6)
N7 = FCO (11,7)
N8 = LIT (11,8)
RC(1) = PC(M1)
RC(2) = PC(M2)
RC(3) = PC(M3)
RC(4) = PC(M4)

```

```

RC$(5) = RC(NS)
RC$(6) = RC(NS)
RC$(7) = RC(NS)
RC$(8) = RC(NS)
ZC$(1) = ZC(NS)
ZC$(2) = ZC(NS)
ZC$(3) = ZC(NS)
ZC$(4) = ZC(NS)
ZC$(5) = ZC(NS)
ZC$(6) = ZC(NS)
ZC$(7) = ZC(NS)
ZC$(8) = ZC(NS)

```

CC  
CC  
CC  
CC

PERFORM GAUSSIAN QUADRATURE INTEGRATION

CC  
C

```

DO 320 I = 1,6
CALL SHAPE(EA(I),ZA(I),SF)
CALL JACCP(EA(I),ZA(I),C,E,RC$,ZC$,RJAC)
DETJ = RJAC(1,1)*RJAC(2,2) - RJAC(1,2)*RJAC(2,1)
DUM1 = INVERSE OF JACOBIAN
DUM1 = RJAC(1,1) / DETJ
RJAC(1,1) = RJAC(2,2) / DETJ
RJAC(1,2) = -RJAC(1,2) / DETJ
RJAC(2,1) = -RJAC(2,1) / DETJ
RJAC(2,2) = DUM1
DC 321 J = 1,8
DNCZ(J) = RJAC(1,1)*D(J) + RJAC(1,2)*E(J)
DNDR(K) = RJAC(2,1)*D(J) + RJAC(2,2)*E(J)

```

321  
100

```

CONTINUE
IF(II,NE,1) GOTO 1J0
CONTINUE

```

CC  
C

FIND RHC, R, AND B FOR NUMERICAL INTEGRATION.

330  
C

```

R+CRB = C,CCO
DC 330 L = 1,ANE
NIIL = NCDE(II,L)
PHORR = NHORR + SF(L)*PHO(NIIL)*RC(NIIL)*B(NIIL)
CONTINUE
SFR = (1.00/(R+CRB))*144.00*12.000

```

305  
C

```

DO 300 J = 1,ANE
IF(II,NE,1) GOTO 309
CONTINUE
DC 310 K = 1,ANE
EMS(J,K) = EMS(J,K) + W(I) * SFR * (DNCZ(J)*DNDZ(K)
+ DNDK(J)*DNDR(K)) * DETJ
+ 144.000

```

100  
100  
200

```

CONTINUE
CONTINUE
CONTINUE

```

CC  
C

ASSEMBLE SYSTEM INFLUENCE MATRIX W/OUT REGARD FOR BOUNDRY CONDITIONS

250  
C

```

N(1) = N1
N(2) = N2
N(3) = N3
N(4) = N4
N(5) = N5
N(6) = N6
N(7) = N7
N(8) = N8
DO 350 IS = 1,ANE
I = N(IS)
DC 350 JS = 1,ANE
J = N(JS)
EM(I,J) = EM(I,J) + EMS(IS,JS)
CONTINUE

```

ZERCIZE CUT EMS( ) FOR NEXT ELEMENT

FILE: TLP9G FCRTRAN A1 NAVAL POSTGRADUATE SCHOOL

```
      DO 370 I2 = 1,ANE
      DC 370 J2 = 1,ANE
      EM(I2,J2) = C.DC
370  CONTINUE
      RECYCLE FOR NEXT ELEMENT
400  CONTINUE
      MODIFY SYSTEM OF EQUATIONS TO INCLUDE BOUNDARY CONDITIONS
      DC 410 I = 1,AN
      DC 410 J = 1,ANBC
      JX = NBC(J)
      F(I) = F(I) - EM(I,JX)*PSI(JX)
      EM(I,JX) = C.DC
      EM(JX,I) = C.DC
      EM(JX,JX) = 1.DC
      F(JX) = PSI(JX)
410  CONTINUE
      RETURN
      ENC
```

```
      SUBROUTINE REPLA(PSI,F,RHS,NADC,NE4,ANE4)
      *****
      *****
      *****
```

```
      IMPLICIT REAL*8(A-H,P-Z)
      INTEGER*4 NREAD,NWRITE,IC,NADC,NE4,ANE4,NROWS,LIMR,LIMI
      COMMON /ACCOUNT/ NCOL,NCOL1,NN,AF
      I,ANE,ANBC,ANNC
      COMMON /ACCOUNT/ NROW,NROW1,KN
      DIMENSION PSI(1),PSIC(1),F(1),RHS(1)
      REPLA PSI(I) WITH SOLUTION VECTOR AND RESET F(I) WITH RHS(I)
      DC 100 I = 1,AN
      PSI(I) = F(I)
      F(I) = RHS(I)
100  CONTINUE
      RETURN
      ENC
```

```
      SUBROUTINE RELAX(RELX,PSI,PSIC,ABC,NADC,NE4,ANE4)
      *****
      *****
      *****
```

```
      IMPLICIT REAL*8(A-H,P-Z)
      INTEGER*4 NREAD,NWRITE,IC,NADC,NE4,ANE4,NROWS,LIMR,LIMI
      COMMON /ACCOUNT/ NCOL,NCOL1,NN,NE
      I,ANE,ANBC,ANNC
      COMMON /ACCOUNT/ NROW,NROW1,KN
      DIMENSION PSI(1),PSIC(1),F(1),RHS(1)
      DIMENSION ABC(1)
      IF KN GE 1, PERFORM UNDER RELAXATION SCHEME
      COMPUTING NEW VELOCITY AND DENSITY DISTRIBUTION.
```

FILE: TLF80 FORTRAN 31 NAVAL POSTGRADUATE SCHOOL

```
C
CC 100 I = 1, NN
DO 200 J = 1, NABC
LTEST = I - NABC(J)
IF(LTEST.EQ.0) GOTO 100
200 CONTINUE
PSI(I) = PSIC(I) + RELX*(PSI(I) - PSIO(I))
100 CONTINUE
RETURN
END
```

```
CCCC
SUBROUTINE NOCCN(X, F, PSI, PSIC, EM, IFL, NNCD, NE4, NNE4)
+++++
+++++
++
++
+++++
+++++
```

```
IMPLICIT REAL*8(A-H, P-Z)
INTEGER*4 NREAC, NWRITE, IC, NNCD, NE4, NNE4, NROWS, LIMR, LIM1
COMMON /ACCUNT/ NCOL, NCOL1, NN, NE
1, NNE, NNEC, NN*BC
COMMON /ACCUNT/ MROW, MROW1, KK
COMMON /LIC/ NREAL, NWRITE
DIMENSION PSI(1), PSIC(1), EM(NNCD, 1), F(1)
WRITE (NWRITE, 1400) KK, X
1400 FPMAT(' ', 'LARGEST EPS FOR ITERATION ', I2, ' IS ', D19.12)
IF (KK.LT.22) GOTO 1500
IFL = 0
GOTO 451
1500 WRITE (NWRITE, 1102) KK
1102 FPMAT(' ', 'ITERATION NO. ', I3, ' COMPLETE', /, ' STREAM FUNCTION CON
VERGENCE NOT YET SATISFIED.', /, ' NEXT ITERATION IS IN PROGRESS.')
```

```
CCCC
PREPARE FOR NEXT ITERATION. ZEROIZE
STIFFNESS MATRIX AND RIGHT HAND SIDE VECTOR
REPLACE PSIO(I) WITH CURRENT VALUE OF PSI.
```

```
IFL = 2
CC 460 I = 1, NN
F(I) = C.DC
PSIO(I) = PSI(I)
DO 460 J = 1, NN
EM(I, J) = C.DC
460 CONTINUE
451 RETURN
END
```

```
CCCC
SUBROUTINE TEST(PSI, PSIO, X, NNCD, NE4, NNE4, NROWS)
+++++
+++++
++
++
+++++
+++++
```

```
IMPLICIT REAL*8(A-H, P-Z)
INTEGER*4 NREAC, NWRITE, IC, NNCD, NE4, NNE4, NROWS, LIMR, LIM1
COMMON /ACCUNT/ NCOL, NCOL1, NN, NE
1, NNE, NNEC, NN*BC
DIMENSION PSI(1), PSIC(1)
CCCC
COMPARE NEW AND OLD STREAM FUNCTION DISTRIBUTIONS
X = 0.DC
```

FILE: TURBO FCRTRAN A1 NAVAL POSTGRADUATE SCHOOL

```
DC 100 I = 1,NN
IF (PSI(I).EQ.C.DO) GOTO 110
EPS = ABS(FSIC(I) - PSI(I))/PSI(I)
GOTO 120
110 EPS = ABS(FSIC(I) - PSI(I))
IF (X.GT.EPS) GOTO 100
X = EPS
CONTINUE
RETURN
END
```

APPENDIX G

SAMPLE PROGRAM OUTPUT

MEMORY SPACE AVAILABLE :  
 REAL 8 = 499    INTEGER = 988    REAL 4 = 424

NASA TASK-1 TRANSONIC COMPRESSOR  
 NO. OF NODES = 222    NO. OF ELEMENTS = 63  
 NO. OF ROWS = 7    NO. OF COLUMNS = 9

NOCE	Z(I)	SUMMARY OF NODAL COORDINATES R(I)	S(I)	ABS FLOW ANG	REL FLOW ANG
1	C.C	C.188780D+02	C.910000D+00	0.0	0.0
2	C.C	C.182000D+02	C.910000D+00	0.0	0.0
3	C.C	C.176924D+02	C.910000D+00	0.0	0.0
4	C.C	C.170532D+02	C.910000D+00	0.0	0.0
5	C.C	C.163099D+02	C.910000D+00	0.0	0.0
6	C.C	C.157194D+02	C.910000D+00	0.0	0.0
7	C.C	C.150091D+02	C.910000D+00	0.0	0.0
8	C.C	C.142614D+02	C.910000D+00	0.0	0.0
9	C.C	C.134734D+02	C.910000D+00	0.0	0.0
10	C.C	C.126343D+02	C.910000D+00	0.0	0.0
11	C.C	C.117397D+02	C.910000D+00	0.0	0.0
12	C.C	C.107696D+02	C.910000D+00	0.0	0.0
13	C.C	C.970091D+01	C.910000D+00	0.0	0.0
14	C.C	C.850010D+01	C.910000D+00	0.0	0.0
15	C.C	C.729900D+01	C.910000D+00	0.0	0.0
16	C.C	C.609790D+01	C.910000D+00	0.0	0.0
17	C.C	C.489680D+01	C.910000D+00	0.0	0.0
18	C.C	C.369570D+01	C.910000D+00	0.0	0.0
19	C.C	C.249460D+01	C.910000D+00	0.0	0.0
20	C.C	C.129350D+01	C.910000D+00	0.0	0.0
21	C.C	C.116433D+02	C.910000D+00	0.0	0.0
22	C.C	C.964628D+01	C.910000D+00	0.0	0.0
23	C.C	C.764923D+01	C.910000D+00	0.0	0.0
24	C.C	C.565218D+01	C.910000D+00	0.0	0.0
25	C.C	C.365513D+01	C.910000D+00	0.0	0.0
26	C.C	C.165808D+01	C.910000D+00	0.0	0.0
27	C.C	C.179124D+02	C.910000D+00	0.0	0.0
28	C.C	C.173216D+02	C.910000D+00	0.0	0.0
29	C.C	C.167106D+02	C.910000D+00	0.0	0.0
30	C.C	C.160775D+02	C.910000D+00	0.0	0.0
31	C.C	C.154154D+02	C.910000D+00	0.0	0.0
32	C.C	C.147352D+02	C.910000D+00	0.0	0.0
33	C.C	C.140010D+02	C.910000D+00	0.0	0.0
34	C.C	C.132372D+02	C.910000D+00	0.0	0.0
35	C.C	C.124265D+02	C.910000D+00	0.0	0.0
36	C.C	C.115591D+02	C.910000D+00	0.0	0.0
37	C.C	C.106212D+02	C.910000D+00	0.0	0.0
38	C.C	C.954131D+01	C.910000D+00	0.0	0.0
39	C.C	C.843402D+01	C.910000D+00	0.0	0.0
40	C.C	C.706903D+01	C.910000D+00	0.0	0.0
41	C.C	C.584460D+01	C.910000D+00	0.0	0.0
42	C.C	C.443402D+01	C.910000D+00	0.0	0.0
43	C.C	C.28720D+02	C.910000D+00	0.0	0.0



NODE	Z(I)	SUMMARY OF NODAL COORDINATES		ABS FLOW ANG	REL FLOW ANG
		R(I)	B(I)		
41	C.45000000+01	C.1504490+02	C.9100000+00	0.0	0.0
42	C.45000000+01	C.1466797+02	C.9100000+00	0.0	0.0
43	C.45000000+01	C.1321440+02	C.9100000+00	0.0	0.0
44	C.45000000+01	C.1154180+02	C.9100000+00	0.0	0.0
45	C.45000000+01	C.9561450+01	C.9100000+00	0.0	0.0
46	C.45000000+01	C.7099000+01	C.9100000+00	0.0	0.0
47	C.60000000+01	C.1840300+01	C.9100000+00	0.0	0.0
48	C.60000000+01	C.1783335+01	C.9100000+00	0.0	0.0
49	C.60000000+01	C.1725240+02	C.9100000+00	0.0	0.0
50	C.60000000+01	C.1664460+02	C.9100000+00	0.0	0.0
51	C.60000000+01	C.1601370+02	C.9100000+00	0.0	0.0
52	C.60000000+01	C.1535630+02	C.9100000+00	0.0	0.0
53	C.60000000+01	C.1470700+02	C.9100000+00	0.0	0.0
54	C.60000000+01	C.1395880+02	C.9100000+00	0.0	0.0
55	C.60000000+01	C.1319170+02	C.9100000+00	0.0	0.0
56	C.60000000+01	C.1233370+02	C.9100000+00	0.0	0.0
57	C.60000000+01	C.1152440+02	C.9100000+00	0.0	0.0
58	C.60000000+01	C.1069280+02	C.9100000+00	0.0	0.0
59	C.60000000+01	C.9571010+01	C.9100000+00	0.0	0.0
60	C.60000000+01	C.8426150+01	C.9100000+00	0.0	0.0
61	C.60000000+01	C.7099000+01	C.9100000+00	0.0	0.0
62	C.60000000+01	C.5692250+02	C.9100000+00	0.0	0.0
63	C.60000000+01	C.4247400+02	C.9100000+00	0.0	0.0
64	C.60000000+01	C.2803220+02	C.9100000+00	0.0	0.0
65	C.60000000+01	C.1318660+02	C.9100000+00	0.0	0.0
66	C.60000000+01	C.1152210+02	C.9100000+00	0.0	0.0
67	C.60000000+01	C.9569500+01	C.9100000+00	0.0	0.0
68	C.60000000+01	C.7839700+01	C.9100000+00	0.0	0.0
69	C.60000000+01	C.6153310+02	C.9100000+00	0.0	0.0
70	C.60000000+01	C.4523450+02	C.9100000+00	0.0	0.0
71	C.60000000+01	C.2863510+02	C.9100000+00	0.0	0.0
72	C.60000000+01	C.1200480+02	C.9100000+00	0.0	0.0
73	C.60000000+01	C.1000480+02	C.9100000+00	0.0	0.0
74	C.60000000+01	C.8000480+02	C.9100000+00	0.0	0.0
75	C.60000000+01	C.6000480+02	C.9100000+00	0.0	0.0
76	C.60000000+01	C.4000480+02	C.9100000+00	0.0	0.0
77	C.60000000+01	C.2000480+02	C.9100000+00	0.0	0.0
78	C.60000000+01	C.1000480+02	C.9100000+00	0.0	0.0
79	C.60000000+01	C.0000480+02	C.9100000+00	0.0	0.0
80	C.60000000+01	C.0000480+02	C.9100000+00	0.0	0.0



NODE	SUMMARY OF MODAL COORDINATES			ABS FLOW ANG	REL FLOW ANG
	Z(I)	R(I)	B(I)		
121	0.18329	0.1557060+02	0.9001670+00	0.0	0.0
122	0.18255	0.14941	0.3994630+00	0.0	0.0
123	0.18255	0.14340	0.3986370+00	0.0	0.0
124	0.18319	0.1376170+02	0.3976990+00	0.0	0.0
125	0.18112	0.1310740+02	0.3966250+00	0.0	0.0
126	0.18145	0.12410	0.3953850+00	0.0	0.0
127	0.18109	0.1167580+02	0.3939450+00	0.0	0.0
128	0.18073	0.1083210+02	0.3922450+00	0.0	0.0
129	0.18036	0.1004750+02	0.3902810+00	0.0	0.0
130	0.18000	0.9125000+01	0.3877430+00	0.0	0.0
131	0.18440	0.1803050+02	0.3701220+00	0.0	0.0
132	0.18454	0.1704550+02	0.3603280+00	0.0	0.0
133	0.18466	0.1503500+02	0.3457210+00	0.0	0.0
134	0.18483	0.15019	0.3355050+00	0.0	0.0
135	0.18493	0.1386320+02	0.3135440+00	0.0	0.0
136	0.18506	0.1261620+02	0.2886390+00	0.0	0.0
137	0.18518	0.1123240+02	0.2622550+00	0.0	0.0
138	0.18533	0.9533000+01	0.2223750+00	0.0	0.0
139	0.20370	0.1767100+02	0.3030410+00	0.0	0.0
140	0.20416	0.1743350+02	0.2903030+00	0.0	0.0
141	0.20469	0.1693350+02	0.2799270+00	0.0	0.0
142	0.20517	0.1652150+02	0.2614450+00	0.0	0.0
143	0.20563	0.1604700+02	0.2338550+00	0.0	0.0
144	0.20618	0.1555760+02	0.2032040+00	0.0	0.0
145	0.20669	0.1505230+02	0.1695490+00	0.0	0.0
146	0.20718	0.1453250+02	0.1336680+00	0.0	0.0
147	0.20767	0.1399710+02	0.9277930+00	0.0	0.0
148	0.20817	0.1342230+02	0.807660+00	0.0	0.0
149	0.20866	0.1283330+01	0.4956800+00	0.0	0.0
150	0.20916	0.1221540+02	0.1543730+00	0.0	0.0
151	0.20966	0.1156600+02	0.1927480+00	0.0	0.0
152	0.21016	0.1087650+02	0.1905410+00	0.0	0.0
153	0.21066	0.1014100+02	0.3877000+00	0.0	0.0
154	0.21116	0.1785350+02	0.9100000+00	0.0	0.0
155	0.21166	0.1686450+02	0.9100000+00	0.0	0.0
156	0.21216	0.1607910+02	0.9100000+00	0.0	0.0
157	0.21266	0.1511400+02	0.9100000+00	0.0	0.0
158	0.21316	0.1408250+02	0.9100000+00	0.0	0.0
159	0.21366	0.1297010+02	0.9100000+00	0.0	0.0
160	0.21416	0.1175240+02	0.9100000+00	0.0	0.0





SYSTEM TOPOLOGY

ELEMENT	NOTES	TYPE OF ELEMENT
0206		
0207		
0208		
0209		
0210		
0211		
0212		
0213		
0214		
0215		
0216		
0217		
0218		
0219		
0220		
0221		
0222		
0223		
0224		
0225		
0226		
0227		
0228		
0229		
0230		
0231		
0232		
0233		
0234		
0235		
0236		
0237		
0238		
0239		
0240		
0241		
0242		
0243		
0244		
0245		
0246		
0247		
0248		
0249		
0250		
0251		
0252		
0253		
0254		
0255		
0256		
0257		
0258		
0259		
0260		
0261		
0262		
0263		
0264		
0265		
0266		
0267		
0268		
0269		
0270		
0271		
0272		
0273		
0274		
0275		
0276		
0277		
0278		
0279		
0280		
0281		
0282		
0283		
0284		
0285		
0286		
0287		
0288		
0289		
0290		
0291		
0292		
0293		
0294		
0295		
0296		
0297		
0298		
0299		
0300		

INLET THERMODYNAMIC VARIABLES ARE AS FOLLOWS

FLOW RATE =  $0.17454 \times 10^3$  LBM/SEC  
TOT DENSITY =  $0.851884 \times 10^{-1}$  LBM CU FT  
TOT PRESSURE =  $0.175000 \times 10^2$  PSI  
TOT TEMPERATURE =  $0.555000 \times 10^3$  DEG RANKINE  
ROTATIONAL SPEED =  $0.697520 \times 10^4$  RPM  
INLET U VELOCITY =  $0.306922 \times 10^3$  FT/SEC  
GAS CONSTANT =  $0.533000 \times 10^2$   
RATIO OF SPECIFIC HEATS =  $0.140000 \times 10^1$   
SPECIFIC HEAT AT CONSTANT PRESSURE =  $0.240000 \times 10^3$   
STATIC DENSITY AT INLET =  $0.922124 \times 10^{-1}$





```

LARGEST EPS FOR ITERATION 1 IS 0.346759559206D+00
ITERATION NO. 1 COMPLETE
STREAM FUNCTION CONVERGENCE CRITERION NOT YET SATISFIED.
NEXT ITERATION IS IN PROGRESS
LARGEST EPS FOR ITERATION 2 IS 0.204902273624D+00
ITERATION NO. 2 COMPLETE
STREAM FUNCTION CONVERGENCE CRITERION NOT YET SATISFIED.
NEXT ITERATION IS IN PROGRESS
LARGEST EPS FOR ITERATION 3 IS 0.135922144523D+00
ITERATION NO. 3 COMPLETE
STREAM FUNCTION CONVERGENCE CRITERION NOT YET SATISFIED.
NEXT ITERATION IS IN PROGRESS
LARGEST EPS FOR ITERATION 4 IS 0.941425824100D-01
ITERATION NO. 4 COMPLETE
STREAM FUNCTION CONVERGENCE CRITERION NOT YET SATISFIED.
NEXT ITERATION IS IN PROGRESS
LARGEST EPS FOR ITERATION 5 IS 0.662198640489D-01
ITERATION NO. 5 COMPLETE
STREAM FUNCTION CONVERGENCE CRITERION NOT YET SATISFIED.
NEXT ITERATION IS IN PROGRESS
LARGEST EPS FOR ITERATION 6 IS 0.469458793800D-01
ITERATION NO. 6 COMPLETE
STREAM FUNCTION CONVERGENCE CRITERION NOT YET SATISFIED.
NEXT ITERATION IS IN PROGRESS
LARGEST EPS FOR ITERATION 7 IS 0.342379259092D-01
ITERATION NO. 7 COMPLETE
STREAM FUNCTION CONVERGENCE CRITERION NOT YET SATISFIED.
NEXT ITERATION IS IN PROGRESS
LARGEST EPS FOR ITERATION 8 IS 0.254317279121D-01
ITERATION NO. 8 COMPLETE
STREAM FUNCTION CONVERGENCE CRITERION NOT YET SATISFIED.
NEXT ITERATION IS IN PROGRESS
PROGRAM TERMINATED ON ITERATION NO. 9
RESULTS WHICH FOLLOW ARE FOR CONVERGENCE EPSILON = 0.189017741652D-01
STREAM FUNCTION CONVERGENCE CRITERION SATISFIED ON ITERATION NUMBER 9
RESULTS ARE AS FOLLOWS FOR CONVERGENCE EPSILON = 0.189017741652D-01

```

FINITE ELEMENT RESULTS

NODE	PSI(1)	VZ	VR	R(1)	DENSITY
1	277794	306522D+03	0.0	1.84780C+02	0.8221240-C1
2	25794	306922D+03	0.0	1.82900D+02	0.8221240-C1
3	21826	306522D+03	0.0	1.76824D+02	0.8221240-C1
4	1984	306922D+03	0.0	1.70532C+02	0.8221240-C1
5	17879	306522D+03	0.0	1.63905D+02	0.8221240-C1
6	15895	306922D+03	0.0	1.57194D+02	0.8221240-C1
7	13910	306522D+03	0.0	1.50340D+02	0.8221240-C1
8	11926	306922D+03	0.0	1.42614D+02	0.8221240-C1
9	9941	306522D+03	0.0	1.34737D+02	0.8221240-C1
10	7956	306922D+03	0.0	1.26367D+02	0.8221240-C1
11	5971	306522D+03	0.0	1.17646D+02	0.8221240-C1
12	3986	306922D+03	0.0	97000D+01	0.8221240-C1
13	1999	306522D+03	0.0	79950D+01	0.8221240-C1
14	0	306922D+03	0.0	62900D+01	0.8221240-C1
15	0	306522D+03	0.0	45810D+02	0.8221240-C1
16	0	306922D+03	-0.460541D+02	1.75030D+02	0.8221240-C1
17	0	306522D+03	-0.277484D+02	0.162375C+02	0.8221240-C1
18	0	306922D+03	-0.211303C+02	0.148666D+02	0.8221240-C1
19	0	306522D+03	-0.155310D+02	0.133552C+02	0.8221240-C1
20	0	306922D+03	-0.103989D+02	0.1164629D+02	0.8221240-C1
21	0	306522D+03	-0.000000D+02	0.799000D+01	0.8221240-C1
22	0	306922D+03	-0.53389D+02	0.134840D+02	0.8221240-C1
23	0	306522D+03	-0.411451D+02	0.174124D+02	0.8221240-C1
24	0	306922D+03	-0.290220D+02	0.233150D+02	0.8221240-C1
25	0	306522D+03	-0.16054536D+02	0.167100D+02	0.8221240-C1
26	0	306922D+03	-0.228207D+02	0.154164D+02	0.8221240-C1
27	0	306522D+03	-0.179725D+02	0.147352D+02	0.8221240-C1
28	0	306922D+03	-0.153050D+02	0.140100D+02	0.8221240-C1
29	0	306522D+03	-0.132974D+02	0.132372D+02	0.8221240-C1
30	0	306922D+03	-0.110535D+02	0.124265D+02	0.8221240-C1
31	0	306522D+03	-0.933358D+01	0.115561D+02	0.8221240-C1
32	0	306922D+03	-0.620627D+01	0.106212D+02	0.8221240-C1
33	0	306522D+03	-0.545475D+01	0.84338C2D+01	0.8221240-C1
34	0	306922D+03	-0.355355D+01	0.709700D+01	0.8221240-C1
35	0	306522D+03	-0.257992C-17	0.184400D+02	0.8221240-C1
36	0	306922D+03	-0.365273D+01	0.172872D+02	0.8221240-C1
37	0	306522D+03	-0.128843D+02	0.172872D+02	0.8221240-C1

FINITE ELEMENT RESULTS

MCDE	PSI(I)	VZ	VR	R(II)	DENSITY
41	0.196246C+02	0.382613D+03	-C.1169E3D+02	0.160445D+02	0.8C5813D-01
42	0.156204C+02	0.377925D+03	-C.0.945150D+01	0.146975D+02	0.8C6993D-01
43	0.116615C+01	0.372207D+03	-C.620554D+C1	0.132144D+02	0.8C8282D-01
44	0.775100C+01	0.371532D+03	-C.413513D+01	0.115475D+02	0.8C8444D-01
45	0.555E2C+C1	0.374785D+03	-C.0	0.709930D+01	0.8C807689D-01
46	0.2777895C+02	0.3933052D+03	-C.735681D+01	0.184040D+02	0.8C232281-01
47	0.257762C+02	0.391295D+03	-C.774821D+01	0.179266D+02	0.8C3761D-01
48	0.238782C+02	0.388416D+03	-C.435324D+02	0.172524D+02	0.8C4467D-01
49	0.216506C+02	0.35536D+03	-C.505014D+01	0.166436C+02	0.8C051549-01
50	0.196321C+02	0.346149C+03	-C.570011D+01	0.160127C+02	0.8C051740-01
51	0.176225C+02	0.301493D+03	-C.515480D+01	0.152369D+02	0.8C61121-01
52	0.156231C+02	0.321038D+03	-C.475397D+01	0.146707C+02	0.8C06220D-01
53	0.136334C+02	0.377121D+03	-C.331115D+01	0.131917D+02	0.8C07147D-01
54	0.116541C+02	0.377383D+03	-C.330920D+01	0.139508D+02	0.8C07057D-01
55	0.985640C+01	0.374235D+03	-C.218440D+01	0.123842D+02	0.8C082244D-01
56	0.77723C+01	0.374235D+03	-C.142233D+01	0.115244D+02	0.8C7677D-01
57	0.57723C+01	0.368008D+03	-C.445145D-01	0.105878C+02	0.8C52249D-01
58	0.383472C+01	0.368402D+03	-C.149632D+01	0.971018D+01	0.8C0158D-01
59	0.192720C+01	0.359431D+03	-C.139945D+00	0.842615D+01	0.8C11184D-01
60	0.777495C+02	0.377407D+03	-C.558674D-13	0.709930D+01	0.8C0707D-01
61	0.277119C+02	0.359150D+03	-C.137524D+00	0.194025D+02	0.8C4328D-01
62	0.190522C+02	0.389020D+03	-C.111373D+01	0.172374D+02	0.8C34328D-01
63	0.156144C+02	0.387553D+03	-C.348864D+01	0.160052D+02	0.8C0665D-01
64	0.156144C+02	0.385119D+03	-C.348864D+01	0.166645D+02	0.8C5237D-01
65	0.116112C+02	0.381643D+03	-C.663060D+01	0.13868D+02	0.8C0607D-01
66	0.779367C+01	0.376340D+03	-C.554022C+01	0.115221D+02	0.8C728D-01
67	0.777895C+02	0.358475D+03	-C.614323D-07	0.950350D+01	0.8C67C7D-01
68	0.257216C+02	0.393380D+03	-C.893952D+00	0.709930D+01	0.8C11369D-01
69	0.23625C+02	0.393357D+03	-C.277521D+01	0.178291D+02	0.8C3227D-01
70	0.216066C+02	0.353535D+03	-C.431057D+01	0.166351D+02	0.8C31337D-01
71	0.196491C+02	0.392325D+03	-C.611907D+01	0.160048D+02	0.8C2923D-01
72	0.154453C+02	0.392103D+03	-C.107059D+02	0.153486D+02	0.8C3663D-01
73	0.154453C+02	0.388658D+03	-C.134124D+02	0.146436C+02	0.8C3331D-01
74	0.134925C+02	0.388729D+03	-C.164344D+02	0.144381D+02	0.8C04359D-01
75	0.113723C+02	0.381019D+03	-C.144555D+02	0.131854D+02	0.8C0528D-01
76	0.935883C+01	0.382078D+03	-C.226876D+02	0.115195D+02	0.8C06115D-01
77	0.736883C+01	0.382078D+03	-C.226876D+02	0.115195D+02	0.8C05823D-01

FINITE ELEMENT RESULTS

ACCE	PSI(11)	VZ	VR	R(11)	DENSITY
01	540672C+01	C.367249D+03	0.262556D+02	0.105893C+02	0.8092C8D-01
02	349044C+01	0.351666D+03	0.205554D+02	0.055866D+01	0.810413D-01
03	168667E+01	0.325666D+03	0.100820D+02	0.842522D+01	0.818268D-01
04		0.313548D+03	0.540917D-01	0.010000D+01	0.820725D-01
05	77785D+02	0.398993D+03	0.127650D+02	0.193935D+02	0.801903D-01
06	236975D+02	0.359646D+03	0.544164D+01	0.160364D+02	0.801676D-01
07	190472C+02	0.354844D+03	0.147315D+02	0.147241E+02	0.801848D-01
08	155084D+02	0.355344D+03	C.251559D+02	0.132741E+02	0.802552D-01
09	143595D+02	0.386276D+03	C.342357D+02	0.116478D+02	0.804547D-01
10	143527E+01	0.373813D+03	0.538599D+02	0.975477D+01	0.806949D-01
11	357495D+01	0.331067D+03	0.349344D+02	0.739000D+02	0.814850D-01
12	77785D+02	0.396727D+03	-C.127087D+01	0.183500D+02	0.802458D-01
13	57725E+02	0.396955D+03	-C.100360D+01	0.178195E+02	0.8024C9D-01
14	237125D+02	0.406828D+03	-C.234215D+01	0.172715E+02	0.799956D-01
15	217125D+02	0.405476D+03	0.151249D+01	0.164944E+02	C.799315D-01
16	156675E+02	0.407428D+03	C.636474C+01	0.160754E+02	C.799755D-01
17	175183E+02	0.403118D+03	C.117510D+02	0.154428D+02	0.800097D-01
18	155057E+02	0.400902D+03	C.117520E+02	0.147928D+02	0.799853D-01
19	135226E+02	0.403345D+03	C.167535E+02	0.140921D+02	0.800669D-01
20	114878E+02	0.403504D+03	0.244768D+02	0.133258D+02	0.800518D-01
21	545945E+01	0.396113D+03	0.344710D+02	0.117975D+02	0.802199D-01
22	50025E+01	0.396475D+03	C.535356E+02	0.117755D+02	0.801886D-01
23	3555E+01	0.331696D+03	0.570117D+02	0.109001D+02	0.804997D-01
24	174824E+01	0.348508D+03	C.723258D+02	0.944333E+01	0.811784D-01
25	77785D+02	0.424285E+03	0.906746D+02	0.768000D+01	0.812846D-01
26	277205E+02	0.425294D+03	C.147240D+02	0.139000D+02	0.795291D-01
27	15655E+02	0.430708D+03	-C.109719D+02	0.172285D+02	0.795173D-01
28	15597E+02	0.432135D+03	C.109157E+01	0.160371E+02	0.793380D-01
29	15745E+02	0.429470D+03	0.358424D+02	0.149103D+02	0.793348D-01
30	155357E+01	0.421738D+03	C.566729D+02	0.135540E+02	0.792782D-01
31	267674E+01	0.411491D+03	C.895060D+02	0.120934E+02	0.7955104D-01
32	77785D+02	0.415901D+03	0.140070D+02	0.104070D+02	0.795523D-01
33	258483E+02	0.435182D+03	0.149040D+02	0.040250D+01	0.801820D-01
34	232333E+02	0.442480D+03	-C.192040D+02	0.141900D+02	0.792516D-01
35	232333E+02	0.400290D+03	-C.205149D+02	0.171902D+02	C.792516D-01
36	156774E+02	0.407470D+03	-C.215122E+02	0.171902D+02	0.795548D-01
37	156774E+02	0.407470D+03	-C.141616E+02	0.166678D+02	0.795560D-01
38	156774E+02	0.477368D+03	-C.305160D+01	0.161628E+02	0.789012D-01

FINITE ELEMENT RESULTS

NCDE	PS(11)	VZ	VR	R(11)	DENSITY
121	0.177573E+02	0.476950D+03	0.613218D+01	0.155706D+02	0.781066D-01
122	0.156982E+02	0.478171D+03	0.184100D+02	0.149419D+02	0.780561D-01
123	0.116151E+02	0.473304D+03	0.304695D+02	0.014390D+02	0.781420D-01
124	0.560208E+01	0.466745D+03	0.384120D+02	0.137617D+02	0.781485D-01
125	0.761048E+01	0.465301D+03	0.568042D+02	0.131034D+02	0.782950D-01
126	0.564781E+01	0.455113D+03	0.877142D+02	0.124101D+02	0.782768D-01
127	0.371115E+01	0.443224D+03	0.877142D+02	0.110892E+02	0.784863D-01
128	0.183061E+01	0.435533D+03	0.125758D+03	0.109475D+02	0.783820D-01
129	0.277785E+02	0.458336D+03	0.154604D+03	0.125006E+01	0.777039D-01
130	0.334384E+02	0.452776D+03	0.511980D+02	0.130305D+02	0.851327D-01
131	0.157688E+02	0.471845D+03	0.200776D+02	0.170855D+02	0.847555D-01
132	0.164195E+02	0.464273D+03	0.249323D+02	0.150190D+02	0.850548D-01
133	0.187160E+02	0.451673D+03	0.490769D+02	0.138602E+02	0.859306D-01
134	0.761285E+01	0.445422D+03	0.726271D+02	0.125167D+02	0.854559D-01
135	0.373981E+01	0.432517D+03	0.133154D+03	0.112341D+02	0.846881D-01
136	0.277785E+02	0.433578D+03	0.133154D+03	0.163300E+01	0.830545D-01
137	0.277785E+02	0.434485D+03	0.331715D+02	0.178710D+02	0.811138D-01
138	0.257195E+02	0.464115D+03	0.531876D+02	0.509070D-01	0.809070D-01
139	0.237334E+02	0.452608D+03	0.322253D+02	0.174325D+02	0.817225D-01
140	0.217209E+02	0.455334D+03	0.322253D+02	0.165218D+02	0.817225D-01
141	0.190337E+02	0.455334D+03	0.216747D+02	0.160470E+02	0.842376D-01
142	0.175580E+02	0.451705D+03	0.189320D+02	0.156576E+02	0.845720D-01
143	0.154797E+02	0.433277D+03	0.406550D+02	0.145295D+02	0.844543D-01
144	0.134510E+02	0.435876D+03	0.306550D+02	0.145295D+02	0.847465D-01
145	0.124805E+02	0.427284D+03	0.527213D+02	0.135871D+02	0.837028D-01
146	0.120098E+01	0.425152D+03	0.626721D+02	0.132813E+02	0.835150D-01
147	0.565146E+01	0.423751D+03	0.731461D+02	0.122164D+02	0.827666D-01
148	0.276472E+01	0.430402D+03	0.432118D+02	0.115660D+02	0.819172D-01
149	0.186731E+01	0.430157D+03	0.168282D+03	0.108765D+02	0.807015D-01
150	0.277785E+02	0.437539D+03	0.144950D+03	0.191410D+02	0.817225D-01
151	0.277785E+02	0.463475D+03	0.654058D+01	0.178535D+02	0.819782D-01
152	0.237334E+02	0.478478D+03	0.218112D+03	0.156600D+02	0.807015D-01
153	0.154173E+02	0.469219D+03	0.156312D+03	0.160710D+02	0.840240D-01
154	0.154173E+02	0.457100D+03	0.182310D+02	0.151140D+02	0.840240D-01
155	0.113373E+02	0.441505D+03	0.605441D+02	0.140829D+02	0.825573D-01
156	0.267565E+01	0.425204D+03	0.811621D+02	0.117524D+02	0.814030D-01

FINITE ELEMENT RESULTS

ACDE	PSI(I)	VZ	VR	R(I)	DENSITY
161	C.277789C+02	0.417646D+03	C.101248D+03	0.103930D+02	0.900633D-01
162	C.277762C+02	0.478634D+03	-0.675492D+01	0.178366D+02	0.515078D-01
163	C.237425C+02	C.489155D+03	-0.421942D+00	0.174211E+02	0.502381D-01
164	C.216637C+02	0.509131D+03	C.109074D+02	0.165960D+02	0.854759D-01
165	C.155755C+02	0.424303D+03	0.147020D+02	0.161122D+02	0.532575D-01
166	C.154091C+02	0.486268D+03	0.160210D+02	0.156112D+02	0.934066D-01
167	C.133786C+02	C.490478D+03	0.248823D+02	0.151772D+02	0.536727D-01
168	C.113878C+02	C.471376D+03	C.301735E+02	0.1466874D+02	0.332072D-01
169	C.113878C+02	0.466029D+03	0.359072D+02	0.141806D+02	0.528849D-01
170	C.142447C+01	C.460245D+03	C.359072D+02	0.136551E+02	0.525452D-01
171	C.748307C+01	0.458066D+03	C.437066D+02	0.131085D+02	0.920361D-01
172	C.577745C+01	0.451583D+03	0.526157D+02	0.125381D+02	0.316443D-01
173	C.269556C+01	0.462827D+03	0.602933D+02	0.119404D+02	0.506551D-01
174	C.181501C+01	0.446247D+03	C.707446D+02	0.113113D+02	0.506551D-01
175	C.777789C+02	0.435438D+03	0.383571D+03	0.106453D+02	0.395332D-01
176	C.237504C+02	C.510663D+03	0.105571D+03	0.106453D+02	0.395332D-01
177	C.156134C+02	C.521489D+03	-0.337745D+01	0.176166D+02	0.848954D-01
178	C.155076C+02	C.521489D+03	C.4330486D+01	0.161557E+02	0.887179D-01
179	C.114764C+02	0.515943D+03	0.998154D+01	0.152482D+02	0.889123D-01
180	C.753846C+01	0.504070D+03	0.181034D+02	0.142785D+02	0.887275D-01
181	C.266650E+01	C.506238D+03	C.311065D+02	0.132412D+02	0.881460D-01
182	C.777789C+02	0.495435D+03	0.492025D+02	0.131149D+02	0.365557D-01
183	C.258302C+02	C.542637D+03	0.554737D+02	0.103725D+02	0.355131D-01
184	C.228733C+02	0.550581D+03	-0.554737D+02	0.178375D+02	0.926671D-01
185	C.228733C+02	C.571703D+03	C.2325124D+01	0.174413D+02	0.816462D-01
186	C.1582204C+02	0.554424D+03	-0.5516124D+01	0.170376D+02	0.803017D-01
187	C.157911C+02	0.551970D+03	-0.551970D+01	0.161595D+02	0.828558D-01
188	C.157911C+02	C.552209D+03	-0.460532D+01	0.157693D+02	0.845056D-01
189	C.117099C+02	C.543012D+03	0.460532D+01	0.152163D+02	0.843690D-01
190	C.117099C+02	0.543332D+03	C.515887D-01	0.148548E+02	0.846645D-01
191	C.580828C+01	0.526337D+03	0.377482D+01	0.143786D+02	0.845056D-01
192	C.787894C+01	0.523303D+03	0.902277D+01	0.138866D+02	0.847792D-01
193	C.292631C+01	0.536651D+03	0.150316E+02	0.133753D+02	0.841797D-01
194	C.195719C+01	0.547955D+03	C.521546D+02	0.122904D+02	0.845342D-01
195	C.277789C+02	0.556189D+03	0.892546D+02	0.117104D+02	0.830268D-01
196	C.277789C+02	0.492100D+03	0.0	0.110300D+02	0.818927D-01
197	C.277789C+02	0.492100D+03	0.0	0.110300D+02	0.818927D-01
198	C.277789C+02	0.492100D+03	0.0	0.110300D+02	0.818927D-01
199	C.277789C+02	0.492100D+03	0.0	0.110300D+02	0.818927D-01
200	C.277789C+02	0.492100D+03	0.0	0.110300D+02	0.818927D-01

FINITE ELEMENT RESULTS

NCDE	PSI(I)	VZ	VR	R(I)	DENSITY
201	C.236547E+02	0.520660D+03	0.528668D+01	0.170408D+02	0.535245D-01
202	C.1520224E+02	0.481502D+03	C.105126D+02	0.162057D+02	0.972544D-01
203	C.111625E+02	0.463783D+03	0.144856D+02	0.153394E+02	C.577364E-01
204	C.125857E+01	0.450237D+03	0.164231D+02	0.133921D+02	0.977777D-01
205	C.346617E+01	0.423253D+03	C.163626D+02	0.123175D+02	0.562319D-01
206	C.27789E+02	0.502808D+03	C.1337515D+01	0.111325D+02	0.540117D-01
207	C.256491E+02	C.620442D+03	C.0	0.178260D+02	0.542072D-01
208	C.235495E+02	0.542338D+03	C.0	0.174444E+02	0.531027D-01
209	C.213624E+02	0.510770D+03	C.0	0.166340D+02	0.526200D-01
210	C.170597E+02	0.510345D+03	C.0	0.162135E+02	0.567674D-01
211	C.145486E+02	C.48913D+03	C.0	0.157819D+02	0.973731D-01
212	C.128979E+02	0.473327D+03	C.0	0.153381D+02	0.574483D-01
213	C.129035E+02	0.473327D+03	C.0	0.148811E+02	0.976513D-01
214	C.106703E+01	0.450412D+03	C.0	0.144065D+02	0.57706D-01
215	C.518260E+01	0.443613E+03	C.0	0.134129D+02	0.976736D-01
216	C.338183E+01	0.426766D+03	C.0	0.128919D+02	0.582955D-01
217	C.162651E+01	C.39275D+03	C.0	0.123447E+02	0.991367D-01
218	C.0	0.362656D+03	C.0	0.117720D+02	0.998775D-01
219	C.0	0.0	C.0	0.0	0.954872D-01
220	C.0	0.0	C.0	0.0	0.0
221	C.0	0.0	C.0	0.0	0.0
222	C.0	0.0	C.0	0.0	0.0













MS  
 1420760+03  
 1407380+03  
 1404500+03  
 1355950+03  
 1353110+03  
 1363820+03  
 1412910+03  
 1419430+03  
 1417750+03  
 1405590+03  
 1404220+03  
 1402270+03  
 1396620+03  
 1392670+03  
 1380210+03  
 13733920+03

WT  
 0.0  
 0.0  
 0.0  
 0.0  
 0.0  
 0.0  
 0.0  
 0.0  
 0.0  
 0.0  
 0.0  
 0.0  
 0.0  
 0.0  
 0.0  
 0.0  
 0.0

VT  
 1853600+01  
 9753600+01  
 5332490+01  
 5587310+01  
 1995320+01  
 3725830+01  
 1418410+02  
 4111580+02  
 5409580+02  
 1800340+02  
 1190250+02  
 9603360+01  
 3219870+01  
 3212140+01  
 5347440+01  
 4375570+01  
 1754560+01  
 1511880+01  
 3471060+01  
 9369550+01  
 1912400+02

FT  
 92150+03  
 1477020+03  
 1474340+03  
 1471880+03  
 1469690+03  
 1466360+03  
 1463840+03  
 1461650+03  
 14591240+03  
 1457740+03  
 1456450+03  
 1454170+03  
 1452930+03  
 1451700+03  
 1449570+03  
 1447420+03  
 1445200+03  
 1443100+03  
 1441060+03  
 1439080+03

MPL(I, I) + C2  
 1517870+02  
 1664200+01  
 1702300+01  
 1721630+01  
 1730170+02  
 1741170+02  
 1752510+02  
 1763600+02  
 1775410+02  
 1787940+01  
 1799400+01  
 1811340+01  
 1823800+01  
 1836730+01  
 1849220+01  
 1861350+01  
 18730340+01  
 1884340+02

NEDE  
 201  
 202  
 203  
 204  
 205  
 206  
 207  
 208  
 209  
 210  
 211  
 212  
 213  
 214  
 215  
 216  
 217  
 218  
 219  
 220



ACDE	TEMP	TTOT	PRES S	PTOT	RHCT
44	4279	5550000+03	1618	1750000+02	8518840-01
44	4304	5550000+03	1622	1750000+02	8518840-01
44	4331	5550000+03	1624	1750000+02	8518840-01
44	4345	5550000+03	1625	1750000+02	8518840-01
44	4352	5550000+03	1626	1750000+02	8518840-01
44	4371	5550000+03	1627	1750000+02	8518840-01
44	4384	5550000+03	1628	1750000+02	8518840-01
44	4397	5550000+03	1629	1750000+02	8518840-01
44	4409	5550000+03	1630	1750000+02	8518840-01
44	4422	5550000+03	1631	1750000+02	8518840-01
44	4434	5550000+03	1632	1750000+02	8518840-01
44	4446	5550000+03	1633	1750000+02	8518840-01
44	4458	5550000+03	1634	1750000+02	8518840-01
44	4470	5550000+03	1635	1750000+02	8518840-01
44	4482	5550000+03	1636	1750000+02	8518840-01
44	4494	5550000+03	1637	1750000+02	8518840-01
44	4506	5550000+03	1638	1750000+02	8518840-01
44	4518	5550000+03	1639	1750000+02	8518840-01
44	4530	5550000+03	1640	1750000+02	8518840-01
44	4542	5550000+03	1641	1750000+02	8518840-01
44	4554	5550000+03	1642	1750000+02	8518840-01
44	4566	5550000+03	1643	1750000+02	8518840-01
44	4578	5550000+03	1644	1750000+02	8518840-01
44	4590	5550000+03	1645	1750000+02	8518840-01
44	4602	5550000+03	1646	1750000+02	8518840-01
44	4614	5550000+03	1647	1750000+02	8518840-01
44	4626	5550000+03	1648	1750000+02	8518840-01
44	4638	5550000+03	1649	1750000+02	8518840-01
44	4650	5550000+03	1650	1750000+02	8518840-01
44	4662	5550000+03	1651	1750000+02	8518840-01
44	4674	5550000+03	1652	1750000+02	8518840-01
44	4686	5550000+03	1653	1750000+02	8518840-01
44	4698	5550000+03	1654	1750000+02	8518840-01
44	4710	5550000+03	1655	1750000+02	8518840-01
44	4722	5550000+03	1656	1750000+02	8518840-01
44	4734	5550000+03	1657	1750000+02	8518840-01
44	4746	5550000+03	1658	1750000+02	8518840-01
44	4758	5550000+03	1659	1750000+02	8518840-01
44	4770	5550000+03	1660	1750000+02	8518840-01
44	4782	5550000+03	1661	1750000+02	8518840-01
44	4794	5550000+03	1662	1750000+02	8518840-01
44	4806	5550000+03	1663	1750000+02	8518840-01
44	4818	5550000+03	1664	1750000+02	8518840-01
44	4830	5550000+03	1665	1750000+02	8518840-01
44	4842	5550000+03	1666	1750000+02	8518840-01
44	4854	5550000+03	1667	1750000+02	8518840-01
44	4866	5550000+03	1668	1750000+02	8518840-01
44	4878	5550000+03	1669	1750000+02	8518840-01
44	4890	5550000+03	1670	1750000+02	8518840-01
44	4902	5550000+03	1671	1750000+02	8518840-01
44	4914	5550000+03	1672	1750000+02	8518840-01
44	4926	5550000+03	1673	1750000+02	8518840-01
44	4938	5550000+03	1674	1750000+02	8518840-01
44	4950	5550000+03	1675	1750000+02	8518840-01
44	4962	5550000+03	1676	1750000+02	8518840-01
44	4974	5550000+03	1677	1750000+02	8518840-01
44	4986	5550000+03	1678	1750000+02	8518840-01
44	4998	5550000+03	1679	1750000+02	8518840-01
44	5010	5550000+03	1680	1750000+02	8518840-01
44	5022	5550000+03	1681	1750000+02	8518840-01
44	5034	5550000+03	1682	1750000+02	8518840-01
44	5046	5550000+03	1683	1750000+02	8518840-01
44	5058	5550000+03	1684	1750000+02	8518840-01
44	5070	5550000+03	1685	1750000+02	8518840-01
44	5082	5550000+03	1686	1750000+02	8518840-01
44	5094	5550000+03	1687	1750000+02	8518840-01
44	5106	5550000+03	1688	1750000+02	8518840-01
44	5118	5550000+03	1689	1750000+02	8518840-01
44	5130	5550000+03	1690	1750000+02	8518840-01
44	5142	5550000+03	1691	1750000+02	8518840-01
44	5154	5550000+03	1692	1750000+02	8518840-01
44	5166	5550000+03	1693	1750000+02	8518840-01
44	5178	5550000+03	1694	1750000+02	8518840-01
44	5190	5550000+03	1695	1750000+02	8518840-01
44	5202	5550000+03	1696	1750000+02	8518840-01
44	5214	5550000+03	1697	1750000+02	8518840-01
44	5226	5550000+03	1698	1750000+02	8518840-01
44	5238	5550000+03	1699	1750000+02	8518840-01
44	5250	5550000+03	1700	1750000+02	8518840-01

ADDR	TEMP	TCGT	PRESEN	PTGT	R40T
881	543707L+03	0550000+03	0162810+02	01750000+02	03518840-C1
882	5446134L+03	0550000+03	0163159L+02	01750000+02	03518840-C1
883	546789L+03	0550000+03	0165450+02	01750000+02	03518840-C1
884	541887L+03	0550000+03	01609500+02	01750000+02	03518840-C1
885	541677L+03	0550000+03	01607810+02	01750000+02	03518840-C1
886	541924L+03	0550000+03	01609570+02	01750000+02	03518840-C1
887	542050L+03	0550000+03	01615150+02	01750000+02	03518840-C1
888	542220L+03	0550000+03	01622130+02	01750000+02	03518840-C1
889	541875L+03	0550000+03	01609380+02	01750000+02	03518840-C1
890	541121L+03	0550000+03	01602500+02	01750000+02	03518840-C1
891	541156L+03	0550000+03	01603510+02	01750000+02	03518840-C1
892	541125L+03	0550000+03	01602210+02	01750000+02	03518840-C1
893	541184L+03	0550000+03	01602210+02	01750000+02	03518840-C1
894	541314L+03	0550000+03	01604500+02	01750000+02	03518840-C1
895	541734L+03	0550000+03	01604500+02	01750000+02	03518840-C1
896	542573L+03	0550000+03	01607950+02	01750000+02	03518840-C1
897	5442395L+03	0550000+03	01616600+02	01750000+02	03518840-C1
898	544687L+03	0550000+03	01618770+02	01750000+02	03518840-C1
899	5399015L+03	0550000+03	01633770+02	01750000+02	03518840-C1
900	539544L+03	0550000+03	01599100+02	01750000+02	03518840-C1
901	539544L+03	0550000+03	01535280+02	01750000+02	03518840-C1
902	539544L+03	0550000+03	01534240+02	01750000+02	03518840-C1
903	540227L+03	0550000+03	01588210+02	01750000+02	03518840-C1
904	540192L+03	0550000+03	01592320+02	01750000+02	03518840-C1
905	5391654L+03	0550000+03	01607730+02	01750000+02	03518840-C1
906	537315L+03	0550000+03	01576150+02	01750000+02	03518840-C1
907	536747L+03	0550000+03	01556110+02	01750000+02	03518840-C1
908	536021L+03	0550000+03	01549350+02	01750000+02	03518840-C1



DATE	TIME	TEMP	YTCT	PRESS	PTOT	PFACT
11	00	536047L+03	0.5550000+03	0.1549370+02	0.1750000+02	0.8518840-01
11	00	535924L+03	0.5550000+03	0.1549370+02	0.1750000+02	0.8518840-01
11	00	5336173C+03	0.5550000+03	0.1550540+02	0.1750000+02	0.8518840-01
11	00	5336580C+03	0.5550000+03	0.1555500+02	0.1750000+02	0.8518840-01
11	00	5336530L+03	0.5550000+03	0.1554500+02	0.1750000+02	0.8518840-01
11	00	53371C4L+03	0.5550000+03	0.1560330+02	0.1750000+02	0.8518840-01
11	00	5337881L+03	0.5550000+03	0.1557430+02	0.1750000+02	0.8518840-01
11	00	5337590L+03	0.5550000+03	0.1563240+02	0.1750000+02	0.8518840-01
11	00	533663752L+03	0.5550000+03	0.1565240+02	0.1750000+02	0.8518840-01
11	00	536657752L+03	0.5849620+03	0.1781440+02	0.20633960+02	0.9440440-01
11	00	5360452L+03	0.5844420+03	0.1749506+02	0.2078400+02	0.9555440-01
11	00	53600770L+03	0.5941860+03	0.1792270+02	0.2082110+02	0.9575990-01
11	00	5355593L+03	0.5836980+03	0.1772810+02	0.2074420+02	0.9550840-01
11	00	5352923L+03	0.5830600+03	0.1782790+02	0.2064700+02	0.9527530-01
11	00	5388711L+03	0.6193920+03	0.1685420+02	0.23371770+02	0.1034520-00
11	00	53591430L+03	0.6212250+03	0.1689550+02	0.2365300+02	0.1028460-00
11	00	5352326L+03	0.6183680+03	0.1936790+02	0.24122180+02	0.1054180-00
11	00	5384267L+03	0.6153010+03	0.2066040+02	0.2423150+02	0.1063720+00
11	00	5385811L+03	0.6148380+03	0.2053310+02	0.2432550+02	0.1066560-00
11	00	5355553L+03	0.6133400+03	0.2037020+02	0.2417100+02	0.1063640+00
11	00	538224352L+03	0.6133550+03	0.2033530+02	0.2410560+02	0.1061810+00
11	00	5360675L+03	0.6125050+03	0.2009760+02	0.2404860+02	0.1058360+00
11	00	5378771L+03	0.6110210+03	0.1979740+02	0.2394970+02	0.1057400+00
11	00	5372655L+03	0.6112000+03	0.1979800+02	0.2390340+02	0.1056600+00
11	00	5368256L+03	0.6096850+03	0.1910400+02	0.2381550+02	0.1054850+00
11	00	5360359L+03	0.6096850+03	0.1905270+02	0.2373750+02	0.1053420+00
11	00	5390408L+03	0.6193920+03	0.1911840+02	0.2371770+02	0.1054530+00
11	00	5385521L+03	0.6152530+03	0.1976110+02	0.2425250+02	0.1064470+00
11	00	5382997L+03	0.6133330+03	0.2033260+02	0.2425250+02	0.1064730+00
11	00	5384433L+03	0.6127100+03	0.2019520+02	0.2398630+02	0.1061730+00
11	00	5367673L+03	0.6111330+03	0.1951190+02	0.2388980+02	0.1056490+00

ADDR	TFMP	TOUT	PRESS	PTOI	RHOI
161	57166CL+C3	0.608685D+03	0.190568D+02	0.237375D+02	0.105362D+00
162	58961UL+03	0.6119392D+03	0.199745D+02	0.237177D+02	0.1033453D+00
163	58705CL+C3	0.622166E+03	0.194937D+02	0.236577D+02	0.102854D+00
164	584005L+C3	0.618269D+03	0.200191D+02	0.241315D+02	0.103046D+00
165	582232L+C3	0.614325D+03	0.202220D+02	0.243218D+02	0.106422D+00
166	582295L+C3	0.614397D+03	0.201466D+02	0.243218D+02	0.106646D+00
167	582271L+C3	0.613333D+03	0.200893D+02	0.241622D+02	0.106374D+00
168	581407L+C3	0.612881D+03	0.199847D+02	0.241022D+02	0.106173D+00
169	580496L+C3	0.612481D+03	0.198947D+02	0.240479D+02	0.105998D+00
170	579137L+C3	0.611948D+03	0.19789D+02	0.239736D+02	0.105830D+00
171	577864L+C3	0.61145D+03	0.196018D+02	0.238943D+02	0.105736D+00
172	577447L+C3	0.609591D+03	0.193009D+02	0.238320D+02	0.105651D+00
173	575557L+C3	0.608985D+03	0.192034D+02	0.238124D+02	0.105480D+00
174	57330L+C3	0.619392D+03	0.190184D+02	0.237375D+02	0.105362D+00
175	571868L+C3	0.619392D+03	0.186177D+02	0.236645E+02	0.105133D+00
176	57085L+C3	0.622166E+03	0.181265D+02	0.236445E+02	0.102717D+00
177	57085L+C3	0.615322D+03	0.18386L+02	0.234172D+02	0.106025D+00
178	571592L+C3	0.614415D+03	0.187952D+02	0.2370115D+02	0.105767D+00
179	566422L+C3	0.611127D+03	0.186129D+02	0.237705D+02	0.105986D+00
180	567642L+C3	0.608445D+03	0.178954D+02	0.23592D+02	0.104742D+00
181	567642L+C3	0.619392D+03	0.173650D+02	0.235712D+02	0.102914D+00
182	564714L+C3	0.622166E+03	0.171644D+02	0.235972E+02	0.102326D+00
183	564714L+C3	0.618603D+03	0.172345D+02	0.235597D+02	0.102326D+00
184	561592L+C3	0.615609D+03	0.174667D+02	0.239446E+02	0.104576D+00
185	560891L+C3	0.614471D+03	0.175586D+02	0.240800D+02	0.105078D+00
186	561925L+C3	0.613421D+03	0.175156D+02	0.241050D+02	0.105187D+00
187	562416L+C3	0.613922D+03	0.176097D+02	0.240038D+02	0.105284D+00
188	560410L+C3	0.613421D+03	0.175648D+02	0.239290E+02	0.105351D+00
189	561715L+C3	0.61295D+03	0.174738D+02	0.239567D+02	0.105149D+00
190	557858L+C3	0.611207D+03	0.175758D+02	0.237355D+02	0.104926D+00
191	554776L+C3	0.61007D+03	0.171805D+02	0.236564D+02	0.104561D+00
192	552933L+C3	0.609285D+03	0.171105D+02	0.235537D+02	0.104317D+00
193	559076L+C3	0.619392D+03	0.167603D+02	0.234535D+02	0.102220D+00
194			0.1709746D+02	0.235712D+02	0.102314D+00

AOCE  
201  
202  
203  
204  
205  
206  
207  
208  
209  
210  
211  
212  
213  
214  
215  
216  
217  
218  
219  
220  
221  
222  
223

TEMP  
G.59418L+03  
G.59498L+03  
G.59497L+03  
G.595339L+03  
G.595455L+03  
G.596042L+03  
G.596071L+03  
G.598171L+03  
G.598734L+03  
G.597010L+03  
G.593648L+03  
G.593378L+03  
G.593306L+03  
G.594978L+03  
G.595337L+03  
G.595868L+03  
G.595424L+03  
G.596575L+03  
G.596781L+03  
G.596569L+03  
G.597698L+03

TICT  
G.621733D+03  
G.614308D+03  
G.613283D+03  
G.612369D+03  
G.610593D+03  
G.608685D+03  
G.619292D+03  
G.621251D+03  
G.617805D+03  
G.615335D+03  
G.614704D+03  
G.614234D+03  
G.613634D+03  
G.613225D+03  
G.612759D+03  
G.612319D+03  
G.611752D+03  
G.610920D+03  
G.609795D+03  
G.606685D+03

PRE SS  
C.207420D+02  
C.215237D+02  
C.215461D+02  
C.215511D+02  
C.218083D+02  
C.208528D+02  
C.206320D+02  
C.210659D+02  
C.212673D+02  
C.215043D+02  
C.215052D+02  
C.215445D+02  
C.216054D+02  
C.216105D+02  
C.217062D+02  
C.218415D+02  
C.220097D+02

PTOT  
0.236139D+02  
0.2401061D+02  
0.2379055D+02  
0.2377981D+02  
0.2365933D+02  
0.2357120D+02  
0.2363433D+02  
0.240014D+02  
0.241154D+02  
0.2406010D+02  
0.2387660D+02  
0.2387635D+02  
0.237006D+02  
0.236278D+02  
0.2353720D+02  
0.234535D+02

RHOT.  
102512D+00  
105825D+00  
105872D+00  
105313D+00  
104874D+00  
104503D+00  
104122D+00  
102814D+00  
102146D+00  
102150D+00  
104959D+00  
105878D+00  
106127D+00  
105828D+00  
105515D+00  
105055D+00  
104852D+00  
104650D+00  
104781D+00  
104122D+00





>DC YOU WISH TO ENTER THE PLOT SEQUENCE?  
1 = YES; 2 = NO.

>DC YOU WISH TO CONTINUE PLOT SEQUENCE?  
1 = YES; 2 = NO.

>DC YOU WISH TO CONTINUE PLOT SEQUENCE?  
1 = YES; 2 = NO.

>DC YOU WISH TO CONTINUE PLOT SEQUENCE?  
1 = YES; 2 = NO.

>DC YOU WISH TO CONTINUE PLOT SEQUENCE?  
1 = YES; 2 = NO.

>DC YOU WISH TO CONTINUE PLOT SEQUENCE?  
1 = YES; 2 = NO.

>DC YOU WISH TO CONTINUE PLOT SEQUENCE?  
1 = YES; 2 = NO.

>DC YOU WISH TO CONTINUE PLOT SEQUENCE?  
1 = YES; 2 = NO.

>DC YOU WISH TO CONTINUE PLOT SEQUENCE?  
1 = YES; 2 = NO.

>DC YOU WISH TO CONTINUE PLOT SEQUENCE?  
1 = YES; 2 = NO.

>DC YOU WISH TO CONTINUE PLOT SEQUENCE?  
1 = YES; 2 = NO.

>DC YOU WISH TO CONTINUE PLOT SEQUENCE?  
1 = YES; 2 = NO.

>DC YOU WISH TO CONTINUE PLOT SEQUENCE?  
1 = YES; 2 = NO.

>DC YOU WISH TO CONTINUE PLOT SEQUENCE?  
1 = YES; 2 = NO.

INITIAL DISTRIBUTION LIST

	<u>No. Copies</u>
1. Defense Technical Information Center Cameron Station Alexandria, Virginia 22314	2
2. Library, Code 0142 Naval Postgraduate School Monterey, California 93940	2
3. Department Chairman, Code 67 Department of Aeronautics Naval Postgraduate School Monterey, California 93940	1
4. Director, Turbopropulsion Laboratory, Code 67Sf Naval Postgraduate School Monterey, California 93940	20
5. LT J. Ferguson Naval Air Systems Command AIR-536 Washington, D.C. 20361	2
6. T. H. Okiishi Department of Mechanical Engineering Iowa State University Ames, Iowa 50011	1